Aalborg Universitet

Ensuring Supply Reliability and Grid Stability in a 100% Renewable Electricity Sector in the Faroe Islands

By Helma Maria Tróndheim

SEV

AALBORG UNIVERSITY
DENMARK

UNIVERSITY OF
THE FAROE ISLANDS

Ensuring Supply Reliability and Grid Stability in a 100% Renewable Electricity Sector in the Faroe Islands

by

Helma Maria Tróndheim

AALBORG UNIVERSITY
DENMARK

UNIVERSITY OF
THE FAROE ISLANDS

SEV

granskingarráðið
RESEARCH COUNCIL FAROE ISLANDS

Abstract

The Power Company in the Faroe Islands, SEV, and the Faroese Government have a vision to reach a 100% renewable electricity production by 2030. A tangible plan is needed in order to reach this ambitious goal, whilst ensuring supply reliability and grid stability in this isolated power system. This is the objective of this research project.

Ensuring the security of supply and resource adequacy in a power system predominately based on renewable energy resources is challenging, due to the weather dependency of the production and available storage options, especially in an isolated system. The first part of this thesis focuses on obtaining a tangible RoadMap with investments in generation, storage and transmission capacity needed to reach a 100% renewable electricity production in the Faroe Islands by 2030 and thus, ensures supply reliability. Existing expansion planning tools primarily consist of optimisation algorithms, which optimise capacities annually. Hence, the capacity of e.g. a specific transmission cable can increase year by year, whilst in reality a cable is either installed or not. This study uses the economic optimisation tool Balmorel, which optimises the investments and dispatch. A method to translate these optimal results to a practical RoadMap, has been developed. This method also considers practical constraints like the local resource potential, power plant locations and sizes.

Multiple scenarios, considering different technologies, have been analysed. Additionally, a sensitivity analysis of investment and fuel costs has been conducted. According to the results investing in renewables is the economically best option up to 87% renewable energy. Reaching 100% renewables in 2030 requires increasing the renewable generation capacity by almost 80% compared to the capacity needed for 87% renewables. The study also shows that if the potential of tidal energy can be unlocked, it has a disruptive influence on the future power system, as 72 MW of tidal power could replace 155 MW of hydro, wind, photovoltaic and battery power and decrease the pumped storage reservoir capacity by 75%.

The second part of the study focuses on investigating the grid stability of the power system through dynamic simulations. This study focuses on the grid on the isolated island of Suðuroy, which has a electricity demand

that is around 10% of the total demand. Starting with Suðuroy will provide valuable lessons learned to the rest of the system. In order to investigate the stability, a model suitable for load flow and dynamic simulations has been developed and validated. The available information about the governors and automatic voltage regulators of the synchronous generators is very limited. Therefore, these have been modelled using standard models. Using some of the existing approaches to parameterise the models, did not result in a model which could be dynamically validated. Therefore, a procedure combining different existing approaches was developed in order to parameterise and validate these models.

Dynamic RMS simulations over a 4.5 hour period without disturbances and shorter simulations, e.g. 30 seconds, with large disturbances have been conducted. The frequency and voltage fluctuations and their dependency on inverter-based generation shares and fluctuations have been investigated through the 4.5 hour simulations. The stability in Suðuroy towards 2030 has been investigated through the shorter simulations with disturbances. The study shows that initiatives are necessary in order to maintain the same frequency and voltage stability at the same level as today. However, according to the RoadMap the grid of Suðuroy should be connected to the main grid in 2026 through a subsea cable. The main grid is significantly larger than the grid of Suðuroy, and therefore contributes with ancillary services to Suðuroy. Two network reduction models and one detailed model have been used to represent the main grid in the simulations post 2026, and the results show that using network reductions causes implications when frequency triggered technologies, in this case batteries, are contributing to the stability. The dynamic stability of Suðuroy should be investigated further, especially scenarios in which the subsea cable to the main grid is out of service. The dynamic stability of the main grid also has to be studied.

The results of this research project are of great significance when in the transition toward a 100% renewable electricity sector in the Faroe Islands. The methods developed and lessons learned can also be applied to other power systems, especially similar power systems.

Resumé

Det færøske elselskab SEV og den færøske regering har en vision om en 100% grøn elproduktion i 2030. En konkret plan er nødvendig for at nå dette ambitiøse mål, og samtidig sikre en pålidelig elforsyning og et stabilt elnet i dette isolerede elsystem. Det er formålet med dette forskningsprojekt.

Når en stor del af den elektriske energi stammer fra vedvarende energikilder, er det en udfordring at sikre nok energi. Dette skyldes at produktionen bliver afhængig af vejret og lagringsmulighederne. Den første del af denne afhandling handler om at udvikle en konkret udbygningsplan med de nødvendige investeringer i produktions-, lagrings- og transmissionkapacitet for at nå en 100% grøn elproduktion på Færøerne i 2030, og samtidig sikre en pålidelig elforsyning. Eksisterende værktøjer til at lave udbygningsplaner med er typisk algoritmer, der optimerer investeringer årligt. Det vil f.eks. sige at kapaciteten af et kabel kan forøges år for år, mens det i virkeligheden enten vil blive installeret eller ej. Dette studie gør brug af værktøjet Balmorel, som økonomisk optimerer produktion og investeringer. En metode til at oversætte disse optimale resultater til en konkret udbygningsplan er blevet udviklet. Denne metode tager højde for praktiske begrænsninger såsom lokale energikilder, samt placeringer og størrelser på kraftværker.

Flere scenarier med forskellige energiteknologier er blevet analyseret. Følsomheden på resultaterne i forhold til investeringspriser og priser på brændstoffer er også analyseret. Resultaterne viser, at vedvarende energi er det bedste økonomiske valg op til 87% grøn elproduktion. Produktionskapaciteten af vedvarende energi skal øges med næsten 80% for at nå en 100% grøn elproduktion i 2030, i stedet for 87%. Analysen viser også, at tidevandsenergi har potentialet til at omvælte hele udbygningsplanen hvis det lykkes at udnytte den. 72 MW af tidevandsenergi kan erstatte 155 MW af vandkraft, vindenergi, solenergi og batterier. Pumpesystemets dæmninger kan også reduceres med 75%.

Den sidste del af projektet drejer sig om at analysere elnettets stabilitet med dynamiske simuleringer. I denne del er fokus på elnettet på øen Suðuroy, som har et elforbrug der svarer til omkring 10% af det samlede elforbrug. Erfaringerne på Suðuroy kan også bruges på resten af systemet. En model til at simulere load flow og dynamikken i elnettet er udviklet

og valideret. Der er få oplysninger om synkrongeneratorernes frekvens- og spændingsregulatorer tilgængelige. De er derfor blevet modelleret med standardmodeller. Resultaterne af at bruge eksisterende tilgange kunne ikke valideres. Derfor blev en metode, der kombinerer forskellige tilgange udviklet til at parametrisere og validere modellerne.

Der er lavet dynamiske simuleringer over 4,5 timer uden forstyrrelser og kortere simuleringer, f.eks. 30 sekunder, med store forstyrelser. Frekvens- og spændingudsving, og sammenhængen mellem udsvingene og fordelingen af inverter-baseret produktion er analyseret med de lange simuleringer. Stabiliteten i elnettet på Suðuroy frem imod 2030 er analyseret med de kortere simuleringer. Analysen viser, at det er nødvendigt med initiativer for at sikre stabiliteten på samme niveau som i dag. Udbygningsplanen indeholder et søkabel mellem Suðuroy og hovednettet i 2026. Hovednettet bidrager med systemydelser til nettet på Suðuroy, da det er betydeligt større. To simple modeller og et detaljeret model er brugt til at repræsentere hovednettet i simuleringere fra 2026. Det viser sig at de simple modeller, ikke er nøjagtige, når batterier på hovednettet bidrager med system ydelser. Den dynamiske stabilitet på Suðuroy bør analyseres yderligere, specielt i situationer hvor søkablet er ude af drift. Den dynamiske stabilitet på hovednettet skal også analyseres.

Resultaterne fra dette forskingsprojekt har en stor betydning for den grønne omstilling på det færøske elnet. Metoderne og erfarningerne kan også bruges til at analysere andre elnet, specielt lignende elnet.

Samandráttur

Elfelagið SEV og føroysku myndugleikarnir hava eina visión um 100% grøna elframleiðslu í 2030. Ein ítøkilig ætlan er neyðug fyri at náa hesum framsøkna máli og samstundis tryggja eina álítandi og støðuga elveiting í hesi lítlu og avbyrgdu elskipan. Hetta er endamálið við hesi granskingarverkætlan.

Tá ið ein stórur partur av elorkuni kemur frá varandi orkukeldum, er tað ein avbjóðing at tryggja, at tað altíð nóg mikið er til av orku tí hesar eru tongdar at veðrinum og goymslumøguleikum. Fyrri parturin av hesi ritgerðini snýr seg um at útvega eina ítøkiliga útbyggingarætlan við tilhoyrandi íløgum í framleiðslumátt, orkugoymslur og flutningsnet fyri at hava eina 100% grøna elorku í Føroyum í 2030 og harvið tryggja eina álítandi elveiting. Núverandi amboð at gera útbyggingarætlanir við eru vanliga algoritmur, ið optimera útbyggingar árliga. Tað vil t.d. siga, at føri hjá einum kaðli kann økjast ár fyri ár, meðan hann í veruleikanum verður íbundin ella ikki. Hendan kanningin nýtir amboðið Balmorel, ið búskaparliga optimerar bæði framleiðslu og íløgur. Ein mannagongd at umseta hesi optimalu úrslitini til eina ítøkiliga útbyggingarætlan er ment. Hendan mannagongdin leggur eisini upp fyri praktiskum avmarkingum sum staðbundnu orkukeldunum, umframt staðseting og støddum av orkuverkum.

Fleiri kanningar við ymsum orkutøknum eru gjørdar. Viðkvæmið hjá úrslitunum í mun til íløgu- og brennievniskostnaðir er eisini kannað. Sambært úrslitunum er grøn orka búskaparliga besta valið upp til 87% grøna orkuframleiðslu. Grøni framleiðslumátturin má økjast við næstan 80% fyri at fáa eina 100% grøna orkuframleiðslu í 2030, í mun til 87%. Kanningin vísir eisini, at sjóvarfalsorka kann kollvelta útbyggingarætlanina, um tað eydnast at gagnnýta hana. 72 MW av sjóvarfalsorku kann minka vindorku-, vatnorku-, sólorku- og battarímáttin við 155 MW. Harumframt minkar tørvurin á goymsluni í pumpuskipanini við 75%.

Seinni parturin av hesi verkætlanini snýr seg um at kanna støðufestið á elnetinum við støði í dynamiskum simuleringum. Í hesum partinum verður dentur lagdur á elnetið í Suðuroy, ið hevur eina elnýtslu á umleið 10% av samlaðu elnýtsluni. Royndirnar úr Suðuroynni kunnu brúkast í víðari kanningum av restini av elnetinum. Eitt modell til at simulera load flow og dynamikkin í elskipanini er ment og validera. Tað eru fáar upplýsin-

gar um frekvens- og spenningsregulatorarnir hjá synkrongeneratorunum tøkar. Tí eru hesir modelleraðir við standard modellum. Úrslitið av at brúka núverandi hættir at parametrisera hesi modell var ikki nøktandi. Tessvegna varð ein mannagongd, ið ger brúk av fleiri háttum, ment til at parameterisera og validera hesi modellini.

Dynamiskar simuleringar yvir 4,5 tímar uttan órógv og styttri simuleringar, t.d. 30 sekund, við stórum órógvum eru gjørdar. Sveiggini í frekvensinum og spenninginum, og teirra samanhangur við sveiggini í og býti av inverter-baseraðari framleiðslu eru kannað út frá teimum longru simuleringunum. Støðufestið í Suðuroy fram ímóti 2030 er kannað við stuttu simuleringunum við órógvum. Kanningin vísir, at neyðugt er við átøkum at tryggja at støðufestið ikki gerst verri enn í dag. Sambært útbyggingarætlanini skal ein sjókaðal knýta Suðuroynna í elnetið á meginøkinum í 2026. Elnetið á meginøkinum er munandi størri enn tað í Suðuroy, og tí stuðlar tað netinum í Suðuroy við skipanarberandi tænastum. Meginøkið er modellera við tveimum einføldum modellum og einum nágreiniligum í simuleringunum frá 2026. Úrslitini vísa at einføldu modellini ikki vísa tað sama sum tað nágreiniliga modellið, tá ið battaríini á meginøkinum stuðla netinum. Dynamiska støðufestið í Suðuroy átti at verið kannað nærri, serliga har gingið verður út frá, at sjókaðalin er óvirkin. Dynamiska støðufestið á meginøkinum átti eisini at verið kannað.

Úrslitini frá hesi granskingarverkætlanini hava stóran týdning fyri orkuskifti á føroyska elnetinum. Mannagongdirnar og royndirnar kunnu eisini brúkast at kanna onnur elnet, serliga líknandi elnet.

Preface

First and foremost, I would like to express my sincere appreciation to my excellent supervisors Claus Leth Bak, Filipe Faria da Silva, Bárður Niclasen and Terji Nielsen for guidance, constructive advise and profound belief in my work. I am also thankful for your encouragements and patience through the difficult periods these past years.

I would like to thank Aalborg University, the University of the Faroe Islands and the Power Company SEV for granting me the opportunity to pursue an industrial dual degree PhD. SEV and the University of the Faroe Islands together with Research Council Faroe Islands are also thanked for making this project possible through funding.

To my colleagues at Aalborg University, University of the Faroe Islands and of course SEV, where I spent the majority of my time; thank you for your valuable inputs and continuous support, both professional and personal.

Special thanks to Prof. Lutz Hofmann at Leibniz University Hannover, Pascal Gartmann and Eckard Quitmann at Enercon GmbH for the virtual study abroad collaboration. I would also like to recognise the assist I have received from AFRY Denmark and EA Energy Analyses for this project.

I am grateful for my family and friends, who have supported me throughout this project and shown interest in my work. To the scout leaders of my scout group; being the group leader, whilst conducting this research project, would have been impossible without the tremendous work you do.

Last but not least, I would like to express my deepest gratitude to my parents Frida and Jakku, my sister Oddvá and my brother Tummas and his family for their love, understanding and for always helping me achieve my goals.

Helma Maria Tróndheim
SEV, April 8, 2022

x

Contents

CHAPTER 1
Introduction

This chapter introduces the topic of this PhD thesis. First, the background of the research is described and then the power system is introduced. This is followed by the project objectives and limitations of the research project. Finally, the dissemination of the research results and the thesis outline are presented.

1.1 BACKGROUND

The integration of renewable energy into electrical power systems is rapidly increasing. According to the IRENA[1] the worldwide installed renewable production capacity has more than doubled over the 2010 to 2020 decade. In 2010 the installed capacity was 1.2 TW and in 2020 it had reached 2.8 TW. The majority of the growth, around 58%, is in Asia, but renewable power plants are being commissioned all around the globe [1]. Limiting climate changes due to pollution from fossil fuelled power generation is the main motivator behind increasing interest. Ambitious goals to minimise the pollution and obtain a cleaner electricity production have been set in many countries. Based on stated policies the CO_2 intensity from electricity generation will decrease from 476 g/kWh in 2018 to 308 g/kWh in 2040 [2].

The Faroe Islands, an 18 island archipelago in the North Atlantic Ocean (see Figure 1.1), are also aiming for a more renewable future. In 2014 the Electrical Power Company SEV announced the company's vision "100by2030", which is to reach a 100% renewable electricity production by 2030 [3]. The total production in 2021 was 424 GWh, which is a 20% increase from 2018 [4]. The majority of the electricity, 61.9%, was produced from fossil fuels, while hydro power plants and wind power plants produced 23.7% and 12.8% of the electricity, respectively. The final 1.6% were produced by a biogas power plant. There are photovoltaic panels in the system as well, but these produced less than 0.1% in 2021 [5]. The 100by2030 vision anticipates a doubling in the electricity demand from around 305 GWh in 2014 to around 600 GWh in 2030 [6]. The anticipated increase is based on the average annual increase, and a

---

[1]International Renewable Energy Agency

potential full electrification of the heating and transport sectors. This ambitious goal has also gained political interest, and was included in the coalition agreement valid from 2015 to 2019 [7]. The current coalition agreement (2019-2023) also states that the pace of the renewable transition should accelerate, but does not include a specific goal of shares of renewables, time span nor degree of electrification [8].

Fig. 1.1: A map showing the location of the Faroe Islands in the North Atlantic Ocean [9].

There are evidently environmental advantages with utilising renewable resources, but renewable energy is also associated with multiple disadvantages. The first obvious disadvantage is the nature of the renewable resources. Renewable energy resources are often undispatchable, fluctuating and intermittency is common. Wind speeds and directions can change suddenly, a cloud can cover the sun and there can be longer periods without any precipitation. The resources are also, to some extent, unpredictable, even though weather forecasts are increasingly accurate. Storage options for electrical energy are limited and expensive. These factors impact the prospect of achieving the required balance between the production and consumption. This is not an issue with fossil based power systems, as they are dispatchable and can therefore easily be controlled to meet the demand. There are some renewable energy resources that are dispatchable, e.g. biofuels and hydro power plants with designated reservoirs. Hydro power plants are however limited by the energy available in the associated storages, whilst power plants operating on biofuels have the same features of fossil generation, when it comes to storage of energy resource, i.e. fuel.

In an isolated power system like the Faroe Islands, the demand has to be supplied by local production, as it is not possible to import or export electricity. Thus, the local renewable resource potential and the combination

of different sources is an important factor when planning for 100% renewable electricity sector. The Faroe Islands have a wet, windy and cold climate, unlike many archipelagos, which typically have a high potential for e.g. solar power. In some islands hydro power might not be an option and in other islands installing wind turbines might be difficult due to e.g. geology. The Faroe Islands also have a potential for tidal energy, and by placing tidal projects at different locations a base load production could be obtained. The configuration of renewable generation will be different from location to location, and the uniqueness of the Faroe Islands geography means that it has to be studied locally. One of the closest isolated power system, is in Iceland. Iceland has a potential for geothermal power, which is not an option in most other power systems, including the Faroe Islands. This is an example of a resource which can have a high share in one system, but be non-existent in another.

The local resource potential also has a high impact on the economic feasibility of any renewable generation project. If a project is infeasible economically, the chances of it becoming a reality is lower than if the project is profitable. Therefore this has to be addressed when planning for 100% renewable electricity sectors. The profitability of renewable technologies also depend on what these are replacing, in the Faroe Islands and many other islanded systems this is diesel power. Purchasing and shipping diesel to a remote location is more expensive than using e.g. coal, and therefore the feasibility of renewable energy technologies can be higher. However, there are also factors that make renewable technologies more expensive in islands than in large grids, e.g. smaller power plants lead to higher costs pr. MW or the need for structural strength of wind turbines and PV panels in the Faroe Islands due to high wind speeds. Thus, the local economic feasibility has to be addressed.

Obtaining and maintaining a balance between production and consumption in power systems with a high penetration of renewables is as mentioned difficult, but from a technical perspective there are several additional challenges, e.g. with regards to the power system stability. The IEEE[2] and the CIGRE[3] have proposed the following definition of power system stability [10]:

> Power system stability is the ability of an electric power system, for a given initial operating condition, to regain a state of operating equilibrium after being subjected to a physical disturbance, with most system variables bounded so that practically the entire system remains intact. [10]

---

[2]Institute of Electrical and Electronics Engineers
[3]International Council on Large Electric Systems

The power system stability can be classified into rotor angle stability, voltage stability and frequency stability, and further subcatagorised depending on the type of disturbance, see Figure 1.2 [10]. The three classifications are related to the ability of the machines to being synchronised, maintain steady busbar voltages and a steady system frequency following a disturbance. This study focuses on the short term frequency and voltage stability.

```
                    ┌──────────────────┐
                    │  Power System    │
                    │    Stability     │
                    └──────────────────┘
          ┌──────────────────┼──────────────────┐
   ┌──────────────┐   ┌──────────────┐    ┌──────────────┐
   │ Rotor Angle  │   │  Frequency   │    │   Voltage    │
   │  Stability   │   │  Stability   │    │  Stability   │
   └──────────────┘   └──────────────┘    └──────────────┘
   ┌──────────┬──────────┐      │      ┌──────────────┬──────────────┐
┌────────────┐┌────────┐      ┌────────────┐┌──────────────┐
│Small-      ││Transient│      │Large-      ││Small-        │
│Disturbance ││Stability│      │Disturbance ││Disturbance   │
│Angle       ││        │      │Voltage     ││Voltage       │
│Stability   ││        │      │Stability   ││Stability     │
└────────────┘└────────┘      └────────────┘└──────────────┘
   ┌──────────┐          ┌──────────┬─────────┐  ┌──────────┐┌──────────┐
   │Short Term│          │Short Term││Long Term│  │Short Term││Long Term │
   └──────────┘          └──────────┴─────────┘  └──────────┘└──────────┘
```
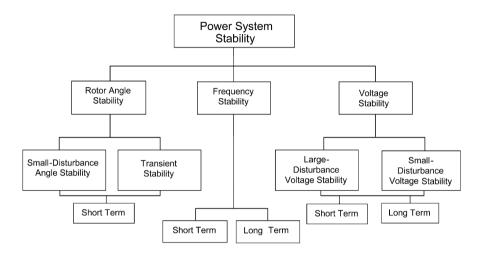
Fig. 1.2: Classification of power system stability [10].

The increase of renewable generation capacity, leads to conventional generators with respected regulating capacity and inertia being partly or totally decommissioned. This causes challenges with the power system stability, as the synchronous generators are traditionally the ones providing the ancillary services needed to maintain a stable supply, i.e. inertia and active/reactive power regulation. Inverter-based generation does not have the same capabilities, e.g. by being decoupled from the grid it does not provide natural inertia, and since the production is based on the renewable resource potential, the regulation capabilities are limited by instant resource potential as well. Thus, the likelihood of generation fluctuations and intermittence due to the nature of the resource are increased, while the regulating capacity is decreased and therefore the power system stability becomes a concern. A study on how the fluctuations of wind power can be minimised by spreading the wind farms around the Faroe Islands is found in [11]. Reference [12]–[14] discuss the issues with high penetrations of renewables and power electronics, the different types of renewable generation and their point of connection lead to different challenges, which are addressed in the following paragraphs.

The challenges associated with a high penetration of wind energy are addressed in references [15]–[18] The interaction and coordination between the

synchronous machines which have an inertia and the wind turbines can be difficult, and therefore finding the right control strategy is a challenge. There are several types of wind turbines, and these cause different issues, e.g. induction machines absorb reactive power, which can have a negative impact on the voltage and the power factor, while variable speed wind turbines are galvanically decoupled from the grid, and thus do not contribute to inertial response, but these can to some degree regulate the reactive power and voltage. The cut in wind speed can also lead to issues, as the wind turbine suddenly starts producing, which can cause the voltage to drop, and thus a high magnetising inrush current, that can damage power electronics and cause instabilities. The variations in the wind speed (thus active and reactive power), tower shadow and turbulence can result in voltage flicker. The effect of the variations are however not significant unless they are equal in size to the variations in the consumption according to [17].

The authors of reference [19] review the power system stability challenges associated with large-scale PV penetration. The study states that a high integration of PV generation, leads to a lower inertia and thus the online synchronous generators are under more stress, which can bring them to instabilities. Other issues addressed are fluctuations, lack of voltage/reactive power control, transient overvoltages etc. Through a literature review Eltawil and Zhao [20] have summarised how the maximum PV penetration levels depends on the following aspects: Ramp rates of main-line generators, cloud transients, harmonics, fast transients, unscheduled tie-line flows, frequency control vs break-even costs, voltage rise, voltage regulation and distribution losses. The penetration limits range form 1.3% (unscheduled tie-line flows) to no limit (harmonics). Harmonics are according to the review not an issue, as the PV inverters produce less harmonics than consumer loads. A simulation analysis of how the power system is affected by different levels of PV penetrations can be found in [21], which concludes that especially the voltage is negatively affected by the increased penetration of renewables.

Renewable production is often distributed generation (DG) [22], [23]. DG can therefore also lead to a lower power quality, as it typically does not contribute with short circuit capacity, and thus, the reliability of the supply is decreased. Contribution to ancillary services is also difficult using renewable DG. The voltage profile can become instable and fluctuating, due to the potential bi-directional flows. The bi-directional flows also make it difficult to tune protection systems, and therefore the effectiveness of protection equipment decreased. The delivery of reactive power with DG is also a challenge, as DG typically are asynchronous or inverter-based. The latter can however inject reactive power to some extent, but on the other hand it can cause harmonics in the system [23].

The challenges addressed here are valid for all power systems, but in an isolated grid like the Faroe Islands, these are even more severe, as these

5

systems are much more prone to disturbances than a large interconnected system [15], [17], [18], [24], [25]. Thus, all of these challenges have to be carefully considered when aiming for a high penetration of renewable generation. Especially in an isolated system like the Faroe Islands.
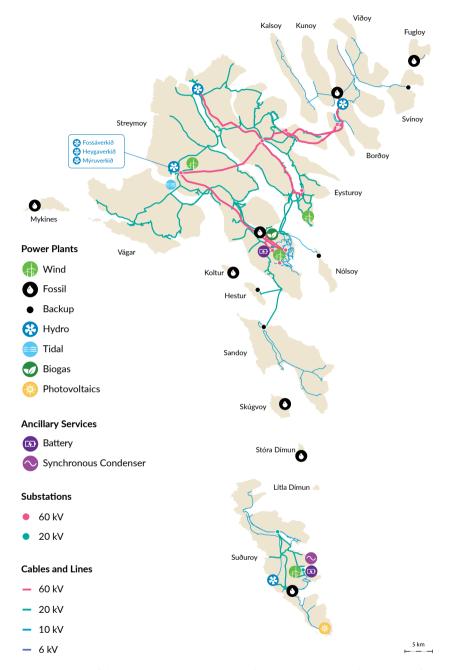
1.2 THE FAROESE POWER SYSTEM

The Faroese power system is operated by the Power Company SEV [26]. SEV was founded on the 1st October 1946 by the municipalities in the following three islands: **S**treymoy, **E**ysturoy and **V**ágar. Today SEV is owned by all the municipalities in the country, and is obliged to deliver power all over the country with a joint and several price structure. SEV has monopoly on grid operation, and currently a de facto monopoly on production, as SEV owns 98% of the installed generation capacity.

The total generation capacity in the Faroe Islands is 168 MW. These 168 MW are distributed between fossil, hydro, wind, biogas and PV power. A demonstration project with tidal power is also a part of the power system. In terms of storage every hydro plant has one or more reservoirs with a storage capacity of 12.3 GWh in total. Two battery systems (2.3 MW/707 kWh and 7.5 MW/7.5 MWh) and a synchronous condenser (8 MVA) are also a part of the system.

The following sections describe the Faroese power system in terms of transmission/distribution grid and generation and storage capacities in its expected stage dated 1st of June 2022. The grids, the power plants and ancillary services are shown on Figure 1.3, tabulated in Table 1.1 and described in subsection 1.2.1, subsection 1.2.2 and subsection 1.2.3.

Fig. 1.3: Overview of the Faroese power system (1st of June 2022) showing the location of power plants, ancillary services, substations, cables and lines.

Table 1.1: Power and storage capacities of power plants and ancillary services in each island as shown in Figure 1.3. The power plants and ancillary services are listed from North to South. *kWh **MVA.

Island	Name	Type	Generation (MW)	Storage (MWh)
Fugloy	Elverkið í Fugloy	Fossil	0.18	-
Svínoy	Elverkið í Svínoy	Backup (fossil)	0.26	-
Borðoy	Elverkið á Strond	Fossil	3.60	-
		Hydro	1.40	24
Eysturoy	Eiðisverkið	Hydro	21.70	5927
	Neshagi	Wind	4.50	-
Streymoy	Mýrarnar	Wind	1.98	-
	Fossáverkið	Hydro	6.30	2577
	Heygaverkið	Hydro	4.80	523
	Mýruverkið	Hydro	2.40	2275
	Minesto	Tidal	0.20	-
	Sundsverkið	Fossil	82.30	-
	FÖRKA	Biogas	1.50	-
	Húsareyn	Battery	2.30	*707
	Húsahagi	Wind	11.70	-
Mykinesi	Elverkið í Mykinesi	Fossil	0.15	-
Koltur	Elverkið í Koltri	Fossil	0.03	-
Hestur	Elverkið í Hesti	Backup (fossil)	0.15	-
Nólsoy	Elverkið í Nólsoy	Backup (fossil)	0.26	-
Sandoy	Elverkið í Skopun	Backup (fossil)	1.78	-
Skúgvoy	Elverkið í Skúgvoy	Fossil	0.23	-
Stóra Dímun	Elverkið í Dímun	Fossil	0.09	-
Suðuroy	Porkerihagi	Wind	6.30	-
	Í Heiðunum	Battery	7.50	*7500
		Synchronous condenser	**8.00	
	Elverkið í Botni	Hydro	3.00	924
	Vágsverkið	Fossil	13.30	-
	Sumba PV	Photovoltaics	0.26	-

1.2.1 TRANSMISSION AND DISTRIBUTION GRIDS

The Faroese power system, consists of seven isolated electrical grids. The main grid connects 11 out of 18 islands, and the demand on the main grid is 90% of the total demand. The other grids supply one island each and the 18th island is uninhabited, and does therefore not have a grid. The demand on the most southern island, Suðuroy, which is electrically isolated is around 10% of the total demand. The five remaining grids: Fugloy, Mykines, Koltur,

Skúvoy and Stóra Dímun, are small, and their demand is less than 0.2% of the total demand. Lítla Dímun is uninhabited and therefore does not have a power supply.

The voltage levels are 60 kV, 20 kV, 10 kV, 6 kV and 0.4 kV. The highest voltage levels, 60 kV and 20 kV, are used for transmission, while 10 kV, 6 kV and 0.4 kV are used for distribution. In the past, overhead lines were used all over the system, but in the end of 2019 88% of the grid was composed of cables [27]. Cables are used in all new connections, and lines are replaced by cables on all voltage levels except for 60 kV. The main reasons behind the transition from overhead lines to cables are the heavy winter storms, which on several occasions have led to blackouts. Figure 1.4 shows an example of a transmission tower after a heavy winter storm.

Figure 1.3 also shows the 60 kV and 20 kV substations. Substations are also combined with the diesel and hydro power plants in several locations, and these are not visible in the figure e.g. the hydro power plant on Eysturoy (Eiðisverkið) or the fossil fuelled power plant on Suðuroy (Vágsverkið).

Fig. 1.4: A transmission tower after a heavy winter storm.

Load

In 2020 the mean load in the main grid was 42.1 MW, with a minimum of 26.8 MW and a maximum of 61.7 MW. The load in Suðuroy is as mentioned previously significantly lower, with a mean of 4.0 MW, and the variations are larger, as the peak load in Suðuroy was 8.0 MW, which is twice as much as the mean load. This large variation is caused by a fish factory, which is not always online, but has a demand of similar size to the total demand in Suðuroy. The minimum, mean and maximum loads for the main grid and the grid on Suðuroy are shown in Table 1.2.
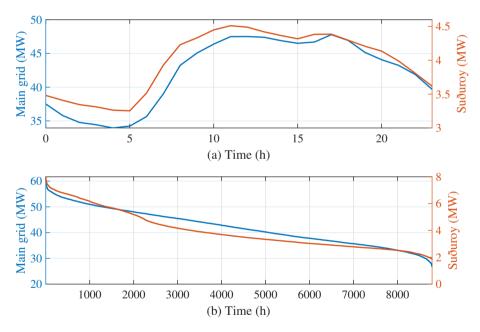
Grid	Minimum	Mean	Maximum
Main	26.8	42.1	61.7
Suðuroy	1.8	4.0	8.0

Table 1.2: Minimum, mean, and maximum load in 2020 in the main grid and in Suðuroy.

Figure 1.5 shows the (a) average daily load profile in 2020 and the (b) duration curve of the load in both the main grid and in Suðuroy. The load in the two grids have a similar behaviour, but the peak in Suðuroy is around noon, while the peak on the main grid is at 17:00.

While the load duration curve in the main grid has a constant slope from 500 to 8500 hours, the grid in Suðuroy shows a higher slope below 2000 hours, than above 2000 hours. This is due to the fish factory, which is online for around 2000 hours in 2020, as also discussed in [28].

Fig. 1.5: Load in the main grid and in Suðuroy in 2020. (a) Average load profile over a day and (b) duration curves.

1.2.2 POWER PLANTS

The description of the power plants is structured in sections for each generation type, i.e. fossil fuel, hydro, wind, biogas, photovoltaic and tidal power.

Fossil Fuel Power Plants

The largest fossil fuel power plant, Sundsverkið, was originally put into operation in 1974. This plant was expanded in 1983, in 1987 and again in 2019. Today the total capacity at Sundsverkið is 82.3 MW.

Elverkið á Strond, which originally was built as a hydro power plant, was expanded with a diesel generator in 1950. The installed thermal generation capacity at Strond is 3.6 MW.

In 1982 Vágsverkið on Suðuroy was commissioned. Vágsverkið has been expanded twice, and today it has a total rated capacity of 13.3 MW distributed between four engines.

The five small isolated islands Fugloy, Mykines, Koltur, Skúvoy and Stóra Dímun all have a fossil fuel plant with 2-3 diesel generators. These plants have a rated capacity between 30 kW and 230 kW.

Finally there are four backup power plants, rated between 0.15 MW and 1.78 MW, located on some of the islands, which are connected to the main grid. Out of these four backup power plant, the one in Svínoy is the most used. This is because Svínoy is connected to the main grid through an overhead line, and sometimes a storm risks in an outage of this line. The other islands with backup plants are connected to the main grid through subsea cables, and therefore these are not as often in risk of an outage, but when they are, it is for a longer period of time.

Hydro Power Plants

In 1921 the very first power plant in the Faroe Islands was inaugurated. This was the hydro power plant "Elverkið í Botni" installed in Suðuroy, see Figure 1.6. There are two turbines at Botnur. The first one (1 MW) produces electricity from water stored in the reservoir Ryskivatn, which at a 244 m altitude can store up to 238 MWh. The water from Miðvatn, a reservoir at 349 m above sea level (a.s.l.), is tapped into Ryskivatn. Miðvatn can store 339 MWh. The second turbine has a rated capacity of 2 MW. This turbine produces electricity using the water stored at Vatnsnesvatn, which is located at 181 m a.s.l. and has a storage capacity of 347 MWh.

The second hydro power plant was put into operation in 1931, this was "Elverkið á Strond". The plant has one turbine with a rated capacity of 1.4 MW. The reservoir associated with Strond can store around 24 MWh at a height of 224 m a.s.l.

There are three hydro power plants in the village of Vestmanna on Streymoy; Fossáverkið, Mýruverkið and Heygaverkið, which all were installed between 1953 and 1963. There are two turbines installed at Fossáverkið with a total capacity of 6.3 MW. The water from the reservoir Vatnið is tapped into Lómundaroyri. In total these two reservoirs have a storage capacity of 2.6

GWh. Lómundaroyri has an altitude of 224 m. The other two hydro power plants in Vestmanna are a cascading system. The water used to produce electricity at Mýruverkið is reused at Heygaverkið. These two plants' reservoirs, Mýrarnar and Heygadalur, are located at 347 m and 108 m and can store 2.3 GWh and 0.5 GWh, respectively. Mýruverkið has a turbine capacity of 2.4 MW and Heygaverkið 4.9 MW.

The final hydro plant is Eiðisverkið. Eiðisverkið was originally built in 1987, and has been expanded by increasing the inflow and by adding turbine capacity. The latest expansion was finished in 2012. Eiðisverkið has a storage capacity of around 5.9 GWh in the Eiðisvatn reservoir, and hence; it is the largest storage capacity in the country. There are three turbines at Eiðisverkið with a total capacity of 21.7 MW.

Fig. 1.6: The hydro power plant Botnur from 1921.

Wind Farms

The first grid connected wind turbine was installed in 1993 at Neshagi. This 150 kW Nordtank wind turbine was in operation until November 2021 when it was struck by lightening, see Figure 1.7. In 2005 the wind generation capacity at Neshagi was expanded with three 660 kW Vestas V47 wind turbines. However, due to a faulty control, two of these wind turbines were destroyed in the winter storms 2011/2012. The third Vestas turbine was decommissioned because of the malfunction, and instead of installing three additional wind turbines in 2012, which were planned prior to storms, five new turbines were installed. The total wind power capacity at Neshagi is 4.5 MW, consisting of five 900 kW Enercon E-44 wind turbines.

In 2003 a private company, Sp/f Vindrøkt, installed three Vestas V47 wind turbines at Mýrarnar in Vestmanna. The total wind power capacity at Mýrarnar is 1.98 MW.

The third wind farm, Húsahagi, is composed of 13 Enercon E-44 wind turbines. The total wind power capacity almost tripled, when this wind farm of 11.7 MW was installed in 2014.

Fig. 1.7: The Nordtank wind turbine strucked by lightening. Photo by B. Á. Rubeksen.

In November 2020 the first wind energy was delivered to the isolated grid of Suðuroy. This energy was produced at the 6.3 MW wind farm in Porkeri. The wind farm consists of 7 Enercon E-44 wind turbines and was officially inaugurated in February 2021.

In 2019 there were two tenders for 18 MW wind farms. SEV won the tender for the wind farm to be located at Eiði, close to the hydro power plant Eiðisverkið, while the privately owned oil company Magn won the other tender for a wind farm to be located next to the 11.7 MW wind farm Húsahagi. Both winning offers consisted of 6 Enercon E-82 wind turbines.

Early in 2021 Sp/f Vindrøkt won an open-door tender for a 25.2 MW wind farm, right next to the 11.7 MW wind farm Húsahagi and Magn's 18 MW wind farm. The 25.2 MW wind farm will consist of six Vestas V117 - 4.2 MW wind turbines.

Biogas

In April 2018 the Faroese salmon farming company Bakkafrost announced, that they were investing in a biogas power plant (FÖRKA), which was commissioned in 2020. The gas is made from cow manure and organic waste from both sea farms and hatcheries. The company sells electricity to the grid, and heat to the district heating system in the capital. The substance left from the process, is a fertiliser utilised by farmers. Figure 1.8 [29] shows a schematic of the process cycle.

The gas engine has a rated capacity of 1.5 MW, and the plant has a limited storage capacity. It is expected that the production has reached its full potential of producing 9.3 GWh/year by 2024. The production will be close to constant at 1 MW [29].
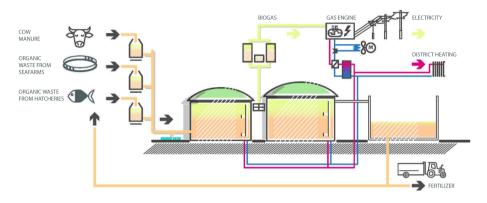
Fig. 1.8: A schematic showing the process cycle of planned biogas power plant [29].

Photovoltaic Power

SEV put the first relatively large photovoltaic (PV) power plant into operation in November 2019. This first grid scale plant is a demonstration project. The plant has capacity of 250 kW and is placed on abandoned football field in Sumba on Suðuroy, see Figure 1.9. Aside from the PV plant in Sumba, the installed capacity of PV is negligible, as very few systems have been installed on rooftops.

Fig. 1.9: The first grid-scale photovoltaic plant in the Faroe Islands.

Tidal Power

The technology to extract tidal energy is still in the development phase, and thus it is difficult to predict how significant a component tidal energy will be in the future. However, tidal energy has gained a lot attention in the Faroe Islands, especially due to the predictability and the fact that it could provide a base load production, as there is a phase shift between the tidal currents at different locations. This is addressed in following chapters. Thus, if the potential of tidal energy could be unlocked, it could change the future energy mix fundamentally.

In November 2018 SEV made a collaboration agreement with the Swedish company Minesto, to do a demonstration project with tidal energy in the Faroe Islands with two DG100 tidal kite generators (100 kW), located in Vestmannasund, i.e. the strait between Vágar and Streymoy. In March 2022 Minesto announced that it will concentrate its operations in 2022 in the Faroe Islands instead of France and Wales, as originally planned. The plan is to install two generators of the newly designed D4 (100 kW), see Figure 1.10b and one D12 generator (1.2 MW) also in Vestmannasund [30]. Through these projects new knowledge will be gained about the feasibility of tidal energy in the Faroe Islands. The previous design DG100 and new design D4 are shown in Figure 1.10.

(a) DG100

(b) D4
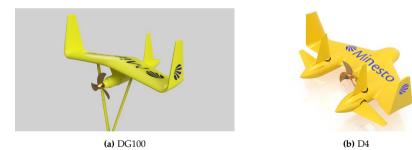
Fig. 1.10: Minesto's tidal generators.

1.2.3 ANCILLARY SERVICES

The first section of this chapter, section 1.1, discussed some of the challenges of the integration of renewable energy, e.g. the decommission of synchronous generators with their inherent ancillary services. This integration in the Faroe Islands has led to additional investments in alternative ancillary services. These are battery systems to provide active power reserves and synchronous condensers to provide inertia, reactive power regulation and short circuit power.

Battery Systems

A battery system of 2.3 MW/707 kWh was installed at the substation Húsareyn next to the wind farm Húsahagi in 2016, see Figure 1.11. The objective is to smooth the production from the wind farm (ramp rate control) and contribute to frequency regulation.
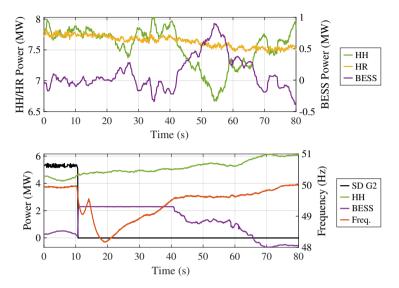
Fig. 1.11: The BESS located at the wind farm Húsahagi.

The upper plot on Figure 1.12 shows an example of the battery in ramp rate control. The production from the wind farm (HH), the output from the battery (BESS) and the summation of these two (HR), i.e. stabilised output, are all shown on the figure. It is clear from the figure that the battery smoothens the wind farm output significantly. An example of the battery system contributing to frequency regulation is shown on the lower plot in Figure 1.12. In this example the wind farm output is relatively stable. An engine at Sundsverkið (SD G2) suddenly drops out, which causes a frequency drop. The battery system reacts to the low frequency and starts to deliver maximum power. Due to the low frequency another unit drops out, and the battery system continues to deliver full power until the frequency has exceeded 49.5 Hz.

A 7.5 MW/7.5 MWh BESS is installed at the substation "Í Heiðunum" in Suðuroy next to the 6.3 MW wind farm there. This BESS is intended for fast frequency control, and does not have a ramp rate control like the BESS at Húsareyn. The power capacity is designed to be able to handle a sudden loss of the whole wind farm, while the energy capacity is designed to have enough time to start up diesel engines or bringing the wind farm back into operation.

As the wind power capacity is set to increase, SEV's plans to increase the BESS capacity in the main grid up to 55 MW, which is the same size as the existing 11.7 MW wind farm Húsahagi and the two new wind farms to be

installed next to Húsahagi, and be considered the largest unit. 12 out of the 55 MW BESS have been ordered.

Fig. 1.12: Examples of the BESS in operation. HH is the power output from the wind farm, BESS the battery system and HR (Húsareyn) the sum of HH and BESS. SD G2 is one of the thermal generators at Sundsverkið and Freq. is the frequency measured at the Húsareyn substation. Upper: Ramp rate control. Lower: Frequency regulation.

Synchronous Condensers

An 8 MVA synchronous condenser is also installed at the substation next to the wind farm in Suðuroy, see Figure 1.13. There are no synchronous condensers in the main grid, but a 16 MVA synchronous condenser has been ordered and SEV's preliminary plans include two more of the same size and also one rated at 6 MVA in the northern isles.

Fig. 1.13: The synchronous condenser at the wind farm substation in Suðuroy.

1.3   PROBLEM FORMULATION AND PROJECT OBJECTIVES

The Faroese Power Company SEV is, as previously mentioned, aiming for a 100% renewable electricity sector in 2030. In order to reach this goal a detailed plan addressing the challenges associated with a renewable production is needed. The aim of this thesis is to investigate two of the challenges, i.e. the energy balance and the power system stability. The main objectives of this industrial PhD project are to answer these two questions:

1. What is the best suited RoadMap in a 100% renewable electricity sector in the Faroe Islands based on energy resources and economics?

2. How can we obtain a stable electricity supply in a 100% renewable electricity sector?

In order to answer the first objective, which is based on the main grid and Suðuroy, the following will be addressed:

(a) State of the art of expansion planning tools and case studies.

(b) Assessment of the available energy resources and potential production in this unique system.

(c) Feasibility of the production and long-term storage technologies, which are relevant to the study case.

(d) Analyses of the optimal mixture between production and long-term storage technologies, and investigations of the impact that different costs and technologies, e.g. tidal energy, can have on the overall system.

(e) Development of a procedure to obtain a tangible RoadMap from an economic optimisation.

(f) Obtaining a tangible RoadMap for the Faroese power system based on the economically optimal energy mixture.

For the second objective, the grid on Suðuroy is in focus, and this objective will be answered by;

(a) State of the art of power system model regulation and modelling.

(b) Model the isolated power system in DIgSILENT's PowerFactory, based on today's configuration and the future developments according to the RoadMap.

(c) Develop and apply validation guidelines for the dynamic power system models. Prepare tests for measurements on the system to obtain data for model validation.

(d) Assessing and analysing the frequency and voltage variations in today's system.

(e) Simulating and analysing the grid with the proposed expansion plan and test scenarios based on common and known grid disturbances, which the grid should be able to ride through. Given that instabilities are an issue; address the need for expansions in ancillary services.

(f) Assess the need for using a detailed simulation model of the larger main grid when analysing the stability on Suðuroy with a cable connection to the main grid.

(g) Provide lessons learned from Suðuroy to the main grid.

1.4 LIMITATIONS

This study investigates two aspects of the transition towards a 100% renewable electricity sector; supply reliability and the grid stability of the system.

The supply reliability is addressed through expansion planning, since this ensures enough generation and storage capacity to meet the demand considering the available energy resources. The expansion planning is conducted through economic optimisation of generation and storage capacities. The study is based on the main grid and the grid of Suðuroy only, not the 5 smaller isolated grids of Fugloy, Mykines, Koltur, Skúgvoy and Stóra Dímun.

The power system stability study is limited to frequency and voltage stability. Some simulations have been conducted including the main grid, but the main focus in the power system stability study is the island of Suðuroy. Analysing the grid of Suðuroy is a building step towards a full analysis of the Faroese power system, as the studies on Suðuroy will be replicated on the main grid. The study includes both dynamic RMS simulations without disturbances over several hours, and also shorter simulation periods with large disturbances. The study does not include EMT simulations.

All studies, both supply reliability and grid stability, focus on the power system at transmission level.

1.5 DISSEMINATION

The research findings of this project have been disseminated through scientific articles, scientific and general presentations and participation in media, e.g. TV and radio. The scientific articles are listed under section 1.5.1, while presentations and media participation can be found under section 1.5.2 and 1.5.3 respectively. Teaching and supervision activities are found under 1.5.4.

1.5.1   SCIENTIFIC ARTICLES

This thesis is written as a monograph, but some of the methods and results have been, or are to be, published as scientific articles. The drafts of the unpublished articles number 6 and 8 are available for the reader in Appendix C. Article number 4, which will be published in July, is not in appendix due to lack of copyrights. However, the results presented in it are based on article number 3, which is found in Appendix C.

1. **H. M. Tróndheim**, B. A. Niclasen, T. Nielsen, C. L. Bak, and F. F. da Silva, "Introduction to the Energy Mixture in an Isolated Grid with 100% Renewable Electricity - the Faroe Islands," in *Proceedings of CIGRE Symposium Aalborg 2019.* Aalborg, Denmark: CIGRE (International Council on Large Electric Systems), 2019.

2. **H. M. Tróndheim**, T. Nielsen, B. A. Niclasen, C. L. Bak, and F. F. da Silva, "The Least-Cost Path to a 100% Renewable Electricity Sector in the Faroe Islands," in *Proceedings of 4th International Hybrid Power Systems Workshop.* Crete, Greece: Energynautics GmbH, 2019.

3. **H. M. Tróndheim**, B. A. Niclasen, T. Nielsen, F. F. D. Silva and C. L. Bak, "100% Sustainable Electricity in the Faroe Islands: Expansion Planning Through Economic Optimization," in *IEEE Open Access Journal of Power and Energy*, vol. 8, pp. 23-34, 2021. Selected as *IEEE Open Access Journal of Power and Energy Trending Topic Paper March 2021*. Licensed under **CC BY 4.0**.

4. J. Cochran, C. L. Bak, P. L. Francos, D. McGowan, A. Iliceto, G. Kiseliovas, J. Rondou, **H. M. Tróndheim**, and J. Whiteford, "Same goal, different pathways for energy transition," in *IEEE Power and Energy Magazine*, vol. 20, no. 4, 2022.

5. **H. M. Tróndheim**, J. R. Pillai, T. Nielsen, C. L. Bak, F. F. da Silva, B. A. Niclasen, "Frequency Regulation in an Isolated Grid with a High Penetration of Renewables - the Faroe Islands," in *2020 Cigre Session: Papers and Proceedings.* Paris, France: CIGRE (International Council on Large Electric Systems), 2020.

6. **H. M. Tróndheim**, F. F. da Silva, C. L. Bak, T. Nielsen, B. A. Niclasen, R. S. Nielsen, and N. Weikop, "Alternative and Combined Procedure for Parameter Identification and Validation of Governor and Automatic Voltage Regulator Dynamic Models," (Working title, to be submitted prior to defence).

7. **H. M. Tróndheim**, L. Hofmann, P. Gartmann, E. Quitmann, F. F. da Silva, C. L. Bak, T. Nielsen, and B. A. Niclasen, "Frequency and Voltage

Analysis of the Hybrid Power System in Suðuroy, Faroe Islands," in *Proceedings of Virtual 5th International Hybrid Power Systems Workshop.* Energynautics GmbH, 2021.

8. **H. M. Tróndheim**, L. Hofmann, P. Gartmann, E. Quitmann, C. L. Bak, F. F. da Silva, T. Nielsen, and B. A. Niclasen, "Frequency and Voltage Stability Towards 100% Renewables in Suðuroy, Faroe Islands," CIGRE Science and Engineering Journal, (Accepted with minor changes, to be published in June 2022).

1.5.2 PRESENTATIONS

- **EA Energy Analyses, 2019:** Presentation on the 100by2030 vision and the research objectives.

- **Granskingardagur, 2019:** Presentation on project objectives and initial results for employees of the University of the Faroe Islands.

- **Minesto, 2019:** Presentation on research results with regards to the influence of tidal energy for the board and management of the Swedish company Minesto.

- **Arctic Circle 2019:** Invited by the Faroese Ministry of Foreign Affairs to present the energy transition in the Faroe Islands, with focus on the 100by2030 vision and the ongoing research project.

- **High Schools, 2019-2021:** Presentations on the 100by2030 vision and the ongoing research results for 5 different high school classes.

- **SEV, 2019-2021:** Presentations on the ongoing research results on multiple occasions for the board, management and engineers.

- **ORKA (Energy Authority), 2020-2021:** Presentation of ongoing research results on two occasions.

- **Viden og vækst, 2021:** Invited to have an oral conference presentation on the project and the cooperation between AAU, UFI and SEV.

- **Vísindavøka 2021 (European Researcher's Night 2021 Faroe Islands):** Poster presentation on power system stability with unstable resources. *Awarded 1st price*.

- **Ljósfest, 2021:** Public presentation about research results at the celebration of 100 years of electricity in the Faroe Islands.

- **Ocean Energy Europe 2021:** Invited by the organisers to present how tidal energy could disrupt the future energy composition in the Faroe Islands.

- **Canadian Embassy in Denmark, 2021:** Presentation on the 100by2030 vision and research results.

- **13th MRIA Marine Renewables Emerging Technologies Industry Forum, 2022:** Invited by organisers to present how tidal energy could disrupt the future energy composition in the Faroe Islands. Invited at Ocean Energy Europe 2021.

1.5.3 MEDIA PARTICIPATION

- **National TV news (Kringvarp Føroya, Dagur og vika), May 2019:** Presented early research finding on the daily TV news.

- **Student's Magazine (MFS, Fjølnir 2020), 2020:** Authored an article on the technical challenges with renewable energy.

- **Podcast (Nýhugsan), September 2020:** Discussed research questions and findings.

- **National newspaper (Dimmalætting), March 2021:** Interview with reference to being selected as *IEEE Open Access Journal of Power and Energy Trending Topic Paper March 2021.*

- **National radio show (Kringvarp Føroya, Breddin), April 2021:** Commentator on challenges with a specific wind farm offer.

- **National newspaper (Sosialurin), April 2021:** Interviewed about the 100by2030 stepping stones.

- **National radio show (Kringvarp Føroya, Breddin), October 2021:** Commentator on the situation in the Faroe Islands with reference to COP26.

- **National TV show (Rás 1, Búskapur og vinna), January 2022:** Explained different aspects of the energy transition in the Faroe Islands.

1.5.4 TEACHING AND SUPERVISION ACTIVITIES

- Co-supervisor for bachelor thesis at the University of the Faroe Islands.

- Assisting a EPSH3 group project at AAU with developing a secondary control of a synchronous generator.

- Teaching assistant for in the course "Power engineering 1" for BSc Energy Engineering at the University of the Faroe Islands.

1.6 THESIS OUTLINE

This industrial PhD thesis consists of 8 chapters, where chapters 2-4 address objective 1 and 5-7 address objective 2. The outline is as follows:

1. **Introduction:** The topics of the thesis are introduced, followed by a description of the Faroese power system. The problem formulation, project objectives and limitations are presented, as well as the dissemination of the research results.

2. **Expansion Planning Theory:** The state of the art expansion planning theory is presented, both based on available tools and case studies. The methodology proposed to improve expansion planning, combining an existing optimisation tool and a new method, is also presented.

3. **Optimisation of the Future Energy System:** This chapter covers the modelling and input of the optimisation model, and then presents the results of the economic optimisation.

4. **100by2030 RoadMap:** This chapter presents the main contribution from the expansion planning studies, i.e. the proposed RoadMap. The optimal investments presented in previous chapters are carefully investigated, and then translated into realistic investment projects. The RoadMap is also validated in this chapter.

5. **Power System Regulation and Modelling Theory:** Traditional and state of the art ancillary services are described, followed by study cases on the Faroese power system. The most common tools to conduct power system studies are presented and the need for validated models is addressed. A new alternative and combined parameterisation and validation procedure of dynamic controllers is developed and presented.

6. **PowerFactory Model of the Faroese Power System:** The PowerFactory model of the Faroese power system, focusing on Suðuroy, is described for each component in the system. The results of the static and dynamic validation of the model via field measurements is also presented.

7. **Dynamic Studies of the Power System on Suðuroy:** This chapter describes the dynamic RMS studies conducted in this research project. First an analysis of frequency and voltage fluctuations with and without inverter-based generation in is presented, followed by a study with short-term large disturbances. The final section of the chapter discussed how the results on Suðuroy can be transferred to the main grid.

8. **Conclusions:** The thesis is concluded with the main contributions of the research and possible future works are proposed.

CHAPTER 2
Expansion Planning Theory

This chapter addresses parts of the first objective. It starts with a state of the art review of the available tools used for expansion planning, presents study cases of Faroe Islands and other systems, both energy resources and expansion planning. The final part of the chapter describes the proposed method to conduct expansion planning studies, which also has been applied to the main grid and the grid of Suðuroy in the study.

2.1 TOOLS AND MODELS

Models and computer tools have been developed for investigations of and planning the energy sector. Several of these have been reviewed in literature [31]–[38]. The focus of the reviews varies from brief overviews, categorising models, discussing the approaches and state of the art challenges associated with expansion planning.

From literature previous to 1999 van Beeck [31] has identified nine ways to classify energy models. 10 energy models are classified based on the identified methods. Jebaraj and Iniyan [32] give an overview of a broad collection of energy models dating up to 2006 including energy planning models, energy supply-demand models, forecasting models, optimisation models, neural network energy models, and emission reduction models. The models are not described in details in terms of logic, approach and methodology. The review has a coverage of 252 references. According to [33], none of the then present-day (2007) energy models adequately address the energy systems and economics of developing countries, as these are significantly different from industrialised countries. Reference [34] reviews computer tools used for analysing the integration of renewable energy, and aims to assist the reader to choose a tool suitable for a specific application. This is done by categorising the tools depending on the type and by describing the application, temporal resolution, any specific focus, included sectors (electricity, heat and transport) and the degree of renewable energy penetration simulated previously. 37 tools are included in the review, while 68 tools were considered initially. A model review focusing on the challenges associated with twenty-first cen-

tury energy is found in reference [35]. The paper describes the paradigms of four types of energy models and addresses the respective challenges, these include resolving time and space, balancing uncertainties, system complexity and human behaviour. Ringkjøb et al. [36] thoroughly review 75 modelling tools. The paper categorises the tools similarly to Connolly et al. [34], but a broader collection of tools is presented. The flowchart of the categorisation is shown in Figure 2.1. First the included models are listed with developer, availability, the used software and relevant literature. The models are then categorised based on their general logic and resolution, i.e. the approach, purpose, methodology and temporal/spatial. Finally the technological and economic parameters are listed.
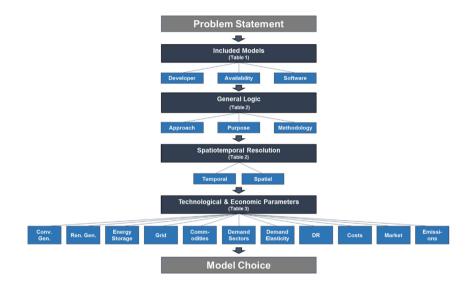
Fig. 2.1: Model categorisation flowchart presented in [36].

Generation expansion planning is not a simple topic, and Koltsaklis and Dagoumas [37] address the challenges with state of the art expansion planning, including risk assessments, integration of electric vehicles, short term operation etc. The different approaches in generation expansion planning are discussed in reference [38]. This review does not contain information about the available tools and models, but compares the different theoretical approaches and discussed the advantages and disadvantages of the approaches.

There is a continuous development of models and tools used for expansion planning, as new challenges have to be addressed and adaptions or new approaches are needed. The number of models and tools is high, and thus choosing the best fitted tool can be difficult, but the published reviews on expansion planning can assist in choosing a suitable tool.

2.2 RELEVANT CASE STUDIES

The following two subsections, i.e. subsection 2.2.1 and subsection 2.2.2, present some of the relevant study cases, both international studies and Faroese studies.

2.2.1 INTERNATIONAL STUDIES

The challenges faced in a power system depend on the characteristics of it. It is therefore important to compare small isolated power systems towards other similar power systems, instead of a large interconnected system, e.g. the European network. The Faroese power system is, according to EU's[1] definition, a micro isolated system, which is a non-interconnected system with an annual consumption less than 500 GWh in 1996 [39]. In 1996 the consumption in the Faroe Islands was 180 GWh [40]. An analysis of other islanded power systems has been conducted, in order to find which systems are the most comparable to the Faroese power system. IRENA has a framework to support SIDS[2] to transit to renewables, i.e. the Lighthouses Initiative. 36 SIDS are participating in the initiative, some of which are comparable to the Faroese power system. EU also has an initiative on renewable islands "Clean Energy for EU Islands". There are also additional archipelagos and islands around the world, not considered as SIDS nor a EU Clean Energy Island, which can be compared to the Faroe Islands in terms of the power system. Table 2.1 contains a list of 10 electrically isolated power systems with a renewable vision and can be found to be similar to the Faroese system in terms of current and future annual generation [>250 GWh,<900 GWh]. The renewable energy shares (RES), types and targets are also included in the table. Archipelagos and islands excluded from the table either have a significantly higher/lower generation, do not have a specific renewable goal and/or are already or plan to be interconnected to the mainland in the nearest future. These are the rest of the SIDS and Clean Energy Islands, the French islands Mauritius and Reunion in the Indian Ocean, the Aegean islands, Malta, Cyprus, the British Shetland Islands, Bermuda, Isle of Man, Guernsey and Jersey, the Oki Islands, Jeju (South Korea), Galapagos (Ecuador) and Tasmania (Australia) amongst others.

The two islands Antigua and Barbuda have individual power systems. There is small penetration of PV panels on Antigua, while Barbuda remains 100% fossil fuelled supplied by a 7.2 MW diesel power plant. The islands have a high potential of wind and solar energy as the average wind speed is around 6.5 m/s - 7.9 m/s and the irradiance 206 W/m^2 - 236 W/m^2 [41]. The

---

[1]European Union

[2]Small Island Developing States as defined by the United Nations Educational, Scientific and Cultural Organization (UNESCO).

potential for hydro power, geothermal and biomass is low, and the potential for ocean energy is unknown. Although the potential for hydro is low, a 10 MW pumped hydro station has been studied in order to balance the system [42]. 10 MW correspond to 25% in ratio of average demand (RAD) according to Table 2.1. IRENA's Renewable Readiness Assessment for Antigua and Barbuda from 2016 [43] proposes that a clear action plan is needed to transit to renewable, but no such plan is publicly available.

Table 2.1: List of archipelagos and islands comparative to the Faroese power system with the annual generation, renewable energy shares (RES), types of renewable and RES targets. *SIDS **EU Clean Energy Island

Archipelago/island	Gen. (GWh)	RES (%)	Types	Target	Sources
Antigua and Barbuda*	350	2	PV	15% in 2030	[42], [44]
British Virgin Islands*	274	1	WP	100% in 2050	[45]
Cabo Verde*	491	17	WP and PV	100% in 2025	[46], [47]
La Palma (Canary Islands)**	281	11	WP, PV and HP	45% in 2025	[48], [49]
Madeira	848	23	HP, WP and PV	50% in 2020	[50]–[52]
Maldives*	658	3	PV and WP	100% in 2050	[53]
Saint Lucia*	400	0	PV	35% in 2020	[54]
San Miguel (Azores)**	440	47	GP, HP and WP	75% in 2018	[55], [56]
Seychelles*	424	2	WP and PV	15% in 2030	[57], [58]
Tahiti (French Polynesia)	518	37	HP and PV	50% in 2020	[59]

The energy potential for hydro, geothermal, ocean and biomass in the British Virgin Islands is unknown, but the potential for wind and solar is high. Necker Island, a privately owned British Virgin Island, is developing a renewable micro-grid consisting of 900 kW of wind power, 300 kW of solar capacity and 500 kWh of storage [60]. Aside from the plans on Necker Islands towards a renewable future, there is no plan on how the British Virgin Islands will reach 100% in 2050 available.

The Republic of Cabo Verde, located in the central Atlantic Ocean, consists of 10 islands. The nine inhabited islands each have an isolated power system. 55% of the electricity demand is on the island Santiago [61]. The resources used to produce electricity on Santiago are thermal power plants, wind, and solar energy [46]. The future potential investments towards a renewable power system in Santiago and the rest of Cabo Verde have been analysed in previous studies. Reference [62] has studied which investments should be made towards 50% in 2020 from an economical and technical perspective. This study shows that on Santiago the solar capacity should be increased from 9 MW to 15 MW (RAD: 29% to 48%), the wind power from 30.6 MW to 48.45 MW (RAD: 99% to 156%) and finally the generation from municipal solid waste should be doubled from 2.5 MW to 5 MW (RAD: 8% to 16%). This would lead to a 57.28% renewable generation according to the simulations software SIMRES, and together with investments on the other islands, the total production in Cabo Verde would be ≥50%. A recent study

[61] analyses Santiago based on the following three scenarios: 1. Business as usual, 2. 100% renewables and 3. 100% renewables with diversified sources. The applied methodology does not consider the intra-daily resource variations, and solar energy is more feasible than wind energy in Santiago. Therefore no investments are made in wind power based on scenario 2. Thus, a diversified structure for renewable power has been introduced in scenario 3, to compensate for the temporal resolution of the model. The optimisation algorithm used was originally developed by [63], and the optimisation has been conducted using the General Algebraic Modelling System (GAMS). The planning period was set to 20 years, and a summary of the results can be found in Table 2.2 together with the plan presented in reference [62].

Table 2.2: Proposed installed capacities (MW) in Santiago, Cabo Verde, according to studies [61], [62].

Year	Pumping	Photovoltaics	Wind	Municipal Solid Waste	RES (%)	Source
Over 20 years	-	360-480	288.8	6.7	100	[61]
2015	20	9	30.6	2.5	45	[62]
2020	20	15	48.5	5.0	57	

A study on the Canary Islands presents possible future energy compositions for each of the islands [64]. In this study the tools MESAP-PlaNet and REMix-OptiMo are combined and used to obtain system transformation pathways and hourly generation and transmission. The study presents scenarios with and without additional subsea cables, and maximum installed generation capacities have been defined. If La Palma remains isolated the capacities will be 224 MW (RAD: 700%) PV, 116 MW (RAD: 363%) onshore WP, 171 MW (RAD: 534%) offshore fixed WP and 26 MW (RAD: 81%) of combined cycle gas turbines (CCGT). With new transmission connections from La Palma to El Hierro, La Gomera and Tenerife, the PV and onshore WP capacity remains the same, but the offshore capacity is reduced to 74 MW (RAD: 231%) and the CCGT to 13 MW (RAD: 41%). The optimal system in 2050 with the new transmission connections is shown in Figure 2.2.

Madeira also has a renewable vision. According to the references found in Table 2.1, the goal was to reach 50% RES in 2020. Case studies of Madeira are found in literature [65], [66]. The decentralised generation requires storage, and Miguel et al. have investigated the need to store energy [65]. The study investigates multiple scenarios with different sizes of battery systems, the highest avoided CO_2 emissions were 3070 tons, and the renewable integration was increased by 1.31 % from the base scenario of 21.02 %. Marcinzinkowski and Barros [66] have applied the tool EnergyPLAN to the system of Madeira, and one of the simulated scenarios imply that with 100 MW (RAD: 103%) of additional PV capacity and 200 MW (RAD: 206%) of additional WP capacity,

the electricity production would be fully renewable if biomass is considered renewable, otherwise the shares are decreased to 77.6%.
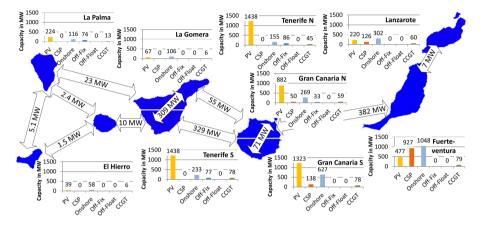
Fig. 2.2: The optimal installed capacity in the Canary Islands in 2050 if new transmission connections from La Palma to El Hierro, La Gomera and Tenerife are considered [64].

In 2015 IRENA published a background report for a renewable energy RoadMap for the Republic of Maldives [67]. The software HOMER has been used to conduct parts of the analysis. According to the study the potential wind power capacity is 20 MW, while the potential for PV is 24 MW in the region of Greater Malé, but the grid stability limit (unspecified) only allows 15 MW of PV and no WP. The capacity limit can be increased by interconnections. Additional regulating capabilities from inverters, battery systems etc. have not been considered in this study. Liu et al. [68] present a feasibility study of the water and energy supply systems in the Maldives, and these claim that Maldives have enough renewable resource potential to be self sufficient, i.e. zero input of energy and water.

Reference [69] presents a development of a RoadMap for Saint Lucia towards a more renewable future. The software HOMER has been utilised. The study is conducted based on multiple scenarios ranging from 0% renewable energy production to 75.3% in 2025. The scenario with the highest renewable shares requires 23 MW (RAD: 50%) of solar, 12 MW (RAD: 26%) of wind, 30 MW (RAD: 65%) of geothermal and 19 MWh (25 min) of storage to be installed in addition to diesel.

San Miguel, one of the Azores, has been analysed using a unit commitment least-cost model in GAMS [55]. The renewable shares are already high, but in order to reach the goal of 75% renewable electricity 50-70 MW (RAD: 100% to 140%) of wind power are required.

The installed capacity in the Seychelles is 116 MW (RAD: 242%) nonrenewable, 3 MW (RAD: 6%) solar and 6 MW (RAD: 12%) wind power [57].

The potential for biomass and solar is high, while the potential for wind power is decent.

Tahiti (French Polynesia) is also aiming for a cleaner electricity production, more specifically 50% renewable energy in 2020 [59]. Tahiti reached 37% renewable energy in 2018.

Additional to the islands and archipelagos mentioned in Table 2.1 it can be mentioned that the energy potential in Ometepe, an island with 30000 inhabitants in Nicaragua, has been investigated. Wind power in Ometepe is estimated to be slightly cheaper than the current diesel production, and solar will be cost-effective within 15 years for non-subsidised customers. The study also estimates a potential of 297 MW of geothermal electricity generation. Due to the fact that the energy resources in Ometepe do not complement each other, there is a need for a storage, and for this the potential of pumped storage was investigated to be 1363 MWh, i.e. 52 days of storage compared to the mean demand in 2014. There is also a potential of Biogas in Ometepe, which could possibly replace e.g. firewood for cooking [70]. For islands with connections to the mainland, e.g. Samsø (Denmark), having a penetration of renewable energy is not as difficult as in fully isolated grids. Some islands like El Hierro (Canary), either already have or have a potential of pumped hydro storage, but others that do not have this, must install other types of storage, e.g. hydrogen [71].

The power systems in Porto Santo (Madeira), Mljet (Croatia), Corvo, Graciosa and Terceira (Azores), Sal (Cap Verde) and Malta have been modelled using the software H2RES [71], [72], which has a hydrogen module. This tool is developed for islanded systems. It optimises the operation, not the investment. Results from the Porto Santo study case in a scenario where the production is 100% renewable, and the generation consists of wind and solar, show that capacity of 10 MW wind power and 20 MW of solar power is needed to meet the demand together with hydrogen storage. 18 scenarios are tested in H2RES in the study case of Mljet. These results show that distributed generation is a viable solution for Croatian Islands. It is however illegal to install wind turbines on Croatian Islands, so these islands must rely on other renewable generation like solar power to reach 100% renewables.

A research study based on the Greek island Sifnos, states that in small isolated systems, the potential of reaching a 100% renewable production depends on the available energy resources and the possibilities of large storage capacities [73]. Another study based on the remote off grid area Rafsanjan in Iran, states that the best economical solution in the study case is to have a wind/diesel/battery based system. The other mixtures tested were: PV/wind/diesel/battery, PV/diesel/battery, and diesel alone [74]. A review on the renewable energy utilisation in 14 selected islands can be found in reference [75]. For further specifications on the different islanded systems, the reader is advised to read the cited literature, i.e. references [44] to [75].

2.2.2 FAROESE STUDIES

The previous Faroese studies are divided into two sections, first studies on the resource potential followed by studies on the energy mixture.

Resource Potential

The wet and windy climate in the Faroe Islands is a great potential for renewable energy. Climatological standard normals for the country are described in reference [76]. The precipitation exceeds 0.1 mm up to 300 days/year, and 10 mm over 100 days/year in various places. In the capital, Tórshavn, the average annual precipitation is 1284 mm, but there are great variations around the country. These depend mostly on the orography. The lowest average precipitation, 823 mm annually, is experienced at the most western island, Mykines. In Hvalvík, a village on Streymoy, the annual precipitation reaches almost 3300 mm. It is possible to expand the hydro power production significantly, but due to environmental concerns, it has been decided not to do this. According to [77], the annual production from hydro power could be expanded with additional 190 GWh, compared to 108 GWh produced by hydro power in 2018. In other words, there is a potential to almost triple the hydro power generation.

According to the climatological standards [76], the average wind speed is 4.5 m/s - 6 m/s in the summer and 6.5 m/s - 10 m/s in the winter. Wind speeds above 40 m/s and gusts above 70 m/s are not uncommon in the autumn and the winter. A meteorological mast next to the Húsahagi wind farm has measured gusts up to 68 m/s [6]. A model based study [78] indicates that the annual average wind speeds are above 7.5 m/s all over the country. The high average wind speeds result in a high wind turbine capacity factor. The capacity factor at Húsahagi varies between 0.4 and 0.45 from year to year. According to inhouse estimations, an additional wind power capacity of 200 MW could be installed at suitable locations in the Faroe Islands.

The solar resources in the Faroe Islands are limited, due to the high altitude and cloud coverage. A normal year in terms of sunshine hours in Tórshavn is 840 hours. There are close to no experiences with extracting solar energy for electricity production in the Faroe Islands, but the few installed systems have shown that annual full load hours above 600 are achievable.

Tidal streams are a predictable source of energy, contrary to other renewable resources. The peak tidal streams around the Faroese isles are above 3.5 m/s at various accessible sites [79]. In addition to the predictability, the advantage with tidal energy in the Faroe Islands, is that there is a phase shift between when the tidal currents turn at the different straits and fiords. Thus, even though the tidal currents in a strait turns every sixth hour, which results in 0 m/s, this does not occur simultaneously at all straits. Therefore, tidal en-

ergy can be used as a base load production if generation units are placed at different fiords and straits. A tidal stream model based on insitu measurements has been developed for the Faroe Islands [79]. According to this model the power in the tidal streams between the islands is up to 2 GW, and 209-780 MW if only locations with depths higher than 40 m and peak velocities higher than 2.5 m/s are considered. However, a maximum of 15% of the available power can be extracted before it affects the tidal streams significantly [80].

As described in the previous paragraphs, the potential for renewable energy is high in the Faroe Islands, based on a diversified mix of resources. The monthly averages of the following four sources: sun hours, precipitation, wind speeds and tidal stream velocities are compared in the upper plot of Figure 2.3 [6], [81]. It is clear that even though the solar resource is relatively low, it can become interesting when combined with the other resources. During the summer, when the wind and hydro potential is relatively low, the potential for solar is relatively high. This means that if photovoltaic power is installed, it will reduce the necessity of the storage capacity. When analysing the potential on an hourly basis, the complementary is not as visible, see the lower plot on Figure 2.3, as there are clearly periods with low resource potential. Tidal is the most predictable and constant resource, although the tidal stream varies by a factor of 2 over the spring neap cycle [81].
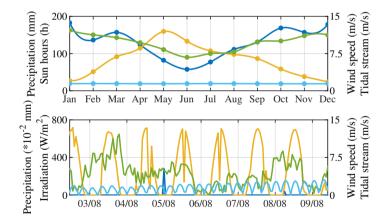
Fig. 2.3: The potential for hydro (blue), photovoltaics (yellow), wind (green) and tidal (cyan) energy on a monthly [6] and hourly basis (2017) [81]

Energy Mixture

There are several studies which investigate the future Faroese power system from different aspects, some of these studies have been briefly reviewed in previous publications [81]–[83]. The first study focusing on a RoadMap towards 100% renewable electricity in 2030 can be found in reference [6]. This

study used the software HOMER. The proposed expansion plan includes wind, photovoltaics and tidal power. The study concludes that without storage the proposed expansion plan would bring the renewable shares up to 85%, but with a pumped storage system implemented in 2026, the renewable shares would reach 100% in 2030. An article published in 2018 states that it is economically interesting to reach an annual renewable production in the Faroe Islands of over 90% based on mainly wind, solar and pumped hydro. It also states that smart grid technologies have to be implemented, when going above 95% RES, without any elaboration on which smart grid technologies have been considered. This is a preliminary study, and more accurate results can be obtained by improving the pumped hydro model, siting of the wind turbines, new demand profiles considering a lower energy usage in buildings etc. [84].
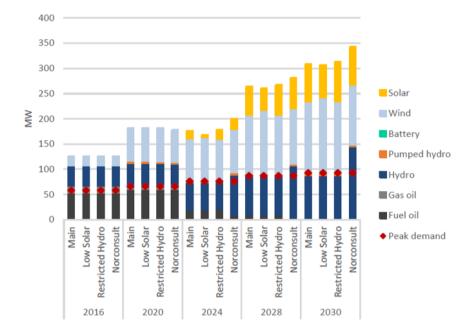
The power system of Suðuroy has been analysed using HOMER by Skeibrok et al. [85]. This study shows that a 100% renewable power system without a cable connection is not feasible as the potential pumped storage system is too small to balance the future system fully. A study on a pumped storage in Suðuroy does however show that the production costs could be lowered significantly with a pumped storage system and a few wind turbines [86]. This pumped storage system is also analysed in [87]. The feasibility of flow batteries in the Faroe Islands has been analysed, and the study states that it could be feasible, but depends highly on the oil prices [88]. A study on the most western island Mykines shows that a more renewable system with fuel cells and wind turbines is more expensive than the existing diesel system [89].

In 2018 an extensive study of the path towards 100% renewables in the Faroe Islands was published by SEV, the local energy authority ORKA and the company Dansk Energi. 12 technical reports and notes were published based on this study [90]–[101]. A brief overview of the study can be found in reference [90]. A note on the feasibility of an subsea cable connection to other countries, especially Iceland, but also Shetland is found in [91]. It is technically possible, and depending on the amount of transmitted power also economically interesting. The results of one previous study showed that the cost of energy through a cable would be 0.70 DKK/kWh with an import of 500 GWh/year, which is more than the actual demand. By comparison wind energy at this time was produced for 0.35 DKK/kWh and production from heavy fuel is >1 DKK/kWh [102]. Another study investigated an undersea cable connection between the Faroe Islands, Iceland and Shetland, with a further connection to the European grid. It is stated that if a connection is made between Iceland and the United Kingdom, the cable would pass through Faroese oceans, and it would therefore be possible to connect the Faroe Islands to this connection [103]. Cable connections to other countries are however not being considered by SEV or the government, as being self-

sufficient regarding the energy sector is more attractive [104].

The study also covered demand projections of the future electricity demand considering an electrification of both the heating and transport sectors [92] based on the coalition agreement 2015 [7], the necessity of storage based on the electrification level and the amount of solar and tidal [97], the possible flexible energy demand [94], and finally 16 scenarios considering the projected demand and different power compositions have been simulated and analysed [93]. The feasibility of alternative production forms, [98], in this case tidal power, and different types of storage [99] have also been considered and discussed.

A thorough investigation of how pumped storage together with solar and wind can be used to obtain a 100% renewable production by 2030, was conducted [96]. This study modifies the already existing hydro systems into pumped storage. The model is based on weather data from several years. This results in a solution that secures a 100% renewable energy balance by 2030, even during dry years with limited hydro resources. The consequences of this are large and expensive systems required to store energy for longer periods of time, that will be unnecessary for years with normal precipitation. The investigation included scenarios where the variable energy sources were grid connected, but also where the sources were off grid and solely used for the pumped storage system. The latter resulted in great energy loss due to the fact that the wind turbines would have to be curtailed more when they operate off grid. This specific study recommends a hydro storage in 2030 of 32.3 GWh. However, other studies with different assumptions and restrictions propose other sizes.

Another analysis was conducted using Balmorel [95]. Balmorel is a least-cost-path optimisation tool, and one of the tools reviewed in [34]. Balmorel has perfect foresight, meaning that it from day 1, knows how much energy must be stored to ensure an energy balance throughout the year. Three scenarios are investigated and compared to the study mentioned in the previous paragraph. One main scenario, one with low solar production and one where there were restrictions on the regulation done by hydro. The three scenarios result in similar amounts of installed capacities of the different technologies, see Figure 2.4 [95]. According to the study, wind and solar should be the dominant technologies together with hydro. In the three different scenarios the recommended hydro storage in 2030 varies between 11.1 GWh and 15.1 GWh, i.e. less than half of what the previous study recommended. The disadvantage with this study is that only one year with normal weather conditions is considered, therefore the recommended expansions are not necessarily enough to reach a 100% renewable production during a dry year, and thus, thermal units will have to be used for backup. As 37 MW at Sundsverkið, see subsection 1.2.2 on page 10, consist of dual fuel units, the fuel used could be carbon neutral. The normal weather conditions are defined as the year

with the median energy resources available. The study gives a better under-
standing of the optimal energy mixture, but some aspects can be improved,
e.g. the biogas system is excluded and the solar data is based on satellite
information.

Fig. 2.4: Generation capacities for the 4 scenarios for 2016, 2020, 2024, 2028 and 2030. Peak
demands are indicated. The orange pumped hydro technology represents the 'pumped hydro'
project in only one place, the other hydro expansion are all shown as dark blue 'hydro' [95].

Table 2.3 compares the proposed generation capacities in the most exten-
sive previous studies of the whole system, i.e. references [6], [95], [96]. Based
on references [90]–[101] a RoadMap has been proposed. The capacities in the
RoadMap are included in Table 2.3. The wind and PV power capacities in
the RoadMap [101] are almost equal to [95], while the RoadMap's pumped
storage capacities are equal to [96]. The needed size of reservoir is however
not included in the RoadMap. In [6] the wind, PV and pumped storage ca-
pacities are lower than in the RoadMap, but a tidal power capacity of 60 MW
is included. The pumped storage capacities in [6] are however closer to the
RoadMap and [96] than [95] is.

The RoadMap is shown in Figure 2.5. For the first 5 years a total of 68 MW
of wind power, 10 MW of solar power and pumped hydro storage of 6 MW
pumping and 4 MW turbines will be installed. From 2024 to 2030 80 MW of
wind power, 70 MW of solar and pumped storage with 140 MW pumping
and 80 MW turbines should be installed. The less developed technologies,

e.g. tidal energy, will have to be reconsidered as time passes. A cable connection to Iceland will not be investigated further according to the proposed RoadMap.

Table 2.3: Summary of most extensive expansion planning studies for the Faroe Islands towards 100% renewables. The table includes required investments in different technologies. Excluding the PS in Suðuroy, as not all studies include this.

Source	WP (MW)	PV (MW)	TP (MW)	Pumped storage Turbines (MW)	Pumps (MW)	Reservoirs (GWh)
[6]	72	30	60	70	100	25
[95]	141	75	-	48	58	7
[96]	235	39	-	105	140	26
[101]	138	72	-	105	140	-
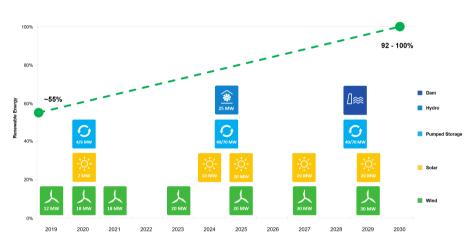
Fig. 2.5: The current road map to a renewable electricity sector by 2030 [101].

In order to improve previous expansion planning studies, the economically optimal energy mixture has been investigated in three publications [81]–[83]. First a simple optimisation algorithm was developed [82], which optimised the investments towards a 100% renewable electricity sector by 2030. The biogas plant, which had been excluded from previous study was considered, and the resource data used to predict the production from PV panels was improved compared to other studies. In reference [95] a Balmorel model of the Faroese power system was developed, and in reference [83] this model was improved by adding the biogas plant and new solar resource data. The contributions from [82], [83] do however meet the requirements of obtaining a realistic and detailed expansion plan for the future Faroese power system. The transmission capacity has not been considered in previous studies, neither has the exact location of the investments, the space constrains, the varia-

tion in demand and resource profiles depending on the location nor the costs of keeping thermal power plants as emergency backup. However, these aspects have been addressed in [81] and are the basis of the following chapters on the expansion planning.

2.3 PROPOSED METHODOLOGY

Although the focus on expansion planning is high and it is in continuous development, the tools and case studies seem to lack a degree of realisability. The tools and studies typically present either an optimal solution without practical considerations, as plant and cable sizes etc. are increased year by year, while in reality investments are conducted in steps of e.g. a full wind farm. In optimisation studies the exact location of investments is typically ignored, as system models are simplified and aggregated. However, in small isolated system it is possible to identify each suitable investment site with respective resource profiles and maximum capacities, whilst maintaining a reasonable computation time. The study conducted on Cabo Verde [62] does define each relevant site, but here the investments are not optimised.

In order to improve this part of expansion planning, a method was developed in reference [81]. The main idea behind the proposed methodology is to translate results from an existing expansion planning tool, in this case Balmorel, to a realistic RoadMap with specific investment projects. This is done by the steps illustrated in Figure 2.6. The first step is to the define the inputs to Balmorel. The required inputs are policy constraints, details about the specific system model, i.e. capacities, demand, costs and emissions, and finally the site specific investment options, local resource potential, maximum capacities per site and costs. The model is then simulated in Balmorel (subsection 2.3.1), which optimises the dispatch and investments simultaneously. From the simulations the optimal investments are obtained, which then are translated into specific investment projects and a RoadMap is obtained (subsection 2.3.2). The capacities in the RoadMap are set as committed capacities in Balmorel, and the system is simulated again without any additional investment options. The optimality of the RoadMap is analysed by comparing the economics of the optimal results and the simulation with the RoadMap, as the proposed RoadMap should be close to the optimal solution (subsection 2.3.3). Additionally, the production using the RoadMap has to meet the requirement of a 100% renewable production in 2030.
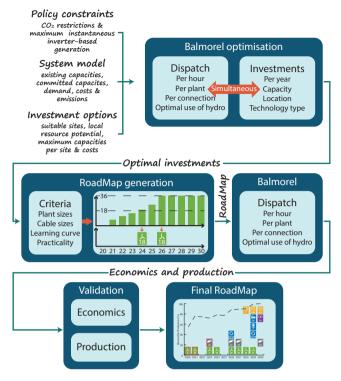
Fig. 2.6: Flowchart of the proposed methodology [81].

2.3.1 BALMOREL

There are, as mentioned previously, multiple tools and models available, which can be utilised for expansion planning. Based on [34] Balmorel was chosen as a suitable tool for this investigation. Balmorel is a partial equilibrium optimisation tool, which optimises the least cost investments annually and the dispatch hourly. It is a open source and transparent tool, which is flexible of new technologies and can be adapted to the specific study case. The disadvantages with Balmorel are that it has perfect foresight throughout a year, and zero foresight across years. This means that the dispatch in Balmorel is optimised to a degree not possible in reality. Due to the zero foresight across years, Balmorel can invest in a lot of wind power in a specific year, without knowing that the capital costs of wind power are reduced significantly the year after. Additionally, Balmorel does not consider the power system operation in details, it can consider unit commitment, but challenges like power system stability are not considered. A thorough review on Balmorel can be found in [105].

The most important Balmorel equations, with regards to this study, are found in Equation 2.1-Equation 2.6, and the parameters from the equations

are found in Table 2.4. Equation 2.1 is the objective function. The parameters considered in the objective function are the generation costs, i.e. variable operation and maintenance (O&M), fuel costs, investment costs in generation, storage and transmission capacities depending on the area/location and fixed O&M costs. The optimisation is subject to meeting the demand (Equation 2.2), the available resource potential (Equation 2.3) and the transmission capacity (Equation 2.4). In order to account for the vision of a 100% renewable generation in 2030, it was necessary to set a policy constraint for the maximum CO_2 emissions, see Equation 2.5. Additionally, a constraint on the maximum allowed instantaneous inverter-based generation have been set Equation 2.6. For further information on the optimisation algorithm, the reader is advised to read [105]–[107].

The output from a Balmorel simulation contains multiple variables. These variables include the generation, transmission, consumption, curtailment, costs, emissions for each location. The results are given in annually and hourly depending on the variable, e.g. investments are given per year, while production is given hourly and annually.

Minimise

$$Z_y = \sum_{g,t} c_{g,t} G_{g,t} + \sum_{g,f,t} c^f_{g,t} F^f_{g,t} + \sum_g (ac^I_g + c^{fix}_g) I_g + \sum xac^I_x I_x \qquad (2.1)$$

subject to

$$\sum_g G_{g,t} + \sum_x (1 - loss) X^{Import}_{x,t} = \sum_x X^{Export}_{x,t} + D_t \qquad (2.2)$$

$$G_{g,t} \leq r^f_t (K_g + I_g) \qquad (2.3)$$

$$X_{x,t} \leq K^x + I^x \qquad (2.4)$$

$$\sum_{g,t} W^f_w F^f_{g,t} \leq T_w \qquad (2.5)$$

$$\frac{\sum_g G^i_{g,t}}{\sum_g G_{g,t}} \leq T_{i,t} \qquad (2.6)$$

Table 2.4: Nomenclature for equations (2.1)-(2.6) [81]

T	Target	g	Technology	F	Fuel consumption
y	Year	G	Generation	K	Existing capacity
a	Area	Z	System costs	W	Emission factor
t	Time	r	Resource	x	Transmission line
c	Costs	I	Investment	X	Transmission capacity
D	Demand	fix	Fixed O&M	i	Inverter based
f	Fuel	w	Emission		

2.3.2 ROADMAP GENERATION

The optimal investments from Balmorel are an input to the RoadMap generation. The criteria set to a realistic RoadMap are that the proposed investments should be conducted in steps of e.g. realistically sized wind farms. Balmorel optimises the investments annually, and thus the size of a wind farm or PV plant can increase year by year, this is however not realistic and should therefore be avoided to the extent possible. Similarly, the cables sizes in the RoadMap should reflect the cables sizes used in the existing 60 kV transmission systems, in this case 44 MW. SEV does not dimension cables for each connection, but uses 44 MW for all new 60 kV connections. Additionally, the fact that the investigated power system is small and each investment in renewable energy has a great impact on the power system operation has to be considered. Thus, it is deemed necessary to account for the learning curve of the power system operators, that have to adapt to the system changes. Therefore, the investments during the first years are smaller, and the time in between the investments is longer. The final criterion is the practicality. The local energy authority makes public tenders for every wind energy project in the Faroe Islands, therefore it is unlikely that multiple tenders will be in the same year.

The flowchart in Figure 2.6 shows an example of the RoadMap generation. The example is from a wind farm with a maximum capacity of 36 MW. In this case Balmorel starts to invest in wind power at this wind farm from 2021, and the capacity then increases until it reaches full capacity in 2026. By 2024 the capacity has reached 20 MW, in the RoadMap it is therefore proposed that the investment in this wind farm is done in two steps, i.e. 18 MW in 2024 and additional 18 MW in 2026. 36 MW in one step is considered to be too much at this stage when the learning curve of the power system operators and thus, the risk of compromising the stability, is accounted for. This example shows how both the plant size and the learning curve has been considered at this specific investment site.

2.3.3 VALIDATION

The final step of the proposed methodology is to validate the proposed RoadMap towards the optimal solution. The capacities in the proposed RoadMap have been used as committed capacities in Balmorel, and the simulation was rerun without any additional investment options. The output variables used for the validation are the production and economics.

The first step of the validation is to check whether or not the production meets the requirement of a 100% renewable production in 2030. The second step of the validation is analyse and compare the economics of the optimal solution to the proposed RoadMap. The RoadMap is not necessar-

ily economically optimal, but it is a realistic and practical oriented RoadMap based on an economic optimisation. The RoadMap should be close to the economically optimal solution, and it is therefore necessary to ensure this by comparing the economic output from the two Balmorel simulations. If both of these parameters can be validated, the RoadMap has been validated.

2.4   CHAPTER SUMMARY

This chapter has presented the state of the art of expansion planning theory with regards to the available tools and models. Power systems of similar sizes with similar visions to the Faroe Islands have been listed and briefly presented, followed by state of the art Faroese studies. Finally some gaps in expansion planning have been identified and a method to improve expansion planning has been proposed. The proposed method combines an economic optimisation with practical considerations and contains a validation as well.

CHAPTER 3
Optimisation of the Future Power System

This chapter presents the economic optimisation used to generate a RoadMap, and thus it addresses the first project objective. First the different scenarios are presented, and then a thorough model description is presented. This is followed by the results of the optimisation and finally a chapter summary.

3.1 INVESTIGATED SCENARIOS

The economically optimal future power system has been investigated through running multiple scenarios in the optimisation tool Balmorel. There are six main scenarios, which consider different technologies, investment sites and restrictions, and 12 sensitivity scenarios, with variations in investment and fuel costs. Each scenario is run from 2020 to 2030, and optimised investments are allowed from 2021 and onward. The aim of investigating multiple scenarios, is to analyse the impact different technologies, restrictions and costs have on the future power composition. Each scenario has been defined in close cooperation with SEV. The six main scenarios are described in subsection 3.1.1 and descriptions of the 12 sensitivity scenarios are found in subsection 3.1.2.

3.1.1 MAIN SCENARIOS

A short description of the main scenarios and their number can be found in Table 3.1. The reference scenario (#1) is defined as a 100% renewable scenario in 2030 with investment options in solely mature technologies. The generation technologies considered are wind power and photovoltaics. In terms of storage both a pumped storage system on the main grid and batteries are included as investment options. Additionally, the model is allowed to invest in transmission capacity. All other scenarios, both main and sensitivity scenarios, are variations of the reference scenario. There is only one change made from the reference scenario to the other scenarios, e.g. removal of one restriction, reduction of one investment cost etc.

Table 3.1: A list of the main scenarios. *See Figure 3.1.

#	Description
1	Reference scenario
2	With tidal power as an investment option
3	With the option to burn biofuel at an existing thermal power plant
4	Without CO_2 emission restriction
5	With a committed pumped storage system in region 7*
6	With an additional wind power investment site

The only difference between the reference scenario and scenario #2 is that the model is allowed to invest in tidal energy. The technology is still in the development phase, but the motivation behind this scenario is to clarify the impacts tidal energy technology could have on the overall energy mixture.

In scenario 3 the model has the option to burn biofuel at an existing thermal power plant, in addition to all the options considered in the first scenario. This scenario is interesting to investigate; because, if possible and economically viable, burning carbon neutral fuels at existing power plants could be an alternative to investing in expensive storage and over capacity of cheap intermittent renewable energy.

In the fourth scenario, the restriction on the CO_2 emissions has been removed, and thus; the model only invests in renewable energy if it is financially feasible. The results of this scenario show how renewable the production can be, whilst still being the most economically feasible solution.

A pumped storage in the most southern island Suðuroy has been discussed and investigated for several years. The configuration of this pumped storage system makes it impossible to optimise the capacities in Balmorel, therefore this system is only included in a separate scenario, i.e. #5. Further details on the configuration of this pumped storage system are given in subsection 3.2.5.

The final scenario (#6) includes an additional investment site for wind power. This site is not included in the reference scenario, because local politicians are against building a wind farm at this exact location, as they plan to build an airport close by. Since this site is very suitable for wind power, possible the best in the country, there is still interest in investigating the potential of the respective site, and analyse the difference it could make in the overall power composition.

Scenarios 5 and 6 do have more local interest than technical, and therefore the analysis focuses on the first four scenarios. Scenarios 1-5 were investigated and published in reference [81]. Scenario 1 and 2 are also compared and presented in [108].

3.1.2 SENSITIVITY SCENARIOS

In order to determine how sensitive the results are to an increase or decrease of the investment costs and fuel costs, a sensitivity analysis has been conducted. This sensitivity analysis has been conducted by running the reference scenario with 20% higher and lower investment costs, changing one cost at the time. A study of the South West Interconnected System of Western Australia [109] similarly conducted a sensitivity analysis using 20% higher and lower costs. The costs changed in the Australian study were the wind power costs and the discount rate. The sensitivity scenarios run in this study are listed in Table 3.2.

Table 3.2: A list of the sensitivity scenarios. Cheap is 20% reduction in investment or fuel costs and expensive is a 20% increase in investment or fuel costs. *See Figure 3.1.

Name	Short description	Name	Short description
cWP	Cheap WP	eWP	Expensive WP
cPV	Cheap PV power	ePV	Expensive PV power
cPS	Cheap PS system in region 1*	ePS	Expensive PS system in region 1*
cBS	Cheap battery systems	eBS	Expensive battery systems
cFU	Cheap fuel	eFU	Expensive fuel
cCA	Cheap transmission cables	eCA	Expensive transmission cables

Through the sensitivity analysis, a range of optimal capacities for each technology will be obtained. This range represents how sensitive the results of study are to the investment costs.

3.2 MODEL DESCRIPTION

The following sections will describe how the power system and its respective technologies have been modelled, together with the investment options considered in the study.

The foundation of the optimisation is the input data. Thus, a data set, which represents the behaviour of the system accurately is a necessity, in order to achieve realistic results. The data used in this optimisation has been chosen based on the following two criteria:

- The data should represent an average weather year, and not a year with abnormally high precipitation, low wind speeds, low irradiation etc. This will assure that the calculated potential production from the different energy types realistically represents an average year.

- The weather and demand data has to be from the same year, as it is known that there is a relationship between the weather and the consumption, as shown in e.g. [110].

45

The resource potential for the different renewable technologies is tabulated in Table 3.3 for 2014-2018. The first row contains the actual hydro production in GWh. It shows that 2017 is the year with the median production for the years considered. The logged potential wind production at existing wind farms expressed in FLH show that 2018 was the median year in terms of wind energy. The final variable in the table is the measured solar irradiation in the capital. 2017 is the median year for solar irradiation alike the hydro production. The tidal streams are independent of the weather, only linked to the gravitational force of the moon and the sun, and thus not included here. The year 2017 has been chosen as the basis of all input data, as it is the median year for both hydro and solar, and that the wind potential in 2017 is only 0.3 % higher than the median wind year 2018.

Table 3.3: The production resources available from 2014 to 2018 for hydro, wind and solar energy. Median year is in bold.

Year	2014	2015	2016	2017	2018
Hydro Production (GWh)	116	127	103	**107**	104
Potential Wind Production (FLH)	3724	4036	3233	3667	**3655**
Solar Irradiation (kWh/m^2)	714	719	745	**729**	759

3.2.1 TRANSMISSION SYSTEM

The Faroese power system is typically investigated as one or two regions; the main grid and Suðuroy. This is also the case for previous Balmorel studies [83], [95]. In this investigation, also published in [81], the Faroese power system has been modelled as 7 regions, see Figure 3.1. The main grid is divided into 6 regions (R1-R6), while Suðuroy is the 7th region (R7). The smaller electrically isolated islands are neglected, as they account for only 0.2% of the total consumption. The definition of the 6 regions in the main grid is based on the structure of the 60 kV transmission system, and the connections represent the actual transmission lines and cables. Hence, the model reflects how the system is operated. Balmorel can only consider transmission capacities as technical constraints and investment options between regions. This means that if the main grid is modelled as only one region, the model does not consider the actual transmission capacity between the locations of the power plants, which can be a limiting factor for how much generation capacity should be placed at a certain location. Therefore, the optimisation results, from a model which is separated into regions, are more realistic from a technical perspective, than models without regions.
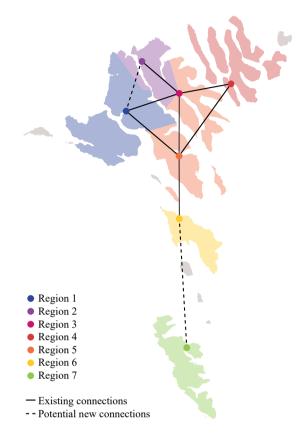
Fig. 3.1: An illustration of the regions in the simulation model.

The demands in R1, R2, R4, R5 and R7 can be supplied by the production in each respective region to a large extent, but it is also necessary to exchange energy. Region 3 represents a connection point between other regions, and does not have a demand nor a generation. There is a demand in R6, but no production, and hence this demand is fed by the production from the main grid. R6 could, due to the lack of production, be a part of R5 in the model. However, the existing transmission capacity between R5 and R6 is a potential bottleneck in the grid. Especially when R7 will be connected to the main grid and when wind power will be installed in R6 in the future. R6 has to be a separate region, if regards should be taken to the potential bottleneck connection R5-R6, since transmission capacities only can be considered between regions in the economic optimisation model.

There are transmission and distribution losses in the power system. This can be seen by comparing the production at the power plants and consumption at the electricity meters, see Table 3.4. The total losses have been around 6% since 2015. Prior to this, the electricity meters were read manually be-

tween November and January. Now the meters are read automatically every day, and the consumption values from 2015 and forward are therefore exactly one calendar year. The varying reading times in the past seem to have affected the calculated losses, as the losses from 2009 to 2014 vary between 4% and 8%.

Balmorel can consider transmission losses and distribution losses. If a distribution loss is defined, this is simply added to the demand. By defining a transmission loss, the loss is calculated based on the energy transmitted from one region to another. In this study distribution and transmission losses of 4% and 2% respectively have been assumed.

Table 3.4: The production, consumption and losses for the whole country and for the regions considered in this investigation. The numbers are rounded to GWh and integer percentages.

	2009	2010	2011	2012	2013	2014	2015	2016	2017	2018
Production (GWh)	276	280	274	292	293	305	314	317	334	352
Consumption (GWh)	259	262	258	268	282	291	295	298	315	329
Losses (%)	6	7	6	8	4	5	6	6	6	6

An increasing demand and thus production will likely require investments in transmission capacities between the regions, depending on the placement of the power plants and the demand. Table 3.5 (upper right corner) contains information about the existing transmission capacities between the regions, and between which regions transmission cables are an investment option (lower left corner). All existing connections except from R5-R6 have a capacity of 35 MW. The 35 MW connections are the following: R1-R3, R1-R5, R2-R3, R3-R4, R4-R5 and R3-R5. The transmission capacity between R5 and R6 is 10 MW. The existing and potential connections are also shown on Figure 3.1. The investment options are based on SEV's plans for the future transmission grid [111].

Table 3.5: The existing transmission capacity (MW) between the regions is shown in the upper right corner. The lower left corner shows whether or not the model is allowed to invest in transmission capacity between the different regions. (✓=Allowed)

	R1	R2	R3	R4	R5	R6	R7
R1		-	35	-	35	-	-
R2	✓		35	-	-	-	-
R3	-	✓		35	35	-	-
R4	-	-	✓		35	-	-
R5	✓	-	✓	✓		10	-
R6	-	-	-	-	✓		-
R7	-	-	-	-	-	✓	

Costs

The average investment cost of 60 kV onshore transmission cables is estimated to 160 EUR/m by SEV's grid department. This cost includes material, excavation and salaries. A cost per MW is required in the simulation model. The new 60 kV transmission cables used in the Faroe Islands can transmit a maximum of 44 MW, and the length of the cables can be estimated, thus a cost per MW can be obtained. The investment costs per MW for onshore transmission cables are summarised in Table 3.6 and vary between 61 818 EUR/MW and 145 455 EUR/MW depending on the length of the cable.

A 10 MW subsea cable between R6 and R7 has been projected, and the investment cost has been estimated to 18 670 000 EUR, i.e. 1 867 000 EUR/MW.

Table 3.6: Estimated cable lengths and investment costs of transmission cables.

Distance	Cable length (km)	Investment cost (EUR)	Cost/capacity (EUR/MW)
R1-R2	40	6 400 000	145 455
R1-R5	24	3 840 000	87 273
R2-R3	18	2 880 000	65 455
R3-R4	17	2 720 000	61 818
R3-R5	35	5 600 000	127 273
R4-R5	52	8 320 000	189 091
R5-R6	29	4 640 000	105 455
R6-R7	40	18 670 000	1 867 000

3.2.2 DEMAND

Annual and hourly demand profiles have to be defined for each region. To some degree the load profiles vary from region to region, as the fishing industry dominates the total demand in some regions. Since the model is in seven regions and previous studies have used one or two regions, new demand projections were required in this analysis.

Historic Annual Demand

The majority of the electricity demand in the Faroe Islands is normal demand, which in this study is considered to be everything except from heating and transport. However, the number of heat pumps and electric vehicles is increasing. The second column in Table 3.7 contains the estimated total number of heat pumps in the Faroe Islands. The second row contains the assumed distribution of the heat pumps between the regions. These numbers based on available data about the locations of the ground source heat pumps,

and is assumed to be representative for the distribution of all types of heat pumps in the Faroe Islands. The data related to the heat pumps have been obtained from the Faroese Energy Authority. It can be seen that the majority of the heat pumps are located in R5, which also is the region with most households.

It can be assumed that a regular household in the Faroe Islands uses around 20 MWh for heating annually [112] and that installed heat pumps have a coefficient of performance factor (COP) of 4 [93]. This corresponds to a 5 MWh consumption of electricity. It is therefore assumed that each heat pump uses 5 MWh annually.

Table 3.7: The assumed number of heat pumps in each region from 2009 to 2018 based on the the total number of heat pumps, and the distribution of the ground source heat pumps. *Assumptions.

Year	Total	R1 (12.7%)	R2 (1.3%)	R4 (9.1%)	R5 (72.8%)	R6 (1.6%)	R7 (2.6%)
2009	238	30	3	22	173	4	6
2010	360	46	5	33	262	6	9
2011	550	70	7	50	400	9	14
2012	605	77	8	55	440	9	16
2013	678	86	9	61	494	11	18
2014	787	100	10	71	573	12	20
2015	*858	109	11	78	625	13	22
2016	*929	118	12	84	676	14	24
2017	1000	127	13	91	728	16	26
2018	*1100	140	14	100	801	17	28

The number of electric vehicles in each region has been obtained from the Faroese Vehicle Administration, see Table 3.8. There are no electric vehicles in R2, and only 1 in R6 and R7. 77 of the EVs, that is 77.7 %, are in R5. The average driver in the Faroe Islands drives 15000 km/year, and with an consumption of 0.2 kWh/km, the annual electricity consumption of an EV can be estimated to 3 MWh [93]. As of March 1st 2022 there are 656 EVs in the Faroe Islands.

The annual demand at the >26000 electricity meters in the country is known, and likewise is the location of the meters. Hence, the demand for each region can be obtained. The historic demand in each region can be seen in Table 3.9. In this table the assumed consumption from the EVs and HPs has been subtracted from the demand measured by the electricity meters. The last row shows that the normal demand has on average increased between 0.2% and 3.6% in each region, based on the past 2009-2018 years.

Table 3.8: The number of electric vehicles in each region from 2011 to 2018 based on the Faroese Vehicle Administration.

Year	R1	R2	R4	R5	R6	R7
2011	0	0	0	3	0	0
2012	0	0	0	3	0	0
2013	0	0	0	6	0	0
2014	0	0	1	8	0	0
2015	0	0	2	10	0	0
2016	0	0	3	15	0	0
2017	0	0	3	30	0	0
2018	11	0	9	77	1	1

Table 3.9: The electricity consumption (rounded to GWh) in each region from 2009 to 2018 based on the electricity meters and extracting of HP and EV demand.

Year	R1	R2	R4	R5	R6	R7
2009	32	9	30	163	6	24
2010	31	9	30	166	5	24
2011	31	9	30	163	5	23
2012	31	10	33	165	5	27
2013	25	10	34	171	5	33
2014	26	10	34	177	4	35
2015	29	10	37	173	5	32
2016	31	10	37	179	5	29
2017	34	10	37	197	6	25
2018	42	10	40	198	6	27
Average increase (%)	3.6	0.9	3.4	2.3	0.2	2.0

Projected Annual Demand

The demand prognosis is an influential factor in the expansion plans of the future power system. Although new projections are required, the approach is similar to previous studies. This means that the demand is separated into three part; traditional, transport and heating demand. This is due to the fact that the annual demand increase in these three categories is assumed to differ from each other, and that the demand profiles are different. It is assumed, that the normal demand will increase with the same pace as it has over the past 10 years (2009-2018). The average increase in each region was presented in Table 3.9. The plan is to build new fish factories in region 7, which will have a high demand relative to the total demand in the region. This demand

is not included in the historic increase in R7, therefore in order to account for this additional demand increase a constant demand of 1 MW and 2 MW is added from 2020 and 2023 respectively.

The 100by2030 vision considers a full electrification of the heating and transport sectors. It is therefore necessary to make assumptions on how the electrification of these two sectors will occur. First of all, the population is increasing and so are the number of households. Table 3.10 contains the number of households in each region from 2009 to 2017. The numbers have been obtained from Statistics Faroe Islands. The number of households has increased between 0% - 1% over the past nine years in the defined regions. This increase is assumed to continue.

Table 3.10: The number of households in each region from 2009 to 2017 based on Statistics Faroe Islands.

Year	R1	R2	R4	R5	R6	R7
2009	1933	561	1895	9714	476	1742
2010	1939	572	1900	9481	480	1731
2011	1956	577	1908	9636	474	1712
2012	1963	575	1911	9767	470	1715
2013	1970	572	1934	9904	471	1730
2014	1980	579	1934	10037	469	1720
2015	1986	595	1961	10233	470	1730
2016	2024	603	1977	10374	481	1752
2017	2060	608	1995	10499	476	1749
Average increase (%)	0.8	1.0	0.6	1.0	0.0	0.1

Similarly the number of personal cars is increasing. Statistics of the personal cars in each region from 2009 to 2018 have been obtained from the Faroese Vehicle Administration. The increase that varies between 1.1% and 2.9% annually, is assumed to continue.

A 50% electrification of the heating and transport sectors by 2025 has been set as a set point in the electrification pace. A 50% electrification of the heating sector by 2025 was one of the goals in the coalition agreement from 2015 [7]. The number of new HPs and EVs pr. year from 2019 to 2025, and 2026 to 2030 has been defined based on this set point. These numbers can be seen in Table 3.12. In other words a linear increase is assumed from 2019-2025, and from 2026-2030, where the later has a higher slope.

Table 3.11: The number of personal cars in each region from 2009 to 2018 based on the Faroese Vehicle Administration.
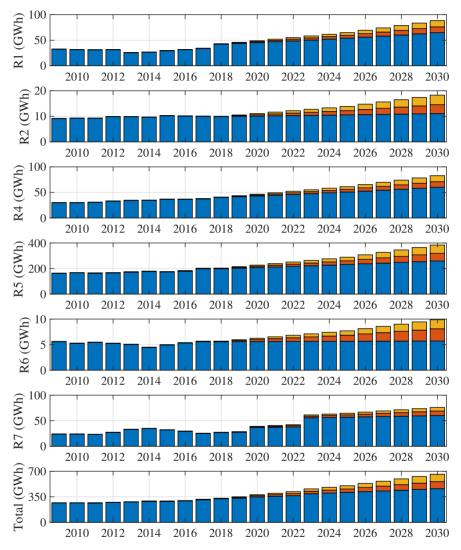
Year	R1	R2	R4	R5	R6	R7
2009	2266	739	2264	12171	477	1775
2010	2238	748	2251	12223	467	1766
2011	2298	751	2240	12299	465	1770
2012	2333	760	2266	12509	458	1778
2013	2393	755	2305	12813	456	1836
2014	2468	760	2381	13207	475	1860
2015	2518	795	2480	13722	490	1891
2016	2695	848	2603	14337	491	1940
2017	2809	872	2748	14954	512	1964
2018	2919	925	2877	15595	524	1994
Average increase (%)	2.9	2.6	2.7	2.8	1.1	1.3

Table 3.12: The assumed number of new HPs and EVs pr. year in each region.

Region	New HPs pr. year		New EVs pr. year	
	2019-2025	2026-2030	2019-2025	2026-2030
1	137	238	253	464
2	45	73	79	140
4	136	224	247	447
5	697	1249	1341	2454
6	32	48	40	63
7	121	177	156	248

Based on just presented numbers, the future energy demand can be projected. The demand is defined for each region and is separated into the normal, heating and transport demand, see Figure 3.2. The values behind the graphs on Figure 3.2 can be found in Table A.1 in Appendix A. There are significant differences between the demand in each region, but this is reasonable, since the population also varies greatly from one region to another. Region 4 and 5 show a linear increase of the historic data, while the demand in R7 peaks in 2014, which is also when R6 has the lowest demand. The demand in the smaller regions is very fragile to changes. There is for example a fish factory on R7 which almost doubles the demand when in operation, thus the demand on R7 depends on the amount of fish caught. In region 6 and 7 the heating demand is higher than the demand for transport, while it is the other way around in the other regions. This is simply due to the fact that the number of cars per household varies from region to region. Overall,

it can be said that the total demand in 2030 will according to this prognosis be 659 GWh, of which 97 GWh is the heating demand and 102 GWh are the transport demand.

Fig. 3.2: The historic (2009-2018) and projected (2019-2030) demand in each region. The normal demand is blue, heating is red and transport is yellow.

Hourly Demand

An hourly demand profile is required for each region and demand type. This profile is then scaled according to the annual demand. The demand profiles

should also be chosen based on 2017, as there is a correlation between the demand the weather.

The hourly normal demand profiles have been obtained for each region from the electricity meters around the country and are shown on the top plot on Figure 3.3. The patterns of the regions in the main grid (R1-R6) are similar, while R7 differs. As previously stated, the load in R7 has great variations due to the heavy industrial load. The figure shows a clear day/night load in R7 for three days, but in the middle of day 4 there is a significant demand increase, which is likely due to a large fish factory being in operation.

Degree days are a parameter which can be used to estimate the daily heating consumption in houses. By subtracting the daily outside temperature from a dimensioning temperature (i.e. 17 °C [110]) the number of degree days is obtained for one day, see Equation 3.1. Fractions of degree days can also be used, if hourly degree days are desired. These are found by using hourly outside temperatures, and dividing with 1/24. Fraction of degree days have been used to estimate the heat demand in previous studies [82], [83], [95]. However, heating the house is not the only heat demand in a household, as hot water is also needed. The hot water use depends highly on the behaviour of the people in the household, i.e. e.g. the timing and frequency of showers taken. This usage is therefore difficult to predict, and therefore fractions of degree days can be misleading. Therefore, the hourly heat demand in this study is fixed daily depending on the average daily outside temperature, this ensures a higher heat demand in the winter than in the summer. The daily temperatures in each region have been extracted from a weather research and forecasting (WRF) model developed by Kjeller Vindteknikk [113]. The heat demand profiles over a week can be seen on the middle plot on Figure 3.3. There are some slight variations in the demand, and these originate from the small variations in temperature.

$$DD = T_{\mathrm{d}} - T_{\mathrm{o}} \tag{3.1}$$

It is assumed that in EVs in the different regions have the same charging pattern, with the highest load during the night. This is how SEV incentives customers to charge, and it fits well with the Faroese driving pattern. The anticipated charging profile can be seen on the bottom plot on Figure 3.3.
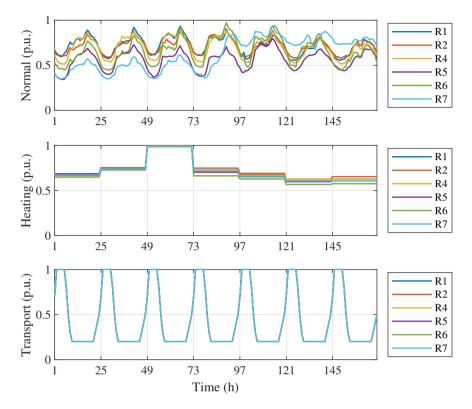
Fig. 3.3: Normalised hourly demand profiles in each region over a week divided into normal, heating and transport.

3.2.3 THERMAL POWER PLANTS

Thermal power plants in Balmorel are modelled using the rated capacity, the fuel type, fuel efficiency and start/end year of operation. The production from the thermal power plants is simply constrained by the rated capacity.

There are, as previously mentioned, eight fossil fuelled power plants in the Faroe Islands and a biogas plant. The five plants on the small islands are neglected in this study. The engines considered in this study are tabulated in Table 3.13. The table contains the plant name, region, rated capacity, fuel type, fuel efficiency and start/end year of operation. Based on internal estimations, it is assumed that all thermal units are available until 2030 or longer. Balmorel cannot decommission the thermal power plants as these will be used as emergency backup in the future.

The generation at the biogas plant is fixed at 1 MW. This is based on information gained from the biogas plant operator.

The model does not see thermal generation as an investment option, but in scenario #3 the model is allowed to burn biofuel using the newest en-

gines at Sundsverkið, 4x9.25 MW. This was also mentioned in the description of the scenarios, see section 3.1. The mentioned engines are dual fuel, and can therefore switch between fuels. This can be modelled in Balmorel using the combined technology option. It is therefore interesting to compare the economic feasibility of an expensive but dispatchable carbon neutral fuel towards inexpensive but undispatchable renewable resources. The exact type of fuel is not discussed here, but the assumption is that this fuel can be classified as carbon neutral and has the same fuel efficiency as fuel oil.

Table 3.13: The plant name, region, capacities, fuel type, efficiencies and start/end year for every thermal unit modelled in Balmorel.

Plant	Region	Capacity (MW)	Fuel type	Fuel efficiency (%)	Start year	End year
Strond	4	3.6	Gas oil	45	1982	2030
Sundsverkið	5	7.85	Fuel oil	42	2001	2030
		7.85	Fuel oil	42	2004	2033
		4.8	Gas oil	45	2015	2044
		12.4	Fuel oil	42	1983	2030
		12.4	Fuel oil	42	1988	2030
		9.25	Fuel oil	43	2020	2050
		9.25	Fuel oil	43	2020	2050
		9.25	Fuel oil	43	2020	2050
		9.25	Fuel oil	43	2020	2050
FÖRKA	5	1.5	Biogas	35	2020	2050
Vágsverkið	7	2.5	Fuel oil	42	1983	2030
		2.5	Fuel oil	42	1983	2030
		4.1	Fuel oil	42	2004	2033
		4.0	Fuel oil	42	2016	2045

Emission

Emission parameters are defined depending on the fuel type. Table 3.14 contains the CO_2, SO_2 and N_2O emissions for fuel oil, gas oil, biogas and biofuel. Additionally, the table contains the renewable shares of the fuels. The emission parameters are taken from the Balmorel fuel dataset, where the fuel type for biofuel to be used in scenario #3 was selected to be biodiesel.

Table 3.14: The renewable shares and the CO_2, SO_2 and N_2O emission for fuel oil, gas oil and biogas.

Fuel type	CO_2 (kg/GJ)	SO_2 (kg/GJ)	N_2O (kg/GJ)	Renewable shares (%)
Fuel oil	78	0.446	0.002	-
Gas oil	74	0.023	0.002	-
Biogas	-	-	0.001	100
Biofuel	-	0.025	0.004	100

Costs

The fixed and variable operation and maintenance (O&M) costs, and the fuel costs are required to model thermal power plants in the Faroese Balmorel model. No investment costs are associated with thermal power, as these are not considered an investment option. The fixed and variable O&M costs for the fuel oil and gas oil power plants are tabulated in Table 3.15. The costs of fuel oil and gas oil are based on experience at SEV and the exact values are taken from the previous Balmorel model [95]. The costs of the biogas plant have been set equal to fuel oil plants. This cost has no affect on the optimisation, as the production is fixed at 1 MW. The O&M costs of biofuel are assumed to be the same as for fuel oil, as the engines are the same.

Table 3.15: The fixed and variable operation and maintenance (O&M) costs for the plants burning fuel oil and gas oil.

Fuel type	Fixed O&M (EUR/kW)	Variable O&M (EUR/MWh)
Fuel Oil	50	8
Gas Oil	141	8

The fuel costs used in this investigation are based on projections from the Danish Energy Agency (Energistyrelsen) [114]. Add-on costs for freight and taxes have been added to the Danish costs. Based on experience these are estimated to 0.95 EUR/GJ, of which 0.37 EUR/GJ are taxes and 0.58 EUR/GJ are freight [95]. The assumed fuel costs are displayed in Figure 3.4 [81]. The biogas fuel costs are, similarly to the O&M costs of biogas, set equal to the fuel oil costs, as the biogas plant with a fixed production does not affect the optimisation. The costs for biofuels are assumptions, due to lack of better data.
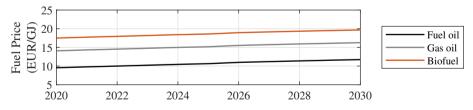
Fig. 3.4: The assumed fuel oil and gas oil costs throughout the simulation period [81].

3.2.4 HYDRO POWER PLANTS

The modelling of hydro power plants with reservoirs requires information about the annual full load hours and the weekly inflow over a year in addition to the capacity specifications and the estimated lifetime of the plants. While

the capacity of the generators are specified with MW, the capacity of the reservoir is defined as the ratio between the reservoir capacity and the annual production.

The weekly inflow can be used during the specific week or saved for future weeks. The storage level is determined by Equation 3.2 [106], where L is the storage level, r is the hydro resource, K is the existing capacity and I is the investments in capacity. The index t represent the time-segment. The storage level is constrained to be between 50% and 100% of the total storage capacity due to technical and environmental constrains.

$$L_{t+1} = L_t + r_t(K + I) - G_t \qquad (3.2)$$

Specific information about the reservoir storages are given in Table 3.16. The hydro power plant Botnur is divided into two, as there are two turbines with separate storages. Some of the reservoirs have two different heights specified; the height above sea level (a.s.l.) and the potential height. The potential height is the height difference between the reservoirs and the turbines. Two reservoirs are connected to Fossáverkið and Botnur 1, and these two reservoirs have the same potential height, because the water from the higher reservoir is tapped to the lower reservoir. The storage capacity for both reservoirs should be included, but the potential energy of the upper reservoir has to be calculated using the same height as the lower reservoir. In 2021 the storage capacity at Strond will increase to 28 MWh, as the dam will be repaired and increased slightly. The increase has been defined as a committed capacity in Balmorel.

Table 3.16: The volumes, heights and storage capacities of the existing hydro reservoirs.

Plant	Reservoir	Volume (m³)	Height a.s.l. (m)	Potential height (m)	Energy (MWh)
Fossáverkið	Vatnið	4 250 000	250.5	224.1	2208
	Lómundaroyra	710 000	224.1	224.1	369
Mýruverkið	Mýrarnar	4 100 000	346.8	239.3	2275
Heygaverkið	Heygadalur	2 100 000	107.5	107.5	523
Eiðisverkið	Eiðisvatn	17 100 000	149.5	149.5	5927
Strond	Strandadalur	46 000	223.5	223.5	24
Botnur 1	Miðvatn	600 000	349.0	243.9	339
	Ryskivatn	420 000	243.9	243.9	238
Botnur 2	Vatnsnesvatn	830 000	180.5	180.5	347

The capacity of the units, the start/end year and the full load hours for the plants are given in Table 3.17. It is estimated that all existing hydro turbines will be available until 2060. The FLH are based on the production in 2017. Both at Botnur 2 and Strond the FLH are expected to increase due to new canals leading water to the reservoir and by increasing the height

of the dam respectively. The increase at Botnur 1 is estimated to 35% and 10% at Strond, both from 2021 and forward. Mýruverkið and Heygaverkið are cascading. When modelling cascading hydro power plants in Balmorel, the FLH have to be based only on the inflow from the associated watershed, not from other plants. It was therefore necessary to calculate the FLH at Heygaverkið, FLH_H, based on the total generation at Heygaverkið, E_H, the generation at Mýruverkið, E_M, the heights of the two reservoirs, h_H and h_M, and the turbine capacity at Heygaverkið, P_H, see Equation 3.3.

$$FLH_H = \frac{E_H - E_M \frac{h_H}{h_M}}{P_H} \tag{3.3}$$

Table 3.17: The capacities, start/end year and full load hours the hydro power plants.

Plant	Capacity (MW)	Start year	End year	Full load hours
Fossáverkið	2.1	1953	2060	3652
	4.2	1956	2060	
Mýruverkið	2.4	1961	2060	5295
Heygaverkið	4.9	1963	2060	1536
Eiðisverkið	14.0	1987	2060	2594
	7.7	2012	2060	
Strond	1.4	1998	2060	1686
Botnur 1	1.0	1965	2060	1154
Botnur 2	2.0	1966	2060	1642

The weekly inflow is assumed to have the same profile as the weekly hydro production. This is considered a reasonable assumption since overflow only occurs a couple of times annually. The normalised inflow profiles can be seen on Figure 3.5. From the figure it can be seen that the inflow at Fossáverkið and Strond is zero for several weeks, and that is because the plants has been out of operation during that period, and the inflow is calculated based on the production. Although this is unfortunate, it is realistic representation, because the units are taken out of operation regularly for maintenance etc.
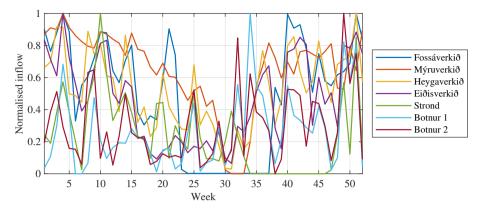
Fig. 3.5: The normalised inflow for Fossáverkið, Mýruverkið, Heygaverkið, Eiðisverkið, Strond, Botnur 1 and Botnur 2.

Costs

The variable O&M costs for hydro plants are negligible, but there is a fixed O&M cost, which is 50 EUR/kW. The model is not allowed to invest in pure hydro power capacity, and thus no investment options or costs are presented here. The model is however allowed to invest in pumped hydro storage, and these costs are presented in subsection 3.2.5.

There are no fuel costs associated with hydro, but in order to optimise the dispatch of hydro energy when the inflow is known for the whole year, a water value, i.e. a fictive price is determined through the optimisation algorithm. This value is based on how much is gained or lost by using hydro at a certain hour. A high water value indicates that the storage level in the reservoir is low, and a high storage level results in a low water value. Figure 3.6 [106] illustrates the impact of the water value. When the water value is higher than the power price, other energy resources will be prioritised before hydro.
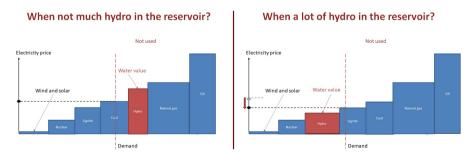
Fig. 3.6: Illustration of the water value [106].

3.2.5 PUMPED HYDRO STORAGE SYSTEMS

Transforming the existing hydro power plants in region 1 and 7 into pumped storage (PS) systems, are considered the best options for pumped storage in the Faroe Islands. The two potential pumped storage systems are shown on Figure 3.7. These transformations will require investments in pumping capacity, additional turbines and possibly expansions of the reservoirs. The potential pumped storage system in R1 would utilise the cascading hydro plants, i.e. Mýruverkið and Heygaverkið. The water that is used to produce at Mýruverkið is reused in Heygaverkið, as it flows through the turbines at Mýruverkið and into the reservoir Heygadalur. By installing a pumping capacity to pump water between the two reservoirs, Heygadalur and Mýrarnar (Figure 3.7a), a pumped storage system can be obtained. The maximum reservoir capacity at the specific location has in previous studies been set to 2.62 GWh and 25.10 GWh for Heygadalur and Mýrarnar respectively [96]. These maximum capacities are used as an upper limit for the allowed investments in reservoir capacities in region 1. It was mentioned previously that the storage level of the reservoirs can be regulated between 50% and 100%, and this is of the initial reservoir size. All additional capacity invested in can also be regulated.

The only difference between modelling a pumped hydro storage system and hydro power plants, is that a loading/pumping capacity with a round-trip efficiency of 70% is added to the plant. The generation, pumping and reservoir capacities at Mýruverkið and Heygaverkið can all be optimised in this study.

(a) PS in region 1 (Mýruverkið/Heygaverkið).

(b) PS in region 7 (Botnur).

Fig. 3.7: The potential pumped storage sites.

The potential pumped storage system in R7 is more complex to model in Balmorel. As previously mentioned, the water from Miðvatn is currently tapped into Ryskivatn, but in case of a pumped storage system, this water would be connected to Vatnsnesvatn. Balmorel is a linear optimisation tool, which means that it cannot optimise using if/then/else logic. An example of if/then/else logic, is given as follows:

- *If...* the model invests in pumped storage in R7

- *then...* the water in Miðvatn should be led to Vatnsnesvatn

- *else...* it should be tapped into Ryskivatn

In other words; Miðvatn can either be tapped to Ryskivatn or the pumped storage system. This means that the system can not be fully optimised. If it is desired to analyse the system with a pumped storage system in Suðuroy, it has to be a committed capacity. Therefore this has been included in a separate scenario (Scenario #5). The turbine and pumping capacities have been set to 4 MW and 6 MW respectively in scenario #5. The potential energy at Miðvatn is reduced in case of a pumped storage system, since the potential height is lowered. This is shown in Table 3.18. Additionally the production at Botnur 1, is reduced. It is assumed that the production at Botnur 1 comes from both reservoirs proportionally to the catchment area. The catchment area for Miðvatn is 1.1 km^2, and for Ryskivatn it is 1.5 km^2, which means that the production at Botnur 1, when a pumped storage system is a committed capacity, is 1.5/2.6 of the production without a pumped storage system [87].

Table 3.18: The energy at Miðvatn with and without a pumped storage system. (*The height of Ryskivatn, **the height difference between Miðvatn and Vatnsnesvatn.)

Scenario	Potential height (m)	Energy [MWh]
Without PS system	*243.9	339
With PS system	**168.5	234

Costs

The costs associated with the pumped storage system in region 1 are the same as the ones used in [95], which are based on actual project estimations [96]. The costs are tabulated in Table 3.19.

Table 3.19: The assumed investment costs, fixed operation and maintenance (O&M) costs, variable O&M costs and the lifetimes related to storage systems [95], [96].

Technology	Investment costs	Fixed O&M (EUR/kW)	Variable O&M (EUR/MWh)	Lifetime (years)
Mýruverkið - pump	220 EUR/kW	50	0	30
Mýruverkið - turbine	266 EUR/kW	50	0	30
Heygaverkið - turbine	591 EUR/kW	50	0	30
Mýrarnar	5 EUR/kWh	0	0	40
Heygadalur	14 EUR/kWh	0	0	40
Pumped storage system R7	61 EUR/kWh	1.29	0	40

3.2.6 WIND POWER PLANTS

Wind power will be a important part of the path towards 100% renewables. Potential wind energy sites have been investigated and mapped based on topology, the infrastructure and a previous study on suitable sites [115]. These sites are mapped on Figure 3.8 together with the existing sites. There are considered 11 wind farm sites in total, and all sites have been named according to the technology type (W is for wind power), the region and if multiple sites are in the same region a letter has been added. W5d is only included as an investment option in scenario #6, due to the planned airport.
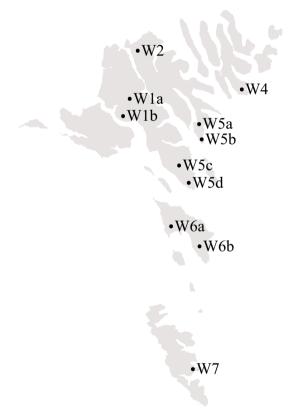
Fig. 3.8: The existing and potential wind energy sites.

A maximum capacity has been set for each site suitable for wind energy. This capacity is based on the technology considered for the site. The existing, committed, and maximum wind power capacities for each site are summarised in Table 3.20. The planned 25.2 MW wind farm, see section 1.2, has not been included in committed, as the study was conducted prior to the wind farm tender.

Table 3.20: Existing, committed and maximum wind power capacities at each wind site. The committed capacities are to be installed in 2021.

Site	Existing capacity (MW)	Committed capacity (MW)	Maximum capacity (MW)
W1a	1.98	-	1.98
W1b	-	-	18.00
W2	-	18.00	33.00
W4	-	-	18.00
W5a	-	-	21.00
W5b	4.65	-	4.50
W5c	11.70	18.00	47.70
W5d	-	-	72.00
W6a	-	-	30.00
W6b	-	-	36.00
W7	6.30	-	11.70

There are two methods to model wind power in Balmorel. The first method uses wind speeds and specifications of the wind turbine technologies to estimate the potential production. In addition to the wind speed profile, the height of the measured or modelled profile and the wind shear factor, α, at the specific site is required. If the hub height is different from the height of the wind speed profile, the wind speed at the hub height is found using the wind shear factor, known wind speed and heights, see Equation 3.4 [106]. The parameter u and h represent the wind speeds and heights. The subscript 1 is the lower height, while 2 is the higher height.

$$u_2 = u_1 \left(\frac{h_2}{h_1} \right)^{\alpha} \tag{3.4}$$

In terms of specifications of the technology a power curve has to be defined and the hub height has to be known. The power curve is defined by Equation 3.5 [106], where P is the power output, γ is the maximum power output reached [p.u.], M is the wind speed at which the maximum growth is reached, g is the maximum slope of the logistic curve, K_w is a smoothening factor for a wind farm and ϵ is an offset in the speed.

$$P = \frac{\gamma}{1 + e^{-gK_w(u-M-\epsilon)}} \tag{3.5}$$

The second method to model wind power is based on historic production data and is therefore suitable to model existing wind farms. The inputs required for this method are the full load hours (FLH) and an hourly power profile at each site. It is important to calculate the FLH based on the potential production rather than the actual production, to avoid curtailment affecting the FLH.

The wind speed is measured with approved MET masts at different heights at the following sites; W2, W5c and W7. However, the measurements at W2 and W7 are not available for 2017, which, as previously mentioned, is the chosen data year. The only site with measured wind speeds available is therefore W5c. The wind speeds over the whole country in a resolution of 500m x 500m have been modelled by Kjeller Vindteknikk [113]. This model has been validated in reference [116]. The hourly wind speeds for 2017 are available from the model.

The methods are prioritised as follows:

1. First method with measured wind speeds

2. Second method based on actual production data

3. First method with modelled wind speeds
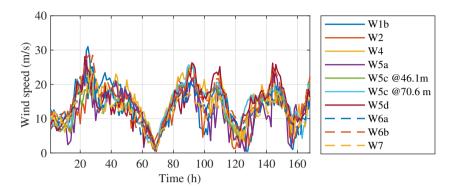
Thus, the second method is applied at the existing wind farms W1a and W5b, where no wind speed measurements are available, while the first method is used for the other wind farms.

The wind speeds at W5c are measured at 46.1 m, 70.6 m and 99 m. The modelled wind speeds are available at the following heights: 10.0 m, 12.3 m, 36.6 m, 60.9 m, 85.3 m, 109.7 m, 134.2 m, 158.3 m, 182.5 m and 207.2 m. The wind shear factors have been calculated based on the wind speeds at the height closest to the hub height using Equation 3.4. The factors are summarised in Table 3.21 together with the height of the wind speed profiles used in the Balmorel. A shear factor between 0.1-0.3 can represent a terrain with smooth hard ground, calm water to small town with trees and shrubs [117]. The calculated wind shear factors are also close to the ones described in reference [78], which is a study of the wind energy study of the Faroe Islands containing a map of the shear factors all over the country. There are two heights specified for W5c, because the existing wind turbines are smaller than the committed turbines.

Table 3.21: The wind shear factor, α, at different wind site and height of measured/modelled wind speed (m). W5c is based on measurements, while the rest is modelled based.

Site	W1b	W2	W4	W5a	W5c	W5d	W6a	W6b	W7
Height	85.3	85.3	85.3	85.3	46.1/70.6	85.3	85.3	85.3	36.6
Shear	0.15	0.15	0.13	0.18	0.09	0.14	0.16	0.12	0.21

Examples of the used wind speed profiles are given for each location in Figure 3.9 over a week. Although all sites show the same pattern, there are some slight variations in the wind speed profiles. Thus, distributing the wind farms over a larger area can result in a smoother wind power production. The

advantage of distributing wind farms in the Faroe Islands has been addressed in reference [118].

Fig. 3.9: An example of the wind speeds at wind sites over one week.

Due to the rough wind conditions on the islands, the turbines installed in the Faroe Islands have to have the highest IEC classification, which is Ia as defined in the IEC 61400 standard for wind turbines. These turbines can withstand the highest wind speeds and turbulence. The Enercon E-44 wind turbine was in 2010 identified as the most suitable wind turbine for Faroese conditions [119]. This turbine is as previously mentioned installed at W5b and W5c. The study mainly considered wind turbines with a power rating around 1 MW. Larger turbines are however now being considered, and the committed 18 MW at W2 and W5c will be 12 E-82 E4 3 MW turbines which also are class Ia. The hub height from E-82 E4 (78 m) will be used in the calculations for all new wind farms except from W7, which has a committed capacity of 7 E-44 turbines. The height of these is 45 m.

The manufacturer's power curve for E-44 has been curve fitted using Equation 3.5 to find the maximum power output reached, γ, the maximum slope of the logistic curve, g, and the wind speed maximum growth is reached, M. The other two parameters; the smoothing factor K_w, and the offset, ϵ, were found by comparing production data with calculated production based on wind speeds and the power curve. This was done by varying K_w (0:0.001:1) and ϵ (0:0.001:5). The most accurate combination of K_w and ϵ was found by calculating the correlation factor between the actual production and the calculated production. The highest correlation factor was found to be 0.94. The respective equation parameters used in this investigation are tabulated in Table 3.22.

Table 3.22: Wind turbine technology characteristics.

γ	g	K_{w}	M	ϵ
1.010	0.585	0.763	9.862	0.886

The manufacturer's power curve, the power curve fitted to Equation 3.5, and the realistic power curve are compared in Figure 3.10. The manufacturer and curve fitted curves are almost identical, while the realistic power curve is different due to the smoothening and offset parameters. Both the E-44 and E-82 E4 are equipped with a storm control, which means that the turbine can deliver rated power up to 28 m/s, and stops at 34 m/s. In the simulations, the power output is assumed to decrease linearly from 900 kW at 28 m/s to zero at 34 m/s.
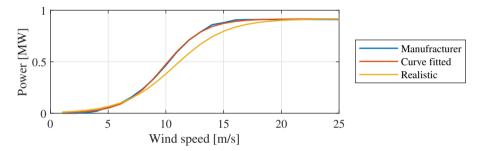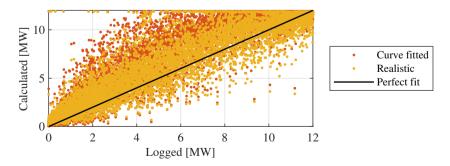
Fig. 3.10: The manufacturer, curve fitted and realistic power curves.

Figure 3.11 shows the difference between calculating the production based on the curve fitted power curve and the realistic power curve. The correlation between the logged potential production from 2017 and the calculated production using wind speeds from 2017 is improved by using the realistic power curve compared to the curve fitted power curve.

Fig. 3.11: Comparison of logged production and calculated production, using a curve fitted and realistic power curve.

The FLH at W1a and W5b can be seen in Table 3.23. In 2017 W5b had higher, which indicates that the wind turbines at W5b were more efficient than those at W1a. This is likely due to a combination of the wind condition at the sites, the two different wind turbine types and the height difference.

Table 3.23: The FLH at W1a and W5b in 2017.

W1a	W5b
3379	3896

Figure 3.12 shows an example of the power output from the E-44 turbines at W1a and the output from the W5b wind farm. These profiles could indicate that W5b is being curtailed, since the rated power is 4.5 MW and reaches a maximum of 1.8 MW, while the rated power of W1a is 1.98 MW, which is being reached at certain times. One explanation of this could be that SEV does not own W1a and cannot control these turbines beside from ON/OFF.
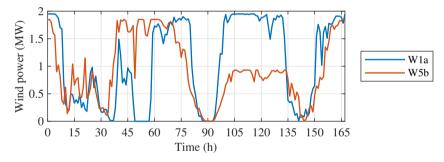
Fig. 3.12: An example of the power output of W1a and W5b over one week.

Costs

Table 3.24 contains the assumed costs and lifetimes associated with wind power. The costs of investing in wind power are based on the committed wind farm in Region 2, and the O&M costs are from reference [95]. The decrease in costs is the same, percentage wise, as in the previous Balmorel study [95]. The lifetimes are based on the Danish technology data catalogue [120], and these are applicable to the Faroe Islands. Due to the accessibility, the investment costs at W4 will be significantly higher than at other sites. The investment cost is assumed to be 70% higher, as estimated by [121].

Table 3.24: The assumed investment costs, fixed operation, and maintenance (O&M) costs, variable O&M costs and the lifetimes related to wind power [95], [120].

Years	Investment costs (EUR/kW)	Fixed O&M (EUR/kW)	Variable O&M (EUR/MWh)	Lifetime (years)
2020-2024	1045	26	7	20
2025-2029	1004	26	7	20
2030	963	26	6	25

3.2.7 PHOTOVOLTAIC POWER

As described in the introduction, photovoltaic (PV) power has the potential to become a very interesting part of the Faroese energy mixture. A maximum wind power capacity is relatively easy to define, as there is a limited amount of suitable areas. On the contrary photovoltaic power can be installed on rooftops, fields and waters. This makes it more difficult to define a maximum capacity. In this study the model is allowed to invest in PV power in all regions except from 3 (which only is a connection point), and no limit has been set on the maximum allowed capacity.

The generation from solar power is modelled based on full load hours and an hourly generation profile. This means that the generation is scaled according to the capacity using the FLH. Due to the very limited measured solar data available, the solar data used in this investigation is from the same model as the modelled wind speeds developed by Kjeller Vindteknikk [113]. A irradiation profile has been selected for each region. The location of the solar profiles has been selected based on the densest built areas in each region. The irradiation profile over a day for each region is shown on Figure 3.13.
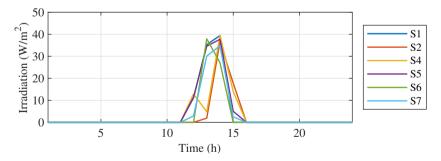
Fig. 3.13: Example of the irradiation at the chosen locations throughout a day.

The full load hours over a year are calculated based on Equation 3.6 [122]. The sum of the irradiance at every hour, G_h, is divided by the irradiance of standard testing conditions, G_{STC}, which is 1 kW/m^2, and multiplied by the

installed power (1 kW) and the performance ratio, η. The performance ratio has been calculated based on the FLH and irradiance measured at existing PV systems. The systems considered are 3 rooftops solution all located within a of radius 2 km. The irradiance, FLH and performance ratio is given for the systems in Table 3.25. The average performance ratio of 81% was used to calculate the FLH in this study. The FLH at each site, which are calculated using Equation 3.6, are summarised in Table 3.26. The FLH vary between 584 in region 5 and 620 in region 6.

$$FLH = \frac{\sum I_h(\text{kW/m}^2)}{G_{\text{STC}}(\text{kW/m}^2)} \cdot P(\text{kW}) \cdot \eta(\%) \qquad (3.6)$$

Table 3.25: Performance ratio of existing PV systems in the Faroe Islands.

System	Year	Irradiance (Wh/m^2)	Performance (Wh/W)	Performance ratio (%)
Vinnuháskúlin	2009-2012	760	620	82
Tannlæknamiðstøðin	2018	759	584	77
Tannlæknamiðstøðin	2019	758	618	82
Umhvørvisstovan	2019	758	627	83
Average		759	616	81

Table 3.26: The full load hours at the solar sites.

S1	S2	S4	S5	S6	S7
590	617	617	584	620	609

Costs

The costs of investing in PV power in the Faroe Islands have been based on the investment costs of the PV plant in Sumba, while the cost reduction and O&M costs are the same as in reference [95]. The lifetimes are taken from the Danish Technology Catalogue [120]. The costs and LT are tabulated in Table 3.27.

Table 3.27: The assumed investment costs, fixed operation and maintenance (O&M) costs, variable O&M costs and the lifetimes related to solar power [95], [120]

Years	Investment costs (EUR/kW)	Fixed O&M (EUR/kW)	Variable O&M (EUR/MWh)	Lifetime (years)
2020-2024	1400	8	0	25
2025-2029	1210	7	0	25
2030	1110	7	0	30
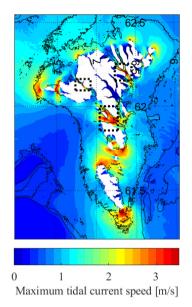
3.2.8 TIDAL POWER PLANTS

Tidal power is considered an investment option in the 2nd scenario, in order to investigate the potential impact of tidal power on the future power composition. There are multiple sites around the islands which are suitable for tidal energy. Three sites are considered in this investigation. These are marked on Figure 3.14a. The three sites have been selected based on the phase shift between the currents at the sites, the accessibility and the current speed, i.e. the potential production. The current speed varies significantly from one point at a site to another. Each site is therefore divided into four zones (A, B, C and D) based on the peak current speed, see Figure 3.14b, Figure 3.14c and Figure 3.14d. A speed profile is obtained for each zone and hence, the accuracy of the calculated potential production and the feasibility is increased, compared to if an average profile was applied to the whole site. The zones have a peak current speed of:
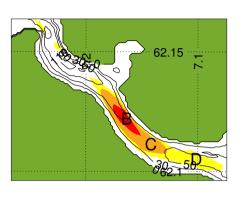
- A: >3.5 m/s

- B: 3.5 m/s - 3.0 m/s

- C: 3.0 m/s - 2.5 m/s

- D: 2.5 m/s - 2.0 m/s

The peak current speed of each point of 100 m x 100 m in the Faroese tidal model [79] is analysed, and the point is grouped into a zone. Additionally, it is known that the installation of the planned tidal turbines, will require an area smaller than 100 m x 100 m. Thus, it is assumed that the maximum capacity is 100 kW/point. This is a conservative estimate. The number of points, the area, and the maximum capacity for each site is tabulated in Table 3.28. The maximum capacities in the table indicate that the implementation of this technology will not be limited by space. However, there is a fifth column "Extraction Limit" which has a stricter limit. This is based on the limitation of how much it is possible to extract from a site without affecting the tidal streams [80]. Using this limit, it is clear that it will not be invested in T1D, T5C, T5D, T6C and T6D, since the extraction limit at the site has been reached utilising the other zones. As shown in the table and the figure, site T1 has three zones (b, c and d) compared to four zones for the other sites. This is because no model point at T1 showed a speed over 3.5 m/s.
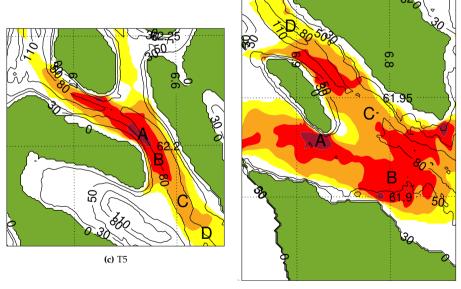
(a) Site overview.

(b) T1

(c) T5

(d) T6

Fig. 3.14: The three tidal sites considered in the study, and the zones A (dark red), B (red), C (orange) and D (yellow).

Table 3.28: The number of points, area and maximum capacity at each site and zone.

Site	Points (#)	Area (km^2)	Maximum Capacity (MW)	Extraction Limit (MW)
T1a	-	-	-	-
T1b	65	0.65	6.5	6.5
T1c	204	2.04	20.4	3.5
T1d	337	3.37	33.7	-
T5a	66	0.66	6.6	6.6
T5b	482	4.82	48.2	23.4
T5c	860	8.60	86.0	-
T5d	1156	11.56	115.6	-
T6a	171	0.17	17.1	17.1
T6b	2323	23.23	232.3	57.9
T6c	2970	29.70	297.0	-
T6d	2021	20.21	202.1	-

Tidal power is modelled using the same method as solar power, i.e. FLH and a generation profile. The FLH are calculated using modelled tidal speeds and a power curve. The potential production from tidal power, is calculated based on the power curve of the DG100 tidal kite from Minesto which is installed in Vestmannasund and the modelled current speed. Figure 3.15 is an example of the tidal speeds at each site throughout a day. Figure 3.15 shows the phase shift between the currents at the different locations, which if utilised ensures a production from tidal energy at all times. Location T6 has the highest speed, and then T5 and T1 respectively.
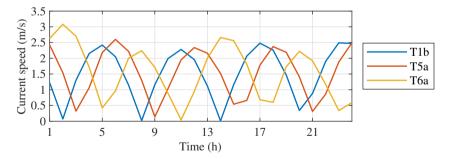
Fig. 3.15: An example of the current speeds at T1b, T5a and T6a over a day.

The power curve for DG100 is shown on Figure 3.16. The cut-in speed is 1 m/s, rated speed is 1.6 m/s and cut-off speed is 3 m/s. This is a preliminary version of the power curve, and thus a conservative estimate, especially with regards to the cut-in speed. The speeds at the three sites (Figure 3.15) are within the same range as the power curve, and the power curve of this technology fits well the available resource potential.
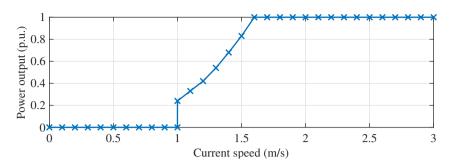
Fig. 3.16: Minesto DG100 power curve.

The full load hours (FLH) for the sites within the extraction limit are tabulated in Table 3.29. The highest potential is at T1b and the lowest at T5b. It is expected that the model will invest in tidal power at T1b first due to the high FLH.

Table 3.29: The full load hours at for the tidal sites.

Site	Full load hours
T1b	4656
T1c	4001
T5a	4395
T5b	3793
T6a	4581
T6b	4009

Costs

The costs of investing in tidal power and the lifetimes are based on input from the manufacturer of the tidal turbine in Vestmannasund, see Table 3.30. The investment costs of tidal power used in [95] are twice the costs used here. This is because the previous study considered the traditional tidal technology, which is more expensive especially with regards to strength, mounting etc. Those costs were based on technical catalogues.

Table 3.30: The assumed investment costs, fixed operation and maintenance (O&M) costs, variable O&M costs and the lifetimes related to tidal power according to the manufacturer.

Years	Investment costs (EUR/kW)	Fix. O&M (EUR/kW)	Var. O&M (EUR/MWh)	Lifetime (years)
2020-2024	2063	26	26	20
2025-2030	1192	18	11	20

3.2.9 BATTERY STORAGE SYSTEMS

Batteries are modelled to stay within the capacity limitations at every hour. The efficiency of the battery systems is assumed to be 80%. In this investigation the battery systems are modelled as short term storages, this means that the energy can only be stored for maximum a week. Batteries are therefore not used for weekly or seasonal storages. The C rating assumed is 0.25C, meaning that the battery discharges in 4 hours.

Costs

The battery cost is only expressed in kWh, as the inverter capacity is assumed to be four times the storage capacity and is included in the costs of the storage capacity. The battery investment costs are based on input from Tesla, which refer to Bloomberg, and can be found in Table 3.31. The fixed and variable O&M costs and the lifetime are taken from [95].

Table 3.31: The assumed investment costs, fixed operation and maintenance (O&M) costs, variable O&M costs and the lifetimes related to battery storage systems.

Investment costs (EUR/kWh)	Fixed O&M (EUR/kW)	Variable O&M (EUR/MWh)	Lifetime (years)
296	2.27	0.2	15

3.2.10 CONSTRAINT ON EMISSIONS

A limitation has been set on the CO_2 emissions from 2021, when the model is allowed to invest in new capacities, and until 2030. With this constraint a 100% renewable production in 2030 is obtained. The emission is expressed in ktonne/year.
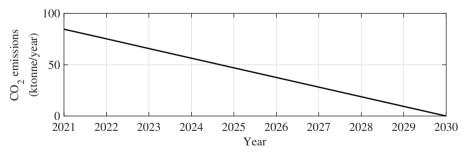
Fig. 3.17: Limit on CO2 emissions from 2020 to 2030.

3.2.11 CONSTRAINT ON THE INVERTER BASED GENERATION

SEV has set a limit of 60% instantaneous inverter based generation in operation. This limit is used to ensure enough inertia, short circuit power and

spinning reserve in the grid. However, in order to reach 100% renewables, it will be necessary to increase the shares of the inverter-based generation. In the simulations conducted in Balmorel, the limit of instantaneous inverter based generation has been set to 60% in 2020 and then increases. It is assumed that in 2021 the limit is set to 80%. This increase is due to new wind farms of 42 MW in total in 2020 and 2021. In order to harvest a large part of this new wind energy, it is necessary to increase the limit. From 2021 to 2030 it is assumed that this limit will increase linearly up to 100% in 2030. The limit in Balmorel has been defined in order to ensure that the optimal investments do not result in a higher instantaneous inverter-based generation, that what is accepted by the power system operator. It was previously stated that the limit of 60% is to ensure the inertia, short circuit power and spinning reserve, this means that in order to increase the limit, other investments in the grid, e.g. synchronous condensers, battery systems, have to replace the synchronous generators, which will be replaced by the inverter based generation.

The limit in the results presented here has been defined for the total hourly production in the main grid and in Suðuroy. It could also be defined separately for the two grids to ensure that the optimised dispatch in each grid prior to the cable connection between Suðuroy and the main grid does not exceed the limit. However, the cable is an optimised investment, which is optimised from 2021 and forward. This means that the main grid and Suðuroy are seen as one system from 2021 and forwards, and when this is the case, the limit should be defined for the whole system. A simulation where the limit was defined pr. grid showed that whether this constraint was defined for the whole system or separately had negligible impact on the optimal investments.

Table 3.32: Limit on the instantaneous inverter based generation.

2020	2021	2022	2023	2024	2025	2026	2027	2028	2029	2030
60%	80%	82%	84%	86%	88%	90%	92%	94%	97%	100%

3.3 ECONOMICALLY OPTIMAL ENERGY MIXTURE

The result of the economic optimisation in Balmorel are presented in this section. The results include the investments in generation, storage and transmission (subsection 3.3.1), additionally information about the dispatch, i.e. the production, curtailment, CO_2 emissions and transmission losses (subsection 3.3.2). The economics of the system are also included as annual costs and cost of energy (subsection 3.3.3). Finally, the sensitivity of the generation, storage and transmission capacities are presented (subsection 3.1.2). The re-

sults are presented by figures, while the data is tabulated in Appendix A. The focus in subsection 3.3.1-3.3.3 is on first four main scenarios (reference, tidal, biofuel and CO_2), while the sensitivity scenarios are presented in subsection 3.1.2. The other two main scenarios (#5 PS in R7 and #6 additional WP site) have, as previously mentioned, local interest and not specifically technical, therefore these are only included in Appendix A. The results obtained with a committed PS in R7 (scenario #5) are very similar to the reference scenario, while the scenario with an additional WP site (scenario #6) varies from the reference scenario, with a lower solar power capacity and higher wind power capacity, but the differences between the reference scenario and scenario 6 are significantly smaller than the differences between the reference scenario and scenarios 2-4. The scenarios presented in section 3.1 are recapped in Table 3.33.

Table 3.33: Investigated scenarios as described in section 3.1.

Main scenarios		Sensitivity scenarios			
Scen.	Description	Scen.	Description	Scen.	Description
#1	Reference	cBS	Cheap batteries	eBS	Expensive batteries
#2	With tidal	cCA	Cheap cables	eCA	Expensive cables
#3	With biofuel	cFU	Cheap fuel	eFU	Expensive fuel
#4	With CO2 emissions	cPS	Cheap PS system in R1	ePS	Expensive PS system in R1
#5	With PS in R7	cPV	Cheap photovoltaic power	ePV	Expensive photovoltaic power
#6	With additional WP site	cWP	Cheap wind power	eWP	Expensive wind power

3.3.1 INVESTMENTS

The economically optimal generation capacities under the given assumptions can be seen in Figure 3.18 and the data is found in Table A.2. From 2020 to 2025 the four presented scenarios have identical generation capacities with small increases in wind and hydro power. In 2025 the tidal scenario (#2) varies slightly from the other three scenarios, and this is because the investment costs of tidal power decreases in 2025 and the technology becomes a feasible option. In 2026 the reference scenario (#1) and the biofuel scenario (#3) also differ from the scenario with CO_2 emissions (#4), this shows that investing in renewable generation is no longer the economically best option, since scenario 4 does not have a restriction on CO_2 emissions. In 2027 there is also a difference between the reference scenario (#1) and the biofuel scenario (#3). This indicates that the feasibility of investing in renewable energy has decreased further, and thus the option to burn biofuel at an existing thermal power plant is utilised. From 2028 solar power becomes a part of the optimal solution in the reference scenario (#1), thus investing in wind power, which has a high resource potential in the Faroe Islands, has become less feasible than investing in solar, which has a low potential. This is due to the challenge of balancing the system during the summer months, when the wind speeds

are lower and solar irradiation is higher. In 2029 and 2030 the variations between the four scenarios become clearer. The total capacities in 2030 can be found in Table 3.34 [81]. The minimum, average and maximum demand in 2030 is 46 MW, 75 MW and 104 MW. Overall, it can be said that:

- Increasing the wind power capacity up to 125 MW and the hydro turbine capacity to 79 MW in 2030 is the economically best solution. Additional investments to reach 100% renewables do not earn back the investments. The added turbine capacity is associated with the PS system in R1, these capacities are shown in Figure 3.20.

- Investing in PV power is not economically feasible under the given assumptions, but it is an important part of the power composition when aiming for 100% renewables and not considering tidal power or biofuel as an option, due to challenge of obtaining a balance in the summer. Under optimal conditions the PV capacity in 2030 could supply the average demand.

- If tidal energy will prove to be as economically viable as assumed in this study, it can have a major impact on the future power composition. 72 MW of tidal power will displace 9 MW of hydro, 66 MW of wind power, 79 MW of PV power and 1 MW of battery power in 2030. PV is not a part of the system anymore, wind power is decreased and there are small reductions in the hydro turbine capacity as well. The tidal resource is available throughout the year and the lack of available energy when the tide turns every six hours can be avoided by utilising different locations and the technology can provide a base load production, this leads to a high reduction in the total power capacity, which is also clear by the fact that the capacities of PV in reference scenario and tidal in scenario #2 are similar, but wind power is significantly decreased. These 72 MW of tidal power could supply the whole demand under optimal tidal stream conditions at times, as the average demand in 2030 is 75 MW.

- The feasibility of biofuels also has a major impact on the final power composition, reducing it from 462 MW to 349 MW. This is due to the technology being dispatchable. PV is eliminated and wind power is reduced from 168 MW to 153 MW. The power plant which in this scenario is assumed to burn biofuel was commissioned in 2019, thus it makes sense to utilised the capabilities of this new dual fuel power plant.

- Scenario 1-3 have a battery capacity, this battery system is located in R7, and is used to balance this remote region. Even with a PS system in R7, battery capacity should be added to balance the system in R7 on a weekly basis.

Table 3.34: The Optimal Generation Capacities (MW) in 2030. Scenarios: 1-reference, 2-tidal, 3-biofuel and 4-CO_2.

Scenario	Fuel oil	Gas oil	Biogas	Hydro	Wind	Solar	Tidal	Battery	Total
1	91	8	2	112	168	79	-	2	462
2	91	8	2	103	102	-	72	1	379
3	91	8	2	94	153	-	-	1	349
4	91	8	2	79	125	-	-	-	305

Fig. 3.18: The Optimal Generation Capacities from 2020 to 2030 for Scenarios 1-4. Scenarios: 1-reference, 2-tidal, 3-biofuel and 4-CO_2.

Storage is vital in order to reach 100% renewables, and there are significant variations between the scenarios with regards to the optimal capacities at the pumped storage system in R1. A schematic of the planned pumped storage system can be seen on Figure 3.19. The optimal capacities can be seen in Figure 3.20 and found in Table A.5 and Table A.4. The optimal capacities in 2030 are tabulated in Table 3.35. The optimal turbine capacity at Heygaverkið (the lower power plant) does not increase until 2026, and varies between 7 MW and 9 MW in 2030. A variation of 2 MW out of 7-9 MW is relatively large, but as this is a very small value considering that it is a hydro turbine, and is therefore considered insignificant.

Greater variations are seen in the optimal turbine capacity at Mýruverkið (upper power plant), ranging with a final value between 40 MW and 71 MW, i.e. all scenarios require significant increases of turbine capacity at Mýruverkið. The increase is high already in 2021, the first year when the model is allowed to optimise investments. Then it increases slowly to 2025. From 2025 and forward the variations between the scenarios become clearer. Until 2030 the tidal scenario (#2) has a much lower capacity than the reference (#1) and biofuel (#3) scenarios, but in order to reach 100% renewables in 2030 the turbine capacity in the tidal scenario (#2) is increased from 28 MW in 2029 to 61 MW in 2030. The capacity in the biofuel scenario (#3) is similar to the

reference scenario (#1) until 2030. In the reference scenario (#1) the capacity increases from 52 MW in 2029 to 71 MW in 2030, while in biofuel scenario (#3) it increases from 50 MW to 54 MW. This is likely due to a lack of undispatchable renewable resources during a specific time, which either a higher turbine capacity or burning biofuels has to compensate for.

Fig. 3.19: Schematic of the planned pumped storage system [123].
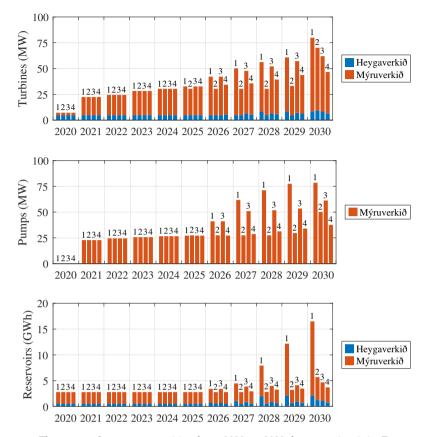
Pumping capacity has to be added to Mýruverkið, to obtain a pumped storage system. Already in 2021 the optimal pumping capacity is 23 MW, and this increases slowly to 27 MW in 2025. In 2026, when investing in renewables is no longer economically optimal, the pumping capacity in reference (#1) and biofuel (#3) scenarios jumps to 41 MW, while the other two scenarios stay at 27 MW. In 2027 the capacity in the reference scenario (#1) exceeds the biofuel scenario (#3). Similar to the turbine capacities the pumping capacity in tidal scenario (#2) is relatively low until 2030, lower than the scenario with CO_2 emissions (#4), but then it jumps by 20 MW in one year. Thus, tidal power results in a 37 MW lower pumping capacity in 2029 compared to the reference scenario (#1), but this difference is decreased to 17 MW when the production has to be 100% renewable. There is a clear need for pumping capacity in all scenarios, as even without a restriction on CO_2 emissions a pumping capacity of 38 MW is optimal, and in order to reach 100% renewables without tidal power and biofuels 78 MW are required. In PS systems the pumping capacity is typically significantly higher than the turbine capacity, see e.g. Figure 2.5, but in this study the pumping capacity in the reference scenario (#1) is only 7 MW higher than the turbine capacity. This indicates that there are periods in 2030 where existing hydro power plants, potential wind and PV sites can not cover the production and thus additional hydro generation capacity is needed.

The optimal reservoir sizes increase from year 2026 and forward, but the expansions in scenario 2-4 are not that large. The reference scenario (#1) requires extensive reservoir increases especially at Mýrarnar, but also at Hey-

gadalur. Heygadalur is increased by 1.6 GWh, 0.7 GWh, 0.6 GWh and 0.2 GWh from 2020 to 2030 in scenario 1 to 4 respectively, while the increases at Mýrarnar vary between 12 GWh and 0.7 GWh. The reservoirs are located above the village Vestmanna, and thus high increases of the associated dams will likely lead to public resistance, but this is necessary in order to reach 100% renewables with the assumptions in this study, especially when neither tidal energy or biofuels are considered a viable option. Since the high increases do not occur until 2028, the demand etc. should be monitored closely, and if necessary the required reservoir sizes should be reevaluated.

To summarise it can be said that Heygaverkið should have what corresponds to 1 day of storage, while the total storage of the pumped storage system corresponds to 8 days in 2030. The turbine power is similar to the average demand in 2030. The pumping capacity corresponds roughly to the wind power capacity minus the average demand, indicating that the surplus wind power is used to pump.

Fig. 3.20: The pumped storage capacities from 2020 to 2030 for scenarios 1-4. From top to bottom: Turbines (MW), pumps (MW) and reservoirs (GWh). Scenarios: 1-reference, 2-tidal, 3-biofuel and 4-CO_2.

Table 3.35: Optimal pumped storage system capacities in 2030. Scenarios: 1-reference, 2-tidal, 3-biofuel and 4-CO_2.

Scenario	H. turb. (MW)	H. res. (MWh)	M. turb. (MW)	M. res. (MWh)	M. pump. (MW)
1	9	2141	71	14355	78
2	9	1232	61	4471	50
3	8	1105	54	3569	61
4	7	750	40	2951	38
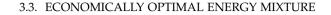
The model invests in transmission capacity at three connections, see Figure 3.21, Table 3.36 and Table A.16. The first connection is between R1 and R5. An increased transmission capacity in this scenario is only necessary in the reference scenario (#1), and the increase is 3 MW. This increase is likely due to the PS system being located in R1, and significant amounts of en-

ergy has to be transmitted to R1 when the PS system is pumping mode, and exported when the PS system is generating.
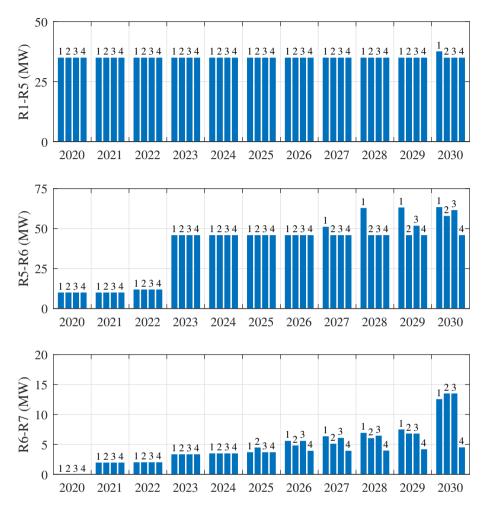
The transmission capacity between R5 and R6 has to be increased significantly, as two large wind power plants are installed in this region according to optimal results, the demand is relatively low, and energy therefore has to be exported. The increase in 2023 is a 44 MW committed transmission cable, which will be installed when an undersea tunnel from R5 to R6 is finished. This cable is however not enough in scenarios 1-3, as the optimal capacity exceeds 44 MW in 2030.

A cable to R7 has to be installed in order to reach 100% renewables in 2030, as all scenarios invest in this connected. This has also been discussed in previous studies e.g. [85]. The tidal (#2) and biofuel scenarios (#3) have a higher transmission capacity between R6 and R7 than the reference scenario (#1). In the reference scenario (#1) 15 MW of PV power are installed in R7, and since PV is not a part of the optimal solution in scenario 2 and 3, and the one available wind farm site is full, the total capacity in Suðuroy is decreased and thus more energy has to be transmitted to R7 from other regions, resulting in a larger cable. Generally, the variations in transmission capacities based on the different scenarios are not as significant, as in the generation and storage capacities.

Table 3.36: Optimal transmission capacities in 2030. Scenarios: 1-reference, 2-tidal, 3-biofuel and 4-CO_2.

Scenario	R1-R5	R5-R6	R6-R7
1	38	63	13
2	35	58	14
3	35	62	14
4	35	46	5
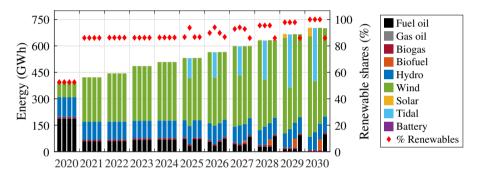
Fig. 3.21: The optimal transmission capacities from 2020 to 2030 for scenarios 1-4. Scenarios: 1-reference, 2-tidal, 3-biofuel and 4-CO_2.

3.3.2 DISPATCH

Balmorel optimises the dispatch simultaneously with the investments. The annual production can be seen in Figure 3.22, the production in 2030 can also be found in Table 3.37, while the data for other years is found in Table A.11. The production is above 80% renewable in 2021 in all scenarios. This is due to the committed wind farms and optimal investments in pumped storage. The committed wind farms have however been postponed, and the pumped storage system is not set to be installed yet, thus; the production in 2021 was not over 80% renewable. In 2025 the tidal scenario (#2) has a higher renewable share than the other scenarios, and this is due to the added tidal capacity and

85

that Balmorel does not curtail tidal energy. The renewable shares in scenario 1-3 are equal, as the CO_2 restriction controls the optimisation. The 79 MW of PV power in 2030 produce 49 GWh, while the 71 MW of tidal power produce 301 GWh, this clearly shows that the potential for solar energy is low in the Faroe Islands. Biofuels produce 62 GWh in biofuel scenario, and this production is enough to reduce the total installed generation capacity by 113 MW, as shown in Table 3.34. When a production of 62 GWh (9% of total) using a dispatchable resource can reduce the total capacity by 25% (reference (#1) vs. biofuel scenario (#3)), it is quite clear that the challenge to balance the production throughout the year is difficult, and doing this using only wind, solar and pumped storage is expensive. In some years the economically optimal generation (scenario #4) reaches 87%, but as the demand increases this is decreased to 86% in 2030.

Fig. 3.22: The optimal production from 2020 to 2030 for scenarios 1-4. The renewable shares are shown on the right y-axis. Scenarios: 1-reference, 2-tidal, 3-biofuel and 4-CO_2.

Table 3.37: Optimal production in 2030 (GWh). Scenarios: 1-reference, 2-tidal, 3-biofuel and 4-CO_2.

Scenario	Fuel oil	Biogas	Biofuel	Hydro	Wind	Solar	Tidal	Battery	Total	Renewable
1	0	9	0	77	569	49	0	0	703	100%
2	0	9	0	102	290	0	301	0	701	100%
3	0	9	62	87	545	0	0	0	702	100%
4	98	9	0	93	501	0	0	0	701	86%

Investing in over capacity of wind power to cover periods with low energy resource potential, leads to high curtailment during other periods. The curtailment from 2020 to 2030 can be seen in Figure 3.23, and the values can be found in Table A.13. The curtailment of wind power is equal in all scenarios until 2024. In 2025 the tidal scenario (#2) has added tidal power capacity, and since Balmorel does not curtail tidal power, a significant amount of wind power is being curtailed. In 2030 the tidal scenario (#2) has the highest curtailment, although it is similar to the reference scenario (#1). In 2026, similar

to other results, the scenario with CO_2 emissions (#4) is different from 1 and 3, and in 2027 all scenarios are different. This is a consequence of the optimised investments. Scenario 4 clearly has the lowest amount of lost energy of 35 GWh, while scenario 1-3 curtail 139 GWh, 147 GWh and 105 GWh respectively. This curtailment can be avoided if the energy can be put elsewhere, e.g. power-to-X technologies or in the electrification of the industry, which is not considered in the demand projections in this study. Some parts of the industry could definitely utilise this excess energy, as the total consumption of the industry on land was 340 GWh in 2020 [124].
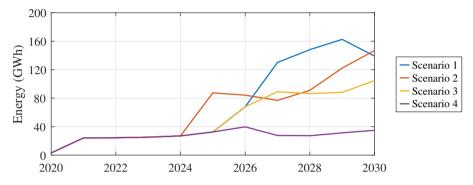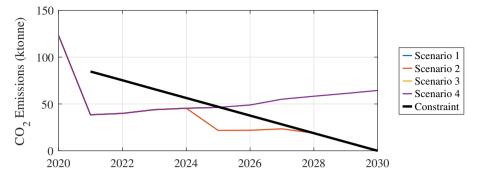
Fig. 3.23: The curtailed wind power from 2020 to 2030 for scenarios 1-4. Scenarios: 1-reference, 2-tidal, 3-biofuel and 4-CO_2.

The CO_2 emissions in the four scenario are illustrated on Figure 3.24, and the data can be found in Table A.14. The constraint is also shown on the figure from 2021. The constraint is not in 2021, as the model is not allowed to invest before 2021, and therefore it is not possible to set a constraint on the emissions. The reference (#1) and biofuel (#3) scenario follow the CO_2 scenario (#4) until 2025, and the constraint from 2026 and forward. The emissions in scenario 2 are lower than the limit and the other scenarios from 2025 to 2027. It was also clear from the production presented previously that the scenario, which allows investments in tidal energy (#2) is more renewable than other scenarios during certain years.

Fig. 3.24: The CO_2 emissions from 2020 to 2030 for scenarios 1-4. Scenario 1 and 3 follow scenario 4 until 2025 and then the constraint from 2026 to 2030. Scenarios: 1-reference, 2-tidal, 3-biofuel and 4-CO_2.

The model was built in 7 regions to account for available transmission capacity and local demand, and this also leads to known transmission losses. The transmission losses in Balmorel are modelled as % of transmitted power, and the losses for scenarios 1-4 are illustrated in Figure 3.25 and tabulated in Table A.15. There is a small variation between the losses in the different scenarios. The difference is caused by generation capacity being located in different regions, depending on which technologies are considered relevant. The transmission losses should be considered, when locating a generation site, as it is best to locate the sites close to the demand, but the losses shown on Figure 3.25, show that the difference in losses is not that large. The losses generally increase from 2020 to 2030, and this is due to more energy being transmitted. The losses in the tidal scenario (#2) are lower than the other scenarios from 2025 to 2029, and this is likely due to a significant amount of tidal power being installed in R1, i.e. in the same region as the pumped storage system.
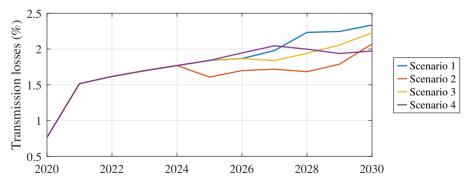
Fig. 3.25: Transmission losses from 2020 to 2030 for scenarios 1-4. Scenarios: 1-reference, 2-tidal, 3-biofuel and 4-CO_2.

3.3.3 ECONOMICS

Annualised fixed O&M costs, variable O&M costs, fuel costs, capital investment costs (generation/storage) and transmission investment costs are shown on Figure 3.26, the full dataset is tabulated in Table A.17, while the total cost from 2020 to 2030 are found in Table 3.38. In terms of investments, the costs presented only include optimised investments, i.e. not previous or committed investments. The transition towards 100% renewables will change the economics of the system, as fuel costs are lower and investment costs are higher. The system costs have a similar behaviour between the different scenarios and years to previously presented results.

The reference scenario (#1) is clearly the most expensive scenario, and by adding the costs over the ten year period and comparing the scenarios, the difference in system costs between the scenarios can be identified, see Table 3.38. Considering only the costs presented here, reference scenario (#1) is 26 mio. EUR more expensive than without any restriction on the CO_2 emission (#4). An interesting observation is the costs of the tidal scenario (#2). In previously presented results it was also clear that the tidal scenario (#2) had a lower emission than other scenarios from 2025 to 2027, i.e. the CO_2 restriction does not limit the investments in scenario 2 from 2025 as in scenario 1 and 3, but from 2028. This also means that the tidal scenario is less expensive than the scenario with CO_2 emissions (#4) from 2025 to 2027. However the tidal scenario is also less expensive in 2028 and 2029, as the fuel costs are significantly lower than in scenario 4, and although the investment costs are higher, the tidal scenario is cheaper than the scenario without the CO_2 restriction (#4) in 2028 and 2029. This results in the tidal scenario being less expensive than in scenario 4 over the 10 year period simulation. The tidal scenario has a total cost of 278 mio. EUR, while the scenario with unrestricted CO_2 emissions costs 285 mio. EUR. The costs of tidal power are however very uncertain, as the technology is not commercially available yet. The scenario with biofuel (#3) is 10 mio. EUR cheaper than the reference scenario, this means that biofuel is a viable competitor even with fuel costs higher than assumed in this study.
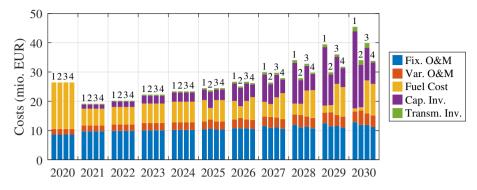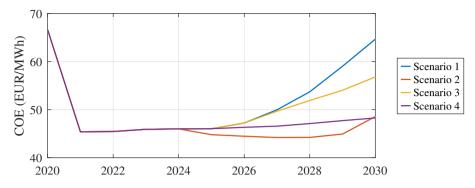
Fig. 3.26: Costs from 2020 to 2030 for scenarios 1-4. Scenarios: 1-reference, 2-tidal, 3-biofuel and 4-CO_2.

Table 3.38: Total costs (mio. EUR) from 2020 to 2030. Scenarios: 1-reference, 2-tidal, 3-biofuel and 4-CO_2.

Scenario	Fixed O&M	Variable O&M	Fuel costs	Capital inv.	Transm. inv. costs	Total
1	118	31	67	88	6	311
2	115	36	61	61	6	278
3	115	32	93	55	6	301
4	113	32	96	41	4	285

The cost of energy (COE) can be found by dividing the annualised costs presented in Figure 3.26 by the annual production presented in Figure 3.22. This gives an indication of how the optimised investments could affect the electricity price. In this case the COE only considers the costs of optimised investments and operation costs of the full system. The COE from 2020 to 2030 is shown in Figure 3.27, and the data is tabulated in Table A.19. The COE decreases significantly from 2020 to 2021, and this is caused by the committed wind farms, i.e. the fuel costs are decreased significantly, see Figure 3.26. After 2021 the costs increase in every scenario. COE of the reference scenario (#1) are highest, but this is also predictable from the annualised costs previously presented. An interesting observation is that the reference scenario (#1) in 2030 is actually lower than in 2020, i.e. although expensive, investing in a 100% renewable power system would not increase the COE based on the data considered in this study. Ancillary services are not included in the COE, and thus the actual COE will be higher.

Fig. 3.27: Cost of energy (COE) considering optimised investments and production from 2020 to 2030 for scenarios 1-4. Scenarios: 1-reference, 2-tidal, 3-biofuel and 4-CO_2.

3.3.4 SENSITIVITY ANALYSIS

The final results of the optimisation that are presented are from the sensitivity analysis. The sensitivity analysis will show how the optimal capacities would be affected, if the costs are higher or lower than assumed in this study. The capacity of wind power in the sensitivity analysis is illustrated in Figure 3.28, and the data can be found in Table A.6 and Table A.7. The figure shows that wind power capacity is not very sensitive to the investment costs, but the variation in the investment costs of wind power and photovoltaic power, has an impact on the optimal capacity. 20% higher investment costs of PV power, would lead to a higher capacity of wind power, and vice versa with a 20% investment cost. In the years 2021 to 2025, a lower fuel cost or higher investment cost of wind power, would also result in a higher wind power capacity.
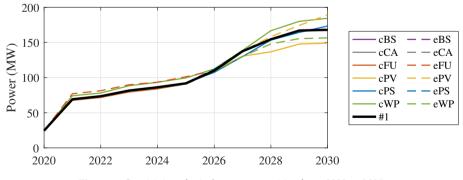
Fig. 3.28: Sensitivity of wind power capacities from 2020 to 2030.

The sensitivity of photovoltaic power can be found in Figure 3.29 and Table A.8. This shows that the PV capacity is sensitive to the investment

costs of PV, PS and WP. A 20% lower investment cost of PV (cPV), would result in 149 MW of PV compared to 79 MW in the reference scenario (#1). This same scenario resulted in a 19 MW reduction of wind power, i.e. 70 MW of PV power have to be installed to compensate for the 19 MW of wind power. Even with a 20% lower solar investment costs, the model does not invest in solar capacity until 2026, this shows that the technology with a 20% cost reduction still is unfeasible, but the challenge is to balance the system in the summer, and therefore the capacity increases significantly.
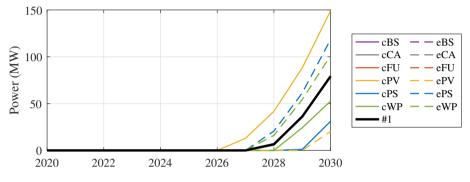
Fig. 3.29: Sensitivity of photovoltaic power capacities from 2020 to 2030.

The battery capacity is small in every scenario, but varies in some of the scenarios, see Figure 3.30. The data behind the figure is available in Table A.9. The largest difference is with a low battery cost (cBS), although the variations might be relatively large, the optimal capacity is so low, that the battery capacity in the expansion plan can be considered insensitive to +/-20% investment costs. Higher costs for the pumped storage system in R1 (ePS) and lower costs of PV power (cPV) increase the battery capacity slightly, this is due to the balancing challenge of region 7, where the battery system is located. A higher investment cost of cables (eCA) also results in a higher optimal battery capacity, as it leads to investing in cables becomes less feasible. This is also explained by the balancing of region 7.
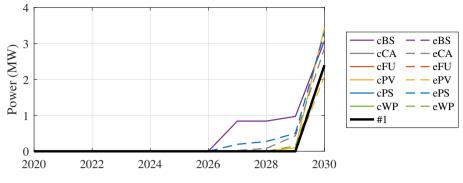
Fig. 3.30: Sensitivity of battery power capacities from 2020 to 2030.

The sensitivity of the turbine capacity at Heygaverkið is shown on Figure 3.31, and the data is found in Table A.5, and the respective data can be found in Table A.5. Seven of the sensitivity scenarios show a turbine capacity varying from the reference scenario (#1), but the variations are small and capacity in 2030 varies between 7 MW and 9 MW. This is the same range the capacity varied in scenario 1-4. More expensive cables (eCA) and less expensive batteries (cBS) have slight variations in 2029 and 2030, and this is likely related to what extent the PS system in R1 has to balance R7. Other variations are in the cost of wind power, PV power and the PS system. Cheap photovoltaic power (cPV) results in the lowest capacity of 7 MW.
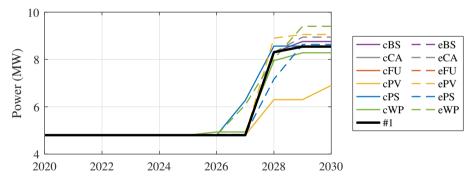
Fig. 3.31: Sensitivity of turbine capacity at Heygaverkið from 2020 to 2030.

The reservoir capacity at Heygaverkið is not significantly sensitive to the investment costs, see Figure 3.32 and Table A.5. There are variations in the optimal capacities caused by lower (cPS) and higher investment costs of PS system (ePS), PV power (cPV/ePV) and wind power (cWP/eWP), but the variations are small and the capacity is stabilised in most scenarios by 2030. Therefore the reservoir capacity at Heygaverkið can be said to not be significantly sensitive to the investment costs.
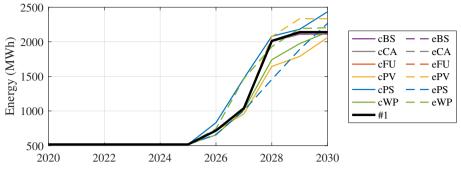
Fig. 3.32: Sensitivity of reservoir capacity at Heygaverkið from 2020 to 2030.

The turbine capacity at Mýruverkið can be found in Figure 3.33 and Table A.4. From 2021 to 2024 a 20% fuel cost reduction (cFU) would lead to a lower turbine capacity, but from 2025 and forward this scenario follows the reference scenario (#1). A cheaper PS system (cPS) would also lead to a slightly higher turbine capacity at Mýruverkið in 2028 and 2029, but in 2030 the capacity reaches the same point as the reference scenario (#1). Other variations are insignificant.
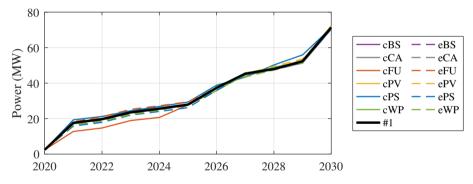
Fig. 3.33: Sensitivity of turbine capacity at Mýruverkið from 2020 to 2030.

A lower investment cost of the PS system (cPS) and a higher cost of photovoltaics (ePV) would lead to a significantly higher reservoir capacity at Mýruverkið and vice versa with a low cost of PS (cPS) and high PV cost (ePV). This once again, illustrates that the challenges is to balance the system in 2030. The sensitivity of the reservoir at Mýruverkið can be found in Figure 3.34 and Table A.4. The investment cost of wind power (cWP/eWP) also has an impact, but this impact is smaller than the other scenarios.
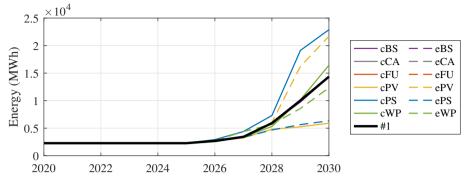
Fig. 3.34: Sensitivity of reservoir capacity at Mýruverkið from 2020 to 2030.

The pumping capacity at Mýruverkið can be seen in Figure 3.35 and Table A.4. The pumping capacity varies slightly when the investment costs of PV power, the PS system, wind power and the fuel costs are increased or decreased. The variations depending on wind power (eWP/cWP) and the PS system (ePS/cPS) are visible throughout the whole period, while the increased/decreased fuel costs (eFU/cFU) only impact the optimal capacity from 2021 to 2025, and the PV costs (ePV/ePV) impact capacity from 2027 to 2030.
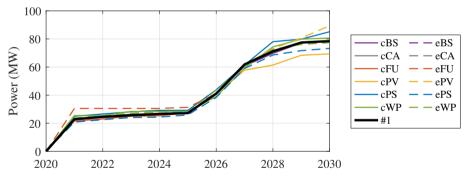
Fig. 3.35: Sensitivity of pumping capacity at Mýruverkið from 2020 to 2030.

The investments in transmission capacity between R1 and R5 is unchanged in all the scenarios until 2030, see Figure 3.36 and Table A.16. If the investment costs of PV are increased by 20% (ePV) the needed transmission capacity increases from 38 MW (scenario 1) to 45 MW, likewise an increase is seen if the PS system (ePS) or wind power is cheaper (cWP).
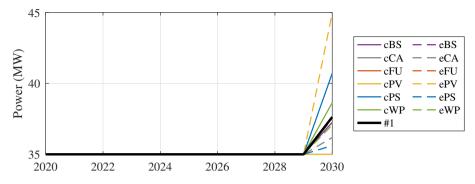
Fig. 3.36: Sensitivity of transmission capacity between R1 and R5 from 2020 to 2030.

Figure 3.37 shows the transmission capacity between R5 and R6. The capacity increases in all scenarios in 2023, and this is caused by the 44 MW committed cable. The reason that not all scenarios are at 44 MW in 2023, is because the optimised capacity from 2022 is added to the committed capacity. Therefore it is more interesting to look at the years from 2027 and forward, when the capacity increases further. Other from the difference in 2028 caused by the cheap PV investment costs (cPV), the variations are small. As all scenarios stabilise between 60 MW and 64 MW in 2030, the capacity of the cable connection between R5 and R6 is not considered sensitive to changes to investment costs. For further information on the data, see Table A.16.
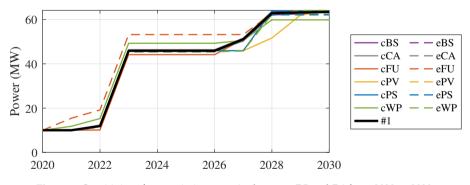
Fig. 3.37: Sensitivity of transmission capacity between R5 and R6 from 2020 to 2030.

The sensitivity of the connection between R6 and R7 is the final results shown from the optimisation in Balmorel. The results are illustrated on Figure 3.38 and tabulated in Table A.16. From 2021 to 2025 the fuel costs (eFU/cFU) have an impact on the transmission capacity, due to the alternative of importing energy from other regions being to burn fuel oil, or in later years were installing PV is considering an alternative. The investment cost of transmission cables (cCA/eCA) also influences the transmission capacity

throughout the period. All scenarios reach 12-13 MW in 2030 and therefore the transmission capacity between R6 and R7 is not considered sensitive to the present variations in investment and fuel costs.
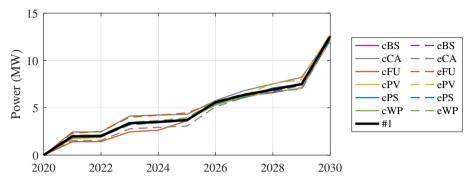
Fig. 3.38: Sensitivity of transmission capacity between R6 and R7 from 2020 to 2030.

3.4 CHAPTER SUMMARY

This chapter started by introducing the scenarios investigated in the study. This introduction was followed by an extensive modelling of the existing Faroese power system in Balmorel, and future potential power plants. The data used in the investigation ranging from demand, renewable resources, technology relevant data, costs etc. has been described in detail. Finally, the results from the economic optimisation were presented. The results show that reaching a 100% renewable production by 2030 is a challenge, especially in terms of balancing the system in the summer, but it is possible. Alternative technologies have the potential to become game changers. In this study investing in tidal power and burning biofuel at an existing thermal power plant were the alternative technologies. These two have a major impact on the future power composition, and the development of tidal energy and the costs of biofuels should be closely monitored. Investing in renewables in the Faroe Islands is the financially best option up to 86%-87% according to this investigation, but after this the renewable percentages do not earn back the investment costs. The sensitivity of the optimal capacities has also been investigated by varying the investment costs of wind power, PV power, battery systems, the PS system, transmission cables and the fuel costs. The majority of the sensitivity analysis results did not show a high sensitivity to the variations, but in some cases e.g. PV power capacity, significant differences are seen when varying the investment costs. Generally, the investment costs of wind power, PV power and the PS system had the greatest impact on the optimal capacities. Although the variations in some cases were noticeable, the variations in the first four scenarios are larger, and therefore one can say

that the optimal capacities are more prone to the development of alterna-
tive technologies than the fuel costs and investment costs of existing mature
technologies. An expansion plan towards 100% in 2030 has to be based on
the first scenario, as this scenario is the most realistic scenario in terms of
reaching the goal. But the development and costs of technologies should be
monitored, and the optimisation should be rerun, when changes occur.

The results in this optimisation are in some cases similar to previous stud-
ies, but the difference is also quite large in some cases. Compared to the main
scenario in the first optimisation of the Faroese power system in Balmorel [95]
the 2030 wind power and PV are quite similar, i.e. 168 MW compared to 141
MW of wind power and 79 MW compared to 75 MW of PV power. The
demand projection in this study is higher than in the previous, which can
explain the higher capacities. This study also uses a power curve for wind
power which has been based on the actual performance of existing wind
turbines, and not just a power curve from the manufacturer. The pumped
storage capacities in this study are however significantly higher than in the
previous study. In the previous study the optimisation could decommission
thermal power plants, but not recommission. This means that if for one year
part of diesel plants are not needed, they will be decommissioned, and can
not be used in the years after. This requires more investments in renewables
in the first years, as the power capacity is needed and the fossil fuelled power
plants can not be used. There is also a difference in when PV power becomes
economically interesting. In the results presented in [95] PV is included from
2024, while in this study it does not become a part of the optimal solution
until 2028. This can be due to the decommissioning of the thermal power
plants, but a higher cost for PV based on actual projects in the Faroe Islands
have also been used in this study.

The optimal wind and PV power capacities in reference [82] vary quite
significantly from this study, with higher PV power capacities and lower wind
power capacities. The exact cause can be difficult to point out. The reason
being that the optimisation is only conducted for 2030 and the optimisation
algorithm used is much simpler than Balmorel. It does not have as many
constraints and the input data is limited to one time series for each resource.
However, the solar data was updated, which can be the cause of the PV
capacities increasing.

Reference [83] and this study are more similar. Similarly to reference [82]
the study suggests higher PV capacities and lower wind power capacities
than this study does, but the deviation is significantly smaller.

CHAPTER 4
100by2030 RoadMap

This is the third and final chapter addressing the first objective. This chapter describes the procedure and results of translating the optimal results to a tangible RoadMap. The validation of the RoadMap is also presented in this chapter.

4.1 TRANSLATION OF OPTIMAL RESULTS

The following section will go through the optimal capacities at each site, according to the reference scenario, and translate them into a realistic RoadMap through the methodology presented in Figure 2.6. The reference scenario has been used as the base for the RoadMap, due to the uncertainties of development of e.g. biofuels and tidal power. Table 4.1 shows the optimal and proposed RoadMap wind power capacities at sites, which Balmorel invests in wind power at.

W6 has a capacity of 6 MW from start, and by 2023 the wind farm in R7 has reached its full capacity at 12 MW according to the optimal results. In the RoadMap W7 remains at 6 MW until 2023, when it is expanded to 12 MW. Thus, the investment at W7 is conducted in one step, when there is a need the full capacity, according to the optimal results.

W6b is a new wind power site, and is assumed to have a maximum power capacity of 36 MW, as presented previously in Table 3.20. The optimal capacity increases from 2021 to 2026, when it reaches its full capacity. In 2024 the capacity is optimised at 20 MW. A 36 MW wind farm in one step in 2026, is considered to be too big, when taking into account the learning curve of the power system operators. Therefore, the investment at W6b is done in two steps. If the investment will be conducted in two steps in reality, it is highly likely that it will be by 2x18 MW. Since the capacity in 2024 is 20 MW, which is only 2 MW higher than half of the wind farm, the RoadMap capacity at W6b is set to 18 MW in 2024 and additional 18 MW in 2026.

In 2026 the capacity at wind farm W1b is optimised at 8 MW and then 18 MW in 2027, which is the maximum capacity at W1b. Therefore the optimal results at wind farm W1b have been translated into a 18 MW investment in

2027.

The optimal capacity at W6a is 17 MW in 2027 and reaches 30 MW the year after. In 2028 it is assumed that the operators have gained more knowledge on operating large wind farms, and that it is possible to increase the capacity in one step by 30 MW, therefore the proposed RoadMap contains an investment of 30 MW at W6a in 2028.

The two final sites, at which Balmorel invests in wind power are in the same region, i.e. wind sites W5a and W5c. The maximum capacities are 21 MW and 18 MW respectively. The optimal investment at W5a is 4 MW, which is too small to be considered a realistic size wind farm in 2029-2030. There is an existing wind farm in R5 of this size, but the technology and knowledge has developed a lot since this wind farm was installed. As W5c is optimised at 43, i.e. 13 additional MW, and W5a is 4 MW, it is recommended to add the capacities at these two wind farms together and install 18 MW at W5c in 2030. W5a should then be the next wind farm to invest in after 2030. The 18 MW investment at W5c in the RoadMap is conducted in 2030. Installing 18-21 MW at W5a instead of 18 MW at W5c has minimal impact on the economic aspect, therefore this wind farm could be moved due to factors other than what is economically optimal. This could e.g. be that in 2030 there are already 30 MW installed at W5c, and an additional wind farm of 18 MW, would likely lead to some technical difficulties, as it increases the risk of a large loss of generation when wind speeds or direction suddenly change.

Table 4.1: The optimal and proposed RoadMap wind power capacities (MW).

Site	Scenario	2020	2021	2022	2023	2024	2025	2026	2027	2028	2029	2030
W7	Reference	6	8	8	12	12	12	12	12	12	12	12
	RoadMap	6	6	6	12	12	12	12	12	12	12	12
W6b	Reference	0	7	11	16	20	26	36	36	36	36	36
	RoadMap	0	0	0	0	18	18	36	36	36	36	36
W1b	Reference	0	0	0	0	0	0	8	18	18	18	18
	RoadMap	0	0	0	0	0	0	0	18	18	18	18
W6a	Reference	0	0	0	0	0	0	0	17	30	30	30
	RoadMap	0	0	0	0	0	0	0	0	30	30	30
W5a	Reference	0	0	0	0	0	0	0	0	4	4	4
	RoadMap	0	0	0	0	0	0	0	0	0	21	21
W5c	Reference	12	30	30	30	30	30	30	30	30	42	43
	RoadMap	12	30	30	30	30	30	30	30	30	30	30

Photovoltaic or solar power can be installed on roof tops, fields and on waters. Therefore, the topic of defining realistic plant sizes has not emphasised when it comes to PV power. Instead, the RoadMap capacities have been set equal to the optimal results. In S7 there are however some small differences as seen in Table 4.2. The capacities in 2029 and 2030 have been rounded

up, to ensure that there is enough power available. The optimal capacities in S7 in 2029 and 2030, rounded to 3 decimals are 14.496 MW and 15.396 MW. From the capacities shown in Table 4.2, it is clear that the need for PV power is especially in R4, and this is likely caused by the fact that the only potential wind farm site is 70% more expensive than other wind farms, and the only hydro power plant is rated at 1.4 MW, which is far from enough to supply this region, which has a relatively large demand. Since there is a loss associated with transmitting energy between the regions, PV becomes a significant part of the optimal solution in this region.

Table 4.2: The optimal and proposed RoadMap solar power capacities (MW).

Site	Scenario	2020	2021	2022	2023	2024	2025	2026	2027	2028	2029	2030
S7	Reference	0	0	0	0	0	0	0	0	7	14	15
	RoadMap	0	0	0	0	0	0	0	0	7	15	16
S4	Reference	0	0	0	0	0	0	0	0	0	22	61
	RoadMap	0	0	0	0	0	0	0	0	0	22	61
S6	Reference	0	0	0	0	0	0	0	0	0	0	3
	RoadMap	0	0	0	0	0	0	0	0	0	0	3

The battery power in the optimal solution and the RoadMap can be found in Table 4.3. The only investment in battery power is 2.4 MW in R7 in 2030. Similarly to the PV capacity the investment has been directly transferred into the RoadMap. Since batteries are modelled with a C rating of 0.25, it has a storage capacity of 9.6 MWh.

Table 4.3: The optimal and proposed RoadMap battery power capacities (MW).

Site	Scenario	2020	2021	2022	2023	2024	2025	2026	2027	2028	2029	2030
R7	Reference	0.0	0.0	0.0	0.0	0.0	0.0	0.0	0.0	0.0	0.0	2.4
	RoadMap	0.0	0.0	0.0	0.0	0.0	0.0	0.0	0.0	0.0	0.0	2.4

There are 5 investments which are optimised at the pumped storage system in R1; two turbines, two reservoirs and one pump. All of these are shown in Table 4.4. Since all five optimised capacities are parts of the same system, the investments in the RoadMap have to be coordinated. According to the optimisation:

- The needed turbine capacity at Heygaverkið in 2030 is 9 MW, which is also needed in 2029.

- The reservoir capacity at Heygaverkið increases to a total of 2141 MWh, which similarly to the turbine, is reached already in 2029.

- The turbine capacity at Mýruverkið increases from 2 to 18 MW already in 2021, and then increases more as the years pass.

- The reservoir capacity at Mýruverkið increases to 14355 MWh in 2030.

- The pumping capacity at Mýruverkið reaches a significant size already in 2021.

The previous RoadMap (Figure 2.5) suggests doing the investments at Mýruverkið in two similarly sized steps. Therefore it has been decided that the expansions are Mýruverkið at conducted in 2026 and 2029. The first step includes adding additional turbine capacity and new pumping capacity. In the second step the reservoir size is increased and Heygaverkið is expanded, both in terms of reservoir size and turbine capacity. The investments in the RoadMap are done in integer values unlike the optimal solution, which has multiple decimals, therefore the numbers in the RoadMap have been rounded up, and thus higher in the RoadMap than in the optimal solution.

Table 4.4: The optimal and proposed RoadMap pumped storage capacities. H: Heygaverkið and M: Mýruverkið.

Site	Scenario	2020	2021	2022	2023	2024	2025	2026	2027	2028	2029	2030
H - Turb. (MW)	Reference	5	5	5	5	5	5	5	5	8	9	9
	RoadMap	5	5	5	5	5	5	5	5	5	9	9
H - Res. (MWh)	Reference	516	516	516	516	516	516	716	1040	2013	2141	2141
	RoadMap	516	516	516	516	516	516	516	516	516	2141	2141
M - Turb. (MW)	Reference	2	18	20	23	26	28	37	45	48	52	71
	RoadMap	2	2	2	2	2	2	37	37	37	72	72
M - Pump. (MW)	Reference	0	23	25	26	27	27	41	62	71	77	78
	RoadMap	0	0	0	0	0	0	41	41	41	79	79
M - Res. (MWh)	Reference	2275	2275	2275	2275	2275	2275	2689	3428	5915	10039	14355
	RoadMap	2275	2275	2275	2275	2275	2275	2275	2275	2275	14355	14355

The optimal investments in transmission capacity are shown in Table 4.5, together with the proposed RoadMap capacities. The onshore 60 kV transmission cables used in the Faroese power system are 44 MW, therefore each investment in onshore transmission capacity is set at 44 MW in the RoadMap. Previously 35 MW were used, and therefore the current capacity between R1-R5 is 35 MW. The R1-R5 capacity is optimised at 38 MW in 2030. This means that according to the optimisation only 3 additional MW are needed to transmit power between these two regions. As there is a need to increase the capacity, a 44 MW connection is added at R1-R5 in 2030.

The connection between R5 and R6 is currently a 20 kV connection, and thus the capacity is lower than between other regions. A new 60 kV connection with a capacity of 44 MW is committed in 2023, when a subsea tunnel will open between the two regions. In 2022 the optimisation suggests that 2 MW of transmission capacity should be added, and when the model is set to switch the 10 MW out with 44 MW, the optimised capacity is added to the 44 MW. This means that although the optimisation says that the optimal

capacity between R5 and R6 is 46 MW, it is not because 44 MW is too little, but rather due to the configuration of the model. However, in 2027 and forward the optimal capacity increases. Therefore, an additional connection of 44 MW is added in 2027.

Finally there is the potential new offshore cable connection between R6 and R7. In 2021 the model optimises a capacity of 2 MW, which then increases steadily to 8 MW in 2029, and then jumps to 13 MW in 2030. A cable connection between these two islands is required to reach a 100% renewable production in R7. In the RoadMap the investment is a 13 MW offshore cable in 2026, which is installed in 2026, as there already at this point is a need for significant transmission capacity.

Table 4.5: The optimal and proposed RoadMap transmission capacity (MW).
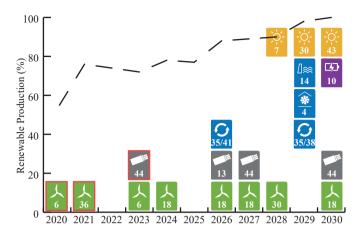
Site	Scenario	2020	2021	2022	2023	2024	2025	2026	2027	2028	2029	2030
R1-R5	Reference	35	35	35	35	35	35	35	35	35	35	38
	RoadMap	35	35	35	35	35	35	35	35	35	35	79
R5-R6	Reference	10	10	12	46	46	46	46	51	63	63	63
	RoadMap	10	10	10	44	44	44	44	88	88	88	88
R6-R7	Reference	0	2	2	3	4	4	6	6	7	8	13
	RoadMap	0	0	0	0	0	0	13	13	13	13	13

4.2 PROPOSED ROADMAP

Based on the translation of the optimal results presented in section 4.1, a figure illustrating the proposed RoadMap has been made, see Figure 4.1. The bottom row shows the wind power plants, the second shows transmission cables, the third and fourth the pumping and turbine capacities of the pumped storage system, the fourth row shows the storage capacities, i.e. reservoir sizes and battery. Finally, the top row shows the PV power. The figure only shows new investments, not existing existing capacity added with investments. The committed wind farms and cable are marked with a red border.

This RoadMap, compared to the previous one i.e. Figure 2.5, is more detailed and realistic. It has been assured that the investments reflect actual plant and cable sizes. The location of the investments, and local practical constraints like e.g. available space have been considered. The potential production is also calculated based on the local resource potential, instead of e.g. using the same wind speed profile for all locations. Since the Balmorel model is expanded to seven regions, the RoadMap also considers different demand profiles around the country, transmission losses and assures that the required transmission capacity is available. Overall, the capacities in the previous and proposed RoadMaps are similar, but there is more information behind the proposed RoadMap and it is therefore better grounded.

Fig. 4.1: Proposed RoadMap. Committed capacities are marked with a red border. All capacities are given in MW except from the second row from the top, where the reservoirs are given in GWh and the battery in MWh.

4.3 ROADMAP VALIDATION

The final step of the proposed methodology is to validate the proposed RoadMap. This is done defining the capacities in the RoadMap as committed capacities in Balmorel, and then rerunning the optimisation algorithm without any additional investment options. The two steps in the validation are to check whether or not the production is 100% renewable in 2030, and if the economics of the RoadMap are similar to the optimal solution.

The left axis of the RoadMap figure, see Figure 4.1, shows the renewable production (%) using the RoadMap as committed capacities. This shows that a 100% renewable production can be reached in 2030 based on the proposed RoadMap. Therefore, the proposed RoadMap can be validated according to the first requirement.

The second validation parameter is the economics. The optimality of the economics of the RoadMap is validated by comparing it to the economically optimal solution, i.e. the reference scenario. This comparison can be seen in Figure 4.2. The costs of transmission cables have not been included in the validation, as these capacities are set significantly higher in the RoadMap than the optimal results require, and these expansion are necessary to transmit the power regardless. According to the figure, the RoadMap scenario (RM) is more expensive for most years, but in 2027 and 2028 the RM is less expensive and in 2020, 2026 and 2030 the values are very similar. The main difference between the two scenarios is that the fuel costs are higher in the RM, as investments in renewables are conducted later. The sums of the costs shown on Figure 4.2 are 305 mio. EUR and 316 mio. EUR for the optimal solution and the RoadMap, respectively. In other words, the RoadMap is 4% more expen-
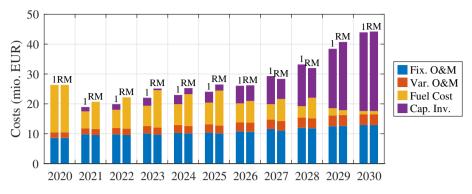
Fig. 4.2: Comparison of the economics of the reference scenario and the RoadMap (RM).

sive over the 10 year period simulated. This is considered to be sufficiently close to the optimal solution, and therefore the economic parameter can also be validated.

4.4 CHAPTER SUMMARY

This chapter has presented the proposed RoadMap towards a 100% renewable electricity sector in 2030 in the Faroe Islands. The RoadMap is based on an economic optimisation, presented in the previous chapter. The optimal solution at each potential investment site has been carefully investigated and translated into actual investment projects. In order to ensure that the proposed RoadMap is close to the optimal solution, the simulation tool was run again using the RoadMap as committed capacities. Then it was validated through a comparison of the economics of the optimal solution and the RoadMap. It is also ensured that the production is 100% renewable in 2030. As the results of the different scenarios investigated in the previous chapter, show that the development of technologies like tidal power and biofuels could change the whole expansion plan, the RoadMap should be re-evaluated as changes in development and costs occur.

Table 4.6 compares the investments in the proposed RoadMap (Figure 4.1), the previous RoadMap (Figure 2.5 on page 37) and international studies (subsection 2.2.1 starting on page 27). As seen in the table the difference between the previous and this RoadMap is limited when only addressing the 2030 capacities, but the real contribution from the updated RoadMap is the placements and many practical considerations which have been made. Comparing the RoadMap to other islands described in subsection 2.2.1 is more difficult, as the basic assumptions, approaches and renewable energy shares (RES) goal of each study vary significantly. One interesting aspect is however the similarities between Madeira and the Faroese

RoadMap. Madeira is located at 33° North, while the Faroe Islands are located at 62° North. This should result in a higher solar potential in the Madeira than in the Faroe Islands, but the RAD values are quite similar. One of the causes could be that Madeira, just like the Faroe Islands, have hydro power. In 2010 the hydro power capacity in Madeira was 50 MW with an anticipated increase up to 80 MW [52], similar to the 40 MW hydro power capacity in the Faroe Islands, which with the first expansion of the pumped storage system will increase up to around 80 MW.

In addition to Madeira, an other interesting observation is the capacities in San Miguel with 75% renewable generation. In 2021, according to the RoadMap, the generation in the Faroe Islands is around 85% renewable with 70 MW of wind power, which corresponds to 150% of the average demand, compared to San Miguel with 140% of wind power. Hydro power is also the cause for the higher renewable shares in the Faroe Islands.

Table 4.6: Comparison of investments in the proposed RoadMap, previous RoadMap and international studies found in subsection 2.2.1 by RAD values. on: onshore, off: offshore.

Study	Comment	Wind, on	Wind, off	Solar	Storage	Waste	Gas	Geothermal
This RoadMap		224%		105%	8-9 days			
Previous RoadMap		202%		106%				
Antigua and Barbuda					25%			
Santiago, Cabo Verde	57% REN	156%		48%		16%		
La Palma, Canary Islands	If isolated	363%	534%	700%			81%	
La Palma, Canary Islands	If interconnected	363%	231%	700%			41%	
Madeira	Added capacity	206%		103%				
Saint Lucia	75% RES in 2025	26%		50%				65%
San Miguel, Azores	75% RES	140%						

CHAPTER 5
Power System Regulation and Modelling Theory

This is the first chapter addressing the second objective. The chapter describes how ancillary services traditionally have been provided and some of the state of the art technologies and approaches. Then Faroese study cases of the power system stability are also presented. Finally the aspect of parameterising and validating power system models is addressed, which includes a development of a procedure for this specific purpose.

5.1 PROVISION OF ANCILLARY SERVICES

The provision of ancillary services is changing as synchronous generators are being decommissioned and replaced by inverter-based generation (IBG) to minimise emissions from the electricity production. The traditional approach to provide ancillary services is described in subsection 5.1.1 followed by state of the art approaches, see subsection 5.1.2.

5.1.1 TRADITIONAL APPROACHES

In conventional power systems synchronous machines provide the ancillary services required to stabilise the system after a disturbance. The motion of a synchronous machine can be described by the swing equation [125],

$$\frac{2H}{\omega_\mathrm{s}} \frac{\mathrm{d}^2 \delta_\mathrm{m}}{\mathrm{d}t^2} = P_\mathrm{m} - P_\mathrm{e} \tag{5.1}$$

where H is the inertia constant of the machine, ω_s is the electrical angular velocity, δ_m is the rotor position, P_m is the mechanical power and P_e is the electrical power. A potential power deficit between mechanical and electrical power, can be caused by a sudden load increase, and this deficit is supplied by the inertia of the machine. When the inertia, is released, the speed of the generator drops, which leads to a frequency drop, due to the machine being synchronised with the grid. Thus, the rate of change of frequency after a disturbance depends on the inertia in the grid and the disturbance itself. This initial response, is known as the inertial response. The inertia in conventional

power systems is primarily from synchronous generation, but frequency dependant loads e.g. motors, can also increase the system inertia [126]. After the inertial response, the frequency drop is stabilised by primary frequency control. This task is performed by the synchronous machines' governors, by detecting the frequency and then adjusting the active power output to stabilise the frequency drop. A governor is a proportional controller; hence, a steady state error from the nominal frequency is obtained after the frequency has been stabilised. In order to correct this error, secondary control has to be applied. Secondary control can be automatic or manual. In the Faroe Islands it is manual. Figure 5.1 show the different stages of frequency control reserves are deployed in the European grid [127]. There are no definitions in the Faroese power system with regards to this. The synchronous machines are also equipped with an automatic voltage regulator (AVR), which regulates the voltage and keeps it stable. As shown in the swing equation the frequency is linked with the active power, but the voltage is primarily linked with the reactive power. The AVR controls the excitation and thus the reactive power of the machine, in order to stabilise the voltage [125].
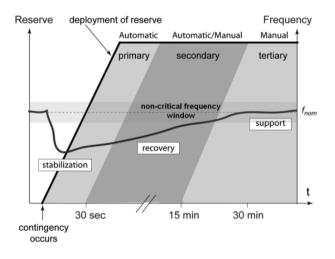
Fig. 5.1: Deployment of frequency control reserves in the European grid [127].

5.1.2 STATE OF THE ART APPROACHES

The state of the art approaches to provide ancillary services utilise wind turbines, photovoltaic (PV) panels, battery systems (BESS), vehicle to grid (V2G), heat pumps (HP) etc. Some of the approaches found in literature are described in the following paragraphs.

Variable speed wind turbines are galvanically decoupled from the grid, through converters. This means that the wind turbine generators are not

synchronised with the grid and therefore do not have the same automatic inertial response and primary frequency regulation, which synchronous generators have. Some types of wind turbines have this automatic reaction, but over 90% of the wind power installed in the Faroe Islands are variable speed turbines. This being said, these variable speed turbines can be controlled to emulate inertia. Inertia emulation can become an important part of the frequency regulation in the Faroe Islands, as the wind penetration is expected to increase significantly. In the purpose of describing this control, one of the proposed wind turbine controllers is shown on Figure 5.2 [128]. This is a simple controller, which emulates both an inertial response (middle branch) and can contribute to primary frequency control (lower branch). The inertia emulation is as shown controlled based on df/dt, while the primary frequency control is controlled based on the deviation from nominal frequency, Δf. Both controls have a deadband. Another, more detailed controller, can be found in [129].
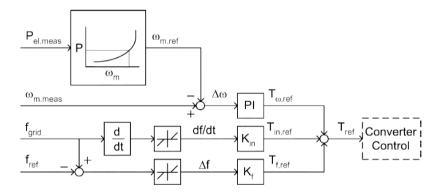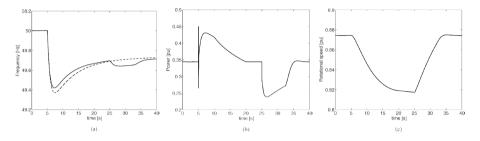
Fig. 5.2: Proposed controller. Upper branch: wind rotor control. Middle branch: inertia emulation. Lower branch: frequency control support [128].

Figure 5.3 shows an example of the response of the controller in Figure 5.2 to a contingency. The minimum frequency (a) reached is slightly higher with the controller on (solid) than off (dashed), this indicates that the controller can improve the frequency response, but (b) and (c) show that there are disadvantages with this controller. When the controller reacts to a contingency, it increases the power output. This is done using the kinetic energy stored in the rotor. When the kinetic energy is extracted the rotational speed decreases, which means that the turbine is spinning with a speed different from the optimal speed. In order to increase the speed after the control, the power output of the turbine drops significantly, as seen at around 25 seconds. Wind turbines are usually not considered for long term regulation, as this would require curtailment of wind turbines, in order to have reserve power. This

would results in a great loss of potential production, and it does not ensure a reserve, as the wind speed and direction can shift rapidly.

Fig. 5.3: Response to disconnection of synchronous generator with controller ON (solid) and controller OFF (dashed). (a) Grid frequency. (b) Wind turbine power. (c) Wind turbine rotational speed. (b) and (c) are with the controller ON [128].

Researchers have also investigated the possibility of using PV panels in frequency regulation [130]. This is done by always producing 10% less than the maximum power point and applying a droop controller. This way a PV system can be shown to support to grid. However, in the Faroe Islands, where the solar resources are low, operating 10% lower than the potential, might not be the most feasible solution to provide regulation, and therefore the financial consequences of down regulation should be analysed and the feasibility should be compared to other control strategies and technologies.

Battery systems are used for frequency regulation in the Faroe Islands, as described in section 1.2, and this has also been investigated in several studies. This is done by controlling the batteries to respond to e.g. a frequency drop. This was studied already in 1993 for the Israeli system [131]. In the Japanese Oki-Islands a demonstration project with a hybrid battery system has been conducted [132]. The aim was to be able to increase the installed capacity of renewables from 3 MW to 11 MW, by implementing a battery system. The minimum demand in the Oki-islands is 10 MW, and thus 11 MW is a high penetration of renewables. Currently, the penetration has reached 8 MW. The battery system consists of a 2.0 MW/0.7 MWh Li-ion battery system and a 4.2 MW/25.2 MWh NaS battery system. The purpose of the Li-ion batteries is to provide short term frequency regulation, while the NaS batteries are used for long term frequency regulation. Figure 5.4 shows an example of the operational performance of the investigated system. From the figure it is clear that the two battery systems do not behave in the same way. The Li-ion battery output is fluctuating on a short term basis, while the NaS output varies more throughout the day.
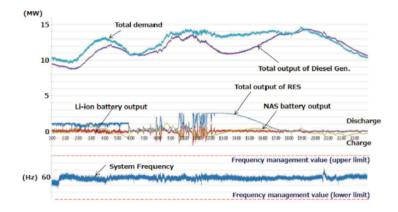
Fig. 5.4: Example of operation performance [132]

The vehicle to grid (V2G) concept, is a concept where electrical vehicles (EV) are used to support system stability [133]. The V2G concept has been investigated in the island of Bornholm (Denmark) [134], [135]. An electrification of the transport sector is anticipated, and therefore this research topic is of great interest. The aim is to use the storage in EVs to support the grid. Two different controller modes are used in [135]. One is a droop control and the other a PI control. The results of the study show that the EVs can contribute to regulation, however the droop control mode requires a larger battery capacity than the PI control. The capacity also depends on the parameters of the controller. In case of using the PI control, a battery capacity that is 30-40% of the installed wind power capacity should be available to meet a sufficient frequency quality. It should be noted, that even though the island is electrically connected to the mainland, this study investigates the grid in isolated operation, making the results relevant for other isolated systems like the Faroe Islands. The disadvantage with using V2G is that not all EVs are capable of this, it requires the EV owners approval and it might also lead to unnecessary wear and tear of the battery of the EVs.

Supplementary load frequency control using heat pumps (HP) was discussed in [136]. This study considered V2G as well. The maximum frequency deviation reached in this study using EVs but not HPs for regulation was 0.251 Hz. Utilising the HPs as well the maximum was reduced to 0.225 Hz. The average frequency deviation was reduced from 0.0272 Hz to 0.0263 Hz when the HPs were added to the controller. In the Faroe Islands it is expected that the heating sector will be electrified, and most houses will be heated using HPs. This makes utilising HPs for frequency regulation highly relevant.

According to [137] both heating and transport can also be used for voltage regulation, not only frequency regulation. The author models electric water

heaters, heat pump water heaters, electrolyser system and electric vehicles as active loads used for voltage regulation. In this study the customers comfort is considered, meaning that the units can only be used for regulation, when this does not affect the customers comfort, i.e. the temperature in the water tank must be at a certain level.

A study case of the South Korean island Jeju with a hybrid voltage control system is described in [138]. This control uses the generators' traditional AVR and passive devices such as capacitors and reactors when the AVR do not meet a sufficient reference. The control was tested for an emergency state and was shown to be feasible.

One study investigated the maximum installed PV capacity per house whilst preventing overvoltages with and without reactive power regulation contribution from PV inverters [139]. According to this study, the maximum allowed PV capacity per house could be increased from 5.3 kW to 7 kW, if the PV inverters were allowed to absorb reactive power. The study also showed that if a transformer overloading of 120% was allowed, the maximum PV capacity could be 8 kW. This means that a grid with a high PV penetration could benefit by allowing the PV inverters to contribute to voltage regulation.

This section has presented the traditional and alternative state of the art methods to provide ancillary services. The state of the art alternatives include control strategies of wind turbines, PV panels, BESS, HPs, EVs etc. that can contribute to power system stability.

5.2 FAROESE POWER SYSTEM STABILITY STUDIES

There are only a handful of previous studies of the power system stability in the Faroese power system, and these can be found in references [100], [140]–[143]. All of these studies have been conducted using power system models of the Faroese power system, but these have not been validated. The final part of this section, i.e. subsection 5.2.1, describes a study [144] conducted in this research project using an aggregated model with standard models and default parameters of governors and AVRs. The results of this study emphasises the need for validated models.

One of stability study [100] was a part of the previously discussed extensive expansion planning study [90]. This study states that there will be a need of grid reinforcement, load shedding, battery systems etc. in the main grid in order to ensure a stable power system in 2030. The power system of Suðuroy should, with the planned battery system, be able to main the stability within acceptable limits.

Reference [140] applies a load shedding control strategy using fish factories. Load shedding contributes to the stability, but the ability to load shed a fish factory depends on the whether or not the freezing units at the fish factory are in use at the time when a disturbance happens.

Østerfelt and Hansen [141] use synchronverters to contribute to grid stability. The simulations show a positive contribution from the synchronverters, but there are some disadvantages, as well. Under short circuit scenarios, the synchronverter draws 75 kA, which is 7 times the nominal current under full load. The harmonics from the synchronverter switching frequency should be investigated further as well, and thus, the reliability of the results can not be assured.
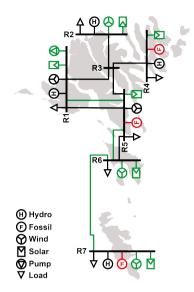
Using and sizing battery systems for inertial response and primary frequency reserve in Suðuroy was addressed in reference [142]. However, following the sizing method used and modelling technique the BESS did not sufficiently support the grid.

Finally using heat pumps for secondary frequency control in Suðuroy has been investigated [143]. The results showed that heat pumps could contribute to the frequency stability, but that the controller, needed additional tuning to have a significant contribution to the system.

5.2.1 STUDY BASED ON AGGREGATED MODELS

One of the studies [144] of this research project has shown the importance of using accurate and detailed models for dynamic analysis of the frequency stability. This study analysed both the main grid as it was in 2019, and the main grid in 2030, which also includes a subsea cable to the isolated grid of the most southern island Suðuroy, i.e. R7 in Figure 5.5. The expansions in generation and storage capacity in 2030 were based on the previous RoadMap [90], as the study behind the updated and expanded RoadMap [81] was not finished. Since the previous RoadMap did not specify the locations of future investments, the wind power plants and PV farms were placed according to best guess from SEV's engineers.

Figure 5.5 shows how the model of the Faroese power system has been aggregated. The system has been aggregated to the regions used in the Balmorel optimisation [81] (previously presented in Figure 3.1 on page 47). This means that if multiple diesel engines are placed in one region, e.g. R5, these are aggregated to one generator, and similarly with wind turbines, hydro turbines and loads. Some of the regions also have multiple substations and power plants, and these are also aggregated to the same level. Also, as shown in Figure 1.3 on page 7, the number of power plants and substations is larger than the number of regions, so it is not only generators which have been aggregated, but the power plants and substations as well.

Fig. 5.5: Single line diagram of the aggregated model of the Faroese power system. Black objects are online both in 2019 and 2030, red objects are offline in 2030 and green objects are only online in 2030 [144].

The diesel generators were modelled with the standard gov_DEGOV1 and avr_IEEET1 models with default parameters, and similarly the hydro turbines were modelled with gov_HYGOV and avr_IEEET1, also with default parameters. The wind turbines and PV panels were modelled as negative loads, where the load is controlled by a time series with production data inversed. The pumped storage system was modelled as a load equal to the excess wind power.

The frequency stability was analysed for the following three scenarios:

1. A dynamic simulation over a whole week day without disturbances, but with minute based varying load, wind power, PV power and pumping consumption.

2. A sudden 5% load increase on all loads. The load in the specific hour in 2019 was 30 MW and 70 MW in 2030.

3. A sudden outage of the line between region 1 and 3.

Running a full day simulation with varying production requires a secondary control, because otherwise the frequency will just increase and decrease depending on the wind power production and demand, and will not be regulated back to 50 Hz. Therefore an automatic secondary frequency controller was developed for this purpose. However, the secondary control in the Faroe Islands is manual. The next chapter will present how the man-

ual secondary controller has been modelled in the validated power system model.

A wind turbine regulator (WTR) was also developed to see how wind turbines could contribute to frequency regulation. Please see reference [144] for further specifications on the WTR and secondary frequency controllers, as the aim of this subsection is to emphasis the need of validated models rather than specific details on modelling approaches.

Figure 5.6 shows the simulated frequency in 2019 and 2030 over a whole day (scenario 1), using the aggregated models with default parameters. The deviations from the nominal frequency are larger in 2030 than in 2019, but the deviations are in both cases significantly smaller than in reality. The frequency in the Faroe Islands can vary between 49.5 Hz and 50.5 Hz under normal operation. However, the frequency varies between 49.974 Hz and 50.029 Hz in 2019 and between 49.969 Hz and 50.033 Hz in 2030. The standard deviation increased by 50% from 2 mHz to 3 mHz, but this deviation is significantly lower than in the actual system. An analysis of the frequency measurements in Suðuroy show that prior to the wind farm, the standard deviation in the frequency was between 45 mHz and 46 mHz from 2018 to 2020, and after the wind farm has been installed, this has increased to 90 mHz. These values are calculated based on Figure 3 in reference [145]. These simulations therefore show that these aggregated models with standard models and parameters, do not reflect the behaviour of the actual system. Hence, there is a need to have a validated model of the Faroese power system, in order to obtain accurate and applicable simulation results.
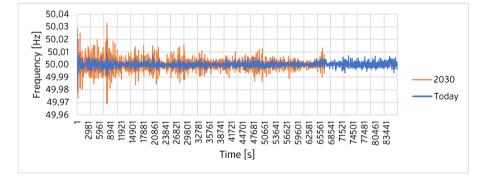
Fig. 5.6: The frequency under steady state operation over one day [144].

The scenario with a 5% load increase is shown in Figure 5.7. This scenario was run with and without the WTR. Again, the frequency is clearly worse in 2030 than in 2019, but the maximum frequency is well within the normal operation limits (49.5 Hz to 50.5 Hz) according to the simulation. A 5% load increase is a quite severe disturbance, and should have a great impact on

any system, but it does not cause any alarming situations in the simulations, which again indicate that the model is not sufficiently accurate to use for realistic dynamic studies of the Faroese power system.
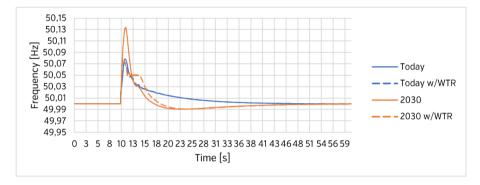
Fig. 5.7: The frequency response in today's system and in 2030 to a 5% load decrease at hour 1 with and without the wind turbine regulators (WTR) [144].

The connection between R1 and R3 is an important connection in the system, and therefore a fault on the line can lead to blackouts in the system. This however depends on how much the line is loaded. In the simulation for 2019 only 0.07 MW are being transmitted, while in 2030 it is 5.6 MW (around 9%). According to the simulations however (Figure 5.8), an event of such leads to a minimum frequency of 49.985 Hz and maximum of 50.005 Hz, which again is well within the limits. Thus, the third scenario also indicates that there are some differences between the simulation and responses which would be observed in the actual system.
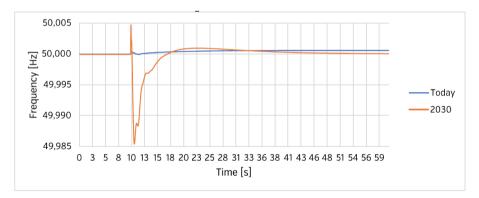
Fig. 5.8: The frequency response to an outage of the line between R1 and R3 [144].

The results shown here clearly indicate that using an aggregated model with standard controllers and default parameters does not lead to accurate

results, and thus can not be used for power system planning. There is a need to obtain a detailed model which can be validated.

5.3 VALIDATION OF DYNAMIC POWER SYSTEM MODELS

This section describes some common approaches to power system model validation, the validation process of the Faroese power system and a finally a new method to parameterise and validate models is presented.

The motivation of validating power system models was emphasised in the previous section, subsection 5.2.1. Other studies, not related to the Faroese power system, have also discussed the need for validated models, which can be used both to analyse previous disturbances, and to plan for the future [146]–[149]. These studies also state that obtaining a validated model can be difficult due to fact that each component and parameter can have a significant impact on the simulations. This is especially difficult when the available information on the different components are limited, and many parameters therefore are unknown. This is the case for e.g. the AVRs in Cyprus [150].

Measured data is required in order to validate a model. In the past it was common to use frequency response measurements [151], [152], while today using active and reactive power measurements together with frequency and voltage is commonly used. This data can either be retrieved from planned tests or unstaged measured disturbances [146], [147]. During a staged tests, there are more known parameters, than during an unstaged tests. This can be an advantage when parameterising. However, a staged test requires access to the grid and permission to conduct the test. This can be a long process in larger grids, but the time to wait for enough data for parameterising based on unstaged tests is unknown and there is no guarantee that the needed data will be obtained at all.

There are several methods to parameterise dynamic models, both manual [150] and automatic [153]–[155]. One way is to by a trial-and-error process vary the parameters. This can be very difficult, and requires a lot of experience. Especially when parameterising a whole system, and not only one controller, as a controller reacts to the performance of other controllers in the synchronised grid. In order to simplify this, many optimisation algorithms have been applied in previous literature [153]–[155]. The objective function of the optimisation is then set to minimise difference between measurements and simulations.

When parameterising a model it is desired to find the global optimum set of parameters, instead of a local optimum. If only one event/disturbance is used to parameterise a model, the likelihood of finding a local optimum is higher than if several events are used. One of the few studies that utilises multiple events to parameterise is reference [149], which parameterises a generator's parameters. This study showed that a better set of parameters were

obtained when multiple events were used.

Reference [156] compares two methods of validating power system models, these are Hybrid Simulations (HS) and System Wide Simulations (SWS). For example HS is by Kosterev in e.g. reference [157], while [158] uses SWS. An example of HS is shown in Figure 5.9. HS is a simulation of a subnetwork and uses measurement data as input. the figure shows a subnetwork consisting of a wind turbine (W) and a synchronous generator (G). The subnetwork is connected to a larger network, here called "External grid". There are measurements at the boundary between the subnetwork and the external grid. Time series of these measurements (V and δ on the figure) are used as input to the simulation, as shown on the right side of the figure, and the performance of the components to be validated are compared to measurements. In a SWS the whole power system is simulated to replicate measurements, i.e. loads, generation etc. are set equal to measurements and the disturbance measured is initiated in the simulations as well. Measurements and simulations are compared.
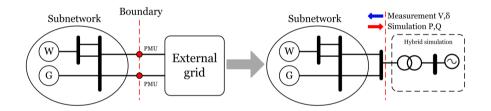
Fig. 5.9: Example of Hybrid Simulation (HS) [156].

The advantage with SWS is that it shows the responses of the whole system and the interactions between different controllers is accounted for, but it can be difficult to validate a whole system simultaneously. HS simplifies the validation significantly, but studies [159], [160] have shown that HS is not always sufficient, although it is important in terms of power system model validation [148]. Reference [160] proposes combining the two approaches using HS for initial parameterisation of the models, and SWS for validation.

5.3.1 ROAD TO A VALIDATED MODEL OF THE FAROESE POWER SYSTEM

Obtaining a validated dynamic RMS model of the Faroese power system, has been a long process. SEV has used consultants to build and maintain the model in DIgSILENT's PowerFactory, first Dansk Energi and currently AFRY Denmark. At the start of this project, AFRY had built a static model, but not validated it. An initial parameterisation of the governors and AVRs had

been conducted, but this had not been validated. The first task of this PhD related to the PowerFactory model was therefore to validate the static load flow model. The causes behind the differences between the simulations and measurements, had to be identified and corrected. The causes were incorrect cable/line parameters, tap changer settings etc. After the load flow model was validated, the accuracy of parameterisation of the dynamic controllers was investigated. This investigation showed that the model could not be validated. Therefore the dynamic controllers had to be parameterised and validated for RMS simulations in this PhD.

Initially the parameterisation was conducted using HS for one scenario for each regulator. The parameters were adjusted manually and when the HS showed a good resemblance with the measurements, the model was said to be validated. This was considered to be good enough until a SWS, with the purpose of replicating an recorded event was conducted, revealed that the simulation with selected parameters could not replicate the measurements accurately.

The other obvious option was to parameterise with SWS, but obtaining correct parameters through manual adjustment of parameters in a multi generator system, can be difficult. Therefore a script which ran simulations with different combination of parameters was developed, and the results from each simulation were then exported from PowerFactory and compared to measurements to find the parameter combination which led to the highest correlation with measurements using MATLAB. This method was used until it became apparent that PowerFactory had a built-in module called System Parameter Identification (SPI).

SPI can optimise the correlation between measurements and simulations by using different parameter settings much faster than the developed script with exports to MATLAB. Thus, it was decided to utilise this this module. Using this module it was also possible to run multiple scenarios at the same time, and this increases the chances of finding a parameter set, which is globally optimal instead of locally, as previously discussed.

Running SPI with multiple scenarios using SWS requires high computational power, which can be minimised using HS, but the previous HS parameterisation did not result in a sufficiently accurate model. Therefore it was decided to use HS for main parameterisation and SWS for parameterisation in cases where HS showed insufficient results. This combines existing approaches to obtain models with increased accuracy. A procedure based on this has been developed as a part of this industrial PhD, and will be published in [161]. The procedure is also described in subsection 5.3.2 in this thesis. The procedure was developed in cooperation with AFRY Denmark.

5.3.2   PROPOSED PROCEDURE

The proposed procedure which combines hybrid simulations, system wide simulations and multiple scenarios, is shown as flowchart in Figure 5.10, and is described in the following sections. This procedure is not limited to this power system, these regulators or using PowerFactory as a software, but adjustment might be necessary depending on the application.
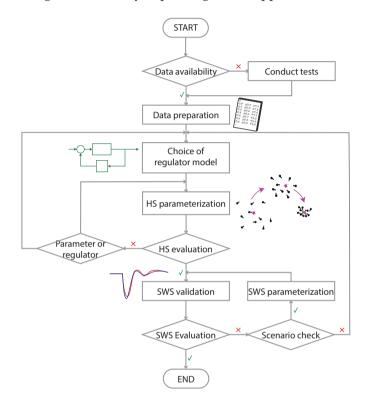
Fig. 5.10: Flowchart of the proposed procedure of parameterising and validating dynamic models [161].

Data Availability

The first step of the proposed procedure is to make sure that enough data is available to apply the procedure. The data used for the validation has to show active and/or reactive power dynamic responses of the generators and has to be without other interruptions, i.e. the system has to be stable before, during and after the event recorded. The scenario used can be either intentional (test) or unintentional disturbances.

The data used in the parameterisation and validation of the Faroese power system is generators' active and reactive power and the busbars' voltage and

frequency all measured with a resolution of 10 Hz, which is enough to capture the dynamic response for RMS simulations.

In order to get parameters, which can accurately represent the dynamic response for a wide range of events, it is important to have more than one scenario for parameterisation and validation. The more scenarios, the more accurate the parameterisation will be, but this also increases the calculation time and complexity of the procedure.

Conduct Tests

It is necessary to conduct tests on the system, if not enough data is available, which meets the requirements described in the previous step, i.e. *Data Availability*. These tests can e.g. be tripping of a generator or a load rejection.

Data Preparation

Depending on the software used, the data has to be prepared for the simulation. In this case the data has been defined as a measurement file in PowerFactory. A measurement file requires data to be stored in columns, of which the first column is a time series. There can be up to 24 columns of other data. This data can then be used to control some variables in PowerFactory. For the hybrid simulations the measured frequency and voltage stored in a measurement file have been used to control the frequency and voltage of a voltage source. The generators' active and reactive power has also been in SPI to compare measured and simulated responses. The data in a measurement file can also be plotted. Ensuring that the data does not have measurement faults, which can disturb the simulation, that parameters are given in the right unit and a suitable length time period is also a part of the data preparation.

Choice of Regulator Model

A model has to be chosen to represent each governor and AVR. The AVR models used are selected based on the IEEE Recommended Practice for Excitation System Models for Power System Stability Studies [162], and on input from the manufacturer. The DEGOV1 model is used for diesel governors and HYGOV model for hydro governors in Suðuroy. This procedure is however not limited to these models, as any model, standard or customised, can be used for parameterisation and validation.

HS Parameterisation

In this study the HS parameterisation has been done using the SPI tool in PowerFactory with particle swarm optimisation (PSO) selected as the optimi-

sation algorithm, see subsection 5.3.3. This is conducted for each regulator separately, but for all scenarios relevant to the regulator simultaneously. In order to do this for multiple scenarios simultaneously, it is necessary to define one HS network (see Figure 5.9) for each scenario in the same simulations. The parameters of the regulator to be parameterised, have to be the same for each HS network. In PowerFactory this is ensured using a configuration script.

HS Evaluation

The hybrid simulation is evaluated qualitative, i.e. the measured and simulated responses are compared and if the responses for all generators are estimated to have a similar pattern, minimum/maximum values and settling times, one continues to the system wide simulation. If the results are insufficient and the response can be improved by additional HS parameterisation, the adjustments have to be made before running a second HS parameterisation, as described in the next step.

Parameter or Regulator

In some cases adjusting a boundary of the optimised parameters can lead to a better parameterisation, while in other cases it can be necessary to conclude that using the chosen regulator will not lead to better results, and thus another regulator has to be used.

SWS Validation

The step *SWS validation* are simulations of the whole system, where the recorded event is replicated. This is conducted for all of the scenarios used for parameterisation.

SWS Evaluation

There are no standards on when a governor or AVR model is accurate enough, and therefore the evaluation is qualitative and based on criteria estimated in each study case. In this study the focus was that the response should have a similar pattern, minimum and/or maximum values and settling time. If the evaluation is successful, the dynamic models of regulators with respective parameters have been successfully validated, if not, a SWS parameterisation is conducted. This parameterisation is however only conducted on the specific regulator, which did not show an accurate response.

Scenario Check

Before the SWS parameterisation is conducted, it is checked whether or not all relevant scenarios have been used for SWS parameterisation. If no scenario is left, it is concluded that an accurate response can not be obtained using the chosen model. Therefore another model has to be used.

SWS Parameterisation

The SWS parameterisation is conducted using SPI on the regulator, which could not be validated after HS parameterisation. The SWS parameterisation is only conducted for one scenario at a time, unlike the HS parameterisation. The SWS can be run on each scenario relevant until accurate parameters have been found and validated through SWS validation.

5.3.3 THE PARTICLE SWARM OPTIMISATION

SPI in PowerFactory uses an optimisation algorithm, and in this study it was decided to use the PSO algorithm. The PSO method is inspired by a swarm of animals looking for food. Animals move according to their individual intelligence as well as the swarm's intelligence [163]. A two dimensional illustration of the PSO method can be seen on the left side of Figure 5.11. A number of particles/animals (the black circles) are moving in the x,y-plane and evaluating an objective function, a function of x,y. Particle A is marked with a red border. The latest position of Particle A (i-1) is to the left of the current position (i). The particle remembers its best previous position and also communicates with the rest of the swarm about their best location. Particle A's position in the next evaluation (i+1) is determined by its previous velocity (red line), the particle's best previous position (blue) and the swarm's best position (green). The right side of Figure 5.11 illustrates the movement of the swarm of particles through the iterations, where the purple star illustrates the best global position.

The PSO is a relatively fast algorithm compared to other options in SPI, e.g. DIRECT, but it does not ensure that the global optimum is found. In this study multiple scenarios are used for parameterisation simultaneously. This decreases the risk of finding a local optimum significantly. PSO is also a recognised method, which is used several similar studies [154], [158], [164], [165]. Hence, due to the fast optimisation and minimised risked of finding a local set of parameters, PSO was used for parameterisation.
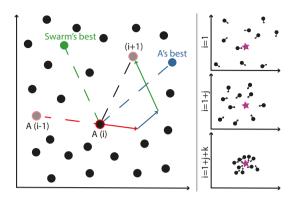
Fig. 5.11: Two dimensional illustration of Particle Swarm Optimisation.

5.4 CHAPTER SUMMARY

This chapter has introduced how ancillary services are provided using traditional methods, i.e. control of synchronous generators. It has also presented some of the state of the art approaches to e.g. use wind turbines, PV panels, BESS, HPs and EVs for ancillary services.

Previous studies of the Faroese power system related to power system stability have been described. The results from a study, which is a part of this PhD, but used aggregated and standard models were presented, and showed the need for validated power system models. There are different methods to parameterise and validate models, but due to insufficient results using existing approaches to validate the model of the Faroese power system, a new method, which combines several existing approaches has been developed. The application of this method is described in the following chapter.

CHAPTER 6
Faroese Power System PowerFactory Model

This chapter introduces the PowerFactory model of the Faroese power system, and thus focuses on the second project objective. It is structured in two sections, the first which describes how the different components have been modelled, and the latter presents the load flow and dynamic RMS validation of the model, where the new procedure proposed in the previous chapter has been applied. Since this is an industrial PhD the modelling includes practical considerations needed when modelling an actual power system, in contrary to a pure theoretical academic study using a standard e.g. IEEE 9 bus system.

6.1 MODEL DESCRIPTION
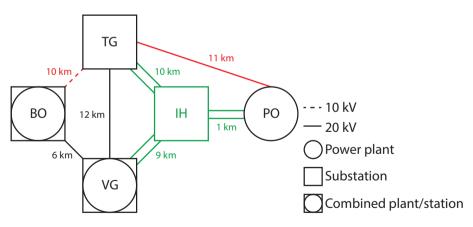
The PowerFactory model of the Faroese power system is suitable for static and dynamic RMS simulations. All components rated above 1000 V are included in the model; hence, the 400 V distribution grid is represented by loads. The dynamic power system analyses conducted in this PhD primarily focus on the grid of Suðuroy; hence, so do the model descriptions and validation. The same methods have been applied to the main grid, but this has been done by the consulting company AFRY Denmark A/S. The main grid has not been as thoroughly validated as the Suðuroy model, i.e. fewer operation scenarios and events have been validated.

The studies in this project have been conducted whilst the grid of Suðuroy has been under a significant transition, going from a system with only hydro, diesel and a small PV system to a system with a relatively large wind farm, a synchronous condenser and a battery system as described in the introduction. Since some of the conducted studies are validation based, while others are focused on the future, the studies have been conducted both with and without the new expansions. Therefore, the model of the power system in Suðuroy, will be described based on primo and ultimo 2022 in the following sections.

The power system of Suðuroy consists of two substations, a power plant and two combined power plants and substations. These are tabulated in Table 6.1. An overview of the power system in Suðuroy is found in Figure 6.1.

This diagram shows the system as it was primo 2022 (red) and how it is expected to be ultimo 2022 (green). The black symbols are a part of the system primo and ultimo 2022. The main difference between the system primo and ultimo 2022 is the new substation IH. This is where the wind farm (PO) is to be connected together with the previously mentioned 8 MVA synchronous condenser and 7.5 MW/7.5 MWh battery energy storage systems. From the start of operation the wind farm was connected to a temporary substation, which is connected to the TG substation. The IH substation has connections to both the TG substation and the thermal power plant VG. Primo 2022 includes a 10 kV line (red dotted) between TG and the hydro power plant BO, this will be removed when the new substation is installed. This line is not used under normal operation. Detailed data, e.g. cable characteristics, dynamic controller's parameters, inertia etc., is not presented in this study due to confidentiality.

Name	Abbreviation	Function
Elverkið í Botni	BO	Hydro power plant and substation
Í Heiðunum	IH	Substation
Porkerishagin	PO	Wind power plant
Tvøroyri	TG	Substation
Vágsverkið	VG	Fossil power plant and substation

Table 6.1: List of power plants and substations in Suðuroy
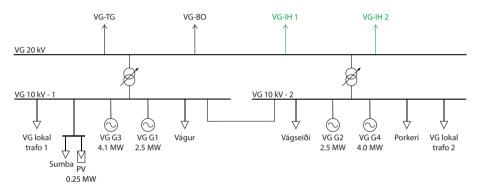
Fig. 6.1: Overview of the grid in Suðuroy. The red symbols are only a part of system primo 2022, while the green symbols are only a part of the system ultimo 2022.

There are currently two connections between the 20 kV busbar at VG and other plants and stations, one to TG and one to BO, see the single line
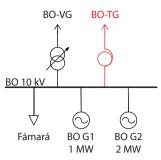
diagram on Figure 6.2. Two new connections to IH will be available ultimo 2022. Two 20 kV/10 kV transformers, with on-load tap changers, transform the voltage to the two 10 kV busbars at VG. These busbars are connected under normal operation. There are three load radials on each busbar, which supply a large part of the island with electricity. A 260 kW PV system is connected in the distribution system of one of the radials (Sumba). This is shown by the additional busbar from VG 10 kV - 1. This is a fictional busbar used to illustrate the location of the PV system. The load and the PV are connected to VG through the same connection. This load is low; thus, when the PV production is high, the excess energy is exported to VG. The thermal generators VG G1 and VG G2 are rated at 2.5 MW, VG G3 at 4.1 MW and VG G4 at 4.0 MW.
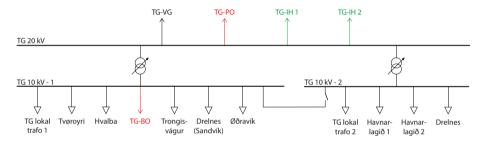
Fig. 6.2: Single line diagram of the combined power plant and substation Vágsverkið (VG). The green symbols are only a part of the system ultimo 2022.

As previously mentioned the only connection to BO in the future is from VG, as the 10 kV line between BO and TG will be decommissioned. There is a 10 kV busbar in BO, which two hydro turbines and a load radial (Fámará) are connected to, as shown by the single line diagram on Figure 6.3. The load is always low, as it only supplies a sheep farm with little to no activity. BO G1 is rated at 1 MW, and BO G2 at 2 MW.

The single line diagram of TG can be found in Figure 6.4. TG was in the past both a thermal power plant and a substation, but today it is only a substation connected to VG and BO (VG and IH ultimo 2022). Similarly to VG, TG has two 10 kV busbars (TG 10 kV - 1 and TG 10 kV - 2), but these are however not connected under normal operation. There are 10 load radials in total at the two 10 kV busbars.
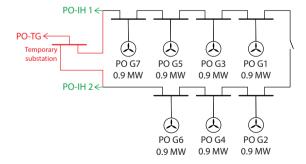
Fig. 6.3: Single line diagram of the combined power plant and substation Botnur (BO). The red symbols are only considered a part of system primo 2022.
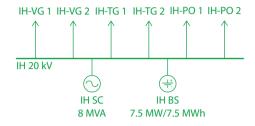
Fig. 6.4: Single line diagram of the substation Tvøroyri (TG). The red symbols are only a part of system primo 2022, while the green symbols are only a part of the system ultimo 2022.

The PO wind turbines are connected to two feeders, with three and four wind turbines. All wind turbines can also be connected together, as illustrated with the switch on the right. As previously mentioned they are currently connected to through a temporary substation connected to TG, but will be connected to the new IH substation. This is shown in Figure 6.5.

Fig. 6.5: Single line diagram of the wind power plant Porkerishagin (PO). The red symbols are only a part of system primo 2022, while the green symbols are only a part of the system ultimo 2022.

Figure 6.6 shows the single line diagram of the substation "Í Heiðunum". As shown on the figure, this is were the battery system (IH BS) and the synchronous condenser (IH SC) are connected.

Fig. 6.6: Single line diagram of the Í Heiðunum substation (IH). Every symbol in green, as the substation is only a part of the system ultimo 2022.

6.1.1   CABLES AND OVERHEAD LINES

The impedance of the lines and cables are not measured when installed in the Faroe Islands. Therefore data from the datasheets has been used to define the characteristics of cables and lines. The length of the cables and overhead lines (OHL) is measured and registered in SEV's geographic information system (GIS), and these lengths have been used when modelling. Some of the connections are combined of sections of different cables and OHL types. The cable/OHL parameters of each section have been defined.

6.1.2   TRANSFORMERS

Each transformer has its own type. The transformer types have been modelled based on data extracted from factory acceptance test (FAT) reports. Some of the transformers have automatic tap changing, and this has been modelled where relevant.

6.1.3   LOADS

The 400 V distribution system is represented by loads at the substations. The dynamic behaviour of the load has not been measured and is therefore unknown. Thus, the loads are modelled as constant PQ static loads. Through the validation process of the governors and AVRs, the impact of the load model was also investigated, due to difficulty of obtaining correct parameters. The load model had insignificant impact on the overall frequency and voltage response in the investigated scenarios.

In some of the analysis the loads are however controlled by a measurement file, meaning that the active and reactive power is set to vary based on a time series found in a measurement file.

129

6.1.4 REACTORS

There are no reactors in Suðuroy in the transmission system today, but in the future there will be at least one installed to compensate the cable to the main grid anticipated in 2026. In simulations from 2026 and forward a reactor has been modelled. This reactor is modelled identical to one of the reactors in the main grid, using the voltage, resistance and reactance. The reactor is modelled as a 3 phase coil with a shunt type of R-L. This specific reactor is rated at 3.9 Mvar.

6.1.5 SYNCHRONOUS GENERATORS

The synchronous generators are modelled with both static and dynamic parameters and dynamic controllers. The static components of the generators' model types consists of the ratings of the generators, i.e. voltage, power and power factor. The local controller of the generators have also been defined. They have been defined as Voltage Q-Droop, as the generators are controlling the voltage with droop. This is typically used when voltage controlling generators are placed close together.

The parameters needed for RMS simulations are the inertia, pole pairs, nominal frequency, the rotor type, reactances and time constants. These values are to a large extent obtained from FAT reports. The manufacturers have not specified the inertia for all generators, and in these cases, the inertia has been calculated from measurements from load rejection tests.

Speed Governors and Automatic Voltage Regulators

All synchronous generators have a governor and AVR. None of the generators on Suðuroy are equipped with a power system stabiliser. Standard models from the PowerFactory library have been used to model the governors and AVRs. The governor and AVR types and models used for each synchronous generator in Suðuroy are listed in Table 6.2. Each diesel governor has been modelled with the DEGOV1 model, while the hydro turbines are modelled with HYGOV. The only other standard diesel governor model is the DEGOV, which only can be used for isochronous diesel governors. HYGOV is one of the most commonly used models to represent hydro governors [166].

The AVR model has been selected based on IEEE's Recommended Practice for Excitation System Models for Power System Stability Studies [162] and input from manufacturer. In Suðuroy this means that all the AVRs are modelled using the IEEE AC8B model. Some of the AVRs in the main grid are modelled using other models, e.g. ST5C.

Table 6.2: Type of governors, AVRs and models for each synchronous generator in Suðuroy.

| Generator | Governor | | AVR | |
	Type	Model	Type	Model
BO G1	Old mechanical regulator	HYGOV	ABB GX 500	AC8B
BO G2	Old mechanical regulator	HYGOV	ABB GX 500	AC8B
VG G1	Woodward UG-8	DEGOV1	Brush TDAVR	AC8B
VG G2	Woodward UG-8	DEGOV1	Brush TDAVR	AC8B
VG G3	Woodward 723 Plus Digital Control	DEGOV1	Basler DECS 125-15	AC8B
VG G4	Wärtsila ESM-20	DEGOV1	ABB Unitrol 1020	AC8B

Secondary Frequency Control

The secondary control in the Faroe Islands is, as previously mentioned, fully manual. This means that when a steady state frequency or voltage deviation occurs, a person has to manually regulate active/reactive power from the generators. In one of the studies of this research project a secondary frequency controller (SFC) was needed, in order to replicate measurements over 4.5 hours in simulations. The study is described in section 7.1.

Modelling a manual control is challenging, due to its dependence on human behaviour. Especially since the staff working at Vágsverkið, where the control center of the power system of Suðuroy is located, do not use an exact guideline on when and how much they should regulate depending on the deviation from rated voltage and frequency. Hence, if the modelling of the secondary control was based on machine learning, it would likely be different depending on the staff. Additionally the individual staff's behaviour might not always be the same. Since the need of including a SFC was identified based on the need to replicate previous measurements, the modelling was based on this.

Figure 6.7 shows how the SFC has been modelled. The box "Secondary Frequency Control" is a measurement file with a time series of the steps in the regulation sent from the control center to the generator (active power up/down) from the period simulated. From the SFC a signal, p_{sfc}, is sent to the governor, here the signal is added to the frequency deviation from the nominal frequency, and a signal, p_{gov}, considering both the manual SFC and the automatic primary control is sent to the generator.
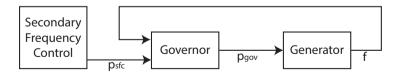
Fig. 6.7: Diagram of how secondary frequency control has been modelled.

The signal from the SFC, i.e. the regulation steps, remains unchanged unless the staff presses power up/down. This means that from the start the signal is equal to zero. When a regulation occurs the value is changed using Equation 6.1. The signal value is kept until the next regulation.

$$p_{\text{sfc},i} = p_{\text{sfc},i-1} + \frac{P_s}{P_r} \cdot R \qquad (6.1)$$

The information needed is the rated power of the generator, P_r, and the droop settings, R. The magnitude of power step change, P_s, when the staff regulate up or down is also needed. This is a fixed value in the control settings, negative if regulated down and positive if regulated up. The droop and power step change for the generators used in the study with SFC (section 7.1) are tabulated in Table 6.3.

Table 6.3: Parameters used to calculate the signal from the secondary frequency controllers to the governors of VG G1, VG G2 and BO G2.

Generator	P_s	R
VG G1	$\pm$100 kW	4%
VG G2	$\pm$100 kW	4%
BO G2	$\pm$50 kW	5%

6.1.6 WIND POWER PLANTS

The Enercon wind power plants are modelled using static generators and the ratings of the generators have been defined. The dynamic models for the wind turbines have been obtained from the manufacturer, and parameter settings and control modes are retrieved from the Enercon SCADA system. The wind turbines are type 4 (full converter). Under normal operation they deliver active and reactive power based on wind speed and setpoints. There are different operating strategies under faults, and the mode activated in the FACTS in Porkeri is currently the QU(ABS)-Strategy. When this operating strategy is used, the wind farm remains in operation up to 5 second during symmetrical and asymmetrical faults. If the voltage recovers within 5 seconds the wind farm goes back to normal operation, otherwise the wind farm shuts down [167].

A model with a high number of dynamic controllers has a higher computational time, than a model with few dynamic controllers. The seven wind turbine generators are identical with identical dynamic controllers. Thus, to reduce the calculation time, they have been modelled using one dynamic model instead of seven and by setting "Parallel machines" to seven. This way the model accounts for all seven turbines with seven controllers, but without increasing the computational time proportionally. This however leads to

the cables between the wind turbines being neglected, but these cables have a maximum length of 520 m (PO G1 to PO G2 on Figure 6.5), and the exclusion of these therefore has a negligible impact on the overall simulations conducted in this study.

6.1.7 FARM CONTROL UNIT

The wind farm is controlled by a Farm Control Unit (FCU). The FCU has 6 active power control types and 11 reactive power control types.

The active power control type used in Porkeri is currently the "P-Type 6 - Power Frequency Control Type 3". This is a PI controller which controls the active power reference value at the controlled bus, and the setpoint is sent to the turbines [168]

"Q-Type 5 - Reactive Power Control" is the used reactive power control at the wind farm in Suðuroy. This type, similarly to the active power control type, uses a PI controller with a delay or parallel integral control, and controls the reactive power reference value at the controlled bus [168].

6.1.8 PHOTOVOLTAIC PANELS

The existing photovoltaic panels are connected to the distribution grid and produce power based on irradiation and with a power factor of 1. Since the distribution grid is simplified to a load, the existing photovoltaic panels are not modelled in details, but included on the load radial where they are placed. The future photovoltaic power plants according to the RoadMap, see Figure 4.1 [81], are assumed be connected to the high voltage system. These are represented by the IEC 614-27-1 WT 4B 2.0MW Hz model, which is commonly used in industry to represent PV and is a full converter model. No plant control has been activated in the simulations. The models are used with default parameters.

6.1.9 BATTERY SYSTEMS

There was no RMS model available for the specific battery system with respective controllers to be installed in Suðuroy at the time of this study. However, there is as previously mentioned, a 2.3 MW battery system in the main grid, which has frequency support capabilities, see Figure 1.12 on page 17. The exact model of this battery system is available from the manufacturer, i.e. Enercon GmbH. This model has been used to model the battery system on Suðuroy. As the system to be installed in Suðuroy will be 7 MW, the model number of "Parallel machines" has been set to 3, i.e. 3x2.3 MW. The static part of the model consists of the battery ratings.

Battery Controllers

The battery is operated in frequency control mode. It controls the frequency at point of connection. The settings of the control mode are found in Table 6.4. The battery reacts to a frequency deviation when the frequency reaches ± 200 mHz from 50 Hz, and delivers full power by a frequency deviation of ± 600 mHz. There is a linear relationship between the frequency deviation and the power delivered by the battery system outside the deadband range, i.e. between ± 200 and ± 600 mHz variations from the nominal frequency. Between 49.8 Hz and 50.2 Hz the battery system does not support the frequency. The power values used in the settings of the BESS are the sum of the maximum charge and discharge power of the BESS in the main grid, as this is the maximum contribution of the battery i.e. if the battery is charging with maximum power, but a frequency dip occurs, the battery can contribute by stopping charging and start discharging, which is a maximum of 3.94 MW. Setting the "Parallel machines" to 3, increases the settings of the frequency control respectively.

Table 6.4: The settings of the frequency control of the battery system.

Frequency (Hz)	Power (kW)
49.4	3940
49.8	0
50.2	0
50.6	-3940

6.1.10 SYNCHRONOUS CONDENSER

The 8 MVA synchronous condenser in Suðuroy has been modelled with a model obtained from the manufacturer ABB. This model includes the actual parameters of the machine in Suðuroy, i.e. ratings, inertia etc.

Controllers

The model received from ABB also included dynamic RMS models of the synchronous condenser's controllers in Suðuroy. However, since the synchronous condenser had not been put into operation at the time of the study, the parameter settings of the controllers had not been tuned. Therefore, the parameters in the model are values received from ABB prior to tuning. The parameters, especially for the AVR, of the dynamic synchronous condenser model are however similar to the parameters used now that the synchronous condenser has been put into operation.

6.2   MODEL VALIDATION

The static and dynamic models of the Faroese power system have been validated. This section presents the validation of the grid on Suðuroy. The static model is validated through a load flow calculation. The parameterisation and validation of the governors and AVRs is presented with SWS and HS parameterisation and validation of events with large disturbances. Three generators have also been validated through a 4.5 hour period using the secondary frequency controller. Finally the performance of the wind turbines' controllers has been tested and the validation has been approved by the manufacturer Enercon GmbH. Thus, the following sections describe an extensive validation of the different models in Suðuroy with many practical considerations.

6.2.1   STATIC MODEL

The validation of the static model is conducted by setting the active and reactive power of loads and generators according to SCADA measurements, simulating a load flow, and check if the current flow is according to the measurements. The tap changers of the transformers are set according to the setting at the time and the synchronous machines are set to operate at the measured voltage. The machines are set to "Voltage Q-droop" control and the droop has been specified, as this is voltage control mode in the system. Three random scenarios have been selected, based on the only condition that each generating unit has to be online for at least one scenario. The selected scenarios are tabulated in Table 6.5, where 'X' indicates that the unit was online. PO is considered to be the whole wind farm, and although the PV system in the Sumba radial is not modelled, it was decided to chose a scenario where there is an export from Sumba, which indicates a PV production higher than the local consumption in the village of Sumba.

All three scenarios showed satisfactory results in the validation. One of the scenario, 01-04-2020 08:29, is presented in this section, while the other scenarios are tabulated in Appendix B.

Table 6.5: Load Flow Validation Scenarios for Suðuroy.

Timestamp	VG G1	VG G2	VG G3	VG G4	BO G1	BO G2	PO	Sumba
01-04-2020 08:29	X	X	X	X	-	X	-	-
01-05-2020 14:26	-	-	X	-	X	-	-	X
01-12-2020 14:30	-	-	X	X	X	-	X	-

Table 6.6 shows the measured and simulated currents in Suðuroy in scenario 1. Missing components are caused by no measurements or the no load/generation. In some locations the current is measured in every phase,

while in other places there is a single current measurement. For the loads the largest difference is 3 A, which is considered to be within an acceptable limit. The phase 1 and 2 measurements for Vágur are likely faulty measurements, since the phase 3 measurement is close to the simulated value, and the load is above zero, i.e. the current should also be higher than zero. The differences between current measurements and simulation for the generators, the busbars, cables/lines and transformers are likewise very small.

The largest numerical difference is the current flow in phase 1 from VG 10 kV - 1 to VG 10 kV - 2, where the difference is 7 A. The current flow measured at VG 10 kV - 1 towards VG 20 kV - 2 and vice versa, should be numerically equal in a phase, but there is a difference of 3 A. This indicates a problem with the accuracy of the measurement. Therefore, this difference of 7 A is not considered to be outside of acceptable limits. Especially when the difference in the other phases is smaller.

The simulated and measured active and reactive power for generation, busbars, lines/cables and transformers are found in Table 6.7. The power of the loads are not included, as these are fixed to the set value in the initialisation. Aside from VG G3 and BO G2 reactive power, the measured and simulated numbers for generating units are identical. The difference in reactive power of BO G2 is 0.01 Mvar, which is insignificant. The differences in VG G3 are slightly bigger, but if any component is not accurately represented in the model and this affects the load flow, the difference has to be compensated by some of the generators. An example could be that the data used for cables is from a datasheet, and not measured, therefore this is an uncertainty in the model. Generally the simulated active and reactive power are close to the measured values, but the active power measurement at the transformer in BO is significantly higher than the simulated value. This large difference can only be explained by a measurement error, as the measured value indicates an import of 1.91 MW, while the only load at BO is 0 MW in this scenario.

Table 6.6: Current (A) in Load Flow Validation of Suðuroy in Scenario 1. HV and LV indicate if the current is measured at the high or low voltage sides of the transformers.

Type	Name	Simulation	Measurement		
			L1	L2	L3
Loads	VG lokal trafo 1	13	13	13	13
	Sumba	9	10	9	9
	Vágur	2	0	0	3
	Vágseiði	65	65	65	64
	VG lokal trafo 2	6	6	6	7
	Tvøroyri	25	25	-	-
	Hvalba	79	82	-	-
	Trongisvágur	2	2	-	-
	Drelnes (Sandvík)	14	14	-	-
	Øðravík	10	10	-	-
	Havnarlagið 1	3	3	3	3
	Havnarlagið 2	43	44	44	43
Generators	VG G1	29	30	-	-
	VG G2	18	18	-	-
	VG G3	147	149	-	-
	VG G4	73	73	-	-
	BO G2	11	13	-	-
Busbars	VG 10 kV: 1->2	66	73	69	68
	VG 10 kV: 2->1	66	70	68	66
Cables/lines	TG-VG	85	86	85	86
	VG-TG	84	86	85	85
	VG-BO	10	11	12	11
Transformers	BO (LV)	11	12	-	-
	BO (HV)	6	7	-	-
	VG 1 (HV)	40	40	-	-
	VG 1 (LV)	80	84	-	-
	VG 2 (HV)	40	40	-	-
	VG 2 (LV)	81	80	-	-
	TG 1 (HV)	63	64	63	63
	TG 1 (LV)	122	122	-	-
	TG 2 (HV)	22	22	22	22
	TG 2 (LV)	42	43	42	42

Table 6.7: Active (MW) and Reactive Power (Mvar) for Load Flow Validation of Suðuroy in Scenario 1. HV and LV indicate if the power is measured at the high or low voltage sides of the transformers.

Type	Name	Active		Reactive	
		Sim.	Meas.	Sim.	Meas.
Generation	VG G1	0.32	0.32	0.42	0.42
	VG G2	0.30	0.30	-0.10	-0.10
	VG G3	2.64	2.74	-0.16	-0.22
	VG G4	1.18	1.18	0.58	0.58
	BO G2	0.11	0.11	0.17	0.18
Busbars	VG 10 kV: 1->2	1.18	1.27	0.07	0.08
	VG 10 kV: 2->1	-1.18	-1.24	-0.07	-0.13
Lines/cables	TG-VG	-2.88	-2.89	-0.72	-0.72
	VG-TG	2.97	2.99	0.72	0.69
	VG-BO	-0.11	-0.11	-0.35	-0.39
Transformers	BO (HV)	-0.11	1.91	-0.17	-0.23
	VG 1 (LV)	1.43	1.43	0.23	0.16
	VG 2 (LV)	1.43	1.45	0.23	0.22
	TG 1 (HV)	2.14	2.13	0.53	0.53
	TG 2 (HV)	0.74	0.75	0.19	0.19
	TG 2 (LV)	-0.74	-0.74	-0.18	-0.19

Table 6.8 shows the measured and simulated voltages. For the 10 kV voltages at BO and VG, the measured and simulated voltages are identical. This is expected, since the machines in the model are set to operate at the measured voltage, and the machines are connected to these busbars. There are some small variations at VG 20 kV and at TG, but again these variations are relatively small.

Table 6.8: Voltage (kV) for Load Flow Validation of Suðuroy in Scenario 1.

Type	Name	Simulation	Measurement		
			L1	L2	L3
Busbars	BO 10 kV	10.39	10.39	-	-
	VG 10 kV - 1	10.38	10.38	-	-
	VG 10 kV - 2	10.38	10.38	-	-
	VG 20 kV	20.87	20.93	-	-
	TG 20 kV	20.16	20.13	20.16	20.14
	TG 10 kV - 1	10.32	10.31	10.33	10.32
	TG 10 kV - 2	10.36	10.34	10.39	10.35

Although there are some small differences in measured and simulated currents, power and voltages, the static model can be validated, as all differences are small or considered faults. Considering the inaccuracy of measurements and using datasheet data for modelling, it would be difficult to decrease the mentioned differences between the model and the measurements.

6.2.2 PRIMARY CONTROL OF SYNCHRONOUS GENERATORS

The implications of obtaining accurate models for dynamic power system models was discussed in Chapter 5. A method to parameterise and validate the models was proposed, see Figure 5.10 on page 120. This method has been applied to the AVRs and voltage transducers in Suðuroy. The parameter settings of the voltage transducers impact the input voltage to the AVRs, thus if these are not parameterised correctly, the dynamic behaviour of the AVRs is impossible to parameterise. Therefore the voltage transducers have been parameterised as well. The method has also been applied to the main grid. In the main grid it has been used to validate governors as well. Both the proposed method and results of the dynamic validation are also to be published in a separate article, see [161].

The initial parameterisation of the governors in Suðuroy with hybrid simulation based on one scenario and manual parameter adjustments, as described in subsection 5.3.1, showed some inaccuracies with the measurements when conducting a SWS. After additional parameter adjustments in SWS, sufficient results were obtained. This was however a very time consuming and difficult adjustment, because manual adjustments have to evaluated one by one, and since there are multiple scenarios each adjustment has to be evaluated in every relevant scenario, and doing such a evaluation qualitative is difficult. If the evaluation is done quantitative, the data from each scenario has to be extracted analysed. Therefore the proposed method was developed and applied to other regulators, i.e. the AVRs in Suðuroy and the AVRs and governors in the main grid. But since a significant amount of time had already been used on the manual adjustment of the governors in Suðuroy and they after this showed a good resemblance with the measurements, the method was not applied to the governors of Suðuroy.

The following sections go through the parameterisation and validation of the governors and AVRs in Suðuroy. In order to parameterise the dynamic models, multiple trip test have been conducted. The results shown in this section have been selected based on the fact that each regulator has to be included in at least on of the events validated. Ten of the tests are part of the description which follows, and are listed in Table 6.9. The machines that are tripped have all had either a high active power and low reactive power, or a low active power and high reactive power, so that the trip affects mainly either the frequency or the voltage and not both simultaneously.

Table 6.9: Overview of of the tests conducted in Suðuroy to parameterise and validate the models and are relevant to the figures and examples presented here.

Event	BO G1	BO G2	VG G1	VG G2	VG G3	VG G4
1	Online	**Tripped**		Online		Online
2	Online	Online			Online	**Tripped**
3	Online	Online	Online	Online	**Tripped**	
4	Online	Online		**Tripped**		Online
5	Online	Online			Online	**Tripped**
6	Online	Online	Online	Online	**Tripped**	
7	Online		**Tripped**		Online	
8	Online		**Tripped**		Online	
9		Online	**Tripped**		Online	
10		Online	**Tripped**		Online	
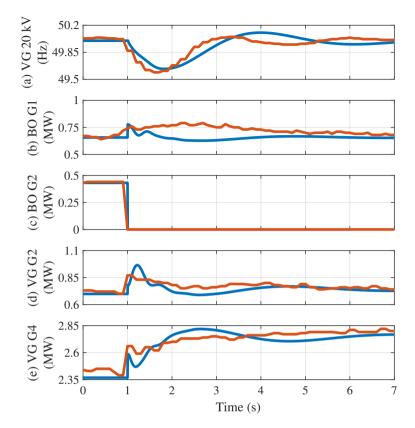
Governors

The validation of the governors is presented by three figures showing the SWS validation (Figure 5.10) of event 1 to 3 in Table 6.9. The first event is shown in Figure 6.8. BO G1, VG G2 and VG G4 are online during event 1, which is a trip of BO G2. BO G1 is producing 440 kW when it is tripped. This results in a measured frequency nadir of 49.59 Hz and simulated of 49.64 Hz; thus, there is not a perfect match between simulations and measurements, but the behaviour is similar with small variations in min/max and settling times.

The simulated active power of BO G1 is not replicating the measurements of BO G1, but no further adjustments were conducted based on the following two reasons:

1. The maximum difference between measurements and simulations is 160 kW, which is less than 4% of the production at that moment.

2. The response of BO G1 is more accurate for event 2 and event 3.

The simulations of VG G2 and VG G4 show some over- and undershoots compared to the measurements. At 1.2 seconds VG G2 shows an overshoot and VG G4 an undershoot, while at 2.5 seconds it is vice versa. These over- and undershoots are of similar sizes, and thus they cancel each other out, and the system frequency is therefore accurately represented. Since VG G2 and VG G4 are connected to the same busbar, some of the interactions between the two engines might be difficult to capture in the parameterisation, and therefore the responses shown in Figure 6.8 are considered to sufficiently accurate.

Fig. 6.8: Comparison of simulated (blue) and measured (red) response from governors to event 1. Plot (a) shows the frequency at VG 20 kV, (b), (c), (d) and (e) the active power of BO G1, BO G2, VG G2 and VG G4 respectively.
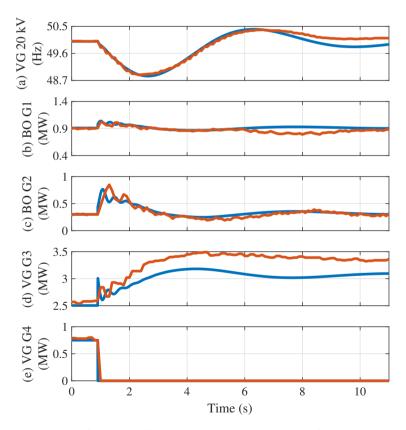
Figure 6.9 shows the SWS validation of event 2, where VG G4 is tripped at 0.78 MW. The simulated frequency matches almost perfectly with the measurements up to 6 seconds. After 6 seconds there is a deviation between the measurements and simulations, and when this deviation is largest it is 270 mHz. This is a significant difference, but the initial response, which matches almost perfectly, is what is of most interest for these simulations. The 270 mHz deviation should however be investigated further, in order to improve the model accuracy.

The simulation of BO G1 replicates the measurements accurately until 6 seconds. The reason why the y axis limits are set to 0.4 MW (minimum) and 1.4 MW (maximum), although the generation is 0.9 MW $\pm$0.1 MW, is that this makes a deviation in one subplot directly comparable to another subplot, as all subplots in Figure 6.9 have a y axis range of 1 MW. This is also done in previous and upcoming figures of the dynamic parameterisation and

validation.

Overall BO G2's simulation and measurements show the same behaviour. The peak in the simulations does however occur slightly before the peak in the measured response, but this difference is so small, and therefore considered insignificant.

Subplot (d) in Figure 6.9 shows the comparison of measured and simulated response of VG G3. The pattern of the response is similar, but not the magnitudes, which leads to a steady state deviation. However, the grid frequency fits perfectly with the measurements up to 6 seconds, and increasing the generation after the event with 200 to 400 kW, would result in a different frequency response. It is more important that the frequency fits well instead of all generators fitting well, the frequency being off. The issue could be in the static model, the lack of dynamic behaviour of the loads or possibly in the measurements. The exact reason should be identified by further analyses.
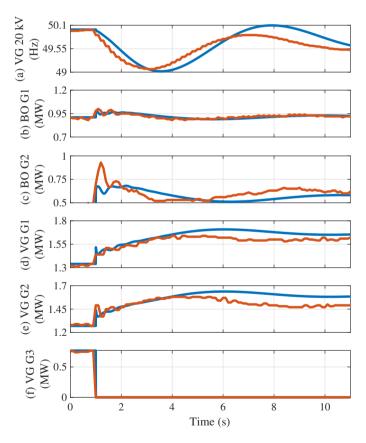
Fig. 6.9: Comparison of simulated (blue) and measured (red) response from governors to event 2. Plot (a) shows the frequency at VG 20 kV, (b), (c), (d) and (e) the active power of BO G1, BO G2, VG G3 and VG G4 respectively.

The final example of the governor validation is shown in Figure 6.10. Here VG G1 and VG G2 are included, which were not online for event 1 and 2. The comparison of the frequency response in event 3 is similar to the one of event 1; i.e. there are variations in the minimum, maximum and settling time, but not any significant differences.

The simulated response of BO G1 shows a good replication of the measurements, while the inertial response of BO G2 in the simulation is lower than in the measurements. In event 2 there also was a difference seen in the inertial response, but not as significant as here. Aside from this, the response is similar.

VG G1 and VG G2 do both show a good replication of the measurements. Especially until 4 seconds. The modelled governor results in a slightly higher steady state value in both generators.

Fig. 6.10: Comparison of simulated (blue) and measured (red) response from governors to event 3. Plot (a) shows the frequency at VG 20 kV, (b), (c), (d), (e) and (f) the active power of BO G1, BO G2, VG G1, VG G2 and VG G3 respectively.

Figure 6.8, Figure 6.9 and Figure 6.10 have shown that generally the modelled governors show a good replication of the actual system. There are some aspects that could be improved, and this could possibly be done by applying the parameterisation and validation method proposed in Figure 5.10 on page 120 to the governors in Suðuroy.

Automatic Voltage Regulators

The validation of the AVRs will show both the HS evaluation and the SWS evaluation, as the proposed procedure has been applied the AVRs in Suðuroy. The HS evaluation is shown for BO G1, BO G2 and VG G3.

Figure 6.11 shows the HS evaluation of BO G1 AVR. When BO G1 AVR was HS parameterised events number 4 to 8 were used. Here one can see that in all of the events there are clear similarities between the measurements and the simulation. This also shows that based on these events, it is not possible to improve the response significantly through HS parameterisation, as they are very similar.
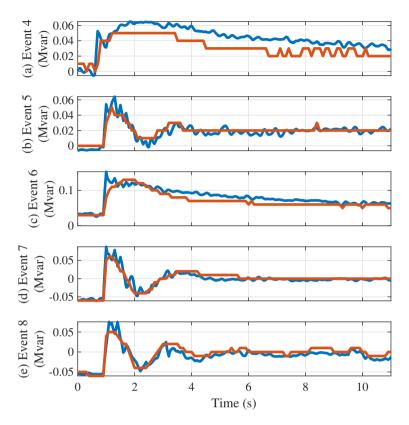
Fig. 6.11: HS evaluation of BO G1 AVR for event 4, 5, 6, 7 and 8. Simulations are blue and measurements are red.

The HS evaluation for BO G2 AVR is shown in Figure 6.12. These results replicate the measurements even better than for BO G1 AVR shown in Figure 6.11. Aside from a slightly lower minimum reactive power in event 5 around 2 seconds, the results are close to identical.
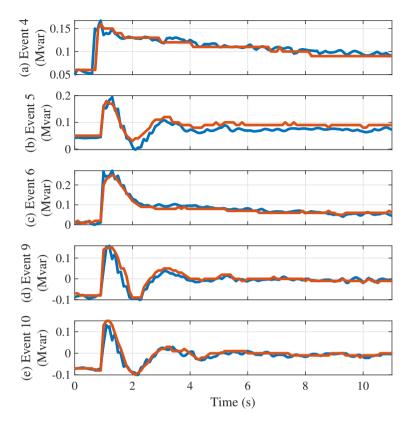
Fig. 6.12: HS evaluation of BO G2 AVR for event 4, 5, 6, 9 and 10. Simulations are blue and measurements are red.

The final HS evaluation presented in this study is for VG G3 AVR, which has been parameterised using event 5 and 7 to 10. The simulations and measurements for events 7 to 10 are very similar, but significant variations are seen in event 5.

Additional HS parameterisation was run with different parameter boundaries, but the simulated response of VG G4 AVR in event 5, did not improve. It was therefore decided to move to the next step in the procedure, which is the SWS validation.
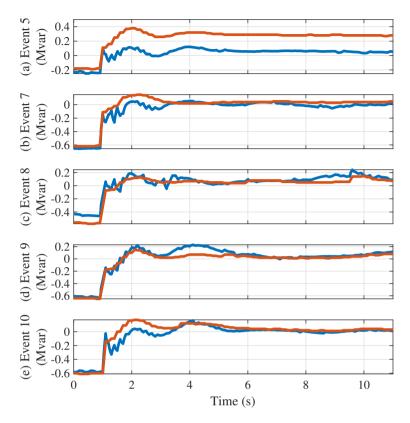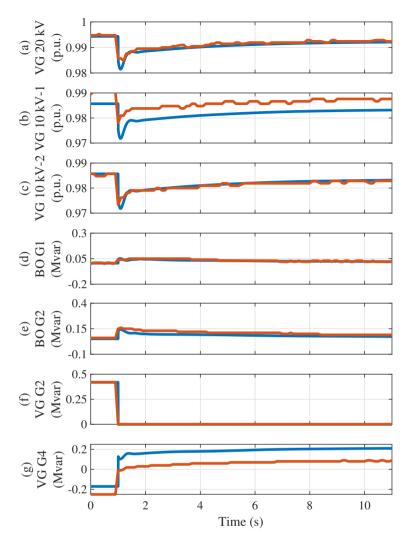
Fig. 6.13: HS evaluation of VG G3 AVR for event 5, 7, 8, 9 and 10. Simulations are blue and measurements are red.

Figure 6.14 show the voltages and reactive power in event 4. The first plot (a) shows the VG 20 kV voltage. The simulated voltage drop is larger than the measured, but the difference is only 64 V, which is considered to be small enough to ignore. The next two plots (b) and (c) are the VG 10 kV - 1 and VG 10 kV - 2 voltages. As these busbars are connected, the voltage should be the same, and this is the case for the simulated response, but in the measurements the voltage at VG 10 kV - 1 is higher. The VG 10 kV-1 is measured at the feeder VG lokal trafo 1, and the VG 10 kV-2 voltage is measured at the VG lokal trafo 2, see Figure 6.2 on page 127. These feeders are connected to auxiliary transformers (10 kV/0.4 kV). They are not modelled, as the model does not include components at 0.4 kV. It is therefore difficult to compare the two responses, and not possible to get both simulated responses identical to the measured responses, when there is a difference in the measurements. Since both generators online at VG are on VG 10 kV - 2, this voltage is used for the validation, and comparing measured and simulated voltages at VG 10 kV - 2 shows that these are close to identical. The only difference is that
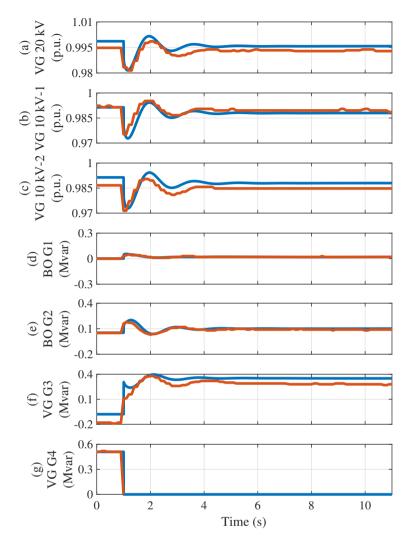
the simulated drop is 20 V larger. The next two responses are the reactive power of the hydro turbines BO G1 and BO G2. Considering the resolution of measurements, the response is considered sufficiently accurate. Finally we have VG G2, which is tripped, and VG G4. The simulated response of VG G4 is likewise very close to the measured response. The reactive power is however slightly lower in the measurements than in the simulations both in the initialisation and throughout the simulation, so the cause of this is that VG G4 is compensating for a reactive power difference in the model compared to the measurements. Considering all the plots on Figure 6.14, the parameterisation of the dynamic models can be validated for this specific scenario.

Fig. 6.14: Comparison of simulated (blue) and measured (red) response from AVRs to event 4. Plot (a) shows the voltage at VG 20 kV, (b) and (c) the voltage at VG 10 kV and (d), (e), (f), and (g) the reactive power of BO G1, BO G2, VG G2 and VG G4 respectively.
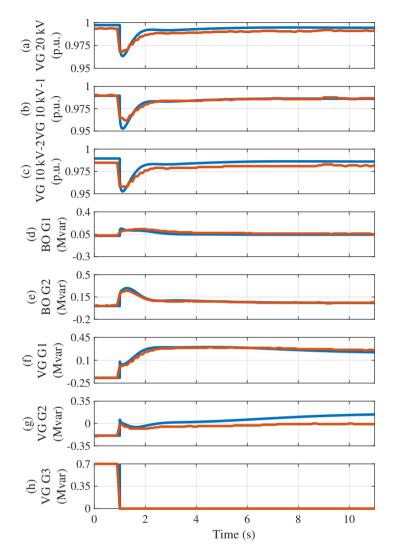
The validation of event 5 is shown on Figure 6.15. There is an 40 V to 80 V offset in the voltage of VG 20 kV, but the patterns of simulated and measured responses are very similar. The measurement offset in VG 10 kV - 1 and VG 10 kV - 2 is again clear, and this time the voltage on VG 10 kV - 1 is very close to the simulated response, and this is due VG G3 being the only generator at VG online after the trip. The voltage drop is around 30 V higher in the simulation than in the measurement, and there is a small offset after the voltage has settled. The reactive power response of BO G1 and BO

G2 are close to identical to the measurement. In BO G1 there is a visible difference at 7.5 seconds, but this is a difference of 10 kvar, which is the resolution of the reactive power measurements, and therefore this difference is considered negligible. The largest differences at BO G2 are 20 kvar. The simulated response of VG G3 is also very close to the measured response. Numerically the differences are larger, but VG G3 is also significantly larger than BO G1 and BO G2. In the parameterisation of VG G3, Figure 6.13, there was a clear difference in event 5, but when simulating the full system, this difference is not apparent. The final plot is VG G4, which is tripped. The parameterisation when considering the second reactive power trip has also been validated through this comparison.

Fig. 6.15: Comparison of simulated (blue) and measured (red) response from AVRs to event 5. Plot (a) shows the voltage at VG 20 kV, (b) and (c) the voltage at VG 10 kV, (d), (e), (f) and (g) the reactive power of BO G1, BO G2, VG G3 and VG G4 respectively.

The full system simulation and measurements for event 6 are compared in Figure 6.16. The simulated and measured responses in this scenario are also very similar, there are some offsets and in some cases differences in the initial voltage drop, but generally the responses can be validated according to this scenario.

Fig. 6.16: Comparison of simulated (blue) and measured (red) response from AVRs to event 6. Plot (a) shows the voltage at VG 20 kV, (b) and (c) the voltage at VG 10 kV, (d), (e), (f), (g) and (h) the reactive power of BO G1, BO G2, VG G1, VG G2 and VG G3 respectively.

Example of Necessity of SWS Parameterisation

The parameterisation and validation of the AVRs in Suðuroy, has shown that an accurate model can be obtained through HS parameterisation. However, in some cases HS parameterisation is not enough, and therefore SWS parameterisation has been included in the proposed procedure as shown in Figure 5.10 on page 120.

The two AVRs at the hydro power plant Fossáverkið in the main grid, could not be validated using only HS parameterisation. Figure 6.17 shows the reactive power response of two hydro turbines at Fossáverkið to one of the staged tests. Blue is the measured reactive power, SWS validation using parameters from the HS parameterisation is in yellow, and red shows the SWS validation after the SWS parameterisation. The yellow curves show a response which is far from the actual response, while the SWS parameterisation clearly improves the responses of both generators, especially for generator 1, i.e. FO G1. A steady state error is shown for FO G2 after HS and SWS parameterisation, but the improvement is significant. Finding suitable parameters for these two AVRs showed to be difficult, because the two generators have a significant influence on each other. A small change in one of the generator can have a significant impact on the response on the other, thus it is possible that additional fine tuning of the parameters, could reduce the steady state error of FO G2 even further.
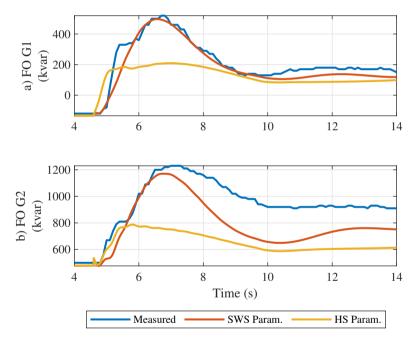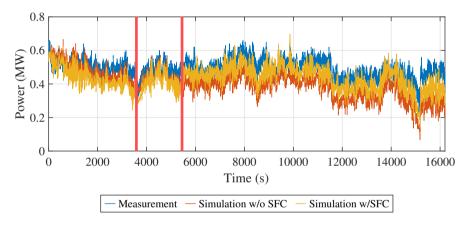
Fig. 6.17: Example of SWS parameterisation at Fossáverkið in the main grid.

6.2.3 SECONDARY FREQUENCY CONTROL

The SFC has been validated for one 4.5 hour scenario. The generators online during the 4.5 hour period are VG G1, VG G2 and BO G2. The following paragraphs will compare the measurements with the simulations (with and without SFC), through illustrated time series of active power and correlation

factors of measured and simulated active power. Both the measurements and the simulations have a 10 Hz resolution.
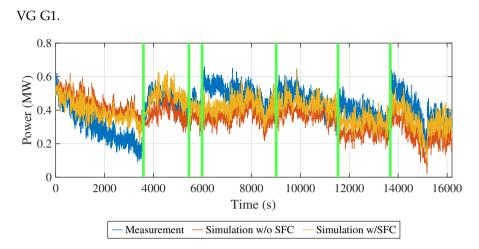
Figure 6.18 shows the measured and simulation active power of VG G1 during the 4.5 hour period with and without the SFC. There are only 2 manual regulations of VG G1 during the period, both of which are down regulations. All time series show a similar behaviour, but the simulation with the SFC is closer to the measurements than the simulation without the SFC. The exact improvement is specified in terms of correlation factors later in Table 6.10. There is not a full agreement between the measurements and the simulation with SFC, but since neither the static model or the primary controllers are 100% accurate when compared to measurements, differences throughout a 4.5 hour period with SFC are unavoidable.

Fig. 6.18: Comparison of VG G1's measured and simulated active power with and without a SFC in the simulation. The red vertical lines mark a manual active power down regulation.
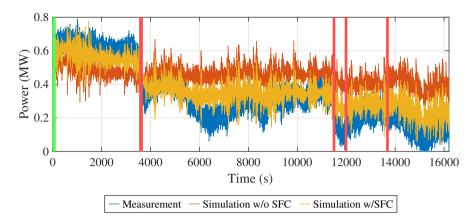
VG G1 and VG G2 are the exact same type of generators with the same regulators, thus they should perform very similarly. Especially since they at the beginning of the time period are both loaded at 0.6 MW; however, as shown on Figure 6.18 and Figure 6.19 this is not the case. The active power of VG G2 decreases as time goes by. The generator is regulated up 6 times during the simulation, but each time the active power decreases. According to the staff at Vágsverkið, this is a known phenomenon, and occurs due to VG G2's governor being damaged. This illustration of the difference between the performance of VG G1 and VG G2, has resulted in a new regulator being ordered.

The faulty operation of VG G2's governor makes it difficult to get an accurate simulation over a long time. There is some improvement seen by implementing the SFC in the simulation, but the deviations between measurements and simulations are significantly more visible for VG G2 than for

VG G1.

Fig. 6.19: Comparison of VG G2's measured and simulated active power with and without a SFC in the simulation. The green vertical lines mark a manual active power up regulation.

The active power of BO G2 without an SFC included does not show any great variations in the production throughout the 4.5 hour period, see Figure 6.20. The measurements do however vary between around 700 kW to 100 kW, not considering fast fluctuations. There are 10 manual regulations in total, only five of which are clearly visible, as 2 up regulations are close together at 50 and 70 seconds, and 5 down regulations occur between 3590 seconds and 3631 seconds. The resemblance between measurements and simulations is significantly improved by adding a SFC to the model. This is especially noticeable at the down regulation around 3600 second and 11500, where the simulation with SFC continuous at the same or similar production, while the measurements show a significant decrease in production. Also at the beginning of the period where the measured power and simulated power with SFC are higher than without the SFC, due to the manual up regulation at 50-70 seconds.

Fig. 6.20: Comparison of BO G2's measured and simulated active power with and without a SFC in the simulation. The red vertical line marks a manual active power down regulation, while the green lines mark a manual active power up regulation.

The precise improvement of implementing a SFC in the simulation is difficult to see in the presented figures, but as a supplement the correlation factors between measured and simulated active power as been tabulated in Table 6.10. The correlation between measurements and simulations for VG G1 is not improved significantly by adding a SFC, but this is also the generator with the least regulations during the period. This means that it is the automatic response of the governor, which is controlling the active power during most of the period. The improvement is much more significant for VG G2 and BO G2, which have 6 and 10 SFC regulations, of which VG G2 has the highest improvement, whilst BO G2 has the highest correlation factor.

Generator	Without SFC	With SFC	Improvement	SFC Regulations
VG G1	0.62	0.68	0.06	2
VG G2	0.22	0.56	0.34	6
BO G2	0.58	0.90	0.32	10

Table 6.10: Correlation factors between measurements and simulations with and without SFC over 4.5 hour dynamic RMS simulation.

Implementing a SFC in the simulation model has decreased the deviations between measured and simulated active power of the generators online. With some additional tuning, this could likely be improved even more, however modelling SFC with a faulty governor is difficult, and since the governor will be replaced soon, this has not been prioritised.

6.2.4 LOAD MODELLING
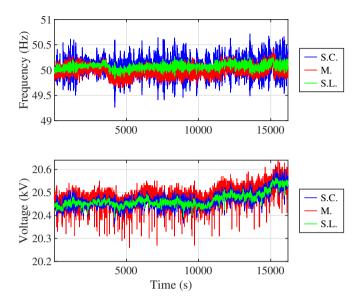
The loads are in some of the analyses defined based on a time series in a measurement file. This means that they are varying over time. PowerFactory interpolates data in time series, either based on a linear or a constant approach. The latter meaning that the value is kept constant until the next value in the time series. This is accurate if the measurements are without deadbands. The load measurements have a deadband of 3%, meaning that the load is logged when the measurement detects a deviation of 3% from the previous measurement. In reference [81] the impact of the interpolation methods (on both loads and wind and PV power production) is presented, see Figure 6.21.

Using a constant interpolation leads to over estimations of the frequency fluctuations, see Figure 6.21. This is due to the deadband in the measurements, which lead to sudden steps in the load series. Another cause of the overestimation can be that the frequency measurements have a resolution of 10 Hz, while the simulation has a resolution of 100 Hz, i.e. some of the fluctuations might not be captured by the measurements.

A linear interpolation underestimates the frequency fluctuations, as it removes all sudden changes in the load profile. Table 6.11 shows the mean and standard deviations of the measurements, simulations with constant interpolation and simulations with linear interpolation. The values show that while the mean frequency using constant interpolation is slightly closer to the measurements, the standard deviation is slightly closer using a linear interpolation.

The voltage fluctuations are underestimated in both cases. This indicates that some of the voltage/reactive behaviour is not captured by the model. The mean voltage is the same with constant and linear interpolation, while the standard deviation with a constant interpolation is 3 V closer to the measurements than the linear interpolation.

Neither of the interpolation methods are perfect, but it was decided to use a constant interpolation in the previous study [81], because of the resolution of the measurements vs simulations and due to the voltage fluctuations. The frequency fluctuations are either over- or underestimated, while the voltage fluctuations are underestimated in both cases, with constant interpolation being closer to the measurements. The constant interpolation has been used in the secondary frequency control validation presented in subsection 6.2.3, and the simulated time period is the same for Figure 6.18, Figure 6.19, Figure 6.20 and Figure 6.21.

Fig. 6.21: Frequency (upper) and voltage (lower) comparison between measurements (M.), simulations with constant interpolation (S.C.) and simulation with linear interpolation (S.L.) for Case 1 [81].

Table 6.11: Frequency and voltage mean and standard deviation for measurements and simulations [81].

	Mean		Standard deviation	
	f (Hz)	U (kV)	f (mHz)	U (V)
Measurement	49.99	20.48	96	38
Simulated, constant	50.05	20.47	153	31
Simulated, linear	50.07	20.47	55	28

6.2.5 WIND POWER PLANTS

The validation of models of the wind turbines and the FCU has been done in cooperation with Enercon GmbH.

Wind Turbines

According to Enercon GmbH the wind turbine controllers should be validated by initiating a voltage dip, and analysing the reactive current response, which should increase. Figure 6.22 shows the voltage at IH 20 kV and PO G1 reactive current component. According to Enercon GmbH, the response

shown in Figure 6.22 shows that the wind turbine model is performing correctly, i.e. the reactive current increases in the shown pattern when the voltage decreases. Thus, the wind turbine model can be validated.
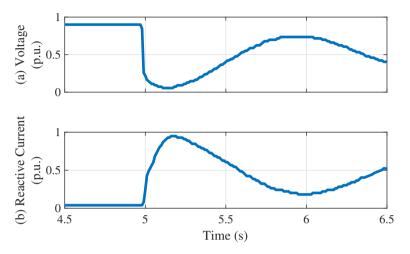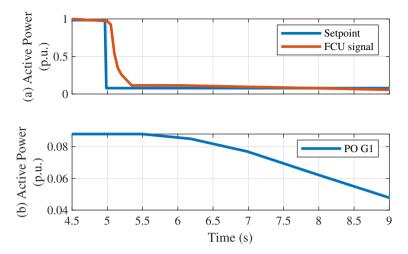
Fig. 6.22: Validation of the wind turbine controllers.

Farm Control Unit

The FCU is correctly implemented and can be validated if increasing or decreasing the active or reactive power setpoint sent to the FCU results in the wind turbines' active or reactive power increasing or decreasing. In the example shown in Figure 6.23, the setpoint is decreased from 1 p.u. to 0.1 p.u. Plot (a) shows the setpoint change and the signal from the FCU to the wind turbines. There is a delay from when the setpoint is changed to when the FCU has down regulated the wind turbines accordingly. Plot (b) also shows that there is an additional delay from when the FCU signal decreases until the active power of the wind turbine decreases. This is due to the production of the wind turbines being below 1 p.u. from the initialisation, not due to setpoint regulation but due to the available wind speed, thus not until the FCU signal reaches a value where the wind turbines actually have to be down regulated, they will react to the setpoint change.

Fig. 6.23: Validation of the FCU. Plot (a) shows the setpoint and the output signal from the FCU. Plot (b) shows the active power of PO G1.

6.3 CHAPTER SUMMARY

This chapter has presented the PowerFactory model of Suðuroy, with some additional comments on how the main grid has been modelled. The static model has been validated and so has the dynamic models of the governors and AVRs. The application of the parameterisation and validation procedure presented in Chapter 5 has shown to be successful. The manual SFC of three generators has also been modelled and validated. Modelling and validating a manual control which depends on the staff's behaviour this is not common in previous literature. The wind turbines and FCU have also been validated in cooperation with the manufacturer. This results in a model of Suðuroy, which can be used for power system analyses and accurate results can be obtained. The model is however not 100% accurate and can therefore likely be improved through the consideration of additional scenarios. This study differs from other studies, due to its many practical considerations of a realistic power system, which are a vital necessity, if accurate and reliable results are desired. Additionally, the validation considers an unusually wide range of the model, i.e. from static load flow calculations to hour long dynamic simulations. This model is the basis for the analyses presented in Chapter 7, and will be used by SEV to investigate the present and future system for future decision making.

CHAPTER 7
Dynamic Studies of the Power System on Suðuroy

This chapter is the final chapter that addresses the second objective. It describes the dynamic studies conducted on the power system of Suðuroy, with and without the subsea cable connection to the main grid. The chapter starts with a study revolving around frequency and voltage fluctuations and their relationship with the inverter-based generation (IBG) in the system today. The next part focuses on short term large disturbances in the system of Suðuroy in 2020, 2023, 2026 and 2030 and how these affect the frequency and voltage stability. The study also addresses the importance of an accurate representation of main grid, after the cable connection between Suðuroy and the main grid has been installed. The studies presented in this chapter are all done using the validated PowerFactory model of the power system in Suðuroy, which was described in Chapter 6.

7.1   FREQUENCY AND VOLTAGE FLUCTUATIONS

The relationship between the IBG and the frequency and voltage fluctuations in the system of Suðuroy has been analysed in order to investigate what impact IBG has on the system. A better understanding of the consequences of increasing the IBG penetration and fluctuations in IBG on power systems in general and especially the Suðuroy power system under steady state conditions is achieved from the analysis described in the following sections. The study has also been published in [28].

The analysis of the impact of IBG on frequency and voltage fluctuations has been conducted based on the system in its stage primo 2022, as described in section 6.1 starting on page 125. It is conducted based on dynamic RMS simulation over a 4.5 hour operation scenario under steady state operation from the past, which meets a set of criteria and the analysis is conducted based on different cases as well. The operation scenario is described in subsection 7.1.1 and the study cases in subsection 7.1.2.

7.1.1 OPERATION SCENARIO

The operation scenario investigated was selected based on criteria for the generation and the demand. These criteria are set to ensure that the selected operation scenario is representative of the system, and suitable for the intended analysis, the set criteria are described in the following paragraphs and summarised in a list.

All generation types should be online, i.e. thermal, hydro, wind and solar. It is quite common that both thermal and hydro power are online, because while hydro is the preferred synchronous generation due to emissions; most of the time it can not serve the demand on the island. As previously shown in Figure 1.5 on page 10, the demand in Suðuroy in 2020 was above 3 MW 6000 hours of the year, which is the rated capacity at the hydro power plant. It was desired to have both wind and solar generation in the scenario, so that the impact of these two can be analysed separately and together, because all IBG is not the same, and the consequences might differ from one technology to another.

The same generation units should be online throughout the whole period. This criteria is set to make sure that start and stops of units throughout the simulation period are avoided. Including starts and stops in a 4.5 hour simulation period complicates the simulation, and does not contribute to the analysis of the IBG impact on the frequency and voltage fluctuations under steady state operation.

Furthermore, there have been conditions set to the renewable energy potential, as the wind speed should be relatively stable, and the irradiation relatively high. The staff of Vágsverkið listed days and hours, which had relatively stable wind conditions and thus production, while the measured production from the PV panels was investigated in order to find days with a relatively high irradiation.

Finally, a normal weekday has been chosen as the best fitted operation scenario, as it is more representative of the whole year than e.g. weekends or holidays. All five criteria are listed as follows:

1. All generation types should be online

2. Same units should be online throughout the period

3. Relatively stable wind speed

4. Relatively high PV power production

5. Normal weekday

This analysis was conducted one to two months after the wind farm in Porkeri had officially been inaugurated in February 2021. Prior to this, the

wind farm had been in test operation for three months. Thus, the data which meets all five criteria is limited, especially with regards to criteria 3 and 4, as there are many storms, i.e. unstable wind conditions, and the solar irradiation is low in the first months of the year. This does not mean that the scenario is not representative, but that the data availability was very limited as the wind farm had recently been inaugurated.

The selected time period is from a Monday in March from 12:00 to 16:30. The total demand during this time period is shown in Figure 7.1. The load varies between 3.8 MW and 2.9 MW. The loads are modelled using measurement files as described in subsection 6.2.4 on page 157.
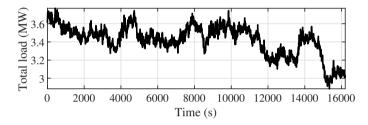
Fig. 7.1: Total load over selected 4.5 hour period [81].

Figure 7.2 shows the production from the wind farm on the left y-axis and the production from the PV plant on the right y-axis during the selected time period. It shows a wind power production varying between 2 MW and 2.4 MW. The step changes in the wind power production e.g. after 14000 seconds, are due to setpoint changes. The setpoint is varying between 0.35 p.u. and 0.41 p.u. The PV production reaches around 0.8 p.u. during the time period, so this is considered a relatively high PV power production considering the time of the year.

The measurements shown in Figure 7.2 are used as an input to represent the production from wind power and PV power in the simulations. This is done by setting a load equal to the measured production, but inverted, using a time series in a measurement file. This means that the dynamic model of the wind turbines has not been used in the simulations, but their dynamic behaviour is captured in the measurements. This is done to ensure that the simulated production replicates the measurements accurately. Controlling the wind power production over a long period of time using e.g. wind speeds as inputs is not possible with the dynamic models of the wind turbines.
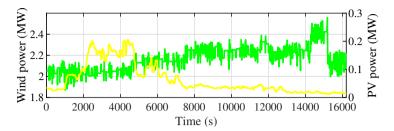
Fig. 7.2: Wind (green) and PV (yellow) power production during the 4.5 hour period [81].

The measurements files (load, wind and PV power) are using a constant interpolation, for further information see subsection 6.2.4 on page 157.

7.1.2 STUDY CASES

In order to investigate the impact of the IBG on the frequency and voltage fluctuations, different cases were studied including and excluding wind and PV power production. The first case is direct replication of the measurements, i.e. both wind and PV power production are set equal to the measured production. This can be considered a base case, which also validates both the secondary frequency control and load models, as discussed in subsection 6.2.3 and subsection 6.2.4. The other cases have been selected in order to make it possible to investigate the impact from the wind power and PV power individually and together. The cases are listed as follows.

- **Case 1:** Replicating the measurements, i.e. the wind and PV power production are set equal to the measurements.

- **Case 2:** The PV power production is removed, while the wind power production remains. The synchronous generation is increased to cover the power deficit caused by excluding PV power.

- **Case 3:** The wind power production is removed, while the PV power production remains. The synchronous generation is increased to cover the power deficit caused by excluding wind power.

- **Case 4:** Both the wind and PV power production are removed and the synchronous generation is increased to cover the power deficit caused by excluding wind and PV power.

7.1.3 COMPARISON OF STUDY CASES

The following sections will compare the simulation results of case 1 to case 2-4 showing the frequency and voltage fluctuations as duration curves, func-

164

tions of IBG shares and functions of fluctuations in the IBG. The frequency and voltage is from VG 20 kV, see Figure 6.2 on page 127.

The duration curves of the fluctuations in the frequency and voltage for the four cases give a general overview of how severe and common the fluctuations are through the simulated period under steady state conditions.

The fluctuations as functions of IBG shares are a good indication of how strong the relationship between the two is, but since the shares do not necessarily mean that the production is unstable, the relationship between the fluctuations in the IBG and the fluctuations in the frequency and voltage is also investigated.
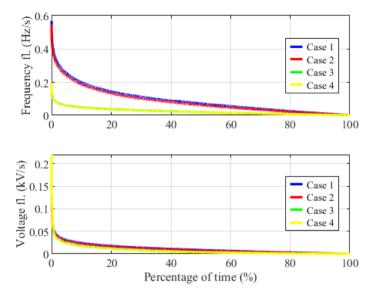
Fluctuation Duration

The duration curves of the frequency and voltage fluctuations in case 1-4 are shown in Figure 7.3 with max, mean and standard deviation fluctuations are tabulated in Table 7.1. The percentage of time with fluctuations above 0.1 Hz/s is also given in the table.

The duration curve of the frequency fluctuations shows that case 1 and 2, which include wind power are very similar, while case 3 and 4, which exclude wind power are very similar. The values in the table also confirm this, but there are some small differences. Case 2 does not include PV power, and this leads to fewer and smaller fluctuations compared to case 1. The maximum fluctuation is reduced by 22 mHz/s, the mean by 9 mHz/s and the standard deviation by 4 mHz/s. Also the duration of fluctuations above 0.1 Hz is decreased from 35.5% of the time to 30.6% of the time. Case 3 and 4 are more similar, as the mean and standard deviation fluctuations are equal, and so is the duration of fluctuations above 0.1 Hz/s. The maximum fluctuation is however decreased by 2 mHz/s. The penetration of wind power is significantly higher than of PV power, and therefore the wind power has a higher impact on the fluctuations. Additionally, the production shown in Figure 7.2 shows that the PV production is more stable than the wind power production.

The differences between the cases are not as clear when it comes to the voltage fluctuations. The standard deviation fluctuations is equal for all four cases, and the max and mean vary within 1 V/s and 4 V/s, respectively. The duration of the fluctuations above 20 V/s vary between 15.6% and 7.5%. The impact of the IBG on the voltage fluctuations is therefore not as clear as the impact of the IBG on the frequency fluctuations. But this voltage is measured at VG 20 kV, whilst the wind farm is connected to TG 20 kV. Since voltage is more local than frequency, there is is a possibility that the fluctuations at TG would be higher than what is measured at VG 20 kV. The reason the voltage used is at VG 20 kV, is because this analysis over 4.5 hours also focused on the validation as shown in previous chapter, and this validation requires fast

frequency measurements, which are not available at TG.

Fig. 7.3: Frequency (upper) and voltage (lower) fluctuation duration curves for cases 1-4 [81].

Table 7.1: Key values for frequency and voltage fluctuations [81].

Frequency	Case 1	Case 2	Case 3	Case 4
Max fluct. (mHz/s)	568	546	197	195
Mean fluct. (mHz/s)	92	83	23	23
Std. fluct. (mHz/s)	80	76	19	19
Fluct. =>0.1Hz/s (% of time)	35.5	30.6	0.6	0.6
Voltage	Case 1	Case 2	Case 3	Case 4
Max fluct. (V/s)	199	199	220	220
Mean fluct. (V/s)	11	10	7	7
Std. fluct. (V/s)	11	11	11	11
Fluct. =>20V/s (% of time)	15.6	13.3	7.5	7.6

Fluctuations as functions of IBG shares

The frequency and voltage fluctuations as functions of the IBG shares are shown in Figure 7.4. Case 4 is excluded from the plots, since no IBG is present in case 4. The difference in the IBG shares in case 1 and 2 compared to 3 is

quite significant, due to wind power being excluded, and this leads to a wide gap in the data coverage from around 6% to 52% IBG shares. Additionally the coverage above 75% is limited. The figure shows the data points, the mean values for each IBG share and a trend line based on all of the values.

Figure 7.4 shows, similarly to the previous figure, i.e. Figure 7.3, that the frequency fluctuations are impacted by IBG more than the voltage fluctuations are. Whilst one can see that the frequency fluctuations are generally higher for the higher IBG shares, the difference in the voltage fluctuations is not as clear, although it has the same tendency. The slope of the frequency trend is 103 mHz, which corresponds to 0.0021 p.u., while the slope of the voltage trend line is 6 V, which is 0.0003 p.u. In order to get a better understanding of the fluctuations as a function of IBG shares, data with a broader coverage of IBG shares should be investigated. As the data used here does not cover above 6% and below 52% IBG penetration.

Fig. 7.4: Frequency (upper) and voltage (lower) fluctuations as a function of IBG shares. All data points (p) and the mean (,) for every IBG share is shown for cases 1-3 (C1-C3). Additionally a linear trend is shown based on all data points [81]. The figure also showed a zoomed plot from 0%-6% IBG and 52%-85% IBG.

Fluctuations as functions of IBG fluctuations
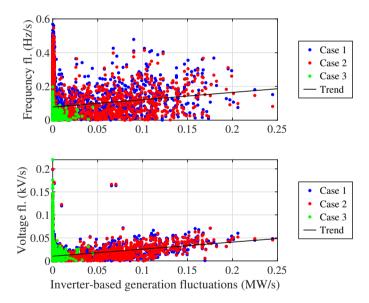
The final presentation of how the frequency and voltage fluctuations are impacted by the IBG is given in Figure 7.5 and Table 7.2. Here the frequency and voltage fluctuations are shown as functions of the IBG power fluctuations, i.e. the fluctuations in the generation from IBG. Frequency and voltage fluctuations are apparent also without IBG fluctuations, which means that there are other factors which have an impact on the frequency and voltage fluctuations. The varying loads in the system could cause this.

Both the figure and the table show that the correlation between the two types of fluctuations (frequency/voltage vs. IBG) are higher for the voltage than the frequency. The correlation factor between the frequency and IBG fluctuations is low, especially with all data considered, but considering only IBG fluctuations above 0.02 MW/s increases the correlation factor somewhat, i.e. 0.08 to 0.28 for case 1. The same thing can be said for the voltage, but the correlation factors are significantly higher than for the frequency.

However, for each MW IBG fluctuations the frequency fluctuates on average by 0.0087 p.u./MW if all data points are considered and 0.0119 p.u./MW, if only the fluctuations above 0.02 MW/s are considered. These values are slightly lower for the voltage at 0.0073 p.u./MW considering all data and 0.0098 considering only fluctuations above 0.02 MW/s. Thus, although the correlation is higher, the impact is lower.

For both the voltage and the frequency the correlation factors for case 2 (without PV) are highest, this indicates that the fluctuations in the wind power have a higher correlation with the fluctuations in the frequency.

Fig. 7.5: Frequency and voltage fluctuations as a function of IBG fluctuations with a linear trend line [81].

Table 7.2: Correlation factors between frequency/voltage fluctuations and inverter-based generation fluctuations [81].

	Frequency		Voltage	
	All data	Fluct. above 0.02	All data	Fluct. above 0.02
Case 1	0.08	0.28	0.23	0.50
Case 2	0.08	0.29	0.25	0.54
Case 3	0.01	0.28	0.04	0.40

Discussion of Frequency and Voltage Fluctuations

From the data represented it is clear that the IBG has a greater impact on the frequency than the voltage, but this is also expected, as the fluctuations are compared to the active power shares and fluctuations of the wind farm, not reactive power. Another factor which can have an impact on this is the location of the voltage measurements. Both the frequency and the voltage is measured at the 20 kV busbar at Vágsverkið and the wind farm is connected to the Tvøroyri substation, and since the voltage is not a global system parameter, the voltage fluctuations seen in Tvøroyri might be different than the ones measured at Vágsverkið.

SEV has no standard on the shape of the voltage and frequency fluctuation duration curves, and thus; although the IBG clearly has a negative impact on these, this can not be used directly as an indicator on whether or not this is acceptable.

The data coverage should be improved in order to make any final conclusions of the fluctuations dependency on the IBG shares, as no data with IBG shares between 6% and 52% have been included here, and data with the high penetrations >75% is also limited.

The correlation between the IBG fluctuations and the frequency and voltage fluctuations has been calculated. The definition of a weak, moderate and strong correlation varies in literature, and thus it can be difficult to state anything specific on the level of the correlation, but the upper limit of a weak correlation is usually between 0.3 and 0.5, while the lower limit of a strong correlation varies between 0.5 and 0.8. According to these limits, the correlation between the frequency and IBG fluctuations is weak to moderate, while the correlation between the voltage and IBG fluctuations is moderate to strong.

7.2   SUĐUROY TOWARDS 2030

The frequency and voltage stability in Suđuroy towards 2030 has been investigated in a submitted paper, which can be found in [145]. This study

builds on Chapter 3 and 4, as the expansions in the grid of Suðuroy and the main grid are taken directly from the proposed RoadMap. Additionally, the operation scenario is based on the input data to the Balmorel optimisation and the optimised dispatch from the optimisation of the RoadMap scenario in Balmorel.

This section describes the expansions in the grid of Suðuroy towards 2030. The base PowerFactory model used is the system of Suðuroy ultimo 2022, i.e. with the new substation, battery energy storage system (BESS) and synchronous condenser (SC), see chapter 6. It also describes the operation scenario simulated and the study cases.

7.2.1 EXPANSIONS IN ACCORDING TO THE ROADMAP

The expansions in Suðuroy based on the RoadMap are shown in Figure 7.6, while the expansions in the main grid are summarised in Table 7.3. The RoadMap accounts for additional 6 MW of wind power in Suðuroy in 2023, and in 2026 a cable connection to the main grid should be installed. From 2028 to 2030 there is a total of 16 MW of solar power installed in Suðuroy. In 2030 there is also a battery installed, but this battery is intended for weekly storage, not ancillary services.
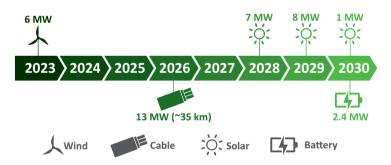
Fig. 7.6: Expansions in Suðuroy according to the RoadMap [81].

The table shows the summed expansion capacities in the main grid from 2020 to 2026 (by 2026), and from 2027 to 2030 (by 2030). The main grid is only analysed together with Suðuroy after the cable connection, i.e. 2026, and only in 2026 and 2030. Suðuroy is investigated isolated in 2020 and 2023 as well. The reason not all years have been investigated, is because the changes in the grid of Suðuroy are limited. The expansions shown in the table are directly taken from the proposed RoadMap [81] which is shown in Figure 4.1 on page 104.

Table 7.3: Additional expansion in wind power, hydro power, pumping power and photovoltaics in the main grid by 2026 and 2030 according to the RoadMap presented in [81]. [145].

By 2026	By 2030
72 MW Wind Power	66 MW Wind Power
35 MW Hydro Power	39 MW Hydro Power
41 MW Pumping Power	38 MW Pumping Power
	40 MW Photovolatics

7.2.2 EXPANSIONS RELATED TO ANCILLARY SERVICES

This study is based on the system ultimo 2022, thus the SC and BESS in Suðuroy are included in the system model. SEV has, as mentioned in section 1.2, preliminary plans to install 3x16 MVA and 1x6 MVA synchronous condensers and a BESS capacity of 30 MW in total. These expansions have been included in the model of the main grid and thus in the simulations for 2026 and 2030.

In this study it was decided to increase the BESS and SC size, when there are issues with the stability of the system. This gives an indication of the initiatives necessary to stabilise the system, but is by no means an optimisation of solving the issues seen. If the simulations show a need for additional BESS capacity, it is increased by adding a parallel battery package of 2.3 MW. The synchronous condenser is increased in intervals of 2 MVA when needed.

7.2.3 SIMULATION OPERATION SCENARIO

A suitable and representative operation scenario has been selected based on the optimisation study, see chapter 3. The input data to Balmorel from 2017 has first been analysed, and all scenarios fitting the following requirements are found.

The system is under pressure in high load scenarios, and therefore it was decided to use a high load scenario. This corresponds to a load above 4.5 MW based on the 2017 input data in Balmorel.

In order to ensure that the potential for wind power is high, the wind speed shall be equal to or higher than the average wind speed i.e. 9.5 m/s in 2017. A high penetration of wind power puts pressure on the system, as it leads to less synchronous generation and increased risk of large generation fluctuations.

Finally the irradiation from the investigated hour should be relatively high, i.e. equal to or above average when night hours are excluded. The average irradiation in Suðuroy in 2017 was 201 W/m^2. This is done to ensure that there in the simulations for 2030, is a production from the solar power,

and so that all components in the system are considered. The requirements set to the input data to Balmorel (2017) are as follows:

1. The operation scenario should be a high load scenario, i.e. $\geq$4.5 MW in 2017.

2. The wind speed at the wind farm Porkerishagi in Suðuroy should be equal to or above average, i.e. 9.5 m/s in 2017.

3. The irradiation in Suðuroy should be equal to or above average, i.e. 201 W/m^2 in 2017. Night hours are excluded from this average calculation.

There are 41 hours in 2017 which meet all three requirements. In order to narrow it down further, the output data from Balmorel, i.e. the optimised dispatch, was analysed. This is done for the investigated years, which are 2020, 2023, 2026 and 2030. A new set of criteria are set to the data and are described in the following paragraphs. This was done to select a representative operation scenario in the system of Suðuroy.

The first criteria is that the IBG shares should be lower than or equal to 60% and 80% in 2020 and 2023 respectively. Although there is a limit on the IBG shares in the dispatch, this is not defined for the two grids independently before the interconnection, see subsection 3.2.11 on page 76. No criteria on IBG shares in Suðuroy after the cable has been installed, i.e. in 2026 and 2030. After the grids are connected, the Balmorel optimisation of the dispatch ensures that the total IBG shares are within the limit set in subsection 3.2.11 on page 76.

The second criteria was that the diesel engines should supply at least 20% in 2020, this to ensure that the diesel engines are loaded above minimum and because this is the first year the wind farm in Suðuroy is in operation, and thus it is unlikely that the system is run only with hydro and wind power.

The shares of PV generation in Suðuroy should be equal to or lower than 20%. This was decided as higher shares will be uncommon, due to the low irradiation caused by the latitude and climate, and because of the installed capacity. If a scenario with high shares of PV was selected as the operation scenario, it would not be representative to draw any general conclusions on.

After Suðuroy is connected to the main grid in 2026, it was decided that the import should be lower than or equal to 40%, so that the analysis includes significant amount of local production. The five criteria are listed as follows:

1. IBR shares: $\leq$60% in 2020 and $\leq$80% in 2023

2. Supply from diesel power plant: $\geq$20% in 2020

3. PV shares: $\leq$25%

4. Import from the main grid: $\leq$40% of the demand in Suðuroy

One hour out of the 41 hours meets all the requirements. This is 12:00 on the 28th of March. The optimised dispatch for this scenario in 2020, 2023, 2026 and 2030 is found in Table 7.4. However this was not used directly, since it is important to have a similar production composition for all years, to be able to compare the impact of the study cases on in different years. The dispatch has been adjusted as listed:

- Wind and PV production values are taken directly from the optimised dispatch.

- Hydro power in Suðuroy is adjusted in 2020, 2026 and 2030, so that it produces 1.8 MW every year.

- In 2020 the thermal production is set lower to compensate for the additional hydro power.

- In 2026 and 2030 the import is decreased to compensate for the interconnection of the main grid, the import is set lower.

Table 7.4: Production and import in the selected operation scenario according to the optimised dispatch in [81] as percentages of demand in Suðuroy (rounded to integers) [145].

	2020	2023	2026	2030
Diesel	42%	15%	0%	-
Hydro	0%	15%	0%	0%
Wind	58%	70%	66%	60%
Import	-	-	35%	18%
PV	-	-	-	23%

The actual generation and pumping settings set in the simulations can be found in Table 7.5. No values are listed for the main grid in 2020 and 2023, since the main grid is not simulated before it is connected to Suðuroy in 2026.

Table 7.5: The generation and pumping settings (MW) used in the simulations.

Year	Suðuroy					Main grid				
	Thermal	Hydro	Wind	Solar	Import	Biogas	Hydro	Pumping	Wind	Solar
2020	1.3	1.8	4.4	-	-	-	-	-	-	-
2023	1.8	1.8	8.2	-	-	-	-	-	-	-
2026	-	1.8	8.2	-	2.2	1.0	4.6	-12.7	72.3	4.0
2030	-	1.8	8.2	3.8	0.7	1.0	3.9	-19.6	80.3	10.7

The load measured at each feeder on Figure 6.2, Figure 6.3 and Figure 6.4 (page 127 to page 128) and the position of the tap changers and circuit breakers have all been extracted from the SCADA system for the specific operation

scenario. The loads have been scaled up to meet the projected demand. This is done for both the main grid and the grid on Suðuroy. In some cases the tap changers positions have been modified for future scenarios when the voltage has been high or low.

7.2.4 STUDY CASES

There are three main events/study cases investigated, which all are large short term disturbances. The first one is a trip of one of the hydro generators in Suðuroy, i.e. BO G1. This is interesting to investigate because in the future the only synchronous generation in Suðuroy will be from the hydro power plant. The size of the loss relative to the total production each year is shown in Table 7.6. This event is also run with/without inertia emulation (IE) from the wind turbines, which is done based on 2020 but without the BESS.

Sudden changes in wind speed and wind direction are not uncommon in the Faroe Islands. Therefore it was decided to simulate the system where the event is that the setpoint of the wind farm changes from 0.7 p.u. to 0.0 p.u. This change can occur within 17 seconds with the installed controllers and respective parameters. A sudden wind change may however happen faster than this in reality, but the dynamic models of the wind farm only accept setpoints as inputs, not wind speeds. This event is also simulated with three different representations of the main grid, i.e. the full size model and approximated models, which are explained in section 7.5.

The final event is a load rejection, which is done at the feeder "TG Havnarlagið 1", which can be seen in Figure 6.4 on page 128. A large fish factory is supplied by this feeder.

Year	2020	2023	2026	2030
BO G1 trip	24%	15%	18% (2%)	14% (2%)
Sudden loss of wind power	58%	70%	82% (10%)	63% (8%)
Load rejection	18%	18%	18% (3%)	18% (3%)

Table 7.6: The size of the events in percentage of the production in Suðuroy. The numbers given in parenthesis are percentage of the total production.

7.3 LARGE SHORT TERM DISTURBANCES

This section presents the main results from simulations with large short term disturbances, which have been presented in the previous section. The disturbances are analysed through plots showing the dynamic frequency and voltage responses.

7.3.1 LOSS OF BO G1

The loss of BO G1 leads to a sudden drop in frequency with a ROCOF of 370 mHz/s in 2020. This is shown in Figure 7.7. The frequency is however stabilised when it reaches 49.8 Hz, as the BESS is controlled to start contributing to frequency regulation ±200 mHz from 50 Hz. The BESS does not have secondary frequency control, and therefore the frequency stabilises with a frequency deficit of 200 mHz.

The frequency responses in 2020 and 2023 are identical. This is because the only difference between 2020 and 2023 is the higher demand, which is supplied by the higher wind power production. The same engines are online and the loss is the same, and therefore the inertial response is the same as well.

In 2026, when the subsea cable connects Suðuroy and the main grid, the system reacts differently to the loss of BO G1. The ROCOF is decreased to 35-40 mHz/s in 2026 and 2030, which is only 9-11% of the ROCOF in 2020 and 2023. The frequency in 2026 does not reach 49.8 Hz, thus the BESS is not contributing to frequency regulation, but in 2030, with a slightly higher ROCOF and thus lower minimum frequency, the BESS contributes, but not significantly. The reason that the ROCOF is higher, is that BO G1 has initialised a higher active power in 2026 than in 2030, thus; although it is smaller disturbance compared to the total production, it is a higher synchronous loss and thus, the ROCOF is higher.

The disturbances on the voltage are very limited. The behaviour in 2020 and 2023 is similar, while the behaviour in 2026 and 2030 is similar. Since the connection to the main grid clearly has an impact on both the frequency and voltage responses, it is important to model the main grid accurately. In the simulations shown here, the main grid has been modelled with a detailed model, i.e. all components above 1000 V.

Based on the simulations with the BO G1 trip, it was not considered necessary to expand the system in Suðuroy with additional BESS and/or SC, because none of the simulations result in instabilities.
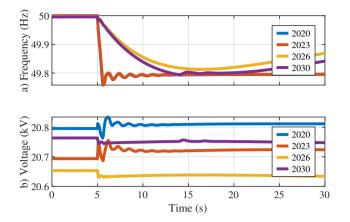
Fig. 7.7: Frequency and voltage response VG-20 kV to the BO G1 trip in 2020, 2023, 2026 and 2030. The 2020 (blue) is behind 2023 (red) [145].

7.3.2   SUDDEN LOSS OF WIND POWER

The second event is a sudden loss of wind power, see Figure 7.8. This means that the wind power production is reduced from 0.7 p.u. to 0.0 p.u. within 17 seconds. The frequency in 2020 drops with a somewhat high ROCOF, but stabilises as the battery starts injecting active power.

In 2023 there are some issues with the frequency. When the frequency reaches 49.6 Hz, the frequency suddenly drops even further. It is increased again, but a second drop happens a few seconds later. The cause of this is the dynamic controllers of wind turbines, since deactivating these solved the issue. The exact cause of this frequency drop has however not been identified, and should be investigated further.

The frequency behaviour in 2023 could possible be caused by the parameter settings, and if so, it could be solved by tuning the parameter settings of the controllers, but in this study the actual current parameter settings at the wind farm have been used and adjusting parameters of existing wind farms is out of scope. Further simulations (2023-1) show that by increasing the battery system by one additional package (2.3 MW) the issue has been resolved.

The connection to the main grid improves the frequency response to the sudden drop of wind power. This again shows that the main grid contributes to the system stability in Suđuroy, with e.g. a decreased ROCOF.

The voltage in 2020 and 2023-1 show the same behaviour but 2023-1 is initialised lower. Similarly 2026 and 2030 (with the cable to the main grid) show the same pattern, but initialisation is different, due to demand and production differences. The cable connection results in a higher voltage drop, due to the import of power from the main grid.

The results in 2023 compared to 2020/2030 show the importance of conducting simulations of the system as it is developing, and not only for start and end scenarios, because some of the issues might not be identified otherwise. Knowing that issues seen in 2023, can be fixed with additional battery capacity of 2.3 MW, but also by further development of the system, might change the approach of solving the issues seen in 2023-1.
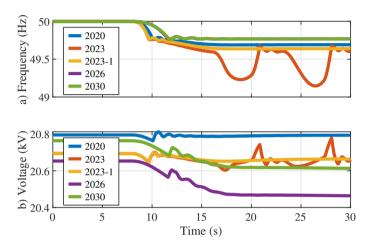
Fig. 7.8: Frequency and voltage response at VG-20 kV to the sudden loss of wind power in 2020, 2023, 2026 and 2030 [145].

7.3.3 LOAD REJECTION

The third event, i.e. the load rejection, is shown in Figure 7.9. Similarly to the previously presented scenarios, it is clear that the ROCOF is higher when Suðuroy is isolated compared to when it is connected to the main grid. The frequency response in 2020 shows that the frequency stabilises after the battery starts to contribute to frequency regulation after 50.2 Hz.

In 2023, there are some oscillations apparent in both the frequency and the voltage response. Further simulations (2023-2) showed that by increasing the synchronous condenser by 4 MVA, from 8 MVA to 12 MVA, these oscillations can be avoided.

Similarly to previous simulations, the voltage behaviour is different depending on interconnection between Suðuroy and the main grid, but the events' impact on the voltage is relatively small in all years.

There are no issues with the frequency nor the voltage after Suðuroy is connected to the main grid. The (expanded) BESS and SC in Suðuroy stabilise the system sufficiently together with the main grid. The frequency is not regulated down to 50 Hz in the simulations due to the secondary control

being manual.

Fig. 7.9: Frequency and voltage response at VG-20 kV to the load rejection in 2020, 2023, 2026 and 2030 [145].

7.4 INERTIA EMULATION FROM WIND TURBINES
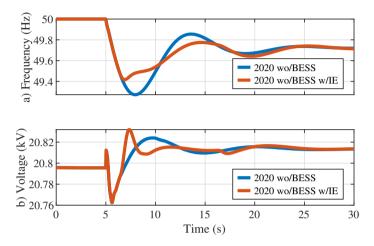
The BO G1 trip event has also been simulated without the BESS located at the Í Heiðunum (IH) substation, see Figure 6.6 on page 129. This was done to show the impact of utilising the inertia emulation (IE) capability of the wind turbines. Since the default settings of inertia emulation is set to not be activated until the frequency reaches 49.5 Hz, and the BESS reacts at 49.8 Hz, the BESS had to be deactivated in order to see the influence of the IE with default settings.

Figure 7.10 shows the comparison of the system response with and without IE. It shows that the system would benefit from activating the inertia emulation, as the frequency nadir is lower without IE.

The IE has little impact on the voltage response. A slightly different pattern is seen, but aside from that the response is similar, with little changes in peak voltage and settling time.

In a case were the event is of such a size, that the BESS can not stabilise the frequency entirely, activating the IE would be beneficial. However, the BESS to be installed in Suðuroy is larger than the wind farm size, and similar to the high load scenarios, so the activation of IE is not a very likely occurrence.

With good coordination between the activation of BESS and IE respectively, the benefit of utilising the IE from the wind turbines could be improved. If IE is proven to be beneficial for the power system, not just in Suðuroy but also in the main grid, it can assist the battery system. The wear

and tear of the batteries and wind turbines when using batteries or IE should be investigated, as this factor should be considered when choosing a control strategy.

Fig. 7.10: Frequency and voltage response at VG-20 kV to the BO G1 trip with and without inertia emulation from wind turbines in 2020, 2023, 2026 and 2030 [145].

7.5 REPRESENTATION OF THE MAIN GRID

Network reductions to represent a large grid connected to a smaller grid is common, when analysing the smaller grid. This is done to decrease the complexity of the system and the calculation time. This section highlights the challenges of representing the main grid with network reductions, in the simulations after the subsea cable has been installed. The accuracy of these models as the penetration of inverter-based technologies increases has to be addressed.

7.5.1 MODELLING

As explained in chapter 6, a detailed RMS model of the main grid is available and has been built, parameterised and validated similarly to the Suðuroy model, although the validation is not done as thoroughly yet. Since this study focuses on the power system Suðuroy, which in the future happens to be connected to a larger grid, the question on whether or not a full detailed model of the main grid was needed or not has been analysed.

In this study two different approximations of the main grid are compared to a detailed model of the main grid. Both approximations have been done using the "External grid" model component in PowerFactory. This "External

grid" model component is a simplified version of synchronous generator, as the saturation and leakage reactances are neglected. The input required is the short circuit power of the grid. This has been calculated from the detailed model. The default acceleration constant is infinite, but it can be changed. In this study the first approximation uses an infinite acceleration constant, while the second approximation uses an acceleration constant, which has been calculated based on the ROCOF of a system disturbance simulation of the main grid in 2026 simulated separately from the grid on Suðuroy, using Equation 7.1 [169]. The transient, substransient time constants and the synchronous and transient reactances can also be defined in addition to the short circuit power and the inertia. The default values have been used for the time constants and reactances.

$$\frac{\mathrm{d}f}{\mathrm{d}t} = \frac{\Delta P}{S_{\text{sys}}} \frac{f}{2H_{\text{sys}}} \tag{7.1}$$

The models of the main grid used in the following sections are:
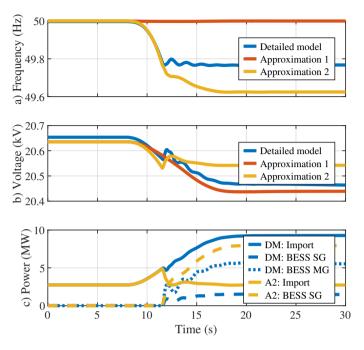
- The full detailed model of the main grid.

- Approximation 1: Simplified synchronous generator defined based on the short circuit power in the grid.

- Approximation 2: Simplified synchronous generator defined based on the short circuit power in the grid and the system inertia.

7.5.2 SIMULATION RESULTS

Figure 7.11 shows the comparison of the frequency and voltage responses to the sudden drop of wind power in 2026 with different representations of the main grid. The figure also shows the power output from the batteries in the main grid and Suðuroy and the import from the main grid to Suðuroy.

Plot a) shows the frequency response. This shows that with approximation 1, the frequency is not affected by the loss of wind power, because the infinite acceleration constant compensates for this. The simulation results with the detailed model show that the frequency decreases to 49.8 Hz when the battery system starts to stabilise the system. The frequency in approximation 2 (subsection 7.5.1) is significantly closer to the detailed model than approximation 1 (subsection 7.5.1), and this is because the inertia constant as been set equal to the actual system. This is also clear from the first seconds after the event, were the detailed model and approximation 2 have the same ROCOF. However, when the battery system in the detailed model injects power the responses differ from each other. This is because the approximated model can not capture the frequency triggered contribution from the battery system in the main grid. Adding the output from the BESS in

the main grid and in Suðuroy using the detailed model, see plot c), gives a higher initial response than the BESS in Suðuroy using the approximated model. There is steady state deviation between the frequency using the detailed model and approximation 2, and this is caused by the limitation of the battery in Suðuroy. The import from the main grid using the detailed model added with the battery system in Suðuroy is higher than the import from approximation 2 added with the battery in Suðuroy. Using approximation 2 the battery is delivering maximum power, and can not increase it further, thus, the total active power regulation with approximation 2 is lower than with the detailed model. Therefore the frequency can not be maintained at the same level as the wind power decreases, when using approximation 2 instead of the detailed model.

The accuracy of the voltage is opposite, i.e. approximation 1 is accurate while approximation 2 is inaccurate. This is because of the relationship between the voltage drop and the import from the main grid. The import from the main grid decreases when the battery in Suðuroy is triggered, and therefore the voltage drop does not increase further. Using approximation 1 the behaviour is sightly different from the detailed model, as the dynamics when the BESS in the main grid is regulating is not capturing, but the overall response is very similar, since the loss is compensated from the main grid whether it is a battery system or an infinite inertia.

Fig. 7.11: Comparison of the dynamic response in Suðuroy using different modelling approaches of the main grid. Plot a) shows the frequency response and plot b) shows the voltage at VG 20 kV. The plot c) shows the import form the main grid (MG) to the Suðuroy grid (SG) and the power output from the BESS using the detailed model (DM) and approximation 2 (A2) of the main grid. The specific scenario is sudden loss of wind power in 2026 [145].

The plots in Figure 7.11 show that there are some implications of using approximating models, especially when it comes to capturing frequency triggered technologies. Therefore the detailed model was used to represent the main grid in the simulations represented in previous sections, i.e. section 7.3 and section 7.4. One method of solving the issue with the approximated model could be to model a battery system parallel to the external grid component at the end of the subsea cable. This means that while the synchronous generation, the transformers and cables are approximated using a simple approximation like e.g. "External grid", the batteries in the main grid should be represented with a battery model. This way Suðuroy should receive the same, or similar, contribution through the cable using the detailed model or approximation 2 with a parallel battery.

7.6 FROM SUÐUROY TO THE MAIN GRID

The dynamic analyses represented here focus on the grid of Suðuroy, which is significantly smaller than the main grid. This section elaborates on how

the results observed in Suðuroy can be transferred to the larger main grid.

The fluctuations seen in Suðuroy due to the IBG, are an issue that is apparent in the main grid as well. The wind farms are larger, especially future wind farms, but the grid is also stronger, with higher inertia and short circuit power. Therefore it is difficult to say anything specific on how the main grid will be affected. The advantage in the main grid is also that there are more wind farm locations, i.e. the generation is distributed and the fluctuations are therefore not directly proportional to the total wind power capacity in the main grid, due to the different wind conditions.

The events analysed in the previous sections are considered large disturbances in Suðuroy; however, in all events it was shown that when Suðuroy is connected to the main grid, the severity of the disturbances decreases significantly. This is of course due to the system becoming larger and the disturbances relatively smaller. Therefore one can not say that since the disturbances analysed in this case do not cause severe issues with the power system stability, that e.g. a sudden wind power drop from 0.7 p.u. to 0.0 p.u. at a wind farm in the main grid, would be insignificant. Because such a reduction depends on the wind farm size and location. Additional simulations are required to conclude anything on this, and the disturbances analysed in the main grid should be large compared to the whole system, not only the grid of Suðuroy.

The approximated models show implications, and if it was the other way around, the same implications would be seen, i.e. if Suðuroy is approximated for an analysis of the main grid from 2026 and onward. The need for simplifying Suðuroy is however not as significant as for the main grid. The issues seen with the approximation are due to the frequency triggered technologies, i.e. in this case the BESS, and this will be an issue in all approximated models of systems which have a significant penetration of frequency triggered technologies.

7.7 CHAPTER SUMMARY

The chapter has analysed and described dynamic studies of the power system in Suðuroy, starting with frequency and voltage fluctuations during steady state operation in the present grid, followed by large disturbances in the grid and main grid network representation.

IBG has a negative impact on the frequency fluctuations in the system, but the impact on the voltage fluctuations is limited. However, as previously discussed, the location of the voltage measurement could be one of the reasons.

It is clear that the IBG can have a negative impact on the stability, but especially the fast reacting BESS in many cases are enough to ensure the stability in the study cases and operation scenarios considered. Large disturbances

in Suðuroy do not appear to be a problem when the system is connected to the main grid, due to ancillary services received from the main grid, and a large disturbance in Suðuroy being significantly smaller compared to the main grid. IE from the wind turbines has the potential to contribute to frequency stability, but as shown here the need of it decreases when there is a BESS in the system, which has been installed for this and other purposes.

Using the simplified models of the main grid lead to inaccuracies of the simulation results, due to the frequency triggered BESS.

The dynamic simulations conducted in this study do not address all aspects which should be addressed when moving towards 100% renewables. Thus, there are many other simulations which should be conducted on both the main grid and the grid in Suðuroy. The system of Suðuroy should be analysed for 2026 and forward with the subsea cable out of service, as this would increase the need for local stabilisation measures in Suðuroy. The system should also be investigated under other scenarios, e.g. with a 100% renewable inverter-based generation. The analyses conducted in the grid of Suðuroy should be adjusted and conducted on the main grid as well.

CHAPTER 8
Conclusions

This thesis has presented a thorough study of the future power system in the Faroe Islands toward a 100% renewable electricity sector. First by investigating the optimal energy mixture and translating it into a tangible RoadMap, and then through dynamic RMS studies of the power system of Suðuroy. This chapter concludes the research through answering the objectives, presenting the main contributions and future works.

8.1 THE FIRST OBJECTIVE

The first objective of this PhD was to determine the best suited RoadMap towards a 100% renewable electricity sector in the Faroe Islands based on the local energy resources and economics. This has been solved through (a) state of the art review, (b) assessment of energy resources, (c) feasibility of technologies, (d) optimisation of the energy mixture, (e) developing a procedure to obtain a tangible RoadMap and (f) obtaining the RoadMap for the main grid and Suðuroy through an application of the developed procedure.

(a) The available expansion planning tools are typically economic optimisations, which optimise the investments annually. This can lead to an increasing capacity at a specific investment site, e.g. a wind farm, every year, whilst in reality investments at a site are either conducted all at once, or in larger construction stages. Therefore an expansion plan based solely on an economic optimisation is not directly applicable to the power system. Hence, a method to obtain a tangible RoadMap should be developed. Multiple Faroese expansion planning studies have been conducted, but a higher level of details was needed, in order to conduct reliable power system analyses and simulations. In terms of similar study cases, the case of Madeira is most similar study case to the Faroese power system, although there are noticeable differences e.g. the potential for PV power.

(b) The potential for renewable energy is high, especially when it comes to wind and hydro power. Although the potential for solar power is lower,

the resource potential complements the wind speeds and precipitation well on a monthly basis, and thus it could become a vital component in the system during the summer. In addition to these, there is a potential for tidal energy as well. Tidal energy has the great advantage that it is not dependant on the weather, and it is predictable. Furthermore, there is a phase shift between the tidal streams at different locations, making it possible for base load production utilisation.

(c) The feasibility and costs of the different technologies has been obtained based on technological catalogues, previous investment projects and input from manufacturers.

(d) The optimal energy mixture has been found based on different scenarios using the economic optimisation tool Balmorel. Including tidal energy as an investment option has been shown to have a disruptive influence. Also utilising biofuels at one of the thermal power plants, could cancel significant investments in power and storage capacity. A sensitivity analysis showed that the results are not significantly sensitive to cost reductions or increases of 20%.

(e) A method to obtain a tangible RoadMap has been developed. This method utilises Balmorel, and translates the optimal results to a RoadMap, of which the economics are close to the economically optimal solution, and meets the goal of 100% renewables by 2030.

(f) The RoadMap for the Faroese power system includes the following wind and solar power capacities of 224% and 105% in ratio of average demand in 2030. In addition to this a 8-9 days of storage at the pumped hydro plant is required.

8.1.1 MAIN CONTRIBUTIONS

The main contributions from the research behind the first objective are the method to develop the RoadMap and the potential influence tidal energy has on the overall power composition.

The method developed to generate a tangible RoadMap bridges the gap between theoretical expansion planning studies and applications in actual power systems. This is done by taking an economic optimisation and translating it to a hands-on expansion plan. In order to make a RoadMap, which is applicable to actual expansion plans, it has to consider a broad aspect of practical constraints; technical, economic, environmental and political, e.g. operation limits, renewable goals and wind farm locations. The method is applicable to other systems [81].

If tidal energy becomes a feasible mature technology, it could reduce the total generation capacity by 18% in 2030. 72 MW of tidal power would replace all solar generation (79 MW), 66 MW of wind power, 9 MW of hydro power and 1 MW of battery power. This because tidal energy, different from hydro and wind power, has the same potential during the, when the wind and precipitation is limited, and the phase shift of the tidal currents at different locations. The needed reservoir capacity at the pumped storage system could also be reduced by 75%, if tidal energy becomes a viable competing technology. These results should motivate continuous development and research in this technology [81], [108].

8.1.2 FUTURE WORKS

The future works related to the first objective are described as follows.

There are constant changes in fuel costs, investment costs, demand progression etc. Therefore the RoadMap has to be updated on a regular basis. This should be done, in order to have the best foundation for making the most beneficial decisions when it comes to expansions of the power system.

The RoadMap generation, i.e. the step between the optimal results and the actual RoadMap, which in this study is manual, could be automatised. This would require the development of an algorithm fed by different criteria set by the expansion planning decision maker.

The RoadMap only considers the main grid and the grid of Suðuroy. The five smaller isolated systems should also be investigated, in order to reach a 100% renewable production in all of the seven grids in the Faroese power systems, although the five small grids account for less than 0.2% of the annual demand in the Faroe Islands.

8.2 THE SECOND OBJECTIVE

The second objective was to analyse how the frequency and voltage stability can be ensured in 100% renewable electricity sector. This objective focused on the power system of Suðuroy and has been answered by the following subobjectives: (a) state of the art review, (b) modelling the power system, (c) developing validation guidelines for power system models, (d) assessing frequency and voltage variations in today's system, (e) analysing the power system stability towards 2030, (f) assessing the need for using a detailed model of the main grid, and finally (g) to provide lessons learned from Suðuroy to the main grid.

(a) As the share of synchronous generation is decreasing, researchers and system operators are looking into alternative methods to provide ancillary services. Multiple control strategies of e.g. wind turbines and pho-

tovoltaics have been developed in previous literature. Previous Faroese power system stability studies have been presented. There are different methods to model (parameterise and validate) power system models, but when applied to the Faroese system insufficient results were obtained.

(b) The power system of Suðuroy has been modelled on transmission level (20 kV and 10 kV) for load flow and dynamic RMS simulations. The modelling of the present system is based on datasheets, test reports and information received from manufacturers. Missing data has estimated based on engineering experience. The type of components in the future system, that exist in today's system are modelled using the same models, e.g. wind turbines, while new types of components, e.g. large PV plants, are modelled with standard models.

(c) A procedure to parameterise and validate standard models of governors and AVRs has been developed. Tests and measurements to use for the parameterisation and validation have been prepared and conducted, and the procedure has successfully been applied to the system of Suðuroy.

(d) The frequency and voltage variations in today's system have been analysed through 4.5 hour simulation period. The impact of wind power and photovoltaic power has been analysed. Wind power has a higher influence on the fluctuations seen in the frequency than PV, but the production from PV is significantly lower and more stable. The impact on voltage fluctuations are limited.

(e) Analysing the system towards 2030 has highlighted some of the implications in the transition towards 100%. However, the connection to the main grid, which is nine times larger, solves some of the implications. This is due to the disturbances becoming relatively smaller, compared to the whole system. Prior to the connection, there is a need to make investments in ancillary services or modify control strategies. The study shows that increasing the battery capacity and synchronous condenser can solve these challenges.

(f) Using simple approximation models of the main grid when analysing the grid of Suðuroy, after the two grids have been connected, led to inaccurate representations. Thus, the dynamic simulations post 2026 were conducted using a detailed model of the main grid as well.

(g) The lessons learned in Suðuroy can to some degree be transferred to the main grid. The parameterisation and validation procedure can be applied to the main grid and other power systems as well. The study highlights the importance of investigating the system throughout the transition period, and not just the start and end, since some of the issues might be uncovered when doing this.

8.2.1 MAIN CONTRIBUTIONS

The main contributions from the research of the second objective are guidelines for parameterising and validating the governors and AVRs, the reflections of the representation of the main grid and how the results on a small grid, in this case Suðuroy, can be transferred to a larger grid, in this case the main grid and the representation of a large grid.

The parameterisation and validation procedure increases the accuracy of the dynamic models. Applications of the existing methods did not result in a model of the Faroese power system, which could be validated, and therefore it is not unlikely that validations of other power systems will face the same implications. The developed method combines existing approaches and increases the accuracy of the models [161].

Representing the main grid using simple network reduction models did not replicate simulations using a detailed model properly. The battery systems, which are frequency triggered, were not captured properly by the network reductions [145].

8.2.2 FUTURE WORKS

The future works related to the second objective are described as follows.

Different operation scenarios and disturbances should be investigated. The system of Suðuroy after the connection the main grid, should also be investigated based on scenarios where the subsea cable is out of service. In this case the system has to be both balanced and stabilised locally. The system was investigated isolated prior to 2026, and these studies showed the need for improved ancillary services. Investigations of the system post 2026 with the cable being out of service should be conducted.

The validation of the main grid should be improved, including more scenarios, to increase the accuracy of the model. The stability of main grid also has to be analysed, in order to get a better understanding of the initiatives necessary to ensure a stable grid towards 100% renewables.

Different ancillary services and control strategies should be investigated in order to chose the best solutions for the specific power system.

The five smaller grids should also be modelled and validated for load flow and dynamic simulations, in order to be able to ensure the future stability of these, in the transition towards 100% renewables.

Recent studies, e.g. [170], have stated that in the future EMT models will be necessary in order to simulate power systems with low system strength. The study shows an example of how simulation results from an RMS model of network with a high penetration of renewables deviates from the results from an EMT model of the same network. RMS simulations might therefore not foresee instabilities in low strength grid accurately. Thus, the Faroese

power system should in the future also be modelled in the EMT domain, in order to obtain accurate results for simulations with fewer synchronous generators/condensers online than the simulations in this PhD.

8.3 CONCLUDING REMARKS

This industrial PhD thesis provides valuable information for the transition of the Faroese power system toward a 100% renewable electricity sector. The methods developed, both to generate a realistic and tangible RoadMap based on an economical optimisation and the method to validate power system models are essential contributions to the industry to ensure a safe and reliable shift away from fossil fuels in the electricity mix in the Faroe Islands. Additionally, the methods are applicable to other power systems as well.

Bibliography

[1]   IRENA, *Renewable capacity statistics 2021*. Abu Dhabi: International Renewable Energy Agency (IRENA), 2021, ISBN: 978-92-9260-356-4.

[2]   International Energy Agency (IEA), *World Energy Outlook 2019*. IEA, 2019, ISBN: 978-92-64-97300-8.

[3]   Elfelagið SEV, *Grønt frambrot*, 2014. [Online]. Available: `https://www.sev.fo/um-okkum/midlar-og-samskifti/tidindi/gront-frambrot/` (visited on 03/09/2020).

[4]   ——, *Elframleiðslan 2020*, 2021. [Online]. Available: `https://www.sev.fo/um-okkum/midlar-og-samskifti/tidindi/elframleidslan-2020/` (visited on 03/09/2022).

[5]   ——, *Methøg elframleiðsla í 2021*, 2022. [Online]. Available: `https://www.sev.fo/um-okkum/midlar-og-samskifti/tidindi/methog-elframleidsla-i-2021/` (visited on 03/09/2022).

[6]   T. Nielsen, *Technical and Economic assessment of a 100% renewable electricity sector in the Faroe Islands in 2030, from the power company perspective*, MBA Thesis, Beuth University, Berlin, Germany, 2016.

[7]   Føroya Landsstýri (Government of the Faroe Islands), *Samgonguskjalið 2015*, Tórshavn, Faroe Islands, Sep. 2015.

[8]   ——, *Samgonguskjalið 2019*, Tórshavn, Faroe Islands, Sep. 2019.

[9]   A. List, *File:Map of faroe islands in europe - english caption.png*, 2005. [Online]. Available: `https://commons.wikimedia.org/wiki/File:Map_of_faroe_islands_in_europe_-_english_caption.png` (visited on 03/09/2020).

[10] P. Kundur, J. Paserba, V. Ajjarapu, G. Andersson, A. Bose, C. Canizares, N. Hatziargyriou, D. Hill, A. Stankovic, C. Taylor, T. Van Cutsem, and V. Vittal, "Definition and Classification of Power System Stability," *IEEE Transactions on Power Systems*, vol. 19, pp. 1387–1401, 2004. DOI: `10.1109/tpwrs.2004.825981`.

[11] T. Poulsen, B. Niclasen, G. Giebel, and H. G. Beyer, "Optimization of wind farm portfolio to minimize the overall power fluctuations -a case study for the faroe islands," *Wind Energ. Sci. Discuss.*, Mar. 2022. DOI: 10.5194/wes-2022-14.

[12] J. Shair, H. Li, J. Hu, and X. Xie, "Power system stability issues, classifications and research prospects in the context of high-penetration of renewables and power electronics," *Renewable and Sustainable Energy Reviews*, vol. 145, p. 111 111, 2021, ISSN: 1364-0321. DOI: https://doi.org/10.1016/j.rser.2021.111111.

[13] "Issues, Challenges, Causes, Impacts and Utilization of Renewable Energy Sources - Grid Integration," vol. 4, no. 3, pp. 636–643, 2014.

[14] L. Meegahapola, A. Sguarezi, J. S. Bryant, M. Gu, E. R. Conde D, R. Cunha, *et al.*, "Power system stability with power-electronic converter interfaced renewable power generation: Present issues and future trends," *Energies*, vol. 13, no. 13, p. 3441, 2020.

[15] D. Weisser and R. S. Garcia, "Instantaneous wind energy penetration in isolated electricity grids: Concepts and review," *Renewable Energy*, vol. 30, no. 8, pp. 1299–1308, 2005. DOI: 10.1016/j.renene.2004.10.002.

[16] T. R. Ayodele, A. A. Jimoh, J. L. Munda, and J. T. Agee, "Challenges of Grid Integration of Wind Power on Power System Grid Integrity: A Review," *International Journal of Renewable Energy Research*, vol. 2, no. 4, pp. 618–626, 2012.

[17] P. S. Georgilakis, "Technical challenges associated with the integration of wind power into power systems," *Renewable and Sustainable Energy Reviews*, vol. 12, no. 3, pp. 852–863, 2008. DOI: 10.1016/j.rser.2006.10.007.

[18] S. D. Ahmed, F. S. M. Al-Ismail, M. Shafiullah, F. A. Al-Sulaiman, and I. M. El-Amin, "Grid Integration Challenges of Wind Energy: A Review," *IEEE Access*, vol. 8, pp. 10 857–10 878, 2020, ISSN: 2169-3536. DOI: 10.1109/ACCESS.2020.2964896.

[19] R. Shah, N. Mithulananthan, R. C. Bansal, and V. K. Ramachandaramurthy, "A review of key power system stability challenges for large-scale PV integration," *Renewable and Sustainable Energy Reviews*, vol. 41, pp. 1423–1436, 2015. DOI: 10.1016/j.rser.2014.09.027.

[20] M. A. Eltawil and Z. Zhao, "Grid-connected photovoltaic power systems: Technical and potential problems-A review," *Renewable and Sustainable Energy Reviews*, vol. 14, no. 1, pp. 112–129, 2010. DOI: 10.1016/j.rser.2009.07.015.

[21] S. Eftekharnejad, V. Vittal, G. T. Heydt, B. Keel, and J. Loehr, "Impact of increased penetration of photovoltaic generation on power systems," *IEEE transactions on Power Systems*, vol. 28, no. 2, pp. 893–901, 2012.

[22] T. Ackermann, G. Andersson, and L. Söder, "Distributed generation: A definition," *Electric power systems research*, vol. 57, no. 3, pp. 195–204, 2001.

[23] G. Pepermans, J. Driesen, D. Haeseldonckx, R. Belmans, and W. D'haeseleer, "Distributed generation: definition, benefits and issues," *Energy Policy*, vol. 33, no. 6, pp. 787–798, 2005. DOI: `10.1016/j.enpol.2003.10.004`.

[24] Y. Tan, L. Meegahapola, and K. M. Muttaqi, "A review of technical challenges in planning and operation of remote area power supply systems," *Renewable and Sustainable Energy Reviews*, vol. 38, pp. 876–889, 2014. DOI: `10.1016/j.rser.2014.07.034`.

[25] O. Erdinc, N. G. Paterakis, and J. P. Catalaõ, "Overview of insular power systems under increasing penetration of renewable energy sources: Opportunities and challenges," *Renewable and Sustainable Energy Reviews*, vol. 52, pp. 333–346, 2015. DOI: `10.1016/j.rser.2015.07.104`.

[26] Elfelagið SEV, *About us*, 2022. [Online]. Available: `https://www.sev.fo/english/about-us/` (visited on 03/10/2022).

[27] ——, *Netroknskapur 2019*, Tórshavn, Faroe Islands, Apr. 2020.

[28] H. M. Trondheim, L. Hofmann, P. Gartmann, E. Quitmann, F. F. da Silva, C. L. Bak, T. Nielsen, and B. A. Niclasen, "Frequency and voltage analysis of the hybrid power system in suðroy, faroe islands," in *Proceedings of the Virtual 5th International Hybrid Power Systems Workshop*, Energynautics GmbH, May 2021.

[29] Bakkafrost, *Bakkafrost og landbúnaðurin samstarva um biogassverk*, 2018. [Online]. Available: `https://www.bakkafrost.com/fo/about-us/news/bakkafrost-og-landbunadurin-samstarva-um-biogassverk/` (visited on 12/02/2020).

[30] Minesto, *Minesto to concentrate Dragon Class operations in the Faroe Islands in 2022*, 2022. [Online]. Available: `https://minesto.com/news-media/minesto-concentrate-dragon-class-operations-faroe-islands-2022` (visited on 03/22/2022).

[31] N. M. J. P. Van Beeck, "Classification of Energy Models; FEW Research Memorandum," *Operations research, Tilburg*, 1999.

[32] S. Jebaraj and S. Iniyan, "A review of energy models," *Renewable and Sustainable Energy Reviews*, vol. 10, no. 4, pp. 281–311, 2006. DOI: 10.1016/j.rser.2004.09.004.

[33] F. Urban, R. M. Benders, and H. C. Moll, "Modelling energy systems for developing countries," *Energy Policy*, vol. 35, no. 6, pp. 3473–3482, 2007. DOI: 10.1016/j.enpol.2006.12.025.

[34] D. Connolly, H. Lund, B. V. Mathiesen, and M. Leahy, "A review of computer tools for analysing the integration of renewable energy into various energy systems," *Applied Energy*, vol. 87, no. 4, pp. 1059–1082, 2010. DOI: 10.1016/j.apenergy.2009.09.026.

[35] S. Pfenninger, A. Hawkes, and J. Keirstead, "Energy systems modeling for twenty-first century energy challenges," *Renewable and Sustainable Energy Reviews*, vol. 33, pp. 74–86, 2014. DOI: 10.1016/j.rser.2014.02.003.

[36] H. K. Ringkjøb, P. M. Haugan, and I. M. Solbrekke, "A review of modelling tools for energy and electricity systems with large shares of variable renewables," *Renewable and Sustainable Energy Reviews*, vol. 96, pp. 440–459, 2018. DOI: 10.1016/j.rser.2018.08.002.

[37] N. E. Koltsaklis and A. S. Dagoumas, "State-of-the-art generation expansion planning: A review," *Applied Energy*, vol. 230, pp. 563–589, 2018. DOI: 10.1016/j.apenergy.2018.08.087.

[38] A. S. Dagoumas and N. E. Koltsaklis, "Review of models for integrating renewable energy in the generation expansion planning," *Applied Energy*, vol. 242, pp. 1573–1587, 2019. DOI: 10.1016/j.apenergy.2019.03.194.

[39] European Parliament, "DIRECTIVE 2003/54/EC OF THE EUROPEAN PARLIAMENT AND OF THE COUNCIL of 26 June 2003 concerning common rules for the internal market in electricity and repealing Directive 96/92/EC THE," *Official Journal of the European Union*, vol. 176, pp. 37–55, 2003.

[40] Dansk Energi, "Notat - Funktionel adskillelse af elsystemet på Færøerne," Tech. Rep. d2018-22131-3.0, 2018.

[41] Department of Sustainable Development of the General Secretariat of the Organization of American States, "Antigua and Barbuda Draft Sustainable Energy Action Plan," Tech. Rep., 2013. [Online]. Available: http://www.scribd.com/doc/197609842/EAP-AntiguaBarbuda-Web.

[42] NREL, *Energy Snapshot Antigua and Barbuda*. Golden, Colorado: National Renewable Energy Laboratory, 2015. [Online]. Available: http://www.nrel.gov/docs/fy15osti/64115.pdf (visited on 10/02/2020).

[43] IRENA, *Renewables Readiness Assessment: Antigua & Barbuda*. International Renewable Energy Acency (IRENA), 2016, ISBN: 9789295111257.

[44] ——, *Country Profile Antigua and Barbuda*. Abu Dhabi: International Renewable Energy Agency (IRENA), 2018. [Online]. Available: `https://islands.irena.org/RE-Progress/Country-Profiles` (visited on 10/02/2020).

[45] ——, *Country Profile British Virgin Islands*. Abu Dhabi: International Renewable Energy Agency (IRENA), 2018. [Online]. Available: `https://islands.irena.org/RE-Progress/Country-Profiles` (visited on 10/02/2020).

[46] ——, *Country Profile Cabo Verde*. Abu Dhabi: International Renewable Energy Agency (IRENA), 2018. [Online]. Available: `https://islands.irena.org/RE-Progress/Country-Profiles` (visited on 10/02/2020).

[47] E. Nordman, A. Barrenger, J. Crawford, J. McLaughlin, and C. Wilcox, "Options for achieving cape verde's 100% renewable electricity goal: A review," *Island Studies Journal*, vol. 14, no. 1, pp. 41–58, 2019. DOI: `10.24043/isj.73`.

[48] A. R. Díaz, F. J. Ramos-Real, G. A. Marrero, and Y. Perez, "Impact of electric vehicles as distributed energy storage in isolated systems: The case of tenerife," *Sustainability*, vol. 7, no. 11, pp. 15 152–15 178, 2015. DOI: `10.3390/su71115152`.

[49] M. Uche-Soria and C. Rodríguez-Monroy, "Special regulation of isolated power systems: The Canary Islands, Spain," *Sustainability*, vol. 10, no. 7, 2018. DOI: `10.3390/su10072572`.

[50] Energynautics GmbH, *Power System in Madeira & Porto Santo*, 2020. [Online]. Available: `https://hybridpowersystems.org/power-system-madeira-porto-santo/` (visited on 03/17/2022).

[51] Electricidade da Madeira, *Mix da oferta do ano 2017 (MWh)*. Funchal, Madeira: Electricidade da Madeira, 2017.

[52] S. R. Abreu, C. Barreto, and F. Morgado-Dias, "Renewable energy characterization of madeira island," in *10th Portuguese Conference on Automatic Control*, Funchal, Portugal, 2012.

[53] IRENA, *Country Profile Maldives*. Abu Dhabi: International Renewable Energy Agency (IRENA), 2018. [Online]. Available: `https://islands.irena.org/RE-Progress/Country-Profiles` (visited on 10/02/2020).

[54] ——, *Country Profile Saint Lucia*. Abu Dhabi: International Renewable Energy Agency (IRENA), 2018. [Online]. Available: `https : / / islands . irena . org / RE - Progress / Country - Profiles` (visited on 10/02/2020).

[55] D. F. Cross-Call, *Matching Energy Storage to Small Island Electricity Systems: A Case Study of the Azores*, MSc Thesis, Massachusetts Institute of Technology, Cambridge, Massachusetts, 2013.

[56] Electricidade dos Açores, *Caracterização das redes de transporte e distribuição de energia elétrica em 2019*. Ponta Delgada, Açores: Electricidade dos Açores, 2019.

[57] IRENA, *Country Profile Seychelles*. Abu Dhabi: International Renewable Energy Agency (IRENA), 2018. [Online]. Available: `https : / / islands . irena . org / RE - Progress / Country - Profiles` (visited on 10/02/2020).

[58] J. V. Vreden, M. Wigan, A. Kruze, K. Dyhr-Mikkelsen, and H. H. Lindboe, *Proposal for Energy Policy of the Republic of Seychelles, 2010-2030*. Seychelles Investment Board.

[59] EDT, *Transition énergétique*. [Online]. Available: `https://www.edt.pf/ transition-energetique-innovation` (visited on 10/02/2020).

[60] NREL, *Energy Snapshot British Virgin Islands*. Golden, Colorado: National Renewable Energy Laboratory, 2015. [Online]. Available: `https: //www.nrel.gov/docs/fy15osti/62703.pdf` (visited on 10/02/2020).

[61] P. V. Ferreira, A. Lopes, G. G. Dranka, and J. Cunha, "Planning for a 100% renewable energy system for the Santiago Island, Cape Verde," *International Journal of Sustainable Energy Planning and Management*, vol. 29, pp. 25–40, 2020. DOI: `10.5278/ijsepm.3603`.

[62] Gesto Energia S.A., "Plano energético renovável Cabo Verde," Algés, Portugal, Tech. Rep., 2011.

[63] S. Pereira, P. Ferreira, and A. I. Vaz, "Optimization modeling to support renewables integration in power systems," *Renewable and Sustainable Energy Reviews*, vol. 55, pp. 316–325, 2016. DOI: `10.1016/j.rser. 2015.10.116`.

[64] H. C. Gils and S. Simon, "Carbon neutral archipelago – 100% renewable energy supply for the Canary Islands," *Applied Energy*, vol. 188, pp. 342–355, 2017. DOI: `10.1016/j.apenergy.2016.12.023`.

[65] M. Miguel, T. Nogueira, and F. Martins, "Energy storage for renewable energy integration: The case of Madeira Island, Portugal," *Energy Procedia*, vol. 136, pp. 251–257, 2017. DOI: `10.1016/j.egypro.2017. 10.277`.

[66]   H. M. Marczinkowski and L. Barros, "Technical Approaches and Insti-
        tutional Alignment to 100% Renewable Energy System Transition of
        Madeira Island—Electrification, Smart Energy and the Required Flex-
        ible Market Conditions," *Energies*, vol. 13, no. 17, p. 4434, 2020.

[67]   IRENA, *Renewable Energy Roadmap for the Republic of Maldives*. Interna-
        tional Renewable Energy Agency (IRENA), 2015. [Online]. Available:
        `https://www.irena.org/publications` (visited on 03/18/2022).

[68]   J. Liu, C. Mei, H. Wang, W. Shao, and C. Xiang, "Powering an island
        system by renewable energy—A feasibility analysis in the Maldives,"
        Applied Energy, vol. 227, pp. 18–27, 2018. DOI: `10.1016/j.apenergy.
        2017.10.019`.

[69]   K. Bunker, S. Doig, J. Locke, S. Mushegan, S. Teelucksingh, and R.
        Torbert, *Developing the Saint Lucia energy roadmap*. Rocky Mountain In-
        stitute, 2016. [Online]. Available: `https://rmi.org/wp-content/
        uploads/2017/03/Islands_Saint_lucia_Energy_Roadmap_Report_
        2016.pdf`.

[70]   C. G. Meza, C. Zuluaga Rodríguez, C. A. D'Aquino, N. B. Amado, A.
        Rodrigues, and I. L. Sauer, "Toward a 100% renewable island: A case
        study of Ometepe's energy mix," *Renewable Energy*, vol. 132, pp. 628–
        648, 2019. DOI: `10.1016/j.renene.2018.07.124`.

[71]   N. Duić and M. Da Graça Carvalho, "Increasing renewable energy
        sources in island energy supply: Case study Porto Santo," *Renewable
        and Sustainable Energy Reviews*, vol. 8, no. 4, pp. 383–399, 2004. DOI:
        `10.1016/j.rser.2003.11.004`.

[72]   G. Krajačić, N. Duić, and M. d. G. Carvalho, "H2RES, Energy plan-
        ning tool for island energy systems - The case of the Island of Mljet,"
        International Journal of Hydrogen Energy, vol. 34, no. 16, pp. 7015–7026,
        2009. DOI: `10.1016/j.ijhydene.2008.12.054`.

[73]   D. A. Katsaprakakis and M. Voumvoulakis, "A hybrid power plant
        towards 100% energy autonomy for the island of Sifnos, Greece. Per-
        spectives created from energy cooperatives," *Energy*, vol. 161, pp. 680–
        698, 2018. DOI: `10.1016/j.energy.2018.07.198`.

[74]   A. Maleki and A. Askarzadeh, "Optimal sizing of a PV/wind/diesel
        system with battery storage for electrification to an off-grid remote
        region: A case study of Rafsanjan, Iran," *Sustainable Energy Technologies
        and Assessments*, vol. 7, pp. 147–153, 2014. DOI: `10.1016/j.seta.2014.
        04.005`.

[75] Y. Kuang, Y. Zhang, B. Zhou, C. Li, Y. Cao, L. Li, and L. Zeng, "A review of renewable energy utilization in islands," *Renewable and Sustainable Energy Reviews*, vol. 59, pp. 504–513, 2016. DOI: 10.1016/j.rser.2016.01.014.

[76] J. Cappelen and E. V. Laursen, "The Climate of The Faroe Islands - with Climatological Standard Normals, 1961-1990," Danish Meteorological Institute (DMI), Copenhagen, Denmark, Tech. Rep., 1998.

[77] Landsbyggifelagið P/f, "Vatnorka, Yvirlit yvir útbyggingarmøguleikar," Elfelagið SEV, Tórshavn, Faroe Islands, Tech. Rep., 2000.

[78] N. Sondell, "Wind Energy Study for the Faroe Islands," Storm Weather Center, Oslo, Norway, Tech. Rep., 2010.

[79] K. Simonsen and B. A. Niclasen, "Analysis of the energy potential of tidal streams on the Faroe Shelf," *Renewable Energy*, vol. 163, pp. 836–844, 2021.

[80] G. Hagerman and B. Polagye, "Methodology for estimating tidal current energy resources and power production by tidal in-stream energy conversion (TISEC) devices," Electric Power Research Institute, Tech. Rep., 2006.

[81] H. M. Tróndheim, B. A. Niclasen, T. Nielsen, F. F. da Silva, and C. L. Bak, "100% Sustainable Electricity in the Faroe Islands: Expansion Planning Through Economic Optimization," *IEEE Open Access Journal of Power and Energy*, vol. 8, pp. 23–34, 2021, Licensed under **CC BY 4.0**. DOI: 10.1109/OAJPE.2021.3051917.

[82] H. M. Tróndheim, B. A. Niclasen, T. Nielsen, C. L. Bak, and F. F. da Silva, "Introduction to the Energy Mixture in an Isolated Grid with 100% Renewable Electricity - the Faroe Islands," in *Proceedings of CIGRE Symposium Aalborg 2019*, Paris, France: CIGRE (International Council on Large Electric Systems), 2019.

[83] H. M. Tróndheim, T. Nielsen, B. A. Niclasen, C. L. Bak, and F. F. da Silva, "The Least-Cost Path to a 100 % Renewable Electricity Sector in the Faroe Islands," in *Proceedings of 4th International Hybrid Power Systems Workshop*, Crete, Greece: Energynautics GmbH, 2019.

[84] D. A. Katsaprakakis, B. Thomsen, I. Dakanali, and K. Tzirakis, "Faroe Islands: Towards 100% R.E.S. penetration," *Renewable Energy*, vol. 135, no. 2019, pp. 473–484, 2019. DOI: 10.1016/j.renene.2018.12.042.

[85] A. M. Skeibrok, M. Eriksen, and J. Stav, *Optimized hybrid microgrid system integrated with renewable energy sources*, BSc Thesis, University of Adger, Kristiansand, Norway, 2019.

[86] J. Burakovskij, C. N. Jacobsen, R. S. Sagoo, and C. Wennerberg, "Fælles nordisk studie om pumped storage," Grontmij, Stockholm, Sweden, Tech. Rep., 2012.

[87] Norconsult AS, "Wind power based pumped storage, Pre-Feasibility Study, Suðuroy, Faroe Islands," Norconsult AS, Tech. Rep., 2013.

[88] D. Buiskikh, B. Zakeri, S. Syri, and P. Kauranen, "Economic Feasibility of Flow Batteries in Grid-Scale Applications," in *2018 15th International Conference on the European Energy Market (EEM)*, 2018. DOI: `10.1109/EEM.2018.8470012`.

[89] P. Enevoldsen and B. K. Sovacool, "Integrating power systems for remote island energy supply: Lessons from Mykines, Faroe Islands," *Renewable Energy*, vol. 85, pp. 642–648, 2016. DOI: `10.1016/j.renene.2015.06.065`.

[90] Umhvørvisstovan, Elfelagið SEV, and Dansk Energi, "Orkugoymslur í Føroyum - yvirskipað frágreiðing," Umhvørvisstovan, Argir, Faroe Islands, Tech. Rep., 2018. [Online]. Available: `https://www.us.fo/Default.aspx?ID=14236` (visited on 03/18/2022).

[91] ORKA, "Kabelforbindelse mellem Færøerne og nabonationer i Nordatlanten - Gennemgang af tidligere arbejde," ORKA, Argir, Faroe Islands, Tech. Rep., 2018. [Online]. Available: `https://www.us.fo/Default.aspx?ID=14236` (visited on 03/18/2022).

[92] Dansk Energi, "Høring vedrørende fremtidsscenarier for energisystemet på Færøerne," Dansk Energi, Copenhagen, Denmark, Tech. Rep. d2016-8677-21.0, 2016. [Online]. Available: `https://www.us.fo/Default.aspx?ID=14236` (visited on 03/18/2022).

[93] ——, "Scenarie notat," Dansk Energi, Copenhagen, Denmark, Tech. Rep. d2016-15912-1.0, 2016. [Online]. Available: `https://www.us.fo/Default.aspx?ID=14236` (visited on 03/18/2022).

[94] ——, "Fleksibelt elforbrug på Færøerne," Dansk Energi, Copenhagen, Denmark, Tech. Rep. d2017-7274-6.0, 2017. [Online]. Available: `https://www.us.fo/Default.aspx?ID=14236` (visited on 03/18/2022).

[95] Ea Energy Analyses, "Balancing a 100% renewable electricity system - Least cost path for the Faroe Islands," Ea Energy Analyses, Copenhagen, Denmark, Tech. Rep., 2018.

[96] Norconsult AS, "100% fornybar kraft, Pumpekraft, vind og sol," Norconsult AS, Sandvika, Norway, Tech. Rep., 2018. [Online]. Available: `https://www.us.fo/Default.aspx?ID=14236` (visited on 03/18/2022).

[97] Dansk Energi, "Sammenfatning af scenarier for energilagring på Færøerne," Dansk Energi, Copenhagen, Denmark, Tech. Rep. d2017-155-3.0, 2017. [Online]. Available: `https://www.us.fo/Default.aspx?ID=14236` (visited on 03/18/2022).

[98] The Power Company SEV, "Notat om alternative produktionsformer," Elfelagið SEV, Tórshavn, Faroe Islands, Tech. Rep., 2018. [Online]. Available: `https://www.us.fo/Default.aspx?ID=14236` (visited on 03/18/2022).

[99] ORKA, "Gennemgang af energilagerteknologier," ORKA, Argir, Faroe Islands, Tech. Rep., 2018. [Online]. Available: `https://www.us.fo/Default.aspx?ID=14236` (visited on 03/18/2022).

[100] Dansk Energi, "Stabilitet og udbygning af elnettet," Dansk Energi, Copenhagen, Denmark, Tech. Rep. d2017-9194-0.31, 2017. [Online]. Available: `https://www.us.fo/Default.aspx?ID=14236` (visited on 03/18/2022).

[101] H. Hansen, T. Nielsen, B. Thomsen, and K. Andersen, "Energilagring på Færøerne - Teknisk opsamlingsrapport," Dansk Energi, Copenhagen, Denmark, Tech. Rep., 2018. [Online]. Available: `https://www.us.fo/Default.aspx?ID=14236` (visited on 03/18/2022).

[102] Jarðfeingi, *Indledende vurderinger af muligheden for at lægge elkabel fra Island til Færøerne*, Hoyvík, Faroe Islands, 2007. [Online]. Available: `https://www.us.fo/Default.aspx?ID=14236` (visited on 03/18/2022).

[103] Orkustofnun, Norges Arktiske Universitet, Energistyrelsen, Jarðfeingi, Shetland Islands Council, and Greenland Innovation Centre, "North Atlantic Energy Network," Orkustofnun, Reykjavik, Iceland, Tech. Rep., 2016. [Online]. Available: `http://os.is/gogn/Skyrslur/OS-2016/North-Atlantic-Energy-Network-Report.pdf`.

[104] P. E. Egholm, F. Jakobsen, B. Bendtsen, K. Mortensen, B. Thomsen, A. Johannesen, J. S. Christensen, and K. Andersen, *Action plan - Report and Recommendations on the future electric energy system of the Faroe Islands*, Tórshavn, Faroe Islands, 2015.

[105] F. Wiese, R. Bramstoft, H. Koduvere, A. Pizarro Alonso, O. Balyk, J. G. Kirkerud, Å. G. Tveten, T. F. Bolkesjø, M. Münster, and H. Ravn, "Balmorel open source energy system model," *Energy Strategy Reviews*, vol. 20, pp. 26–34, 2018. DOI: `10.1016/j.esr.2018.01.003`.

[106] EA Energy Analyses, *Balmorel - User guide*. Copenhagen, Denmark: EA Energy Analyses, 2018.

[107] H. Ravn, *The Balmorel Model Structure*. 2005, vol. 2.12 Alpha. [Online]. Available: `http://www.balmorel.com/Doc/BMS212A.pdf` (visited on 10/03/2020).

[108] J. Cochran, C. L. Bak, P. L. Francos, D. McGowan, A. Iliceto, G. Kiseliovas, J. Rondou, H. M. Tróndheim, and J. Whiteford, "Same goal, different pathways for energy transition," *IEEE Power and Energy Magazine*, no. 4, 2022.

[109] B. Lu, A. Blakers, and M. Stocks, "90–100% renewable electricity for the South West Interconnected System of Western Australia," *Energy*, vol. 122, pp. 663–674, 2017. DOI: `https://doi.org/10.1016/j.energy.2017.01.077`.

[110] T. D. H. Balle, *A Study of weather effects on heat consumption in buildings using heat pumps in the Faroe Islands*, B. Sc. Thesis, University of the Faroe Islands, Tórshavn, Faroe Islands, 2016.

[111] Elfelagið SEV, *60 kV netið í framtíðini, Uppskot*, Vestmanna, Faroe Islands, 2018.

[112] P/f Fjarhitafelagið, *Miðal nýtsla í kWh býtt út á økir*, 2018. [Online]. Available: `https://www.fjarhiti.fo/fjarhitabr%C3%BAkari/mi%C3%B0aln%C3%BDtsla-%C3%AD-kwh-b%C3%BDtt-%C3%BAt-%C3%A1-oekir/` (visited on 05/25/2020).

[113] A. S. Haslerud, "Faroe Islands, Detailed wind maps," Kjeller Vindteknikk, Lillestrøm, Norway, Tech. Rep. KVT/ASH/2019/R032, 2019.

[114] Energistyrelsen, *Fremskrivning af brændselspriser og CO2-kvotepris*, Copenhagen, Denmark, 2019.

[115] J. P. Magnussen, "Vindmyllustaðseting - Val av økjum til vindmyllulundir í Føroyum og dømi um staðsetingar," Orkudeildin á Umhvørvisstovuni, Tórshavn, Faroe Islands, Tech. Rep., 2017.

[116] T. Poulsen, B. A. Niclasen, G. Giebel, and H. G. Beyer, "Validation of WRF generated wind field in complex terrain," *Meteorologische Zeitschrift*, vol. 30, no. 5, pp. 413–428, Oct. 2021. DOI: `10.1127/metz/2021/1068`.

[117] G. M. Masters, *Renewable and efficient electric power systems*, 2nd ed. John Wiley & Sons, 2013.

[118] T. Poulsen and H. G. Beyer, "Spectral characteristics and spatial smoothing of wind power - a case study of the Faroe Islands," *Meteorologische Zeitschrift*, vol. 29, no. 6, pp. 427–438, Nov. 2020. DOI: `10.1127/metz/2020/1041`.

[119] E. Sæta, "Vindturbiner for Færøyene," Norconsult AS, Sandvika, Norway, Tech. Rep. 5014424, 2010.

[120] Energistyrelsen and Energinet, *Technology Data - Generation of Electricity and District Heating*, Copenhagen, Denmark, 2019.

[121] J. P. Magnussen, *Wind Power Project in the Northern Faroe Islands*, B. Sc. Thesis, University of the Faroe Islands, Tórshavn, Faroe Islands, 2016.

[122] H. G. Beyer and I. P. Custodio, "The Possible Role of PV in the Future Power Supply of the Faroe Islands," in *35th EU PVSEC*, Brussels, Belgium, 2018. DOI: 10.1017/CB09781107415324.004.

[123] T. Nielsen, *Pumpuskipan í vestmanna*, Power point presentation, 2018.

[124] Orkuskifti, *Í 2020 var orkunýtslan í Føroyum 3819 GWh*, 2021. [Online]. Available: http://www.os.fo/t%C3%AD%C3%B0indir/%C3%AD-2020-var-orkun%C3%BDtslan-%C3%AD-foeroyum-3819-gwh/ (visited on 01/30/2022).

[125] H. Saadat, *Power System Analysis*, 3rd editio. PSA Publishing, 2010, ISBN: 9780984543861.

[126] P. Tielens and D. Van Hertem, "The relevance of inertia in power systems," *Renewable and Sustainable Energy Reviews*, vol. 55, no. 2016, pp. 999–1009, 2016. DOI: 10.1016/j.rser.2015.11.016.

[127] A. Oudalov, D. Chartouni, and C. Ohler, "Optimizing a battery energy storage system for primary frequency control," *IEEE Transactions on Power Systems*, vol. 22, no. 3, pp. 1259–1266, 2007. DOI: 10.1109/TPWRS.2007.901459.

[128] S. de Haan, J. Morren, J. Ferreira, and W. Kling, "Wind Turbines Emulating Inertia and Supporting Primary Frequency Control," *IEEE Transactions on Power Systems*, vol. 21, no. 1, pp. 433–434, 2006, ISSN: 0885-8950. DOI: 10.1109/TPWRS.2005.861956.

[129] J. M. Mauricio, A. Marano, A. Gomez-Exposito, and J. L. Martinez Ramos, "Frequency regulation contribution through variable-speed wind energy conversion systems," *IEEE Transactions on Power Systems*, vol. 24, no. 1, pp. 173–180, 2009. DOI: 10.1109/TPWRS.2008.2009398.

[130] P. Pourbeik, S. Soni, A. Gaikwad, and V. Chadliev, "Providing primary frequency response from photovoltaic power plants," *Cigre Science and Engineering - Innovation in the Power Systems industry*, pp. 5–11, 2018.

[131] D. Kottick, M. Blau, and D. Edelstein, "Battery energy storage for frequency regulation in an island power system," *IEEE transactions on energy conversion*, vol. 8, no. 3, pp. 455–459, 1993.

[132] M. Mikawa, J. Shimabayashi, and H. Sasaki, "Demonstration project utilizing hybrid battery energy storage system with high penetration of renewable energy sources in the oki-islands," *Cigre Science and Engineering - Innovation in the Power Systems industry*, pp. 13–19, 2018.

[133] S. Han, S. Han, and K. Sezaki, "Development of an optimal vehicle-to-grid aggregator for frequency regulation," *IEEE Transactions on smart grid*, vol. 1, no. 1, pp. 65–72, 2010.

[134] C. Binding, D. Gantenbein, B. Jansen, O. Sundström, P. B. Andersen, F. Marra, B. Poulsen, and C. Træholt, "Electric vehicle fleet integration in the danish edison project-a virtual power plant on the island of bornholm," in *IEEE PES general meeting*, IEEE, 2010, pp. 1–8.

[135] J. R. Pillai and B. Bak-Jensen, "Vehicle-to-grid for islanded power system operation in bornholm," in *IEEE PES General Meeting*, IEEE, 2010, pp. 1–8.

[136] T. Masuta and A. Yokoyama, "Supplementary load frequency control by use of a number of both electric vehicles and heat pump water heaters," *IEEE Transactions on smart grid*, vol. 3, no. 3, pp. 1253–1262, 2012.

[137] I. D. de Cerio Mendaza, *An interactive energy system with grid, heating and transportation systems*. Department of Energy Technology, Aalborg University, 2014.

[138] S.-S. Seo, Y.-H. Choi, S.-G. Kang, B.-J. Lee, J.-H. Shin, and T.-K. Kim, "Hybrid control system for managing voltage and reactive power in the jeju power system," *Journal of Electrical Engineering and Technology*, vol. 4, no. 4, pp. 429–437, 2009.

[139] E. Demirok, P. C. Gonzalez, K. H. Frederiksen, D. Sera, P. Rodriguez, and R. Teodorescu, "Local reactive power control methods for overvoltage prevention of distributed solar inverters in low-voltage grids," *IEEE Journal of Photovoltaics*, vol. 1, no. 2, pp. 174–182, 2011.

[140] M. A. A. Al-nakeeb and S. V. Jensen, "Dynamic Modelling of the Faroe Islands Electric Grid Dynamisk Modellering af det Færøske Elnet," no. March, 2013.

[141] S. Østerfelt and J. Hansen, "Transient stabilitet i elnet drevet af vedvaren- de energikilder," 2021.

[142] H. M. Tróndheim, *A Battery System Utilized for Ancillary Services - the Faroe Islands*, 2018.

[143] "Aggregation and Control of Flexible Thermal Demand for Wind Power Based Power System Analysis," Aalborg University, Aalborg, Denmark, Tech. Rep., 2018.

[144] H. M. Tróndheim, J. R. Pillai, T. Nielsen, C. L. Bak, and B. A. Niclasen, "Frequency Regulation in an Isolated Grid with a High Penetration of Renewables - the Faroe Islands," in *CIGRE e-Session 2020*, CIGRE, 2020.

[145] H. M. Tróndheim, L. Hofmann, P. Gartmann, E. Quitmann, C. L. Bak, F. F. da Silva, T. Nielsen, and B. A. Niclasen, "Frequency and Voltage Stability Towards 100% Renewables in Suðuroy, Faroe Islands," *CIGRE Science and Engineering Journal*, Note: Accepted with minor changes, to be published in June 2022.

[146] J. Feltes and L. Lima, "Validation of dynamic model parameters for stability analysis; industry need, current practices and future trends," in *2003 IEEE Power Engineering Society General Meeting (IEEE Cat. No.03CH37491)*, vol. 3, 2003, pp. 1295–130. DOI: 10.1109/PES.2003.1267336.

[147] L. T. G. Lima, "Dynamic model validation for compliance with nerc standards," in *2009 IEEE Power Energy Society General Meeting*, 2009, pp. 1–7. DOI: 10.1109/PES.2009.5275452.

[148] E. Allen, D. Kosterev, and P. Pourbeik, "Validation of power system models," in *IEEE PES General Meeting*, 2010, pp. 1–7. DOI: 10.1109/PES.2010.5589874.

[149] K. Mahapatra and H. Wang, "Generator dynamic model calibration using multiple disturbance events," in *2020 IEEE Power Energy Society Innovative Smart Grid Technologies Conference (ISGT)*, 2020, pp. 1–5. DOI: 10.1109/ISGT45199.2020.9087727.

[150] S. Stavrinos, A. Petoussis, A. Theophanous, S. Pillutla, and F. Prabhakara, "Development of a validated dynamic model of Cyprus transmission system," in *7th Mediterranean Conference and Exhibition on Power Generation, Transmission, Distribution and Energy Conversion (MedPower 2010)*, IET, 2010, pp. 238–238, ISBN: 978 1 84919 319 1. DOI: 10.1049/cp.2010.0946.

[151] K. Bollinger and R. Gilchrist, "Voltage Regulator Models Using Automated Frequency Response Equipment," *IEEE Transactions on Power Apparatus and Systems*, vol. PAS-101, no. 8, pp. 2899–2905, 1982, ISSN: 0018-9510. DOI: 10.1109/TPAS.1982.317616.

[152] M. Gibbard and Q. Kaan, "Identification of excitation system parameters," *IEEE Transactions on Power Apparatus and Systems*, vol. 94, no. 4, pp. 1201–1207, 1975. DOI: 10.1109/T-PAS.1975.31955.

[153] A. A. Hajnoroozi, F. Aminifar, and H. Ayoubzadeh, "Generating unit model validation and calibration through synchrophasor measurements," *IEEE Transactions on Smart Grid*, vol. 6, no. 1, pp. 441–449, 2015. DOI: 10.1109/TSG.2014.2322821.

[154] S. Kittiwattanaphon, W. Wangdee, and S. Katithummarugs, "Generator excitation system parameter identification and tuning by using pso," in *2019 7th International Electrical Engineering Congress (iEECON)*, 2019, pp. 1–4. DOI: 10.1109/iEECON45304.2019.8939048.

[155] C. Li and J. Zhou, "Parameters identification of hydraulic turbine governing system using improved gravitational search algorithm," *Energy Conversion and Management*, vol. 52, no. 1, pp. 374–381, 2011. DOI: https://doi.org/10.1016/j.enconman.2010.07.012.

[156] T. L. den Boer, *Validation of Dynamic Power System Models using Synchrophasor Measurements*, M.Sc. Thesis, TU Delft, 2019.

[157] D. Kosterev, "Hydro Turbine-Governor Model Validation in Pacific Northwest," *IEEE Transactions on Power Systems*, vol. 19, no. 2, pp. 1144–1149, 2004, ISSN: 0885-8950. DOI: 10.1109/TPWRS.2003.821464.

[158] M. Sajjadi, H. Seifi, and H. Delkhosh, "A new approach for system-wide power system frequency model validation via measurement data," *Engineering Reports*, 2021, ISSN: 2577-8196. DOI: 10.1002/eng2.12446. [Online]. Available: https://onlinelibrary.wiley.com/doi/10.1002/eng2.12446.

[159] J. E. Gomez, I. C. Decker, and R. A. Leon, "Hybrid simulations, a smart way to perform parameter validation in power systems," in *2011 IEEE PES Conference on Innovative Smart Grid Technologies Latin America (ISGT LA)*, 2011, pp. 1–7. DOI: 10.1109/ISGT-LA.2011.6083184.

[160] R. Chen, W. Wu, H. Sun, and B. Zhang, "A two-level online parameter identification approach," in *2013 IEEE Power Energy Society General Meeting*, 2013, pp. 1–6. DOI: 10.1109/PESMG.2013.6672162.

[161] H. M. Tróndheim, F. F. da Silva, C. L. Bak, T. Nielsen, B. A. Niclasen, R. Nielsen, and N. Weikop, "Alternative combined parameter identification andvalidation of dynamic models procedure - appliedto the faroese power system," To be submitted.

[162] "IEEE recommended practice for excitation system models for power system stability studies," *IEEE Std 421.5-2016 (Revision of IEEE Std 421.5-2005)*, pp. 1–207, 2016. DOI: 10.1109/IEEESTD.2016.7553421.

[163] J. S. Arora, "Nature-Inspired Search Methods," in *Introduction to Optimum Design*, 2017, ISBN: 9780128008065. DOI: 10.1016/b978-0-12-800806-5.00001-9.

[164] P. Yu and J. Zhang, "Parameter identification of excitation system based on field data and pso," in *2010 International Conference on E-Product E-Service and E-Entertainment*, 2010, pp. 1–4. DOI: 10.1109/ICEEE.2010.5660858.

[165] C.-H. Lin, C.-J. Wu, J.-Z. Yang, and C.-J. Liao, "Parameters identification of reduced governor system model for diesel-engine generator by using hybrid particle swarm optimisation," *IET Electric Power Applications*, vol. 12, no. 9, pp. 1265–1271, 2018. DOI: `https://doi.org/10.1049/iet-epa.2017.0851`. eprint: `https://ietresearch.onlinelibrary.wiley.com/doi/pdf/10.1049/iet-epa.2017.0851`. [Online]. Available: `https://ietresearch.onlinelibrary.wiley.com/doi/abs/10.1049/iet-epa.2017.0851`.

[166] DIGSILENT GmbH, *DIgSILENT PowerFactory, User Manual*, Gomaringen, Germany, 2021.

[167] Enercon GmbH, *Technical description Operating strategies FACTS 2.0 ENERCON EP1, EP2, EP3, EP4 wind energy converters*, 2020.

[168] ——, *Technical description ENERCON SCADA Farm Control Unit E2 (FCU E2) SAP 630896*, 2019.

[169] V. Knap, S. K. Chaudhary, D. L. Stroe, M. J. Swierczynski, B.-I. Craciun, and R. Teodorescu, "Sizing of an energy storage system for grid inertial response and primary frequency reserve," *IEEE Transactions on Power Systems*, vol. 31, no. 5, pp. 3447–3456, 2016. DOI: `10.1109/TPWRS.2015.2503565`.

[170] B. Badrzadeh, Z. Emin, E. Hillberg, D. Jacobson, L. Kocewiak, G. Lietz, F. da Silva, and M. Val Escudero, "The need or enhanced power system modelling techniques and simulation tools," *CIGRE Science & Engineering*, vol. 17, no. Febr, pp. 30–46, 2020.

APPENDIX A
Expansion Planning Data

Table A.1: Historic (2009-2018) and projected (2019-2030) electricity demand (MWh) in regions 1-7 divided into normal (N), heating (H) and transport (T) demand.

Year	R1			R2			R4		
	N	H	T	N	H	T	N	H	T
2009	32410	151	0	9172	15	0	29951	108	0
2010	31331	228	0	9284	23	0	30103	163	0
2011	31103	349	0	9304	36	0	30464	249	0
2012	31347	384	0	9894	39	0	33054	274	0
2013	25406	430	0	9804	44	0	34192	307	0
2014	26480	500	0	9621	51	0	34444	357	3
2015	29280	545	0	10214	56	0	36520	389	6
2016	31438	590	0	10127	60	0	36600	421	9
2017	33689	635	0	9983	65	0	37203	453	9
2018	42276	698	33	9924	71	0	40267	499	27
2019	43807	1382	791	10015	296	237	41632	1177	767
2020	45394	2067	1549	10108	521	474	43044	1856	1507
2021	47038	2751	2307	10201	746	710	44503	2534	2247
2022	48741	3435	3065	10295	971	947	46012	3212	2988
2023	50507	4119	3823	10390	1195	1184	47572	3891	3728
2024	52336	4803	4581	10486	1420	1421	49185	4569	4468
2025	54231	5488	5339	10583	1645	1658	50853	5248	5208
2026	56195	6675	6731	10680	2009	2078	52577	6367	6549
2027	58231	7863	8123	10779	2373	2498	54360	7487	7890
2028	60340	9050	9515	10878	2737	2918	56203	8606	9231
2029	62525	10238	10908	10978	3101	3339	58108	9726	10572
2030	64790	11425	12300	11080	3465	3759	60079	10845	11913

Year	R5			R6			R7		
	N	H	T	N	H	T	N	H	T
2009	162867	866	0	5587	18	0	23717	31	0
2010	165847	1310	0	5266	28	0	23716	47	0
2011	162943	2002	9	5445	43	0	22910	71	0
2012	165009	2202	9	5231	47	0	27269	78	0
2013	170867	2468	18	5004	53	0	33143	88	0
2014	176844	2865	4	4430	61	0	34515	102	0
2015	172675	3123	0	4913	67	0	32252	111	0
2016	178900	3381	45	5303	72	0	29454	120	0
2017	197002	3640	90	5583	78	0	25298	130	0
2018	198152	4004	231	5571	85	3	26740	142	3
2019	202631	7487	4253	5582	243	124	27265	750	470
2020	207212	10970	8275	5593	401	245	36560	1357	938
2021	211896	14453	12297	5604	559	366	37106	1964	1405
2022	216686	17936	16320	5616	717	486	37662	2571	1872
2023	221584	21419	20342	5627	874	607	55749	3178	2340
2024	226593	24902	24364	5638	1032	728	56328	3785	2807
2025	231715	28385	28386	5649	1190	849	56917	4393	3275
2026	236953	34632	35747	5661	1428	1037	57519	5276	4018
2027	242309	40879	43108	5672	1666	1225	58132	6160	4761
2028	247786	47126	50468	5684	1904	1412	58757	7043	5504
2029	253388	53373	57829	5695	2142	1600	59395	7927	6247
2030	259115	59620	65190	5706	2380	1788	60044	8810	6990

Table A.2: Optimal generation capacities for scenario 1-6, cBS, cCA and cFU.

Scenario	Type	2020	2021	2022	2023	2024	2025	2026	2027	2028	2029	2030
#1	Fuel oil	91	91	91	91	91	91	91	91	91	91	91
	Gas oil	8	8	8	8	8	8	8	8	8	8	8
	Biogas	2	2	2	2	2	2	2	2	2	2	2
	Hydro	40	55	57	61	63	65	75	83	89	93	112
	Wind	24	69	74	82	86	92	110	137	155	167	168
	Solar	0	0	0	0	0	0	0	0	7	36	79
	Battery	0	0	0	0	0	0	0	0	0	0	2
#2	Fuel oil	91	91	91	91	91	91	91	91	91	91	91
	Gas oil	8	8	8	8	8	8	8	8	8	8	8
	Biogas	2	2	2	2	2	2	2	2	2	2	2
	Hydro	40	55	57	61	63	63	63	63	63	66	103
	Wind	24	69	74	82	86	86	86	86	86	86	102
	Tidal	0	0	0	0	0	25	32	38	51	72	72
	Battery	0	0	0	0	0	0	0	0	0	0	1
#3	Fuel oil	91	91	91	91	91	91	91	91	91	91	91
	Gas oil	8	8	8	8	8	8	8	8	8	8	8
	Biogas	2	2	2	2	2	2	2	2	2	2	2
	Hydro	40	55	57	61	63	65	75	80	84	90	94
	Wind	24	69	74	82	86	92	110	124	130	139	153
	Battery	0	0	0	0	0	0	0	0	0	0	1
#4	Fuel oil	91	91	91	91	91	91	91	91	91	91	91
	Gas oil	8	8	8	8	8	8	8	8	8	8	8
	Biogas	2	2	2	2	2	2	2	2	2	2	2
	Hydro	40	55	57	61	63	65	67	68	72	76	79
	Wind	24	69	74	82	86	92	99	102	109	117	125
#5	Fuel oil	91	91	91	91	91	91	91	91	91	91	91
	Gas oil	8	8	8	8	8	8	8	8	8	8	8
	Biogas	2	2	2	2	2	2	2	2	2	2	2
	Hydro	40	55	57	59	61	64	71	78	85	89	108
	PS R7	0	0	0	4	4	4	4	4	4	4	4
	Wind	24	69	74	82	87	93	110	136	154	170	170
	Solar	0	0	0	0	0	0	0	0	7	37	74
	Battery	0	0	0	0	0	0	0	0	0	0	2
#6	Fuel oil	91	91	91	91	91	91	91	91	91	91	91
	Gas oil	8	8	8	8	8	8	8	8	8	8	8
	Biogas	2	2	2	2	2	2	2	2	2	2	2
	Hydro	40	55	57	61	63	65	73	81	89	93	112
	Wind	24	69	74	82	86	92	112	135	156	176	182
	Solar	0	0	0	0	0	0	0	0	0	12	40
	Battery	0	0	0	0	0	0	0	0	0	0	2
cBS	Fuel oil	91	91	91	91	91	91	91	91	91	91	91
	Gas oil	8	8	8	8	8	8	8	8	8	8	8
	Biogas	2	2	2	2	2	2	2	2	2	2	2
	Hydro	40	55	57	61	63	65	75	82	88	93	112
	Wind	24	69	74	82	86	92	110	137	154	168	168
	Solar	0	0	0	0	0	0	0	0	7	37	80
	Battery	0	0	0	0	0	0	0	1	1	1	3
cCA	Fuel oil	91	91	91	91	91	91	91	91	91	91	91
	Gas oil	8	8	8	8	8	8	8	8	8	8	8
	Biogas	2	2	2	2	2	2	2	2	2	2	2
	Hydro	40	55	57	61	63	65	74	82	89	93	112
	Wind	24	69	73	82	86	92	110	137	155	167	168
	Solar	0	0	0	0	0	0	0	0	6	36	79
	Battery	0	0	0	0	0	0	0	0	0	0	2
cFU	Fuel oil	91	91	91	91	91	91	91	91	91	91	91
	Gas oil	8	8	8	8	8	8	8	8	8	8	8
	Biogas	2	2	2	2	2	2	2	2	2	2	2
	Hydro	40	50	52	56	58	65	75	83	89	93	112
	Wind	24	68	72	80	84	91	110	137	155	167	168
	Solar	0	0	0	0	0	0	0	0	7	36	79
	Battery	0	0	0	0	0	0	0	0	0	0	2

Table A.3: Optimal generation capacities for cPV, cPS, cWP, eBS, eCA, eFU, ePV, ePS and eWP.

Scenario	Type	2020	2021	2022	2023	2024	2025	2026	2027	2028	2029	2030
cPV	Fuel oil	91	91	91	91	91	91	91	91	91	91	91
	Gas oil	8	8	8	8	8	8	8	8	8	8	8
	Biogas	2	2	2	2	2	2	2	2	2	2	2
	Hydro	40	55	57	61	63	65	75	81	87	92	112
	Wind	24	69	74	82	86	92	110	131	137	148	149
	Solar	0	0	0	0	0	0	0	13	42	88	149
	Battery	0	0	0	0	0	0	0	0	0	0	3
cPS	Fuel oil	91	91	91	91	91	91	91	91	91	91	91
	Gas oil	8	8	8	8	8	8	8	8	8	8	8
	Biogas	2	2	2	2	2	2	2	2	2	2	2
	Hydro	40	56	58	62	64	67	76	82	91	97	112
	Wind	24	69	73	82	87	92	107	130	154	164	173
	Solar	0	0	0	0	0	0	0	0	0	1	31
	Battery	0	0	0	0	0	0	0	0	0	0	2
cWP	Fuel oil	91	91	91	91	91	91	91	91	91	91	91
	Gas oil	8	8	8	8	8	8	8	8	8	8	8
	Biogas	2	2	2	2	2	2	2	2	2	2	2
	Hydro	40	54	57	61	63	65	73	82	89	93	112
	Wind	24	74	78	88	93	100	112	139	167	180	184
	Solar	0	0	0	0	0	0	0	0	0	24	53
	Battery	0	0	0	0	0	0	0	0	0	0	2
eBS	Fuel oil	91	91	91	91	91	91	91	91	91	91	91
	Gas oil	8	8	8	8	8	8	8	8	8	8	8
	Biogas	2	2	2	2	2	2	2	2	2	2	2
	Hydro	40	55	57	61	63	65	75	83	89	93	112
	Wind	24	69	74	82	86	92	110	137	155	167	168
	Solar	0	0	0	0	0	0	0	0	7	36	79
	Battery	0	0	0	0	0	0	0	0	0	0	2
eCA	Fuel oil	91	91	91	91	91	91	91	91	91	91	91
	Gas oil	8	8	8	8	8	8	8	8	8	8	8
	Biogas	2	2	2	2	2	2	2	2	2	2	2
	Hydro	40	54	56	60	62	65	74	83	88	93	112
	Wind	24	69	74	82	86	92	110	137	155	167	168
	Solar	0	0	0	0	0	0	0	0	7	37	79
	Battery	0	0	0	0	0	0	0	0	0	0	3
eFU	Fuel oil	91	91	91	91	91	91	91	91	91	91	91
	Gas oil	8	8	8	8	8	8	8	8	8	8	8
	Biogas	2	2	2	2	2	2	2	2	2	2	2
	Hydro	40	55	58	62	64	67	75	83	89	93	112
	Wind	24	77	81	90	93	101	110	137	155	167	168
	Solar	0	0	0	0	0	0	0	0	7	36	79
	Battery	0	0	0	0	0	0	0	0	0	0	2
ePV	Fuel oil	91	91	91	91	91	91	91	91	91	91	91
	Gas oil	8	8	8	8	8	8	8	8	8	8	8
	Biogas	2	2	2	2	2	2	2	2	2	2	2
	Hydro	40	55	57	61	63	65	75	83	91	95	112
	Wind	24	69	74	82	86	92	110	137	158	174	189
	Solar	0	0	0	0	0	0	0	0	0	0	20
	Battery	0	0	0	0	0	0	0	0	0	0	2
ePS	Fuel oil	91	91	91	91	91	91	91	91	91	91	91
	Gas oil	8	8	8	8	8	8	8	8	8	8	8
	Biogas	2	2	2	2	2	2	2	2	2	2	2
	Hydro	40	53	55	59	61	63	73	82	87	92	111
	Wind	24	69	73	82	86	93	112	139	155	166	169
	Solar	0	0	0	0	0	0	0	0	21	61	119
	Battery	0	0	0	0	0	0	0	0	0	0	3
eWP	Fuel oil	91	91	91	91	91	91	91	91	91	91	91
	Gas oil	8	8	8	8	8	8	8	8	8	8	8
	Biogas	2	2	2	2	2	2	2	2	2	2	2
	Hydro	40	54	56	59	62	65	75	82	88	93	113
	Wind	24	68	72	80	85	91	109	130	148	156	157
	Solar	0	0	0	0	0	0	0	0	16	54	101
	Battery	0	0	0	0	0	0	0	0	0	0	2

Table A.4: Optimal capacities at Mýruverkið.

Scenario	Technology	2020	2021	2022	2023	2024	2025	2026	2027	2028	2029	2030
#1	Reservoir (MWh)	2275	2275	2275	2275	2275	2275	2689	3428	5915	10039	14355
	Turbines (MW)	2	18	20	23	26	28	37	45	48	52	71
	Pumps (MW)	0	23	25	26	27	27	41	62	71	77	78
#2	Reservoir (MWh)	2275	2275	2275	2275	2275	2275	2275	2275	2275	2560	4471
	Turbines (MW)	2	18	20	23	26	26	26	26	26	28	61
	Pumps (MW)	0	23	25	26	27	27	27	27	27	30	50
#3	Reservoir (MWh)	2275	2275	2275	2275	2275	2275	2689	3008	3091	3180	3569
	Turbines (MW)	2	18	20	23	26	28	37	41	45	50	54
	Pumps (MW)	0	23	25	26	27	27	41	51	52	53	61
#4	Reservoir (MWh)	2275	2275	2275	2275	2275	2275	2275	2384	2648	2797	2951
	Turbines (MW)	2	18	20	23	26	28	29	30	34	37	40
	Pumps (MW)	0	23	25	26	27	27	27	29	31	34	38
#5	Reservoir (MWh)	2275	2275	2275	2275	2275	2275	2520	3326	5756	8803	14940
	Turbines (MW)	2	18	20	22	24	26	34	41	44	48	67
	Pumps (MW)	0	23	25	25	25	25	34	56	65	77	77
#6	Reservoir (MWh)	2275	2275	2275	2275	2275	2275	2504	3217	4960	6759	12562
	Turbines (MW)	2	18	20	23	26	28	35	44	49	53	72
	Pumps (MW)	0	23	25	26	27	27	39	54	66	86	88
cBS	Reservoir (MWh)	2275	2275	2275	2275	2275	2275	2689	3419	5896	9751	14293
	Turbines (MW)	2	18	20	23	26	28	37	45	48	51	70
	Pumps (MW)	0	23	25	26	27	27	41	61	70	77	78
cCA	Reservoir (MWh)	2275	2275	2275	2275	2275	2275	2683	3426	5931	9947	14366
	Turbines (MW)	2	18	20	24	26	28	37	45	48	52	71
	Pumps (MW)	0	23	25	26	27	27	41	62	72	77	79
cFU	Reservoir (MWh)	2275	2275	2275	2275	2275	2275	2689	3428	5914	10039	14355
	Turbines (MW)	2	13	15	19	21	28	37	45	48	52	71
	Pumps (MW)	0	22	23	25	25	27	41	62	71	77	78
cPV	Reservoir (MWh)	2275	2275	2275	2275	2275	2275	2689	3239	4795	5251	5894
	Turbines (MW)	2	18	20	23	26	28	37	44	48	53	72
	Pumps (MW)	0	23	25	26	27	27	41	58	61	68	69
cPS	Reservoir (MWh)	2275	2275	2275	2275	2275	2275	2923	4387	7302	19128	22887
	Turbines (MW)	2	19	21	24	27	29	39	43	50	56	71
	Pumps (MW)	0	25	27	28	29	29	44	61	78	80	85
cWP	Reservoir (MWh)	2275	2275	2275	2275	2275	2275	2550	3371	5310	10171	16437
	Turbines (MW)	2	17	20	23	25	28	36	45	49	52	71
	Pumps (MW)	0	25	25	28	28	28	39	59	74	80	81
eBS	Reservoir (MWh)	2275	2275	2275	2275	2275	2275	2689	3428	5915	10039	14355
	Turbines (MW)	2	18	20	23	26	28	37	45	48	52	71
	Pumps (MW)	0	23	25	26	27	27	41	62	71	77	78
eCA	Reservoir (MWh)	2275	2275	2275	2275	2275	2275	2704	3459	5908	9928	14340
	Turbines (MW)	2	17	19	23	25	27	37	45	48	52	70
	Pumps (MW)	0	23	24	25	26	27	42	62	71	77	77
eFU	Reservoir (MWh)	2275	2275	2275	2275	2275	2275	2689	3427	5916	9964	14346
	Turbines (MW)	2	18	21	25	27	29	37	45	48	52	71
	Pumps (MW)	0	31	31	31	31	31	41	62	71	78	79
ePV	Reservoir (MWh)	2275	2275	2275	2275	2275	2275	2689	3428	6057	16216	21696
	Turbines (MW)	2	18	20	23	26	28	37	45	49	54	71
	Pumps (MW)	0	23	25	26	27	27	41	62	73	81	89
ePS	Reservoir (MWh)	2275	2275	2275	2275	2275	2275	2564	3351	4672	5643	6334
	Turbines (MW)	2	16	18	22	24	26	36	45	47	51	70
	Pumps (MW)	0	21	23	24	24	26	38	59	69	72	73
eWP	Reservoir (MWh)	2275	2275	2275	2275	2275	2275	2739	4376	5688	8575	12337
	Turbines (MW)	2	16	19	22	25	28	38	43	47	51	71
	Pumps (MW)	0	24	25	27	28	28	44	61	73	76	77

Table A.5: Optimal capacities at Heygaverkið.

Scenario	Technology	2020	2021	2022	2023	2024	2025	2026	2027	2028	2029	2030
#1	Reservoir (MWh)	516	516	516	516	516	516	716	1040	2013	2141	2141
	Turbines (MW)	5	5	5	5	5	5	5	5	8	9	9
#2	Reservoir (MWh)	516	516	516	516	516	516	516	516	546	650	1232
	Turbines (MW)	5	5	5	5	5	5	5	5	5	5	9
#3	Reservoir (MWh)	516	516	516	516	516	516	716	857	894	933	1105
	Turbines (MW)	5	5	5	5	5	5	5	6	7	7	8
#4	Reservoir (MWh)	516	516	516	516	516	516	516	547	622	678	750
	Turbines (MW)	5	5	5	5	5	5	6	6	6	6	7
#5	Reservoir (MWh)	516	516	516	516	516	516	642	996	1942	2020	2067
	Turbines (MW)	5	5	5	5	5	5	5	8	9	9	9
#6	Reservoir (MWh)	516	516	516	516	516	516	631	945	1586	2451	2622
	Turbines (MW)	5	5	5	5	5	5	5	5	7	7	7
cBS	Reservoir (MWh)	516	516	516	516	516	516	716	1036	2004	2112	2112
	Turbines (MW)	5	5	5	5	5	5	5	5	8	9	9
cCA	Reservoir (MWh)	516	516	516	516	516	516	714	1040	2020	2143	2143
	Turbines (MW)	5	5	5	5	5	5	5	5	8	9	9
cFU	Reservoir (MWh)	516	516	516	516	516	516	717	1040	2013	2141	2141
	Turbines (MW)	5	5	5	5	5	5	5	5	8	9	9
cPV	Reservoir (MWh)	516	516	516	516	516	516	716	958	1645	1789	2063
	Turbines (MW)	5	5	5	5	5	5	5	5	6	6	7
cPS	Reservoir (MWh)	516	516	516	516	516	516	831	1473	2080	2182	2436
	Turbines (MW)	5	5	5	5	5	5	5	6	9	9	9
cWP	Reservoir (MWh)	516	516	516	516	516	516	653	1015	1741	1974	2141
	Turbines (MW)	5	5	5	5	5	5	5	5	8	8	8
eBS	Reservoir (MWh)	516	516	516	516	516	516	716	1040	2013	2141	2141
	Turbines (MW)	5	5	5	5	5	5	5	5	8	9	9
eCA	Reservoir (MWh)	516	516	516	516	516	516	723	1051	2009	2107	2107
	Turbines (MW)	5	5	5	5	5	5	5	5	8	9	9
eFU	Reservoir (MWh)	516	516	516	516	516	516	716	1040	2013	2132	2132
	Turbines (MW)	5	5	5	5	5	5	5	5	8	9	9
ePV	Reservoir (MWh)	516	516	516	516	516	516	716	1040	2076	2335	2335
	Turbines (MW)	5	5	5	5	5	5	5	5	9	9	9
ePS	Reservoir (MWh)	516	516	516	516	516	516	660	1007	1457	1891	2269
	Turbines (MW)	5	5	5	5	5	5	5	5	7	9	9
eWP	Reservoir (MWh)	516	516	516	516	516	516	744	1468	1929	2192	2204
	Turbines (MW)	5	5	5	5	5	5	5	6	8	9	9

Table A.6: Optimal wind power capacities (MW) in R1 and R5.

Scenario	Wind site	2026	2027	2028	2029	2030
#1	W5a	0	0	4	4	4
	W5c	30	30	30	42	43
	W1b	8	18	18	18	18
#3	W5a	0	0	0	0	3
	W1b	8	18	18	18	18
#4	W1b	0	0	7	15	18
#5	W5a	0	0	4	4	4
	W5c	30	30	30	45	45
	W1b	8	18	18	18	18
#6	W1b	0	0	0	2	7
	W5d	9	33	54	72	72
cBS	W5a	0	0	4	4	4
	W5c	30	30	30	43	43
	W1b	8	18	18	18	18
cCA	W5a	0	0	5	5	5
	W5c	30	30	30	42	43
	W1b	8	18	18	18	18
cFU	W5a	0	0	4	4	4
	W5c	30	30	30	42	43
	W1b	8	18	18	18	18
cPV	W1b	8	18	18	18	18
cPS	W5a	0	0	0	7	7
	W5c	30	30	33	37	46
	W1b	5	18	18	18	18
cWP	W5a	0	0	12	12	16
	W5c	30	30	34	48	48
	W1b	10	18	18	18	18
eBS	W5a	0	0	4	4	4
	W5c	30	30	30	42	43
	W1b	8	18	18	18	18
eCA	W5a	0	0	4	4	4
	W5c	30	30	30	43	44
	W1b	8	18	18	18	18
eFU	W5a	0	0	4	4	4
	W5c	30	30	30	42	43
	W1b	8	18	18	18	18
ePV	W5a	0	0	3	6	21
	W5c	30	30	35	48	48
	W1b	8	18	18	18	18
ePS	W5a	0	0	5	6	6
	W5c	30	30	30	39	43
	W1b	10	18	18	18	18
eWP	W5c	30	30	30	35	36
	W1b	7	18	18	18	18

Table A.7: Optimal wind power capacities (MW) in R6 and R7.

Scenario	Wind site	2020	2021	2022	2023	2024	2025	2026	2027	2028	2029	2030
#1	W6a	0	0	0	0	0	0	0	17	30	30	30
	W7	6	8	8	12	12	12	12	12	12	12	12
	W6b	0	7	11	16	20	26	36	36	36	36	36
#2	W7	6	8	8	12	12	12	12	12	12	12	12
	W6b	0	7	11	16	20	20	20	20	20	20	36
#3	W6a	0	0	0	0	0	0	0	4	10	18	30
	W7	6	8	8	12	12	12	12	12	12	12	12
	W6b	0	7	11	16	20	26	36	36	36	36	36
#4	W6a	0	0	0	0	0	0	0	0	0	0	5
	W7	6	8	8	12	12	12	12	12	12	12	12
	W6b	0	7	11	16	20	26	33	36	36	36	36
#5	W6a	0	0	0	0	0	0	0	16	30	30	30
	W7	6	8	8	12	12	12	12	12	12	12	12
	W6b	0	7	11	16	21	27	36	36	36	36	36
#6	W7	6	8	8	12	12	12	12	12	12	12	12
	W6b	0	7	11	16	20	26	36	36	36	36	36
cBS	W6a	0	0	0	0	0	0	0	17	30	30	30
	W7	6	8	8	12	12	12	12	12	12	12	12
	W6b	0	7	11	16	20	26	36	36	36	36	36
cCA	W6a	0	0	0	0	0	0	0	17	30	30	30
	W7	6	8	8	11	12	12	12	12	12	12	12
	W6b	0	7	11	16	20	26	36	36	36	36	36
cFU	W6a	0	0	0	0	0	0	0	17	30	30	30
	W7	6	8	8	11	12	12	12	12	12	12	12
	W6b	0	6	10	14	18	25	36	36	36	36	36
cPV	W6a	0	0	0	0	0	0	0	10	17	28	29
	W7	6	8	8	12	12	12	12	12	12	12	12
	W6b	0	7	11	16	20	26	36	36	36	36	36
cPS	W6a	0	0	0	0	0	0	0	10	30	30	30
	W7	6	8	8	12	12	12	12	12	12	12	12
	W6b	0	7	11	16	21	26	36	36	36	36	36
cWP	W6a	0	0	0	0	0	0	0	19	30	30	30
	W7	6	9	9	12	12	12	12	12	12	12	12
	W6b	0	11	15	22	27	33	36	36	36	36	36
eBS	W6a	0	0	0	0	0	0	0	17	30	30	30
	W7	6	8	8	12	12	12	12	12	12	12	12
	W6b	0	7	11	16	20	26	36	36	36	36	36
eCA	W6a	0	0	0	0	0	0	0	17	30	30	30
	W7	6	8	9	12	12	12	12	12	12	12	12
	W6b	0	7	11	15	20	26	36	36	36	36	36
eFU	W6a	0	0	0	0	0	0	0	17	30	30	30
	W7	6	8	9	12	12	12	12	12	12	12	12
	W6b	0	15	19	24	27	35	36	36	36	36	36
ePV	W6a	0	0	0	0	0	0	0	17	30	30	30
	W7	6	8	8	12	12	12	12	12	12	12	12
	W6b	0	7	11	16	20	26	36	36	36	36	36
ePS	W6a	0	0	0	0	0	0	0	18	30	30	30
	W7	6	8	8	12	12	12	12	12	12	12	12
	W6b	0	7	11	16	20	26	36	36	36	36	36
eWP	W6a	0	0	0	0	0	0	0	10	28	30	30
	W7	6	8	8	11	12	12	12	12	12	12	12
	W6b	0	7	10	15	19	24	36	36	36	36	36

Table A.8: Optimal PV capacities (MW).

Scenario	Location	2027	2028	2029	2030
#1	S4	0	0	22	61
	S6	0	0	0	3
	S7	0	7	14	15
#5	S4	0	0	21	58
	S7	0	7	16	16
#6	S4	0	0	0	26
	S7	0	0	12	14
cBS	S4	0	0	22	60
	S6	0	0	0	1
	S7	0	7	15	20
cCA	S4	0	0	22	61
	S6	0	0	0	3
	S7	0	6	14	15
cFU	S4	0	0	22	61
	S6	0	0	0	3
	S7	0	7	14	15
cPV	S1	0	0	0	4
	S2	0	0	0	4
	S4	8	28	53	81
	S6	0	0	18	35
	S7	5	14	18	25
cPS	S4	0	0	0	18
	S7	0	0	1	13
cWP	S4	0	0	14	40
	S7	0	0	11	13
eBS	S4	0	0	22	61
	S6	0	0	0	3
	S7	0	7	14	15
eCA	S4	0	0	21	60
	S6	0	0	0	3
	S7	0	7	15	16
eFU	S4	0	0	22	60
	S6	0	0	0	3
	S7	0	7	14	15
ePV	S4	0	0	0	11
	S7	0	0	0	9
ePS	S2	0	0	0	2
	S4	0	11	42	73
	S6	0	0	2	20
	S7	0	9	18	23
eWP	S4	0	5	38	69
	S6	0	0	0	15
	S7	0	11	16	17

Table A.9: Optimal battery capacities (MW) in S7.

Scenario	2027	2028	2029	2030
#1	0	0	0	2
#2	0	0	0	1
#3	0	0	0	1
#5	0	0	0	2
#6	0	0	0	2
cBS	1	1	1	3
cCA	0	0	0	2
cFU	0	0	0	2
cPV	0	0	0	3
cPS	0	0	0	2
cWP	0	0	0	2
eBS	0	0	0	2
eCA	0	0	0	3
eFU	0	0	0	2
ePV	0	0	0	2
ePS	0	0	0	3
eWP	0	0	0	2

Table A.10: Optimal tidal power capacities (MW) in scenario #2.

Location	2025	2026	2027	2028	2029	2030
T1b	6	6	6	6	6	6
T1c	0	2	4	4	4	4
T5a	7	7	7	7	7	7
T5b	0	0	4	16	23	23
T6a	12	17	17	17	17	17
T6b	0	0	0	2	15	15

Table A.11: Optimal generation (GWh) in scenario 1-6, cBS, cCA and cFU.

Scenario	Resource	2020	2021	2022	2023	2024	2025	2026	2027	2028	2029	2030
#1	Fuel oil	188	59	61	67	69	71	57	43	29	14	0
	Biogas	9	9	9	9	9	9	9	9	9	9	9
	Hydro	112	102	101	99	99	99	96	91	85	81	77
	Wind	88	252	273	310	331	354	403	456	507	542	569
	Solar	0	0	0	0	0	0	0	0	4	22	49
	Battery	0	0	0	0	0	0	0	0	0	0	0
#2	Fuel oil	188	59	61	67	69	33	33	36	29	14	0
	Biogas	9	9	9	9	9	9	9	9	9	9	9
	Hydro	112	102	101	99	99	104	105	105	105	105	102
	Wind	88	252	273	310	331	271	274	281	267	236	290
	Tidal	0	0	0	0	0	113	143	167	220	301	301
	Battery	0	0	0	0	0	0	0	0	0	0	0
#3	Fuel oil	188	59	61	67	69	71	57	43	29	14	0
	Biogas	9	9	9	9	9	9	9	9	9	9	9
	Biofuel	0	0	0	0	0	0	0	12	32	50	62
	Hydro	112	102	101	99	99	99	96	94	93	91	87
	Wind	88	252	273	310	331	354	403	441	471	503	545
	Battery	0	0	0	0	0	0	0	0	0	0	0
#4	Fuel oil	188	59	61	67	69	71	75	84	89	93	98
	Biogas	9	9	9	9	9	9	9	9	9	9	9
	Hydro	112	102	101	99	99	99	98	97	96	95	93
	Wind	88	252	273	310	331	354	384	410	439	469	501
#5	Fuel oil	189	59	61	64	66	67	57	43	29	14	0
	Biogas	9	9	9	9	9	9	9	9	9	9	9
	Hydro	111	102	101	102	102	101	99	93	88	84	79
	PS R7	0	0	0	-5	-4	-5	-4	-3	-4	-4	-3
	Wind	88	252	273	314	336	359	403	457	507	541	573
	Solar	0	0	0	0	0	0	0	0	4	23	45
	Battery	0	0	0	0	0	0	0	0	0	0	0
#6	Fuel oil	188	59	61	67	69	71	57	43	29	14	0
	Biogas	9	9	9	9	9	9	9	9	9	9	9
	Hydro	112	102	101	99	99	99	97	92	87	82	77
	Wind	88	252	273	310	331	354	402	454	508	554	591
	Solar	0	0	0	0	0	0	0	0	0	7	24
	Battery	0	0	0	0	0	0	0	0	0	0	0
cBS	Fuel oil	188	59	61	67	69	71	57	43	29	14	0
	Biogas	9	9	9	9	9	9	9	9	9	9	9
	Hydro	112	102	101	99	99	99	96	91	86	82	77
	Wind	88	252	273	310	331	354	403	456	507	541	569
	Solar	0	0	0	0	0	0	0	0	4	23	49
	Battery	0	0	0	0	0	0	0	0	0	0	0
cCA	Fuel oil	188	58	60	66	68	70	57	43	29	14	0
	Biogas	9	9	9	9	9	9	9	9	9	9	9
	Hydro	112	102	101	99	99	98	96	91	85	81	77
	Wind	88	253	274	312	333	355	403	456	508	542	569
	Solar	0	0	0	0	0	0	0	0	3	22	49
	Battery	0	0	0	0	0	0	0	0	0	0	0
cFU	Fuel oil	188	64	66	73	75	72	57	43	29	14	0
	Biogas	9	9	9	9	9	9	9	9	9	9	9
	Hydro	112	103	102	101	100	98	96	91	85	81	77
	Wind	88	246	266	303	324	353	403	456	507	542	569
	Solar	0	0	0	0	0	0	0	0	4	22	49
	Battery	0	0	0	0	0	0	0	0	0	0	0

Table A.12: Optimal generation (GWh) in cPV, cPS, cWP, eBS, eCA, eFU, ePV, ePS, eWP and RoadMap.

Scenario	Resource	2020	2021	2022	2023	2024	2025	2026	2027	2028	2029	2030
cPV	Fuel oil	188	59	61	67	69	71	57	43	29	14	0
	Biogas	9	9	9	9	9	9	9	9	9	9	9
	Hydro	112	102	101	99	99	99	96	92	88	85	82
	Wind	88	252	273	310	331	354	403	447	482	505	522
	Solar	0	0	0	0	0	0	0	8	26	54	92
	Battery	0	0	0	0	0	0	0	0	0	0	-1
cPS	Fuel oil	188	58	60	66	68	70	57	43	29	14	0
	Biogas	9	9	9	9	9	9	9	9	9	9	9
	Hydro	112	102	101	99	99	98	95	91	84	75	70
	Wind	88	253	274	312	333	355	404	456	513	571	606
	Solar	0	0	0	0	0	0	0	0	0	1	19
	Battery	0	0	0	0	0	0	0	0	0	0	0
cWP	Fuel oil	188	53	56	59	61	62	57	43	29	14	0
	Biogas	9	9	9	9	9	9	9	9	9	9	9
	Hydro	112	103	102	100	100	100	97	91	86	81	75
	Wind	88	257	278	318	339	361	402	456	509	548	586
	Solar	0	0	0	0	0	0	0	0	0	15	32
	Battery	0	0	0	0	0	0	0	0	0	0	0
eBS	Fuel oil	188	59	61	67	69	71	57	43	29	14	0
	Biogas	9	9	9	9	9	9	9	9	9	9	9
	Hydro	112	102	101	99	99	99	96	91	85	81	77
	Wind	88	252	273	310	331	354	403	456	507	542	569
	Solar	0	0	0	0	0	0	0	0	4	22	49
	Battery	0	0	0	0	0	0	0	0	0	0	0
eCA	Fuel oil	188	59	62	68	70	72	57	43	29	14	0
	Biogas	9	9	9	9	9	9	9	9	9	9	9
	Hydro	112	102	102	100	99	99	96	91	86	81	77
	Wind	88	251	272	309	330	352	403	456	507	541	569
	Solar	0	0	0	0	0	0	0	0	4	23	49
	Battery	0	0	0	0	0	0	0	0	0	0	0
eFU	Fuel oil	188	47	50	56	59	59	57	43	29	14	0
	Biogas	9	9	9	9	9	9	9	9	9	9	9
	Hydro	112	102	102	100	99	99	96	91	85	81	77
	Wind	88	264	284	321	341	365	403	456	507	542	569
	Solar	0	0	0	0	0	0	0	0	4	22	49
	Battery	0	0	0	0	0	0	0	0	0	0	0
ePV	Fuel oil	188	59	61	67	69	71	57	43	29	14	0
	Biogas	9	9	9	9	9	9	9	9	9	9	9
	Hydro	112	102	101	99	99	99	96	91	85	76	71
	Wind	88	252	273	310	331	354	403	456	512	570	611
	Solar	0	0	0	0	0	0	0	0	0	0	12
	Battery	0	0	0	0	0	0	0	0	0	0	0
ePS	Fuel oil	188	60	62	68	70	71	57	43	29	14	0
	Biogas	9	9	9	9	9	9	9	9	9	9	9
	Hydro	112	103	102	100	99	99	96	91	88	85	82
	Wind	88	250	271	309	330	353	402	456	495	522	539
	Solar	0	0	0	0	0	0	0	0	13	38	73
	Battery	0	0	0	0	0	0	0	0	0	0	-1
eWP	Fuel oil	188	60	63	68	71	72	57	43	29	14	0
	Biogas	9	9	9	9	9	9	9	9	9	9	9
	Hydro	112	102	101	99	99	98	95	91	86	82	78
	Wind	88	251	272	309	330	353	403	456	501	530	555
	Solar	0	0	0	0	0	0	0	0	10	33	62
	Battery	0	0	0	0	0	0	0	0	0	0	0
RoadMap	Fuel oil	188	101	114	135	110	120	68	68	61	15	0
	Biogas	9	9	9	9	9	9	9	9	9	9	9
	Hydro	112	113	113	113	113	113	95	96	97	78	76
	Wind	88	198	206	226	274	287	394	425	462	545	569
	Solar	0	0	0	0	0	0	0	0	4	23	49
	Battery	0	0	0	0	0	0	0	0	0	0	0

Table A.13: Curtailment (GWh) from 2020 to 2030.

	2020	2021	2022	2023	2024	2025	2026	2027	2028	2029	2030
#1	3	24	24	25	27	32	68	130	148	163	139
#2	3	24	24	25	27	87	84	77	91	122	147
#3	3	24	24	25	27	32	68	89	86	88	105
#4	3	24	24	25	27	32	40	28	27	31	35
#5	3	24	24	23	27	32	67	126	145	174	141
#6	3	24	24	25	27	32	78	132	175	223	208
cBS	3	24	24	25	27	32	68	130	148	166	140
cCA	3	23	23	24	25	31	67	129	148	162	139
cFU	3	23	22	23	24	30	68	130	148	162	139
cPV	3	24	24	25	27	32	68	111	101	123	112
cPS	3	23	23	24	28	33	56	99	139	122	123
cWP	3	43	42	52	55	63	80	136	193	207	185
eBS	3	24	24	25	27	32	68	130	148	163	139
eCA	3	26	26	27	28	34	70	130	148	165	141
eFU	3	51	52	55	53	67	68	130	149	164	140
ePV	3	24	24	25	27	32	68	130	159	163	179
ePS	3	26	26	27	28	37	77	135	161	177	175
eWP	3	21	21	21	22	27	62	99	129	130	109
RoadMap	3	36	27	27	69	56	39	85	171	88	136

Table A.14: CO_2 emissions (ktonne) from 2020 to 2030.

	2020	2021	2022	2023	2024	2025	2026	2027	2028	2029	2030
#1	123	38	40	44	45	46	38	28	19	9	0
#2	123	38	40	44	45	22	22	23	19	9	0
#3	123	38	40	44	45	46	38	28	19	9	0
#4	123	38	40	44	45	46	49	55	58	61	64
#5	123	39	40	42	43	44	38	28	19	9	0
#6	123	38	40	44	45	46	38	28	19	9	0
cBS	123	38	40	44	45	46	38	28	19	9	0
cCA	123	38	40	43	45	46	38	28	19	9	0
cFU	123	42	43	48	49	47	38	28	19	9	0
cPV	123	38	40	44	45	46	38	28	19	9	0
cPS	123	38	39	43	44	46	38	28	19	9	0
cWP	123	34	36	38	40	41	38	28	19	9	0
eBS	123	38	40	44	45	46	38	28	19	9	0
eCA	123	39	40	45	46	47	38	28	19	9	0
eFU	123	31	33	36	39	39	38	28	19	9	0
ePV	123	38	40	44	45	46	38	28	19	9	0
ePS	123	39	41	45	46	46	38	28	19	9	0
eWP	123	39	41	45	46	47	38	28	19	9	0
RoadMap	123	66	75	88	72	79	45	44	40	10	0

Table A.15: Transmission losses (%) from 2020 to 2030

	2020	2021	2022	2023	2024	2025	2026	2027	2028	2029	2030
#1	0,8%	1,5%	1,6%	1,7%	1,8%	1,8%	1,9%	2,0%	2,2%	2,2%	2,3%
#2	0,8%	1,5%	1,6%	1,7%	1,8%	1,6%	1,7%	1,7%	1,7%	1,8%	2,1%
#3	0,8%	1,5%	1,6%	1,7%	1,8%	1,8%	1,9%	1,8%	1,9%	2,1%	2,2%
#4	0,8%	1,5%	1,6%	1,7%	1,8%	1,8%	1,9%	2,0%	2,0%	1,9%	2,0%
#5	0,8%	1,5%	1,6%	1,6%	1,7%	1,8%	1,8%	1,9%	2,1%	2,1%	2,3%
#6	0,8%	1,5%	1,6%	1,7%	1,8%	1,8%	1,9%	1,9%	2,0%	2,0%	2,0%
cBS	0,8%	1,5%	1,6%	1,7%	1,8%	1,8%	1,9%	2,0%	2,2%	2,2%	2,3%
cCA	0,8%	1,5%	1,6%	1,7%	1,8%	1,9%	1,9%	2,0%	2,2%	2,2%	2,3%
cFU	0,8%	1,5%	1,6%	1,6%	1,7%	1,8%	1,9%	2,0%	2,2%	2,3%	2,3%
cPV	0,8%	1,5%	1,6%	1,7%	1,8%	1,8%	1,9%	1,9%	2,1%	2,2%	2,4%
cPS	0,8%	1,5%	1,6%	1,7%	1,8%	1,9%	2,0%	2,0%	2,3%	2,4%	2,4%
cWP	0,8%	1,5%	1,6%	1,7%	1,8%	1,8%	1,8%	1,9%	2,1%	2,1%	2,2%
eBS	0,8%	1,5%	1,6%	1,7%	1,8%	1,8%	1,9%	2,0%	2,2%	2,2%	2,3%
eCA	0,8%	1,5%	1,6%	1,7%	1,8%	1,8%	1,9%	2,0%	2,2%	2,2%	2,3%
eFU	0,8%	1,5%	1,6%	1,7%	1,8%	1,9%	1,9%	1,9%	2,2%	2,2%	2,3%
ePV	0,8%	1,5%	1,6%	1,7%	1,8%	1,8%	1,9%	2,0%	2,2%	2,4%	2,4%
ePS	0,8%	1,5%	1,6%	1,7%	1,8%	1,8%	1,8%	2,0%	2,1%	2,2%	2,3%
eWP	0,8%	1,5%	1,6%	1,7%	1,8%	1,9%	1,9%	2,0%	2,2%	2,3%	2,4%
RoadMap	0,8%	1,2%	1,2%	1,2%	1,3%	1,4%	2,0%	1,7%	2,0%	2,4%	2,3%

Table A.16: Optimal transmission capacities (MW).

Connection	Scenario	2020	2021	2022	2023	2024	2025	2026	2027	2028	2029	2030
R1-R5	#1	35	35	35	35	35	35	35	35	35	35	38
	#6	35	35	35	35	35	35	35	35	35	50	50
	cBS	35	35	35	35	35	35	35	35	35	35	37
	cCA	35	35	35	35	35	35	35	35	35	35	38
	cFU	35	35	35	35	35	35	35	35	35	35	38
	cPS	35	35	35	35	35	35	35	35	35	35	41
	cWP	35	35	35	35	35	35	35	35	35	35	39
	eBS	35	35	35	35	35	35	35	35	35	35	38
	eCA	35	35	35	35	35	35	35	35	35	35	36
	eFU	35	35	35	35	35	35	35	35	35	35	37
	ePV	35	35	35	35	35	35	35	35	35	35	45
	ePS	35	35	35	35	35	35	35	35	35	35	36
	eWP	35	35	35	35	35	35	35	35	35	35	37
R5-R6	#1	10	10	12	46	46	46	46	51	63	63	63
	#2	10	10	12	46	46	46	46	46	46	46	58
	#3	10	10	12	46	46	46	46	46	46	52	62
	#5	10	10	12	46	46	46	46	46	57	58	58
	cBS	10	10	12	46	46	46	46	50	62	63	63
	cCA	10	10	12	46	46	46	46	52	64	64	64
	cFU	10	10	10	44	44	44	44	51	63	63	63
	cPV	10	10	12	46	46	46	46	46	52	62	64
	cPS	10	10	12	46	46	46	46	46	64	64	64
	cWP	10	12	15	49	49	49	49	51	60	60	60
	eBS	10	10	12	46	46	46	46	51	63	63	63
	eCA	10	10	11	45	45	45	45	50	62	62	62
	eFU	10	15	19	53	53	53	53	53	63	63	63
	ePV	10	10	12	46	46	46	46	51	62	62	62
	ePS	10	10	12	46	46	46	46	51	62	62	62
	eWP	10	10	11	45	45	45	45	46	62	64	64
R6-R7	#1	0	2	2	3	4	4	6	6	7	8	13
	#2	0	2	2	3	4	4	5	5	6	7	14
	#3	0	2	2	3	4	4	6	6	6	7	14
	#4	0	2	2	3	4	4	4	4	4	4	5
	#6	0	2	2	3	4	4	5	6	7	8	13
	#5	0	2	2	2	3	3	4	5	6	6	9
	cBS	0	2	2	3	4	4	6	6	7	7	12
	cCA	0	2	2	4	4	4	6	7	8	8	13
	cFU	0	1	1	2	3	4	6	6	7	8	13
	cPV	0	2	2	3	4	4	6	6	7	7	12
	cPS	0	2	2	3	4	4	5	6	7	8	13
	cWP	0	2	2	3	4	4	5	6	7	8	13
	eBS	0	2	2	3	4	4	6	6	7	8	13
	eCA	0	2	2	3	3	3	5	6	7	7	12
	eFU	0	2	2	4	4	4	6	6	7	8	13
	ePV	0	2	2	3	4	4	6	6	8	8	13
	ePS	0	2	2	3	3	4	6	6	7	7	12
	eWP	0	2	2	4	4	4	6	6	7	7	13

Table A.17: Costs of optimal results for scenario 1-6, cBS, cCA and cFU.

Scenario	Cost type	2020	2021	2022	2023	2024	2025	2026	2027	2028	2029	2030
#1	Fixed O&M	9	10	10	10	10	10	11	11	12	13	13
	Variable O&M	2	2	2	2	3	3	3	3	3	4	4
	Fuel cost	16	6	6	7	7	7	6	5	4	2	1
	Capital investments	0	1	2	3	3	4	6	9	14	20	26
	Transmission investments	0	0	0	0	0	0	1	1	1	1	2
#2	Fixed O&M	9	10	10	10	10	11	11	11	11	11	12
	Variable O&M	2	2	2	2	3	3	4	4	4	5	5
	Fuel cost	16	6	6	7	7	4	4	4	4	2	1
	Capital investments	0	1	2	3	3	6	6	7	8	10	15
	Transmission investments	0	0	0	0	0	1	1	1	1	1	2
#3	Fixed O&M	9	10	10	10	10	10	11	11	11	12	12
	Variable O&M	2	2	2	2	3	3	3	3	4	4	4
	Fuel cost	16	6	6	7	7	7	6	7	9	11	11
	Capital investments	0	1	2	3	3	4	6	8	8	9	11
	Transmission investments	0	0	0	0	0	0	1	1	1	1	2
#4	Fixed O&M	9	10	10	10	10	10	11	11	11	11	11
	Variable O&M	2	2	2	2	3	3	3	3	4	4	4
	Fuel cost	16	6	6	7	7	7	8	9	10	10	11
	Capital investments	0	1	2	3	3	4	4	5	6	6	7
	Transmission investments	0	0	0	0	0	0	0	0	0	0	1
#5	Fixed O&M	9	10	10	10	11	11	11	12	12	13	13
	Variable O&M	2	2	2	2	3	3	3	3	3	4	4
	Fuel cost	16	6	6	6	7	7	6	5	4	2	1
	Capital investments	0	1	2	3	3	4	6	9	14	19	26
	Transmission investments	0	0	0	0	0	0	0	1	1	1	1
#6	Fixed O&M	9	10	10	10	10	10	11	11	12	13	13
	Variable O&M	2	2	2	2	3	3	3	3	3	4	4
	Fuel cost	16	6	6	7	7	7	6	5	4	2	1
	Capital investments	0	1	2	3	3	4	6	9	12	17	24
	Transmission investments	0	0	0	0	0	0	1	1	1	1	1
cBS	Fixed O&M	9	10	10	10	10	10	11	11	12	13	13
	Variable O&M	2	2	2	2	3	3	3	3	3	4	4
	Fuel cost	16	6	6	7	7	7	6	5	4	2	1
	Capital investments	0	1	2	3	3	4	6	9	14	20	26
	Transmission investments	0	0	0	0	0	0	1	1	1	1	1
cCA	Fixed O&M	9	10	10	10	10	10	11	11	12	13	13
	Variable O&M	2	2	2	2	3	3	3	3	3	4	4
	Fuel cost	16	6	6	7	7	7	6	5	4	2	1
	Capital investments	0	1	2	3	3	4	6	9	14	20	26
	Transmission investments	0	0	0	0	0	0	1	1	1	1	1
cFU	Fixed O&M	9	10	10	10	10	10	11	11	12	13	13
	Variable O&M	2	2	2	2	3	3	3	3	3	4	4
	Fuel cost	13	5	5	6	6	6	5	4	3	2	1
	Capital investments	0	1	2	2	3	4	6	9	14	20	26
	Transmission investments	0	0	0	0	0	0	1	1	1	1	2

Table A.18: Costs of optimal results for cPV, cPS, cWP, eBS, eCA, eFU, ePV, ePS and eWP.

Scenario	Cost type	2020	2021	2022	2023	2024	2025	2026	2027	2028	2029	2030
cPV	Fixed O&M	9	10	10	10	10	10	11	11	12	12	13
	Variable O&M	2	2	2	2	3	3	3	3	3	3	3
	Fuel cost	16	6	6	7	7	7	6	5	4	2	1
	Capital investments	0	1	2	3	3	4	6	10	14	19	25
	Transmission investments	0	0	0	0	0	0	1	1	1	1	1
cPS	Fixed O&M	9	10	10	10	10	10	11	11	12	12	13
	Variable O&M	2	2	2	2	3	3	3	3	4	4	4
	Fuel cost	16	6	6	7	7	7	6	5	4	2	1
	Capital investments	0	1	2	3	3	4	6	9	13	18	24
	Transmission investments	0	0	0	0	0	0	1	1	1	1	2
cWP	Fixed O&M	9	10	10	10	10	11	11	12	12	13	13
	Variable O&M	2	2	2	2	3	3	3	3	3	4	4
	Fuel cost	16	5	6	6	6	7	6	5	4	2	1
	Capital investments	0	2	2	3	3	4	5	8	12	18	24
	Transmission investments	0	0	0	0	0	0	1	1	1	1	1
eBS	Fixed O&M	9	10	10	10	10	10	11	11	12	13	13
	Variable O&M	2	2	2	2	3	3	3	3	3	4	4
	Fuel cost	16	6	6	7	7	7	6	5	4	2	1
	Capital investments	0	1	2	3	3	4	6	9	14	20	26
	Transmission investments	0	0	0	0	0	0	1	1	1	1	2
eCA	Fixed O&M	9	10	10	10	10	10	11	11	12	13	13
	Variable O&M	2	2	2	2	3	3	3	3	3	4	4
	Fuel cost	16	6	6	7	7	7	6	5	4	2	1
	Capital investments	0	1	2	3	3	4	6	9	14	20	26
	Transmission investments	0	0	0	0	0	0	1	1	1	1	2
eFU	Fixed O&M	9	10	10	10	10	11	11	11	12	13	13
	Variable O&M	2	2	2	2	3	3	3	3	3	4	4
	Fuel cost	19	6	6	7	7	7	7	6	4	3	1
	Capital investments	0	2	3	3	4	5	6	9	14	20	26
	Transmission investments	0	0	0	0	1	1	1	1	1	1	1
ePV	Fixed O&M	9	10	10	10	10	10	11	11	12	12	13
	Variable O&M	2	2	2	2	3	3	3	3	4	4	4
	Fuel cost	16	6	6	7	7	7	6	5	4	2	1
	Capital investments	0	1	2	3	3	4	6	9	14	20	26
	Transmission investments	0	0	0	0	0	0	1	1	1	1	2
ePS	Fixed O&M	9	10	10	10	10	10	11	12	12	13	13
	Variable O&M	2	2	2	2	3	3	3	3	3	3	3
	Fuel cost	16	6	6	7	7	7	6	5	4	2	1
	Capital investments	0	2	2	3	3	4	6	10	15	21	28
	Transmission investments	0	0	0	0	0	0	1	1	1	1	1
eWP	Fixed O&M	9	10	10	10	10	10	11	11	12	12	13
	Variable O&M	2	2	2	2	3	3	3	3	3	4	4
	Fuel cost	16	6	6	7	7	7	6	5	4	2	1
	Capital investments	0	2	2	3	3	4	7	11	16	22	28
	Transmission investments	0	0	0	0	0	0	1	1	1	1	2

Table A.19: Levelised cost of energy (EUR/MWh) from 2020 to 2030.

	2020	2021	2022	2023	2024	2025	2026	2027	2028	2029	2030
#1	67	45	45	46	46	46	47	50	54	59	65
#2	67	45	45	46	46	45	44	44	44	45	49
#3	67	45	45	46	46	46	47	50	52	54	57
#4	67	45	45	46	46	46	46	47	47	48	48
#5	67	45	46	46	46	46	47	50	53	59	64
#6	67	45	45	46	46	46	47	49	51	56	61
cBS	67	45	45	46	46	46	47	50	54	59	65
cCA	67	45	45	46	46	46	47	50	53	59	64
cFU	59	43	43	43	44	44	45	49	53	59	65
cPV	67	45	45	46	46	46	47	50	53	57	62
cPS	67	45	45	46	46	46	46	49	52	56	61
cWP	67	45	45	45	45	45	46	48	51	56	62
eBS	67	45	45	46	46	46	47	50	54	59	65
eCA	67	45	46	46	46	46	47	50	54	59	65
eFU	74	48	48	48	48	48	49	51	55	60	65
ePV	67	45	45	46	46	46	47	50	54	59	65
ePS	67	46	46	46	46	46	48	51	55	61	67
eWP	67	46	46	47	47	47	49	52	56	61	67

APPENDIX B
PowerFactory Model Validation

This appendix contains the comparison of load flow measurements and simulations for scenario 2 and 3, as presented in Table 6.5. Table B.1, Table B.2 and Table B.3 contain the current, active and reactive power and voltages, respectively. Table B.4 contains the current for scenario 3, Table B.5 the active and reactive power and Table B.6 the voltage.

Table B.1: Current (A) in Load Flow Validation of Suðuroy in Scenario 2. HV and LV indicate if the current is measured at the high or low voltage sides of the transformers.

Type	Name	Simulation	Measurement		
			L1	L2	L3
Loads	VG lokal trafo 1	10	9	10	10
	Sumba	8	8	8	9
	Vágseiði	50	51	50	49
	VG lokal trafo 2	5	4	4	5
	Tvøroyri	27	28	-	-
	Hvalba	54	53	-	-
	Trongisvágur	2	2	-	-
	Drelnes (Sandvík)	15	15	-	-
	Øðravík	9	10	-	-
	Havnarlagið 1	3	3	3	3
	Havnarlagið 2	23	23	23	24
Generation	VG G3	169	170	-	-
	BO G1	15	15	-	-
Busbars	VG 10 kV: 1->2	110	111	105	107
	VG 10 kV: 2->1	110	110	105	103
Cables/lines	TG-VG	63	66	65	65
	VG-TG	63	64	64	63
	VG-BO	9	11	11	11
Transformers	BO (LV)	15	14	-	-
	BO (HV)	8	8	-	-
	VG 1 (HV)	27	28	-	-
	VG 1 (LV)	56	59	-	-
	VG 2 (HV)	28	29	-	-
	VG 2 (LV)	56	-	-	-
	TG 1 (HV)	52	53	53	52
	TG 1 (LV)	101	102	-	-
	TG 2 (HV)	11	12	12	12
	TG 2 (LV)	22	23	22	23

Table B.2: Active (MW) and Reactive Power (Mvar) for Load Flow Validation of Suðuroy in Scenario 2. HV and LV indicate if the power is measured at the high or low voltage sides of the transformers.

Type	Name	Active		Reactive	
		Sim.	Meas.	Sim.	Meas.
Generation	VG G3	3.03	3.08	0.36	0.22
	BO G1	0.27	0.27	0.01	0.09
Busbars	VG 10 kV: 1->2	1.95	1.91	0.35	0.30
	VG 10 kV: 2->1	-1.95	-1.87	-0.35	-0.38
Lines/cables	TG-VG	-2.22	-2.28	-0.31	-0.33
	VG-TG	2.27	2.29	0.27	0.24
	VG-BO	-0.27	-0.26	-0.19	-0.30
Transformers	BO (HV)	-0.27	1.85	-0.01	-0.13
	VG 1 (LV)	1.00	1.05	0.06	-0.02
	VG 2 (LV)	1.00	1.03	0.06	0.02
	TG 1 (HV)	1.83	1.84	0.22	0.23
	TG 2 (HV)	0.39	0.40	0.09	0.08
	TG 2 (LV)	-0.39	0.00	-0.08	0.00

Table B.3: Voltage (kV) for Load Flow Validation of Suðuroy in Scenario 2.

Type	Name	Simulation	Measurement		
			L1	L2	L3
Busbars	BO 10 kV	10.39	10.36	-	-
	VG 10 kV - 1	10.39	10.39	-	-
	VG 10 kV - 2	10.39	10.34	-	-
	VG 20 kV	21.30	21.17	-	-
	TG 20 kV	20.75	20.57	20.59	20.59
	TG 10 kV - 1	10.64	10.56	10.56	10.56
	TG 10 kV - 2	10.60	10.52	10.50	10.51

Table B.4: Current (A) in Load Flow Validation of Suðuroy in Scenario 3. HV and LV indicate if the current is measured at the high or low voltage sides of the transformers.

Type	Name	Simulation	Measurement		
			L1	L2	L3
Loads	VG lokal trafo 1	12	12	12	11
	Sumba	14	15	13	14
	Vágur	2	3	3	0
	Vágseiði	71	71	72	71
	VG lokal trafo 2	5	5	5	5
	Tvøroyri	33	34	-	-
	Hvalba	37	37	-	-
	Trongisvágur	4	4	-	-
	Drelnes (Sandvík)	17	18	-	-
	Havnarlagið 1	87	89	88	90
	Havnarlagið 2	87	88	88	88
	PO	69	73	70	71
Generation	VG G3	187	187	-	-
	VG G4	42	43	-	-
	BO G1	12	13	-	-
Busbars	VG 10 kV: 1->2	99	96	93	94
	VG 10 kV: 2->1	99	97	96	94
Cables/lines	TG-VG	67	66	65	66
	VG-TG	66	66	65	66
	VG-BO	99	97	96	94
Transformers	BO (LV)	6	7	-	-
	BO (HV)	12	13	-	-
	VG 1 (HV)	30	28	-	-
	VG 1 (LV)	61	63	-	-
	VG 2 (HV)	30	32	-	-
	VG 2 (LV)	61	61	-	-
	TG 1 (HV)	47	48	47	48
	TG 1 (LV)	90	90	-	-
	TG 2 (HV)	90	91	91	91
	TG 2 (LV)	174	176	176	177
	BO 2 (LV)	1	1	-	-

Table B.5: Active (MW) and Reactive Power (Mvar) for Load Flow Validation of Suðuroy in Scenario 3. HV and LV indicate if the power is measured at the high or low voltage sides of the transformers.

Type	Name	Active		Reactive	
		Sim.	Meas.	Sim.	Meas.
Generation	VG G3	3.35	3.33	0.34	0.29
	VG G4	0.61	0.61	0.45	0.45
	BO G1	0.22	0.22	0.01	0.08
Busbars	VG 10 kV: 1->2	1.77	1.68	0.15	0.15
	VG 10 kV: 2->1	-1.77	-1.69	-0.15	-0.24
Lines/cables	TG-VG	-2.34	-2.24	-0.56	-0.59
	VG-TG	2.40	2.49	0.53	0.52
	VG-BO	-0.22	-0.23	-0.20	-0.29
Transformers	BO (HV)	-0.22	-0.21	-0.02	-0.07
	VG 1 (LV)	1.09	1.11	0.19	0.10
	VG 2 (LV)	1.09	1.10	0.19	0.16
	TG 1 (HV)	1.65	1.66	0.30	0.32
	TG 2 (HV)	3.14	3.14	0.76	0.77
	TG 2 (LV)	-3.13	-3.13	-0.65	-0.67

Table B.6: Voltage (kV) for Load Flow Validation of Suðuroy in Scenario 3.

Type	Name	Simulation	Measurement		
			L1	L2	L3
Busbars	BO 10 kV	10.37	10.34	-	-
	VG 10 kV - 1	10.39	10.35	-	-
	VG 10 kV - 2	10.39	10.34	-	-
	VG 20 kV	21.30	21.17	-	-
	TG 20 kV	20.75	20.57	20.59	20.59
	TG 10 kV - 1	10.64	10.56	10.56	10.56
	TG 10 kV - 2	10.60	10.52	10.50	10.51

APPENDIX C
Scientific Papers

Three of the published and unpublished papers are included in this appendix. The published article included, has been included as it is considered a main contribution. Two of the unpublished included are included in order for the reader to have access to unpublished material, which is considered as significant importance.

- Starting on page 232: **H. M. Tróndheim**, B. A. Niclasen, T. Nielsen, F. F. D. Silva and C. L. Bak, "100% Sustainable Electricity in the Faroe Islands: Expansion Planning Through Economic Optimization," in *IEEE Open Access Journal of Power and Energy*, vol. 8, pp. 23-34, 2021. Licensed under **CC BY 4.0**.

- Starting on page 244: **H. M. Tróndheim**, F. F. da Silva, C. L. Bak, T. Nielsen, B. A. Niclasen, R. S. Nielsen, and N. Weikop, "Alternative and Combined Procedure for Parameter Identification and Validation of Governor and Automatic Voltage Regulator Dynamic Models," (Working title, to be submitted prior to defence).

- Starting on page 256: **H. M. Tróndheim**, L. Hofmann, P. Gartmann, E. Quitmann, C. L. Bak, F. F. da Silva, T. Nielsen, and B. A. Niclasen, "Frequency and Voltage Stability Towards 100% Renewables in Suðuroy, Faroe Islands," CIGRE Science and Engineering Journal. (Accepted with minor changes, to be published in June 2022)

100% Sustainable Electricity in the Faroe Islands: Expansion Planning Through Economic Optimization

HELMA MARIA TRÓNDHEIM[1,2,3], **BÁRÐUR A. NICLASEN**[2], **TERJI NIELSEN**[1],
FILIPE FARIA DA SILVA[3] **(Senior Member, IEEE), AND**
CLAUS LETH BAK[3] **(Senior Member, IEEE)**

[1]Research and Development Department, SEV (Power Company), 100 Tórshavn, Faroe Islands
[2]Department of Science and Technology, University of the Faroe Islands, 100 Tórshavn, Faroe Islands
[3]Department of Energy Technology, Aalborg University, 9220 Aalborg East, Denmark
CORRESPONDING AUTHOR: H. M. TRÓNDHEIM (hmt@sev.fo)

ABSTRACT SEV, the Faroese Power Company, has a vision to reach a 100% renewable power system by 2030. SEV is committed to achieve this, starting from a 41% share of renewables in 2019. A detailed expansion plan for the generation, storage and transmission is needed to reach this goal. This is the focus of this study. Practical constrains e.g. resource potential and available space must be considered. Balmorel, an optimisation tool, has been used to optimise investments and dispatch. A method to translate optimal results to a realistic RoadMap was developed and applied. The impact of different technologies and costs has been investigated through multiple scenarios. In ratios of average consumption in 2030, installed power will be 224% wind, 105% solar with 8-9 days of pumped hydro storage according to the proposed RoadMap. The plan is economically favorable up to 87% of renewables, but in order to reach a 100% renewable production in an average weather year, the renewable generation capacity has to be increased by 80%. The study also shows that if biofules or tidal technologies become viable, these will be game changers needing a significantly lower total sum of installed renewable power.

INDEX TERMS Expansion planning, sustainable energy, economic optimisation, Balmorel, islanded system.

I. INTRODUCTION

THE Faroe Islands are aiming for a 100% renewable electricity sector by 2030. A vision set by SEV, the local power company. The power system consists of 7 isolated grids: The main grid connects 11/18 islands (90% of the consumption), the most southern island Suðuroy (10%) and 5 small systems (0.2% in total). The generation capacity is 102 MW of thermal power using fuel oil (FO) and gas oil (GO), 41 MW of hydro power (HP) with reservoirs, 18 MW of wind power (WP), 0.25 MW of photovoltaic (PV) power and 1.5 MW of biogas (BG) power. 42 MW of new WP and a pilot project with 0.2 MW of tidal power (TP) are committed. The generation in 2019 was 387 GWh of which 14% was wind energy and 27% hydro. Demand ranges between 22 MW and 60 MW.

The average wind speed north-west of the capital Tórshavn measured at 104 m is 10.1 m/s [1], the average precipitation

is 1284 mm [2] and the annual hours of bright sunshine are 840 [2]. On a monthly basis these resources complement each other, as seen on the upper plot on Fig. 1 [3]. The monthly wind speeds are average values based on the years from 2011 to 2015. The precipitation and solar data are monthly averages based on 2007-2015. The complementary is also apparent when analysing a specfic year, i.e. not average values. Although the potential for solar energy is relatively low, it complements the wind and hydro resources which could make it interesting for the Faroese power system. The average monthly tidal streams are close to constant throughout the year. Even though the four resources complement each other very well on an average monthly basis, there are periods with a low renewable energy potential, see lower plot on Fig. 1. Tidal is clearly the most constant resource, but varies by a factor of two over the shown spring–neap cycle.

232
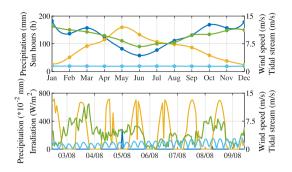
FIGURE 1. The potential for hydro (blue), photovoltaics (yellow), wind (green) and tidal (cyan) energy on a monthly [3] and hourly basis (2017).

The Faroese power system is rarely studied or discussed in peer-reviewed literature. However, the system has been analysed in other studies and technical reports. These are typically initiated or conducted by SEV. The most extensive study, summarised in [4], included a projection of the future energy demand [5], production simulations using different demand and generation technology combinations [6], the role of flexible loads [7], the economically optimal investments towards 2030 [8], expansions required to assure renewable production also during dry years [9], analysis of needed storage capacities with different compositions of renewables [10], the feasibility of tidal energy [11], relevant types of energy storages [12], feasibility of a cable to neighbouring countries [13] and an initial study of the future power system stability [14]. A technical overview of the mentioned studies can be found in reference [15]. The main conclusion is an expansion plan (a RoadMap) that includes 148 MW of wind power, 80 MW of PV power and hydro pumped storage (PS) systems with 146 MW of pumping capacity and 109 MW of generation capacity towards 2030. The need for larger reservoirs should be evaluated later. Another conclusion is that a cable to neighbouring countries is not financially viable [16], nor is it interesting politically as a self sufficient energy system is desired [17]. Finally, that tidal energy technology is currently not mature enough to be considered as a part of the power system in the near future. Other studies have analysed different aspects e.g. economic optimisations of future investments using tools like HOMER [3], [18], Balmorel [19] (also used in ref. [8]) and simpler manual approaches [20]. A few studies have also analysed the system with different scenarios using fixed capacities, i.e. not an optimisation [21]–[23]. Finally some studies have focused on the feasibility of specific components e.g. flow batteries [24] and fuel cells [25]. The presented studies have been conducted using different approaches and focusing on different components of the system. The majority of the studies do conclude that wind power together with PV and pumped storage is the most feasible combination to reach a high penetration of renewables in the Faroe Islands.

One of the remaining challenges towards a 100% renewable power system is the power system stability when increasing the penetration of inverter-based technologies. In order to conduct a realistic investigation of this, it is necessary to have a very detailed RoadMap, which should consider: 1. The exact location of each investment (generation, storage and transmission), 2. Constraints based on available space for new plants, 3. Variation in demand and renewable resources based on location, 4. If the necessary transmission capacity is sufficient or reinforcements are needed and 5. The costs of keeping thermal power plants as back up. The present RoadMap towards a 100% renewable electricity sector in the Faroe Islands [4] is based on studies, which have either simplified or ignored these aspects. Thus, this study aims to present an updated RoadMap considering these details, which then can be used for future power system analyses.

Multiple energy system modelling tools have been developed, and can be used for expansion planning. A broad range of energy system models have been discussed, categorised, and compared in [26]–[31]. The focus in the mentioned review studies varies, e.g. reference [27] focuses on categorising the tools in order to guide the reader to choose the best fitted tool, while others focus on comparing the different approaches [30] and identifying state of the art issues with regards to expansion planning [31]. Based on [27], Balmorel has been chosen as the most suitable tool for this investigation as it can optimise the future investments annually and the dispatch hourly. In addition, it is an open source and transparent tool, that is flexible in terms of immature technologies. Balmorel has been applied to multiple energy systems and is under continous development, see [32].

A disadvantage with Balmorel and other optimisation tools is that an economically optimal solution might not be realistic nor practical, as the capacity of a cable, reservoir or generation unit increases annually, where in reality it has to be installed or not. In order to tackle this challenge, a very detailed model in Balmorel addressing the aspects mentioned previously was defined, and then a method to translate the optimal results to a RoadMap with realistic projects, that are close to the optimal solution, was developed. Other related studies, Faroese [3], [8], [9], [15], [18]–[21] or international [33]–[38], do not transform the optimal results into an actual action plan. Reference [34] analyses the feasibility and security level of a highly renewable power system in the Mainland Portugal using the tool EnergyPLAN and a single predefined scenario. A model focusing on the integration of unit commitment problem is developed in [35] and tested on the Greek power system. The annually optimal investments are obtained. The operation challenges in a renewable system are integrated in a model proposed by [33]. An expansion planning study of Santiago, Cabo Verde, defines each suitable location for renewables and the available capacity, but investments are not optimised [36].

The applied and detailed approach used in this study, based on the tacit knowledge from a system provider actively pushing the limit for variable renewable energy penetration in
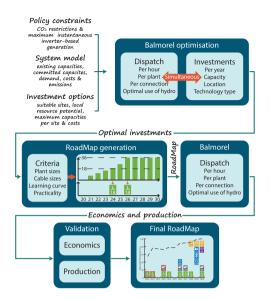
233

FIGURE 2. A flowchart illustrating the methodology followed in this study.

TABLE 1. Nomenclature for Equations (1)-(6).

T	Target	g	Technology	F	Fuel consumption
y	Year	G	Generation	K	Existing capacity
a	Area	Z	System costs	W	Emission factor
t	Time	r	Resource	x	Transmission line
c	Costs	I	Investment	X	Transmission capacity
D	Demand	fix	Fixed O&M	i	Inverter based
f	Fuel	w	Emission		

mentioned in the introduction and more scenarios have been simulated analysing the impact of different technologies, constraints and costs. In Balmorel the least-cost investments are optimised annually, while the least-cost dispatch is optimised hourly. Balmorel seeks to minimise the total costs of the electrical power system through a linear optimisation problem. The costs considered are for fixed operation and maintenance (O&M), variable O&M, investments in generation, storage and transmission capacity (1). The optimisation is subject to meeting the power demand in each region (2), the production not exceeding the hourly available resources (3) nor the transmission capacity (4). Additionally, two policy constrains have been set. The first one limits the CO_2 emissions to decrease linearly to zero in 2030 (5). The other limits the maximum instantaneous inverter based generation. The current inverter based operation limit is set to 60%, with the three planned wind farms this limit is increased to 80% in 2021, and then increases linearly to allow 100% instantaneous inverter-based generation in 2030 (6). The years from 2020 to 2030 have been optimised based on different scenarios (Table 2). The results obtained are the optimal hourly dispatch etc. and the annual optimal investments from 2021 and forward. For further details on the optimisation algoritm: [39].

Minimise

$$Z_y = \sum_{g,t} c_{g,t} G_{g,t} + \sum_{g,f,t} c_{g,t}^f F_{g,t}^f + \sum_g (ac_g^I + c_g^{fix}) I_g$$
$$+ \sum xac_x^I I_x \quad (1)$$

subject to

$$\sum_g G_{g,t} + \sum_x (1 - loss) X_{x,t}^{Import} = \sum_x X_{x,t}^{Export} + D_t$$
$$(2)$$

$$G_{g,t} \le r_t^f (K_g + I_g) \quad (3)$$

$$X_{x,t} \le K^x + I^x \quad (4)$$

$$\sum_{g,t} W_w^f F_{g,t}^f \le T_w \quad (5)$$

$$\frac{\sum_g G_{g,t}^i}{\sum_g G_{g,t}} \le T_{i,t} \quad (6)$$

The annual optimal investments from Balmorel are used as an input to the *RoadMap generation* (Fig. 2). The left box shows the criterias set to a realistic RoadMap, which are as follows: 1) Each investment in a power plant needs to be a reasonable size, e.g. a full wind farm in one year

an isolated grid, differs from the other expansion planning studies we have found, as these are typically more academical in motivation and outcome. The approach presented in this study is especially applicable for other small systems, where it is possible to map out every relevant renewable generation and define the local resource potential and maximum capacities. In addition to the developed methodology, the study also presents very interesting results that show the influence the relatively persistent tidal source and dispatchable biofuels can have on the future power composition. The study is based on political decisions in the Faroe Islands, and the actual power system considering the local constrains, which makes this a realistic RoadMap that will be used in the expansion planning of the power system. The structure of the paper is: The topic is introduced in section I, methodology and modelling in section II. The results are presented and discussed in section III. Section IV concludes the study.

II. METHODOLOGY AND MODELLING

The method used to generate a RoadMap, consists of two parts; an economic optimisation in the partial equilibrium model Balmorel, and a translation of the optimal results to a realistic expansion plan. This chapter starts by describing the methodology and then the modelling of the system, technologies, investment options and the different scenarios, which have been run in this study.

Fig. 2 shows the applied methodology. The inputs required to Balmorel are specifications on the system, investment options and policy constraints. The previous Faroese Balmorel models [8], [19] have been developed futher in to a significantly more detailed model, considering the aspects

234

instead of multiple small investments. 2) It is not possible to increase the capacity of a cable year after year, therefore these investments need to be conducted in one step. Additionally the investments need to reflect the capacity of the onshore cables used in the transmission system, i.e. 44 MW. 3) The learning curve of the system operators has to be considered, as each investment has a big influence on the power system operation, and the operators should have a chance to adapt to the new investments. This means that the sizes of the first wind farms are smaller and with more time inbetween the investments. 4) The energy authority in the Faroe Islands makes tenders for each new wind farm. Thus, from a practical perspective it is highly unlikely that the authority will make several tenders during the same year. This should therefore be avoided to the extent possible, in order to obtain a realistic RoadMap. The four criterias are considered by manually investigating the optimal investments for each site/connection separately. An example from on of the wind farms is found in the right box in *RoadMap generation* in the flowchart. This site has a maximum capacity of 36 MW, and by 2024 just above half of this is needed (20 MW), by 2026 the wind farm reaches full capacity. As the figure shows, these optimal results have been transformed into a two step investment by installing 18 MW in 2024 and 18 MW in 2026. 36 MW is considered too much in one step from a power system operation point of view, and therefore the commission is in halves. This is also in relatively good correspondence with the optimal results. This example shows how the plant size, the learning curve, i.e. the operational experience of the system operators, and practicality have been considered at this specific site.

The next step is to define the proposed RoadMap as committed capacities in Balmorel and rerun the simulation, without any additional investment options. The Balmorel outputs used from the second run are the economic and production data. The RoadMap has then been validated by comparing the economical results to the optimal solution. This is done to ensure that the RoadMap is close to the economically optimal solution. Additionally, the production using the proposed expansion plan has to be 100% renewable in 2030, for the RoadMap to be validated. The final output of the applied methodology is a RoadMap, which is based on an optimisation, but has been translated into a realistic hands-on expansion plan.

A. MODELLING THE POWER SYSTEM

The 5 small isolated (islands) systems are ignored in this study as these are neglectable compared to the rest of the system. The power system has been modelled by dividing the main grid into 6 regions (R1-R6), based on the existing transmission grid, and by defining Suðuroy as region 7 (R7). Any production or consumption has to be related to a specific region. If the region demand is higher than the region production, energy has to be transmitted from another region which results in a 2% loss of the transmitted power. The regions are illustrated in Fig. 3. Region 3 is a connection point (a busbar) without demand and production. The existing transmission
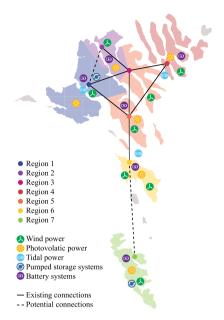
FIGURE 3. The regions in the modelled power system, existing and potential connections between regions and the generation/storage investment options.

capacities are 35 MW, except from the R5-R6 connection which is 10 MW, which will be increased to 44 MW in 2023. The model is allowed to invest in transmission capacity in every connection shown in the figure, except from R1-R3. The investment options are defined based on internal plans for the transmission system [40].

Demand profiles are assigned to the regions. The demand consists of three parts; normal, heating and transport. The normal demand includes everything except for electricity which is needed for heating and transport. The future demand in the Faroe Islands has been investigated and projected previously [3], [5], based on either one or two regions. This model is divided into 7 regions which means new projections are required. The projection assumes that the normal electricity demand, the number of households, and cars in each region continue to increase with the same pace that has been seen from 2009 to 2018. This historic data is obtained from every electricity meter in the Faroe Islands, Statistics Faroe Islands and the Faroese Vehicle Administration. It is assumed that 50% of the heating and transport sectors will be electrified in the year 2025 and 100% in 2030. This is a worst case scenario in terms of investments required to meet the demand. The annual consumption of an electric vehicle is set to 3 MWh [6]. Heat pumps are assumed to consume 5 MWh annually, based on a heat pump coefficient of performance factor of 4 [6] and that for the annual heat demand of a house 20 MWh [41] can be considered a reasonable assumption. The demand in region 7 has an addtional demand increase due to planned new fish
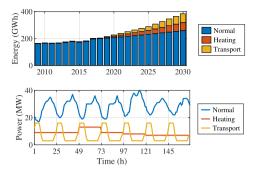
FIGURE 4. The upper plot shows the historic and projected electricity demand (GWh) in R5. The lower plot shows the projected hourly demand in R5 throughout week 1 in 2030.

TABLE 2. A List of the scenarios investigated.

#	Scenario description
1	Main
2	Incl. tidal energy as an investment option
3	Incl. permission to burn BF at FO plant in R5
4	Excl. restrictions on CO_2 emissions
5	Incl. PS system in R7

TABLE 3. Existing and committed generation capacities [MW]. The committed capacities are in parentheses.

	R1	R2	R4	R5	R6	R7
Fuel oil	-	-	-	77	-	13
Gas oil	-	-	4	5	-	-
Biogas	-	-	-	2	-	-
Hydro	14	22	1	-	-	3
Wind	2	(18)	-	16 (18)	-	(6)

factories. These factories are assumed to add a constant load of 1 MW and 2 MW from 2020 and 2023 respectively. The total demand is projected to 659 GWh in 2030. Additionally, a 4% loss is added to the demand, representing distribution losses. An example of the demand projections and the historic demand (R5) can be found in Fig. 4 as well as the hourly demand profiles. The pattern of the hourly profiles for the normal demand is obtained from the electricity meters. The profile of the heating demand is assumed to be constant throughout a day, but varying from day to day based on the outside temperature, as there is a correlation between these two [42]. The majority of the electric vehicles are assumed to charge during the night, due to financial incentives. These profiles are then scaled to meet the annual demand. Similar assumptions have also been made in references [3], [6].

B. SCENARIOS INVESTIGATED

Multiple scenarios, all emerging from the 2030 vision, have been simulated in this study in order to analyse how different technologies and restrictions can affect the future energy mixture. The scenarios are listed below. The main scenario considers wind power, photovoltaic power, a pumped storage system in R1, batteries and transmission capacity as investment options. Scenario 2-5 are all variations of the main scenario. Scenario 2 additionally considers tidal energy as an investment option. Although previously claimed not sufficiently developed, the technology is considered very interesting in the Faroe Islands, which because of the predictability could provide a type of base load generation. In scenario 3 the model is allowed to burn biofuel (BF) at the thermal plant in R5. In scenario 4 the constraint on the CO_2 emissions has been removed, and thus the feasibility of investing in renewable energy is shown. Scenario 5 includes a PS system in R7, which is a highly discussed topic in the Faroe Islands.

A sensitivity analysis of the results has been conducted. This sensitivity analysis is made by increasing and decreasing the investment costs of WP, PV, the PS system in R1, BS, transmission cables and fuel costs by 20% one at a time.

C. MODELLING GENERATION AND STORAGE TECHNOLOGIES

The location of the existing and committed generation capacities, which are considered in this study, are given in Table 3. The modelling of these and the investment options are described in the following subsections. All resource data, i.e. wind speeds, solar irradiation and precipitation, is from 2017 which showed to be the year with the median resources available in the years from 2014 to 2018.

1) THERMAL POWER

The inputs required to model existing thermal power generators are capacity, lifetime (LT), fuel type and efficiency. The efficiency of the FO engines is set to 42%, the GO engines have an efficiency of 45%, while the efficiency of the BG plant is set to 35% [8]. The emissions and energy content depend on the fuel type. No new investments in thermal power are allowed, however one of the thermal plants in R5 is modelled as a combined technology in one of the scenarios, meaning that it is possible to burn BF at this plant, which originally uses FO. The model is not allowed to decommission the thermal power plants, as they will be kept as emergency backup due to the possibility of a lack of renewable resource potential, e.g. a summer with less than average sun hours, wind speeds and precipitation. The fixed O&M costs of these units therefore have to be included in the optimisation.

2) HYDRO POWER

HP with reservoirs is modelled using the turbine and reservoir capacities, the inflow to the reservoirs, the full load hours (FLH) and specification of how much of the reservoir can be regulated. The reservoir capacity used in this study is set lower than the actual reservoir capacity, in order to account for total losses associated with the power plants. The losses are assumed to be 15% [43]. Overflow is rare (a couple of times annually), and thus it is assumed that the weekly inflow can be estimated using logged production data and the water level in the reservoir. The FLHs for each turbine are

available from production data. These vary between 1154 and 5295 and depend on the local precipitation and the reservoir sizes. The water level of the reservoirs can not go below 50% of the current storage capacity. The model is not allowed to invest in new hydro capacity, as there is a political and public resistance towards HP.

3) PUMPED STORAGE SYSTEMS

Two of the locations with one or more HP plants are considered suitable for PS systems. PS systems are modelled as long-term storages which can be used to balance the system throughout the year. The first one, located in R1, will utilise two of the existing cascading HP plants. In this PS system, all components are optimised, i.e. pumps, turbines and reservoir sizes. The reservoirs are however limited the highest capacity proposed in a previous study [9]. 100% of the new invested storage capacity can be used to balance the system. The other investment option in a PS system is in R7. This system is however not optimised. The turbine and pumping capacities are fixed to 4 and 6 MW respectively, and the system is assumed to be commissioned in 2023. Due to the system not being optimised, it is only considered in one of the simulation scenarios.

4) WIND POWER

There are two methods to model WP in Balmorel. The first method is to use production data, i.e. FLH and an hourly generation profile, or wind speeds and a power curve (7) can be used. The second method requires information about the height of the wind turbines and measured/modelled wind speeds, and finally the shear factor per wind site.

$$P = \frac{\gamma}{1 + \exp(-g \cdot K \cdot (u - M - \epsilon)} \quad (7)$$

The symbols in the power curve (7) are P: power output (p.u.), $\gamma = 1.01$ p.u. is the maximum power output, $g = 0.58$ p.u./ms^{-1} is the maximum slope of the logistic curve, $K = 0.76$ is a wind farm smoothening parameter, u is the hourly wind speed (m/s), $M = 9.86$ m/s is the speed at which g is reached and finally $\epsilon = 0.89$ m/s is an offset in the wind speed. The power curve of Enercon's E44 wind turbine was curve fitted to find γ, g and M. K and ϵ were found by optimising the correlation between actual production data and calculations using wind speeds and the equation given. WP is also modelled with storm control, meaning that it is assumed that wind turbines are producing rated power up to 28 m/s, and then decrease linearly to 0 MW at 34 m/s.

Existing wind farms where no wind speed measurements are available have been modelled using FLH and generation profiles from logged production data, while all the other wind sites are modelled using measured wind speeds or modelled wind speeds [1]. The model is allowed to invest in WP in 8 different locations as shown in Fig. 3. Each site has been chosen based on a previous study [44] and internal estimations at SEV. A maximum capacity is defined for every location.

TABLE 4. O&M Costs of existing and comitted power plants.

	FO	GO	BG	HP	WP
Fix. O&M (EUR/kW)	50	151	50	50	37
Var. O&M (EUR/MWh)	8	8	8	0	3

5) PHOTOVOLTAIC POWER

The hourly solar irradiation in each region has been extracted from the Faroese WRF model [1], and validated against the only long-term measurements available. The performance ratio of PV systems in the Faore Islands has been calculated based on three pilot projects, and is found to be 81%. The expected FLH and generation profiles, which are the inputs necessary to model PV power in Balmorel, can be obtained by multiplying irradiance with the performance ratio [45]. The FLH in the regions based on the calculations computed vary between 584 and 620. PV power is not as site specific as e.g. WP. This technology is therefore assumed to be installed all over the region, and no maximum capacity has been defined.

6) TIDAL POWER

Similary to PV power, the necessary inputs to model TP are a generation profile and the FLH. A model of the tidal streams around the Faroe Islands has been developed by Simonsen and Niclasen [46]. Using these tidal streams and a power curve supplied by Minesto, the generation profiles and FLH hours can be calculated. The FLH vary between 3793 and 4656. A limit has been set on the maximum installed capacity in each location based on space requirements and that no more than 15% of the power can be extracted [47]. In total, it is possible to install 115 MW in the chosen three locations shown on Fig. 3, assuming each installation is 100 kW.

7) BATTERY STORAGE SYSTEMS

The battery systems (BS) in this study are modelled as short-term storage, i.e. the energy can be stored for a week. The C rating is 0.25C, meaning that the batteries have a discharge time of 4 hours. The round trip efficiency of a BS is set to 80%. As shown on Fig. 3 the model can invest in BS in every region except for R3.
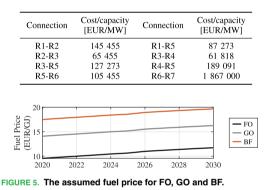
8) COSTS

Table 4 contains the costs of existing power plants. The costs for FO, GO, HP and WP are based on experience at SEV [8], while the cost of BG and BF are set to be equal to FO.

The capital costs of WP are based on the costs of the committed wind farm in R2 with a learning rate and LT based on [8], [48]. The capital costs of WP in R4 are assumed to be 70% higher than the other wind farms, due to difficult accessibility [49]. Investing in PV in the Faroe Islands has proven to be relatively expensive. The capital costs in this study are based on the existing 250 kW PV plant with a learning rate, O&M costs and LT based on [8], [48]. All costs for tidal energy are based on input from the manufacturer of the committed tidal generators in R1. The costs

TABLE 5. Costs Associated with the different investment options. The components of the PS system are: Pump (P), Turbine (T), Reservoir (R), Upper (U) and Lower (L). *EUR/kWh.

Tech.	Years	Capital (EUR/kW)	Fix. O&M (EUR/kW)	Var. O&M (EUR/MWh)	LT
WP	'20-'24	1045	26	7	20
	'25-'29	1004	26	7	20
	'30	963	26	6	25
PV	'20-'24	1400	8	0	25
	'25-'29	1210	7	0	25
	'30	1110	7	0	30
TP	'20-'24	2063	28	26	20
	'25-'30	1192	18	11	20
PS - P	'20-'30	220	50	0	60
PS - U.T.	'20-'30	266	50	0	60
PS - L.T.	'20-'30	591	50	0	60
PS - U.R.	'20-'30	14*	0	0	60
PS - L.R.	'20-'30	5*	0	0	60
BS	'20-'30	296*	2	0	15

TABLE 6. Estimated investment costs of transmission cables.

Connection	Cost/capacity [EUR/MW]	Connection	Cost/capacity [EUR/MW]
R1-R2	145 455	R1-R5	87 273
R2-R3	65 455	R3-R4	61 818
R3-R5	127 273	R4-R5	189 091
R5-R6	105 455	R6-R7	1 867 000

FIGURE 5. The assumed fuel price for FO, GO and BF.

of pumped storage systems are based on previous studies [8], [9]. The battery capital costs for a 0.25C battery are based on input from Tesla, which refers to Bloomberg New Energy Finance, and using a LT from the Danish Technology Catalogue [48]. The mentioned costs can be found in Table 5. The cost of onshore transmission cables has been estimated internally to 160 EUR/m, and the capacity of the cables used is 44 MW which leads to costs between 61.818 EUR/MW and 145.455 EUR/MW depending on the connection. The potential subsea cable between R6 and R7 is estimated to 1.867.000 EUR/MW. Cable costs are found in Table 6.

The fuel prices for FO and GO are based on Danish prices [50] with add-on costs for transport and taxes [8]. BF costs are assumptions due to lack of better data. Fig. 5 contains the fuel prices.

III. RESULTS AND DISCUSSION

The following sections will present the results of the economic optimisation described in the previous chapter. First the results of the scenarios (Table 2) are presented with focus on the main scenario. There are significant differences
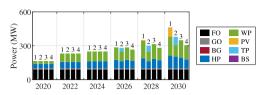
FIGURE 6. Optimal generation capacities (MW) every other year from 2020 to 2030 in four scenarios. The scenario number is shown above the bars.

TABLE 7. The optimal generation capacities in 2030.

	FO	GO	BG	HP	WP	PV	TP	BS	Total
1	91	8	2	112	168	79	-	2	462
2	91	8	2	103	102	-	72	1	379
3	91	8	2	94	153	-	-	1	349
4	91	8	2	79	125	-	-	-	305

between the scenarios, except from scenario 5, which is close to identical to the main scenario and thus, not included in the figures and tables. The results from the sensitivity analysis are also presented, followed by the proposed RoadMap based on the optimal results. The execution time of running all scenarios simultaneously through the Balmorel algorithm was 2 hours and 5 minutes using a Hewlett Packard Enterprise x64 equipped with Intel Xeon CPU E5-2667 v4 @ 3.20GHz 3.20GHz (2 processors) and 192 GB RAM.

A. GENERATION CAPACITIES

The economically optimal generation capacities every other year from 2020 to 2030, based on four of the scenarios (Table 2) are shown in Fig. 6, and the final capacities are tabulated in Tabel 7. As previous studies have suggested, the optimal solution in the main scenario includes significant amounts of WP complemented with PV and PS. The generation capacity of the PS system is included in HP. A small battery capacity is also a part of the optimal solution. This BS is placed in R7, and is used to balance this remote region. It is expected that a significantly higher BS capacity is needed for grid stability, but this will be addressed in another publication. Although they are initially similar, the scenarios give rise to significant differences in power composition by 2030. If TP will reflect the assumptions, it could reduce the total generation capacity by 84 MW. PV is no longer a part of the optimal solution, there is a significant decrease of WP, while HP and the BS capacities are also slightly decreased. This shows that the feasibility of TP could have a significant impact on the future energy mixture. The 3rd scenario, where it is possible to burn BF at a FO plant, shows that burning BF with the assumed fuel costs is a better solution financially than installing PV plants. There is also a significant decrease in WP compared to scenario 1. The total capacity is also reduced by 113 MW. The large reduction is due to BF being a dispatchable technology. Finally, the unrestricted CO_2 scenario shows that investing in WP and PS systems
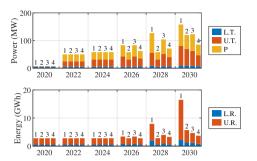
238

FIGURE 7. Optimal capacities of the lower turbine (L.T.), upper turbine (U.T.), pumping capacity (P), lower reservoir (L.R.) and upper reservoir (U.R.) in the PS system in R1 every other year from 2020 to 2030.

TABLE 8. The optimal transmission capacities (MW) between the regions were reinforcements and new connections are required.

Year	'21	'22	'23	'24	'25	'26	'27	'28	'29	'30
R1-R5	35	35	35	35	35	35	35	35	35	38
R5-R6	10	12	46	46	46	46	51	63	63	63
R6-R7	2	2	3	4	4	6	6	7	8	13

is more profitable than thermal generation up to a certain point. From 2026 and forward the capacities in scenario 4 start to differ from scenario 1. This shows that the final renewable percentages do not earn back the investment, given the assumed development in oil prices. What this scenario also shows is that PV power is not economically feasible in the Faroe Islands under the given assumptions. The fact that PV complements WP and HP seasonally is however important in order to reach 100% renewables, as the alternative is increased storages, which are expensive. Based on these results, the best strategy is to aim for 100% (main scenario) while being open to significant adaptations in the later half of the RoadMap time span, especially with regards to the development of TP and the cost of BF.

B. PUMPED STORAGE SYSTEM

Storage is vital in order to reach 100% renewables. The optimal pumping, generation and storage capacities of the proposed pumped storage system in R1 are shown in Fig. 7. These results show that it is feasible to invest in both pumping and more generation capacity in 2022, but that there is no need to increase the storage capacity until 2026. A 100% renewable production, where neither TP nor BF are an option, does require a significant increase in reservoir capacity. Investing in storage capacity is part of the optimal solution in all scenarios, but the variations are large, especially between the main scenario and other scenarios. These results, similarly to the previously presented results, show the importance of ongoing evaluations of expansion plans, as the feasibility of technologies can change over time and this can have a major impact on the optimal expansions. The demand increase should also be monitored, as the large investments in scenario 1 do not occur until 2028 and these increases might not be necessary if the demand does not increase as assumed. Increasing the storages to the level of scenario 1 in 2030 would require significant increase in dam sizes above populated areas, which could lead to public resistance due to the environmental impact, but these investments are

necessary in order to reach 100% renewables with the presented assumptions and currently available technologies.

C. TRANSMISSION CAPACITIES

New transmission cables and reinforcements are required in order to transmit the power from production to consumption. A new connection is needed between R6 and R7, while reinforcements are required between R1-R5 and R5-R6. Table 8 shows the investments required based on the main scenario. This shows that the committed R5-R6 connection of 44 MW will not meet the future requirements. R1-R5 connection needs to be reinforced in 2030, and that is likely due to the PS system being located in R1, while the majority of the consumption is in R5. The R6-R7 capacity increases slowly from 2021 and forward, but in 2030 the capacity increases from 8 MW to 13 MW, in order to reach 100% renewables in R7. All scenarios showed similar results in terms of transmission capacity.

D. PRODUCTION

The main focus of this study is expansion planning, but Balmorel also optimises the hourly production. Fig. 8 shows the optimal annual production in the four presented scenarios, which are almost identical until 2026. In scenario 1, 3 and 4 WP is dominating the production, while in scenario 2 TP is a large part of the generation. This is caused by the restriction that TP can not be curtailed while WP can; thus, the curtailment of WP in scenario 2 is high. BF produces a small part of the energy in scenario 3, which means that the energy composition is not changed significantly even though the power composition is, and this is due to the technology being dispatchable. It is noteworthy how tidal takes on a role similar to base production and how BF seems like an obvious candidate for backup power in less energetic years. The production in scenario 4 is up to 87% renewable in certain years, but in 2030, when the demand has increased more, the financially optimal renewables shares have decreased to 86%. There are small variations between the total production of the scenarios. This is due to the transmission losses which differ, depending on the location and capacity of the different generation and storage units. It should be noted that HP shows the netto production, i.e. pumping, has been subtracted and therefore the shares of hydro power are low.

E. ECONOMICS

The annual optimised capital costs, O&M costs and fuel costs for every other year are shown in Fig. 9 together with the
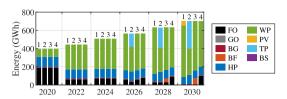
239

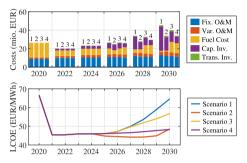**FIGURE 8.** Production in the four scenarios every other year from 2020 to 2030.

FIGURE 9. Annualised costs of the optimal solutions every other year from 2020 to 2030 in the four scenarios.

TABLE 9. Generation capacities [MW] in 2030 in the main scenario and all the sensitivity analysis scenarios. c - 20% Cheaper, e - 20% more expensive, FU - Fuel, CA - Cable.

	1	cBS	cCA	cFU	cPV	cPS	cWP	eBS	eCA	eFU	ePV	ePS	eWP
HP	112	112	112	112	112	112	112	112	112	112	112	111	113
WP	168	168	168	168	149	173	184	168	168	168	189	169	157
PV	79	80	79	79	149	31	53	79	79	79	20	119	101
BS	2	3	2	2	3	2	2	2	2	3	2	3	2

FIGURE 10. The proposed RoadMap towards 2030, which has been made based on the optimisation results from Balmorel. All the values are given in MW, except for the reservoirs (GWh) and BS (MWh) in row 5 from the bottom.

levelised cost of energy (LCOE), i.e. annual costs from the optimisation (upper plot) divided by annual energy production (Fig. 8). The figure does not include the annual capital costs of committed or existing capacity. This figure shows that out of all the scenarios, the most expensive scenario is the main scenario where a 100% renewable production is required and it is not possible to invest in TP, nor is it possible to burn BF at existing FO plants. The difference between scenarios 1/2 and 3/4 are the increased capital costs and decreased fuel costs. This shows that even with higher fuel costs for biofuel, it would still be more feasible than the main scenario. Scenario 2 is shown to be cheaper than scenario 4 until 2030, when it is slightly more expensive. However, the sum of the annual costs from 2020 to 2030 in the four scenarios are 311, 278, 301 and 285 mio. EUR respectively. This means that over the range of 10 years, a 100% sustainable power system with the assumed costs of TP is more feasible than a power system without restrictions on the CO_2 emissions, where it is not possible to invest in TP. The LCOE decreases from 2020 to 2021, and this is due to the increased renewable production, i.e. decreased fuel costs. Although the LCOE of the main scenario is significantly higher than the other scenarios, it is still lower in 2030 with a 100% renewable power system than in 2020.

F. SENSITIVITY ANALYSIS OF GENERATION CAPACITIES

The sensitivity analysis did not show any significant differences in the generation capacities. The generation capacities of hydro, wind, PV and battery in 2030 for every sensitivity scenario and the main scenario are shown in Table 9. The

capacites of batteries and the pumped storage system are close to constant for all the scenarios. The wind power capacity is also quite constant but varies between 149 MW and 189 MW, so although wind is by far the cheapest renewable source, by 2030 it has obtained close to a saturation level where added production is out of sync with local consumption. This finding is interesting as it to some degree opposes recent political dogma. It states, that introducing a free local electrical market will not only generate new business opportunities, due to lower energy prices, but also help solve the nations transition to a 100% renewable electrical grid. If there is a clear saturation limit for the only existing economically viable renewable energy source (WP), any additional investments will not help the transition to a purely renewable electrical grid. The solar capacity is the only capacity that deviates significantly. The differences are especially visible if the PV or PS costs are decreased or increased, reflecting that the main challenge is power supply in the summer months with reduced wind power.

G. ROADMAP

Fig. 10 shows the proposed RoadMap, which is based on the main scenario. The RoadMap includes committed WP and cables (red border). The locations of the optimised investments are tabulated in Table 10. The location number indicates the region. In the case where multiple WP investment sites are in one region, the region number is followed by the site number, which has been numerated from the top and down (Fig. 3).

Most of the investments are conducted as 2030 comes closer. This is when the CO_2 restrictions will be hardened, and more investments will be needed in order to meet the

240

TABLE 10. The location of the optimised investments presented in Fig. 10. *MWh **GWh.

Year	Tech.	Power (MW)	Location
2023	WP	6	7
2024	WP	18	6.2
2026	WP	18	6.2
	CA	13	6-7
	PS - U.T./P	35/41	1
2027	WP	18	1
	CA	44	5-6
	BS	10*	
2028	WP	30	6.1
	PV	7	7
2029	PS - U.T./P	35/38	1
	PS - L.T.	4	1
	PS - U.R./L.R.	12/2**	1
	PV	22/8	4/7
2030	WP	18	5.2
	CA	44	1-5
	PV	39/3/1	4/6/7

requirements. All investments in onshore cables have been set to 44 MW, even though the needed capacity in some cases is significantly lower, but the onshore cables used in the Faroe Islands can transmit 44 MW. Comparing the proposed RoadMap to the previous simpler one [4], we see that the overall results are quite similar, even though several factors have been modified. The underlying reasons seem to be that the cheapest energy source (WP) reaches a saturation level of installed power over two times the average consumption in 2030 (75 MW), while the expensive but seasonally out of sync energy source (PV), must be able cover the average load on calm summer-days. There are some differences related to the pumped-storage configuration, but these seem to be driven by a trade-off between small storage with rapid response vs. larger storage with relative slower response. One important difference is also that this study aims at a renewable solution for an average year and not any year.

There is a need to validate the optimality the RoadMap, by rerunning Balmorel using the RoadMap as committed capacities. Fig. 10 includes the renewable shares of the production based on the RoadMap. According to simulation results it is possible to reach above 80% renewables already in 2021. Using the proposed RoadMap, it should be possible to reach 100% renewables by 2030. The second validation parameter was the cost of the system. The sum of the annual capital costs, fuel costs and fixed and variable O&M costs from 2020 to 2030 in the main scenario are 305 mio. EUR, while the RoadMap is 4% more expensive at 316 mio. EUR. The difference is caused by a higher fuel consumption, due to the investments in the RoadMap occuring slightly later than the optimal results. Based on the presented results, the proposed RoadMap is considered valid and applicable.

IV. CONCLUSION
This study has analysed the energy balance of the future Faroese power system using Balmorel. The study shows that the feasiblility of technologies has to be carefully considered,

as development of e.g. TP and BF can impact the RoadMap significantly. Therefore constant revising and partial investments along the way could be the best approach when aiming for 100% renewables. This has been shown through different scenarios. The study has also shown that the presented results are not very sensitive to variations in the investment and fuel costs. A RoadMap towards reaching the goal of 100% renewable production in 2030 has been generated, based on a method developed for the purpose of achieving a realistic RoadMap from an economical optimisation. A method which is applicable to other, especially small and isolated, power systems. This RoadMap shows the exact location and capacity of added generation, storage, and transmission. The locations of new generation and storage plants have been carefully considered and constraints like available space and local renewable resources have been considered. These assure the realisability of the proposed investments. It is assured that the needed transmission system is capable of transmitting the power between the regions. Overall it can be said that investing in renewables is financially the best option up to 86%-87% renewable production shares depending on year, demand and power composition. The WP capacity should be 224% of the average demand, while PV should be 105% and a storage capacity of 8-9 days is needed in the pumped storage system. The development of the realistic RoadMap and the unveiling of the impact tidal energy has on the energy mix and the economics are the key findings in this study.

FUTURE WORKS
Balmorel has perfect foresight throughout a year, but no across years. This means that Balmorel knows which resource is available every hour throughout the year and can optimise the dispatch to a degree which is not possible in reality. The optimisation is unfamiliar with cost reductions or increases across the years, which means that the model can e.g. do a large investment in wind power in 2024, without knowing that the cost reduced significantly in 2025. In order to address this in Balmorel the algorithm has to be enhanced. Otherwise the power system must be analysed using other tools with different approaches, but with the same inputs, so that it is possible to see the influence this has on the expansion plan.

The presented RoadMap will be used in the expansion planning of the Faroese power system towards 100% renewables, and thus long term follow up studies will be conducted and the RoadMap will be reevaluated in case new technologies beccoming feasible. Following this RoadMap, analyses of the dynamic behavoir of the power system in order to ensure a stable and reliable power supply are necessary. The following studies will focus on the system frequency- and voltage stability, and will be presented in other publications.

241

University (Denmark) and the Department of Science and Technology at the University of the Faroe Islands.

The authors would like to thank Mikael Togeby and Nina Dupont at Ea Energianalyse A/S, Copenhagen, Denmark, for cooperation, training and assistance in Balmorel.

REFERENCES

[1] A. S. Haslerud, "Faroe islands, detailed wind maps," Kjeller Vindteknikk, Lillestrøm, Norway, Tech. Rep. KVT/ASH/2019/R032, 2019.

[2] J. Cappelen and E. V. Laursen, "The climate of the Faroe Islands: With climatological standard normals, 1961-90," Danish Meteorol. Inst., Copenhagen, Denmark, Tech. Rep. 98-14, 1998.

[3] T. Nielsen, "Technical and Economic assessment of a 100% renewable electricity sector in the Faroe Islands in 2030, from the power company perspective," MBA thesis, Dept. Bus. Admin. Social Sci., Beuth Univ., Berlin, Germany, 2016.

[4] *Orkugoymslur í føroyum—Yvirskipað frágreiðing*, Umhvørvisstovan, Power Company SEV, Dansk Energi, Argir, Faroe Islands, 2018.

[5] K. Andersen, "Høring vedrørende fremtidsscenarier for energisystemet på Færøerne," Dansk Energi, Frederiksberg, Denmark, Tech. Rep. d2016-8677-21.0, 2016.

[6] H. Hansen, "Scenarie notat," Dansk Energi, Frederiksberg, Denmark, Tech. Rep. d2016-15912-1.0, 2016.

[7] P. J. Douglass, "Fleksibelt elforbrug på Færøerne," Dansk Energi, Frederiksberg, Denmark, Tech. Rep. d2017-7274-6.0, 2017.

[8] Ea Energy Analyses, "Balancing a 100% renewable electricity system—Least cost path for the Faroe Islands," Ea Energy Analyses, Copenhagen, Denmark, Tech. Rep., 2018.

[9] F. Ludescher-Huber, "100% fornybar kraft, Pumpekraft, vind og sol," Norconsult AS, Sandvika, Norway, Tech. Rep. 5172432, 2018.

[10] H. Hansen, "Teknisk notat Sammenfatning af scenarier for energilagring på Færøerne," Dansk Energi, Frederiksberg, Denmark, Tech. Rep. d2017-155-3.0, 2017.

[11] The Power Company SEV, "Notat om alternative produktionsformer," Power Company SEV, Tórshavn, Faroe Islands, Tech. Rep., 2018.

[12] *Gennemgang af Energilagerteknologier*, ORKA, Umhvørvisstovan, Argir, Faroe Islands, 2018.

[13] *Kabelforbindelse mellem Færøerne og nabonationer i Nordatlanten—Gennemgang af tidligere arbejde*, ORKA, Umhvørvisstovan, Argir, Faroe Islands, 2018.

[14] H. Hansen, "Teknisk notat—Stabilitet og udbygning af elnettet," Dansk Energi, Frederiksberg, Denmark, Tech. Rep. d2017-9194-0.31, 2017.

[15] H. Hansen, T. Nielsen, B. Thomsen, and K. Andersen, "Energilagring på Færøerne—Teknisk opsamlingsrapport," Dansk Energi, Frederiksberg, Denmark, Tech. Rep., 2018.

[16] *Indledende vurderinger af muligheden for at lægge elkabel fra Island til Færøerne*, Jarðfeingi, Tórshavn, Faroe Islands, 2007.

[17] P. E. Egholm, F. Jakobsen, B. Bendtsen, K. Mortensen, B. Thomsen, A. Johannesen, J. S. Christensen, and K. Andersen, "Action plan—Report and Recommendations on the future electric energy system of the Faroe Islands," Faroese Ministry Trade Ind., Tórshavn, Faroe Islands, Tech. Rep., 2015.

[18] A. M. Skeibrok, M. Eriksen, and J. Stav, "Optimized hybrid microgrid system integrated with renewable energy sources," B.Sc. thesis, Dept. Eng., Univ. Agder, Kristiansand, Norway, 2019.

[19] H. M. Tróndheim, T. Nielsen, B. A. Niclasen, C. L. Bak, and F. F. Da Silva, "The least-cost path to a 100 % renewable electricity sector in the Faroe Islands," in *Proc. 4th Int. Hybrid Power Syst. Workshop*. Crete, Greece: Energynautics, 2019, pp. 1–6.

[20] H. M. Tróndheim, B. A. Niclasen, T. Nielsen, C. L. Bak, and F. F. Da Silva, "Introduction to the energy mixture in an isolated grid with 100% renewable electricity—The Faroe Islands," in *Proc. CIGRE Symp. Aalborg*. Paris, France: CIGRE, 2019, pp. 1–12.

[21] D. A. Katsaprakakis, B. Thomsen, I. Dakanali, and K. Tzirakis, "Faroe islands: Towards 100% R.E.S. penetration," *Renew. Energy*, vol. 135, pp. 473–484, May 2019.

[22] J. Burakovskij, C. N. Jacobsen, R. S. Sagoo, and C. Wennerberg, "Fælles nordisk studie om pumped storage," Grontmij, Stockholm, Sweden, Tech. Rep., 2012.

[23] F. Ludescher-Huber, "Wind power based pumped storage," Norconsult AS, Sandvika, Norway, Tech. Rep., 2013.

[24] D. Buiskikh, B. Zakeri, S. Syri, and P. Kauranen, "Economic feasibility of flow batteries in grid-scale applications," in *Proc. 15th Int. Conf. Eur. Energy Market (EEM)*, Jun. 2018, pp. 1–5.

[25] P. Enevoldsen and B. K. Sovacool, "Integrating power systems for remote island energy supply: Lessons from mykines, Faroe Islands," *Renew. Energy*, vol. 85, pp. 642–648, Jan. 2016.

[26] S. Jebaraj and S. Iniyan, "A review of energy models," *Renew. Sustain. Energy Rev.*, vol. 10, no. 4, pp. 281–311, Aug. 2006.

[27] D. Connolly, H. Lund, B. V. Mathiesen, and M. Leahy, "A review of computer tools for analysing the integration of renewable energy into various energy systems," *Appl. Energy*, vol. 87, no. 4, pp. 1059–1082, Apr. 2010.

[28] S. Pfenninger, A. Hawkes, and J. Keirstead, "Energy systems modeling for twenty-first century energy challenges," *Renew. Sustain. Energy Rev.*, vol. 33, pp. 74–86, May 2014.

[29] H.-K. Ringkjøb, P. M. Haugan, and I. M. Solbrekke, "A review of modelling tools for energy and electricity systems with large shares of variable renewables," *Renew. Sustain. Energy Rev.*, vol. 96, pp. 440–459, Nov. 2018.

[30] A. S. Dagoumas and N. E. Koltsaklis, "Review of models for integrating renewable energy in the generation expansion planning," *Appl. Energy*, vol. 242, pp. 1573–1587, May 2019.

[31] N. E. Koltsaklis and A. S. Dagoumas, "State-of-the-art generation expansion planning: A review," *Appl. Energy*, vol. 230, pp. 563–589, Nov. 2018.

[32] F. Wiese *et al.*, "Balmorel open source energy system model," *Energy Strategy Rev.*, vol. 20, pp. 26–34, Apr. 2018.

[33] C. Vrionis, V. Tsalavoutis, and A. Tolis, "A generation expansion planning model for integrating high shares of renewable energy: A meta-model assisted evolutionary algorithm approach," *Appl. Energy*, vol. 259, Feb. 2020, Art. no. 114085.

[34] J. G. Gomes, J. M. Pinto, H. Xu, C. Zhao, and H. Hashim, "Modeling and planning of the electricity energy system with a high share of renewable supply for Portugal," *Energy*, vol. 211, Nov. 2020, Art. no. 118713.

[35] N. E. Koltsaklis and M. C. Georgiadis, "A multi-period, multi-regional generation expansion planning model incorporating unit commitment constraints," *Appl. Energy*, vol. 158, pp. 310–331, Nov. 2015.

[36] "Plano energético renovável cabo verde," Gesto Energia S.A., Algés, Portugal, Tech. Rep., 2011.

[37] H. C. Gils and S. Simon, "Carbon neutral archipelago–100% renewable energy supply for the Canary Islands," *Appl. Energy*, vol. 188, pp. 342–355, Feb. 2017.

[38] P. V. Ferreira, A. Lopes, G. G. Dranka, and J. Cunha, "Planning for a 100% renewable energy system for the Santiago Island, Cape Verde," *Int. J. Sustain. Energy Planning Manage.*, vol. 29, pp. 25–40, Sep. 2020.

[39] Ea Energy Analyses, "Balmorel—User guide," Ea Energy Analyses, Copenhagen, Denmark, Tech. Rep., 2018.

[40] *60 kV netið í framtíðini, Uppskot*, Power Company SEV, Vestmanna, Faroe Islands, 2018.

[41] P/f Fjarhitafelagið. (2018). *Miðal nýtsla í kWh býtt út á økir.* Accessed: May 25, 2020. [Online]. Available: https://www.fjarhiti.fo/apptil-e-veiting-prísir-oa/miðal-nýtsla-í-kwh-býtt-út-á-oekir/

[42] T. D. H. Balle, "A study of weather effects on heat consumption in buildings using heat pumps in the Faroe Islands," B.Sc. thesis, Dept. Sci. Technol., Univ. Faroe Islands, Tórshavn, Faroe Islands, 2016.

[43] M. T. Gatte and R. A. Kadhim, "Hydro power," in *Energy Conservation*, vol. 1. Rijeka, Croatia: InTech, Oct. 2012, p. 13.

[44] J. P. Magnussen, "Vindmyllustaðseting—Val av økjum til vindmyllulundir í Føroyum og dømi um staðsetingar," Orkudeildin á Umhvørvisstovuni, Argir, Faroe Islands, Tech. Rep., 2017.

[45] H. G. Beyer and I. P. Custodio, "The possible role of PV in the future power supply of the Faroe Islands," in *Proc. 35th EU PVSEC*, Brussels, Belgium, no. 9, 2018, pp. 1–15.

[46] K. Simonsen and B. A. Niclasen, "Analysis of the energy potential of tidal streams on the Faroe Shelf," *Renew. Energy*, vol. 163, pp. 836–844, 2021.

[47] G. Hagerman and B. Polagye, "Methodology for estimating tidal current energy resources and power production by tidal in-stream energy conversion (TISEC) devices," Electr. Power Res. Inst., Washington, DC, USA, Tech. Rep. EPRI-TP-001 NA Rev 2, 2006.

[48] *Technology Data—Generation of Electricity and District Heating*, Energistyrelsen, Copenhagen, Denmark, 2019.

[49] J. P. Magnussen, "Wind power project in the northern Faroe Islands," B.Sc. thesis, Dept. Sci. Technol., Univ. Faroe Islands, Tórshavn, Faroe Islands, 2016.

[50] *Fremskrivning af brændselspriser og CO2-kvotepris*, Energistyrelsen, Copenhagen, Denmark, 2019.

242

HELMA MARIA TRÓNDHEIM received the B.Sc. degree in energy and environmental engineering from the University of the Faroe Islands in 2016 and the M.Sc. degree in energy technology with a specialization in electrical power systems and high-voltage engineering from Aalborg University, Denmark, in 2018. She is currently pursuing the industrial dual Ph.D. degree with SEV (Power Company), Faroe Islands, Aalborg University, and the University of the Faroe Islands. Her research project is titled "Ensuring Grid Stability and Supply Reliability in a 100% Renewable Electricity Sector in the Faroe Islands."

BÁRðUR A. NICLASEN received the M.Sc. degree in geophysics from the University of Copenhagen, Denmark, in 2003, and the Ph.D. degree in oceanography from the University of the Faroe Islands in 2007. He is currently an Associate Professor in physics with the Faculty of Science and Technology, University of the Faroe Islands. His research interests are data analyses of oceanographic, meteorological and power data, numerical modeling of waves, currents and physical systems, and applied science relevant for local industries.

TERJI NIELSEN received the B.Sc. degree (Hons.) in electrical engineering from the Engineering College, Aarhus University, Denmark, in 1999, and the M.B.A. degree from the Beuth University of Applied Sciences, Germany, in 2016. He is currently the Head of the Research and Development Department, SEV (Faroese Power Company), where he has more than 20 years of experience from various positions. His main focus is on the company's vision of a 100% renewable electricity sector by 2030 in the Faroe Islands. His research interests are integration of renewable energy in islanded hybrid power systems, resource assessments, and techno-economic analysis of realistic RoadMaps in hybrid power systems.

FILIPE FARIA DA SILVA (Senior Member, IEEE) received the M.Sc. degree in electrical and computers engineering from the Instituto Superior Tecnico, Portugal, in 2008, and the Ph.D. degree in electric power systems from Aalborg University, Denmark, in 2011. He was with EDP-Labelec in 2008 and the Danish TSO Energinet from 2008 to 2011. He is currently an Associate Professor with the Department of Energy Technology, Aalborg University, where he is also Semester Coordinator for the Electrical Power System and High Voltage Engineering master program and the Vice-Leader of the Modern Power Transmission Systems research program. His research focuses on power cables, electromagnetic transients, system modeling, network stability, HVdc transmission, and HV phenomena. He is an active member of CIGRE, currently being the Head of Denmark's IEEE-PES, the Danish Representative for CIGRE SC C4 System Technical Performance, and the Convener of CIGRE WG C4.46.

CLAUS LETH BAK (Senior Member, IEEE) received the M.Sc. degree in electrical power engineering and the Ph.D. degree with the thesis EHV/HV underground cables in the transmission system from Aalborg University, Denmark, in 1994 and 2015, respectively. He is currently a Professor with the Department of Energy Technology, Aalborg University. His main research areas include corona phenomena on overhead lines, power system modeling and transient simulations, underground cable transmission, power system harmonics, power system protection, and HVdc-VSC offshore transmission networks. He is a member of CIGRE JWG C4-B4.38, CIGRE SC C4, and SC B5 study committees and the Chairman of the Danish CIGRE National Committee. He is also the Head of the Energy Technology Ph.D. Program and the Section of Electric Power Systems and High Voltage, Aalborg University. He is a member of the Ph.D. Board with the Faculty of Engineering and Science.

• • •

Alternative and Combined Procedure for Parameter Identification and Validation of Governor and Automatic Voltage Regulator Dynamic Models

Helma Maria Tróndheim[1,2,3], Filipe Faria da Silva[2], Claus Leth Bak[2], Terji Nielsen[1], Bárður A. Niclasen[3], Rasmus Skov Nielsen[4] and Nicolas Weikop[4]

The Power Company SEV[1], Aalborg University[2], The University of the Faroe Islands[3] and AFRY Copenhagen[4]

Abstract: The Faroe Islands are aiming for a 100% renewable electricity generation. The complexity of operational power systems with a high level of renewable generation necessitates accurate dynamic models. Many power systems, including the Faroe Islands, do however contain generation units with old governors and automatic voltage regulators, in which suitable models and parameters are unknown. Obtaining dynamic models with parameters that replicated measurements proved to be challenging using existing procedures. Therefore, this paper presents an alternative and combined procedure for identifying and validating the controllers and parameters. The procedure utilizes measurement data from trip tests, standard controller models, an optimization algorithm, and combines hybrid simulations and system wide simulations. A successful application of the proposed procedure on the power system of the Faroe Islands is presented. The proposed approach can be applied to other power systems and is especially suitable for other island power systems of similar size to the Faroese power system.

1. Introduction

Climate changes due to carbon emissions is a global concern, and a big contributor to this is electrical power generation. The electricity and heat sectors have previously been estimated to be 25% of the global greenhouse gas emissions (1). Power systems worldwide are however replacing the carbon-based generation by renewables to decrease the emissions. The thermal generators are replaced by wind turbines, photovoltaic panels (solar), nuclear power plants and hydro turbines, depending on the local geography and resources available. The environmental advantages with renewable energy are quite obvious, but there are several disadvantages regarding the power system operation, e.g. the intermittent nature of wind speeds and solar irradiation. Intermittent production from a wind power plant or photovoltaic power plant is especially an issue in small power systems, as in larger systems it can be evened out by other power plants. In addition to this, the consumption in islands is small and fluctuating, which is why oil and if possible, hydro have traditionally been used to produce electricity in islands. Some countries are in a better position than others, when it comes to the renewable resources available. Isolated parts of Greenland have hydro in the summer due to melting ice, while Iceland has hydro from both rain and melting ice and of course hydrothermal energy. Norway and Danish islands have a renewable production

on average, i.e. they have a seasonal surplus of hydro power and wind power, respectively, which evens out purchasing carbon based power from other countries/islands other times of the year.

In 2014 the Faroe Islands, see Figure 1, announced its so-called green vision (100by2030), becoming 100% green in terms of electricity production by 2030. The islands are surrounded by an abundancy of renewable resources in terms of wind, hydro, tidal streams and to certain extent solar energy, but balancing the system at 100% is challenging. The Faroe Islands are, out of the mentioned countries, the most densely populated area after Denmark and followed by Norway (Denmark: 137.65/km2, Faroe Islands: 38.1/km^2, Norway: 14.0/km^2). Although the hydro resource is available, it is limited relative to the size. Also, the mild climate and moderate mountains means that hydro does not get a seasonal input from melting ice.
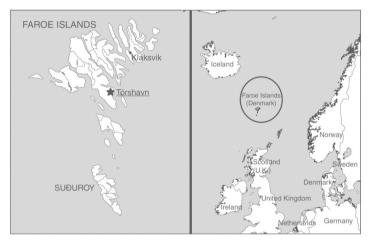
Figure 1 Map of the Faroe Islands (2)

An economically optimized and tangible RoadMap ensuring a balance between supply and demand in the years under investigation (2020-2030), considering the local resources, best available technologies, their attributable investment and O&M costs, has been made for the Faroese power system (3). This study reveals that wind power will be the main provider of energy complemented with solar energy in the summer months when the wind resources typically are low. To bridge the energy gap at times with low renewable resources available, a relatively large-scale pumped hydro system is proposed. The mentioned RoadMap study also showed that tidal energy, if delivered at predicted price, can have a disruptive influence on the future power composition, as it could reduce the pumped hydro reservoir capacity by 75% and the total generation capacity by 18%. Even though tidal energy is being tested, also in the Faroe Islands in cooperation with SEV, this technology is still in the development phase.

The increasing penetration of intermittent and inverter-based renewable energy into a relatively small, isolated power system, calls for precise and validated simulation models to ensure the frequency- and voltage stability in the power system as the inverter-based technologies steadily substitute the synchronous generators and their inherent system services. These system services are inertia, short circuit power and active/reactive power regulation. The active and reactive power regulation after a disturbance is conducted by the governors and automatic voltage regulators (AVR), which compensate for the power deficit between the generation and demand.

High accuracy power system models are essential in power system planning and operation. Analyses and validation of these models has to occur continuously (4–7). A power system model, which has not been validated with measurements, can only be used for academic exercises (6), and states that assessing power systems without computer simulations is inconceivable (5). The application of dynamic power system models is not only for analyses after large disturbances, but also relevant for voltage- and frequency stability studies, protection schemes and restoration plans. A validated power system model can minimize disruption in the operation and risks to equipment (4). However, obtaining a full system validated model can be difficult, as one sub-model (4) or even one single parameter (5), can change the simulation results significantly. Old generation units, e.g. diesel generators and hydro turbines, are commonly found in small isolated grids, like the power system in the Faroe Islands. The available information about suitable computer models and respective parameters is limited or even non-existent, which makes the task of obtaining a fully validated model even more challenging. Even with correct models this is a difficult task, as each parameter is associated with an inaccuracy.

Validation of power system models is usually conducted as either System Wide Simulations (SWS) or Hybrid Simulations (HS), see e.g. reference (8) and (9) respectively. These two methods have been compared by den Boer (10). The first method is a simulation of a full system replicating a previously recorded event. The dynamic response is compared to field measurements. In HS a sub-network is isolated, and then e.g. voltage and frequency time series are injected to this sub-network. The dynamic behaviour of the sub-network, e.g. generators' active and reactive power, is compared to measurements. A study case (10) shows that neither method showed a perfect resemblance with the measurements. HS showed a better resemblance with the measurements, but it must be considered that this is a simulation with measured frequency and voltage as inputs. This means that the measurements are partly controlling the simulation results. Validating a whole network (using SWS) instead of a sub-network (using HS), obviously gives a better indication of the accuracy of the system model, but it can lead to high computational time due to the complexity of the system model. The advantage of using HS in the validation process is the simplification to a sub-network and it is said to be crucial for validations (6), but complementary tools are needed (11), as HS is not always sufficient. This issue is also addressed in another study (12), which proposes a two-level online parameter identification, by parameterizing models using HS and then validating throughout the whole system.

Measurement data used for parameterization is usually obtained from planned tests, but studies have also suggested using actual disturbances (4,5). The advantage with staged tests, is that the unit is typically isolated from the power system for the test, which makes it easier to parameterize, while the advantage with online validation is that it does not require taking a unit out of service. It can however take a long time to obtain enough data from natural disturbances to be able to accurately parameterise models, and a staged test might not reflect some of the interactions and dynamic behaviour between the different governors and voltage regulators etc.

The parametrization of models can be done manually, by trial-and-error varying the parameters, but it can be very difficult to find the correct parameters, especially when looking at a whole system as many parameters are inter-dependent. Thus, multiple optimization algorithms have been applied to parameterize dynamic models, by minimizing the difference between measured and simulated dynamic response, see e.g. references (13–16). In the past parameterization was commonly conducted using frequency response (17,18), but this is not common in newer literature. Huang et al. (19) use a Kalman filter with event playback (of disturbance). However, the need to improve the event playback method due to limitations of phasor measurement units (PMU) has also been identified (20). This is done by using a multi model

adaptive Kalman filtering, a singular spectrum analysis and initialising the event playback after the first fast transients, which cannot be captured by the PMU. The particle swarm optimisation algorithm (PSO), is also commonly used to identified parameters, but a previous study (8) proposes a modified version of PSO to improve the results. This study also states that parameters can be identified using different events. Weaknesses have not only been identified with the algorithms used, but also with the standard models available. A study (21) claims that the standard models must be extended with frequency ramp rate, activity range and deadband to accurately represent reality. In reference (22) the diesel governors on Kinmen island (Taiwan) are parameterised and validated using a reduced order governor, as high order models are complicated, and the risk of finding a local optimum with high order optimisation is higher, than when fewer parameters are validated. The study utilised the HS method using a PSO algorithm to find suitable parameters. The generators, governors and AVRs in Cyprus have been validated based on past disturbances by Stavrinos et al. (23) using a manual approach. Information about generators and governors was available, while AVRs were modelled using standard models with default parameters. In cases where the resemblance between measured and simulation was not good enough, the parameters were adjusted. A study on the validation of a generating unit in Poland combines a genetic algorithm with a gradient algorithm (24). Reference (9) focuses validating hydro governors in three power plants in the Pacific North West in North America. Another attempt of validating a power system is found in (25), in which Bonaire Island (Caribbean Sea) is the study case. This study does not explain how the power system has been modelled, but emphasis on validating the load models as well, as the air conditioners in Bonaire are a significant contributor to the dynamic system response. These few study cases show that different approaches and algorithms are used to validate power system models, from manual adjustment to using optimisation algorithms to find suitable parameters.

Most previous studies use one event to parameterize models, which could result in finding a very specific local set of fitting parameters, i.e. the found parameters might only be valid for one particular event. Using multiple scenarios for parameterization can prevent this, if not obtaining a global parameter set, it at least fits for a wider range of events (4,7). Reference (7) used multiple events to parameterize generator parameters, and a better set of parameters was obtained compared to a parameterization using one event.

The model of the Faroese power system has been developed in DIgSILENT's PowerFactory over several years. The model has been load-flow validated, while the dynamic validation showed to be a challenging task. It started with using HS validation with manual adjustment of parameters, but the SWS simulation using these HS manually adjusted parameters did not replicate the measurements. The need to use automatization to test different combinations of parameters was identified. A script was written to test different combinations using SWS, and through a brute force algorithm, the simulation closest to the measurements could be identified. It was however difficult to find the best parameters, and even with the small system of the Faroe Islands, the computational time was an issue. The authors then utilized the system parameter identification (SPI) tool in PowerFactory, which, as the name implies, is suitable for this type of assignments.

This paper presents an alternative combined procedure for identifying and validating parameters of governors and AVR of a whole system using multiple staged tests/disturbances, in which most models and respective parameters are unavailable. The advantage with the proposed procedure is that it uses the simple HS for initial parameterization by SPI and validates the models with SWS. The parameterisation is conducted using multiple events simultaneously to prevent obtaining a local set of suitable parameters. In the case where the validation shows that the parameterization with HS is insufficient, which is an issue addressed previously, a second parameterization with SWS is conducted. Using SWS for parameterisation is

computationally heavy, which is why HS is preferred in cases where the response is acceptable. This procedure is ideal for islanded power systems of similar sizes of the Faroe Islands. The main disadvantage with SWS is the computational time, so system smaller than the power system in the Faroe Islands can parameterise models without issues using only SWS parameterisation. For systems significantly larger than the Faroese power system, the time required for SWS parameterisation is too high, so this is not even considered an option. This study does not focus on the optimisation algorithm itself, but rather the improvement of the combined procedure of parameterization and validation, described further in section 2. The proposed procedure has been applied to two independent grids in the power system in the Faroe Islands, as seen in section 3. The dynamic simulation results show satisfactory resemblance with the 10 Hz online measurements.

2. Proposed Procedure

A flowchart of the proposed approach is shown in Figure 2. To utilize this approach, a validated static load-flow model is required. The method has been applied using DIgSILENT's PowerFactory. Generally, the procedure is not restricted to PowerFactory only, but adaptions might be necessary when using other software tools. The proposed methodology combines SWS and HS. The main idea is that the primary controllers are parameterized using HS together with PowerFactory's System Parameter Identification (SPI) tool, and then validated with SWS. If the SWS shows a behaviour deviating significantly from the measurements, a second parameterization of user-selected parameters using SWS with SPI is conducted. SPI minimizes the difference between measured and simulated response, by optimising user-selected parameters. In this study case the Particle Swarm Optimisation (PSO) algorithm was used, mainly due to its computational efficiency. SPI is a time demanding process, and thus utilizing HS is a great advantage as the simplification of the grid makes the parameterization faster. However, when validating the parameters in SWS, the parameters did not replicate the measurements accurately in all cases, which is why it is necessary to run SPI with SWS for regulators which cannot be validated after HS parameterisation. Each step of the flowchart is described in detail in the following paragraphs.
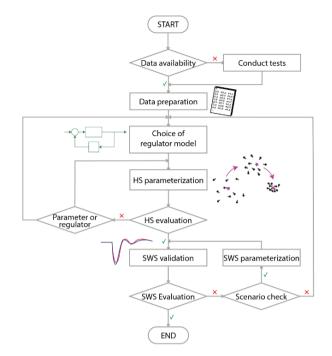
Figure 2 Flowchart for proposed parameter identification and validation procedure

- **Data availability:** The first step of the proposed procedure is to check whether useful measurement data are available. In order for data to be classified as useful, the generators' have to have had a clear primary response, which has been measured with a sufficient resolution e.g. 10 Hz. This data can originate from previous disturbances or by tests conducted for the purpose. The data, which was used in this study case, was the active and reactive power of the generators online and the frequency and voltages measured at the generators' busbars. The measurements with the highest resolution in the Faroese power system are 10 Hz, and these were the measurements used in the examples described in this paper. Each generator has to be online in e.g. 3 datasets, in order to ensure that the parameterisation, and thus, validation is valid for multiple events.
- **Conduct tests:** In the case where no useful data is available, it is necessary to conduct tests on the system and record needed measurements with a suitable resolution (e.g. 10 Hz). This could for example be generator trip or sudden load changes, which result in a clear primary response for the remaining generators online.
- **Data preparation:** The data needed for the parameterization and validation must be prepared according to the required setup of the simulations and made suitable for the specific software. This can be extracting irrelevant parameters from a date file, limiting the period, converting parameters to p.u. etc. Also, the data must be analysed and corrected for any faulty data points.
- **Choice of regulator model:** A model for each regulator can be chosen from the software library or custom designed. It can be challenging to find a model, which fits the regulator exactly, but the IEEE Recommended Practice for Excitation System Models for Power System Stability Studies (26) and support from the manufacturer can be helpful or even required sometimes.

249

- **HS parameterization:** Each regulator is parameterized separately using HS and SPI with PSO, but with all relevant datasets for the regulator simultaneously. This is done by making multiple identical sub-networks all representing the same generator, but with voltage and frequency inputs from different scenarios. The default parameters are used as start values. A so-called "configuration script" for the regulator is used to make sure that the regulators in each subnetwork keep the same parameters when running SPI, so the parameters are optimized according to all relevant scenarios.
- **HS evaluation:** A qualitative evaluation of whether or not the responses can be improved through additional HS parameterization, or if one should proceed to the SWS validation.
- **Parameter or regulator:** A qualitative evaluation of whether optimizing other regulator parameters or using different boundaries can improve the response, or if another regulator model has to be used.
- **SWS validation:** The validation is an RMS simulation (SWS) which replicates the tests/disturbances and compares the simulation results with recorded measurements.
- **SWS evaluation:** The validation is evaluated qualitative, and if the results are sufficient with regards to pattern, min/max and settling time, it is concluded that an accurate model has been obtained. There are no standards for defining when a model is sufficiently accurate, and thus this is up to the engineer criteria. If the results for a specific regulator are insufficient, a second parameterization is required.
- **Scenario check:** The second parameterization can be done for all relevant scenarios individually. This step check wether any available scenarios, have not been SWS parameterized. If SWS parameterization has been run for every relevant scenario, and the validation still is insufficient, it is concluded that a sufficient result cannot be obtained with the specific regulator model, and thus, the process should be restarted with another regulator model.
- **SWS parameterization:** The second parameterization uses SPI with SWS. It is not possible to run multiple scenarios simultaneously with SWS, thus the SWS parameterization is conducted for one scenario, and the new parameters are validated and evaluate. If these are insufficient the SWS parameterization is run again with another scenario. SPI is in this case configured to optimize only the parameters of the regulator(s), which show insufficient results.

3. Application to the Faroese Power System

The procedure proposed in the previous section has been applied to the Faroese power system, specifically the synchronous generators in the main grid which connects 11 out of 18 islands, and the isolated grid in the island of Suðuroy. The synchronous generation capacity, i.e. diesel and hydro, is 124 MW in the main grid and 17 MW in Suðuroy. A list of power plants, the respective grid, the type, number of units and the total generation capacity at the plant can be found in Table I (27). In addition to the synchronous generation capacity, the Faroese power system includes wind turbines of 24,5 MW in total and a small photovoltaic plant of 0.24 MW. Models for all wind turbines (except the 3x660kW windfarm at Mýrarnar) with the actual parameters have been provided by the manufacturer, and the performance has been validated using SWS simulations, thus the need for a validation procedure considering the wind turbines is not needed. The photovoltaic plant of 0.24 MW is relatively small, is not equipped with any active or reactive power regulation capabilities to support the grid and is connected in the distribution grid, thus this plant has not been modelled. The biogas plant is likewise relatively small and placed in the distribution grid and has not been modelled. The generator is a synchronous machine, but the active and reactive power regulation from this unit is negligible.

Grid	Power plant	Type	Units (#)	Plant capacity (MW)
Main	Sundsverkið	Heavy fuel oil	9	82,5
	Elverkið á Strond	Heavy fuel oil and hydro	2	5
	Eiðisverkið	Hydro	3	22,1
	Fossáverkið	Hydro	2	6,5
	Heygaverkið	Hydro	1	5,4
	Mýruverkið	Hydro	1	2,4
	Neshagi	Wind	5	4,5
	Húsahagi	Wind	13	11,7
	Mýrarnar	Wind	3	2
	Förka	Biogas	1	1,5
Suðuroy	Vágsverkið	Heavy fuel oil	4	13,6
	Botnur	Hydro	2	3
	Porkerishagi	Wind	7	6,3
	Sumba	Photovoltaics	-	0,24

Multiple staged tests have been conducted to obtain enough measurement data to parameterise and validate the governors and AVRs in the main grid and in Suðuroy. The tests were done by tripping one of the online generators. In most of the tests the generator, which was tripped, had a high production of either active or reactive power, not both. This was done in order to capture e.g. a frequency drop, which was mostly associated with the loss of active power, not impacted by a large voltage drop due to reactive power loss. This makes it possible to parameterise the AVRs in a scenario where the response from the governors was limited. Some of the tests were however conducted by tripping a generator with a high production of both active and reactive power. This paper highlights the results from three examples of the parametrisation and validation.

Figure 3 shows an example of the reactive power and voltage validation of one of the events in Suðuroy with the final regulator parameters. In this scenario it was not necessary to conduct a second parameterisation using SWS, i.e. the parameters were identified using the HS parameterisation only. The staged test in this example, is that a diesel generator (VG G4) producing 80 kW and 510 kvar is tripped. The other generators online are two hydro turbines (BO G1 and BO G2) and another diesel generator (VG G3). The plot clearly shows a good resemblance between measured (blue) and simulated (red) response. For BO G1, there are two relatively high spikes in the measurements after the event, and these are not seen the simulation. However, this inaccuracy looks worse than it is, as it is due to the resolution of the measurement, 0.01 MW. The generator is small and is only producing 20 kvar steady state, which is why this difference is so visible. There is also an offset for VG G3, but this is caused by an overall reactive power offset in the static load flow model. An offset in the static model has to be compensated by from one of the generators in the dynamic simulation, and in this case, it is VG G3, the largest generator online during the test.
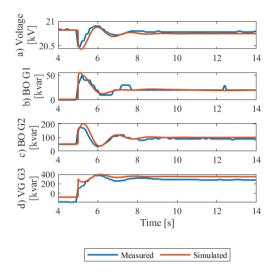
Figure 3 Example from reactive power/voltage validation (SWS) in Suðuroy. Red is simulated and blue is measured.

An example with active power and frequency validation for the main grid is shown in Figure 4. The total generation capacity in the main grid is significantly larger in the main grid than in Suðuroy and the number of generation units is higher, see Table I. This makes the task of validating the model of the main grid more difficult than the grid in Suðuroy. Figure 3 shows the grid frequency and active power for one of the diesel engines which was online (SD G6) and two of the hydro turbines (EI G2 and HE G1) during the staged test. Other engines were online, but these are some of the largest, and thus, some of the most interesting units. The measurements and simulations show very similar behaviour, for both EI G2 and SD G6, the simulation response is much more stable prior, during and post the event. The generators shown here were parameterised trough HS only. There is a difference between the simulated and measured inertial response for HE G1, but the difference might be associated with limitations in the measurements rather than the simulation, as the measured inertial response for HE G1 seems to happen in two steps rather than one continuous. The grid frequency shows acceptable ROCOF, frequency nadir and steady state frequency. The consequences of applying a method which would not lead to an as good validation, is that the model could not be used to plan future expansion or analyse past disturbances to the same degree. The frequency does have a steady state deviation from 50 Hz, due to the secondary control in the Faroe Islands being manual.

Gomez et al. (2011) states, as previously discussed, that HS parameterisation does not always lead to simulation results which can be validated, and this was also experienced during the validation of the Faroese power system, which is why SWS parameterization was included as a step in Figure 1. Figure 5 shows the reactive power response of two hydro turbines in one plant (Fossáverkið in Table I) to one of the staged tests. Blue is the measured reactive power, SWS validation using parameters from the HS parameterisation is in yellow, and red shows the validation after the SWS parameterization. The yellow curves show a response which is far from the actual response, while the SWS parameterisation clearly improves the responses of both generators, especially FO G1. The response of FO G2 has a steady state error but is improved significantly during the first seconds after the test, and the steady state deviation is also smaller than using only HS parameterisation.
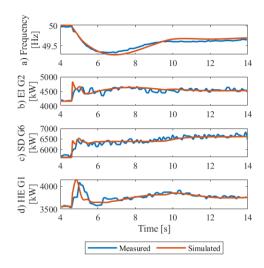
Figure 4 Example from active power/frequency validation (SWS) in the main grid. Red is simulated and blue is measured.
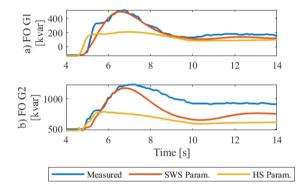

Figure 5 Example where SWS parameterization was needed to improve resemblance between simulated and measured response. Blue is measured, yellow is simulation after only HS parameterization and red is after SWS parameterization.

4. Conclusion

There are many methods and approaches to parameterise and validate power system models. Validating the power system model of the Faroe Islands has been a long process, and different approaches have been used ending with procedure combining different approaches available, which has resulted in a successful application to two isolated grids in the Faroe Islands. The proposed method, which is a significant scientific contribution, takes advantage of the simple and fast HS parameterisation, but also identifies the need for SWS in validation and parameterization, as HS in some cases leads to system wide simulations which cannot be validated. The method also considers multiple staged tests, to ensure that the parameters found can be validated for multiple scenarios, which also increases the possibility to find a global optimum during the parameter optimisation, rather than a local optimum. Power systems smaller than the Faroe Islands

might not see the need to use HS parameterisation instead of SWS, while SWS parameterisation is not an option for larger systems, due to the complexity and computational time, which is why the method shown here is especially interesting for islanded power systems of similar sizes as the Faroe Islands. In the application to the Faroese power system PowerFactory was used together with the PSO algorithm, but the approach can be used in other software and with other optimisation algorithms. It is expected that this procedure will show similar improvements in finding controller parameters of similar island systems.

References

1. IPCC. Mitigation of climate change. Contrib Work Gr III to Fifth Assess Rep Intergov Panel Clim Chang. 2014;1454.

2. Schug MG, Gottlieb A, DeLoache J. "Equal Children Play Best": Raising Independent Children in a Nordic Welfare State. In: A World of Babies [Internet]. Cambridge: Cambridge University Press; 2016. p. 261–92. Available from: https://www.cambridge.org/core/product/identifier/9781316480625%23CT-bp-9/type/book_part

3. Trondheim HM, Niclasen BA, Nielsen T, Silva FF Da, Bak CL. 100% Sustainable Electricity in the Faroe Islands: Expansion Planning Through Economic Optimization. IEEE Open Access J Power Energy. 2021;8(August 2020):23–34.

4. Feltes JW, Lima LTG. Validation of dynamic model parameters for stability analysis; industry need, current practices and future trends. In: 2003 IEEE Power Engineering Society General Meeting (IEEE Cat No03CH37491). 2003. p. 1295-1301 Vol. 3.

5. Lima LTG. Dynamic model validation for compliance with NERC standards. In: 2009 IEEE Power Energy Society General Meeting. 2009. p. 1–7.

6. Allen E, Kosterev D, Pourbeik P. Validation of power system models. In: IEEE PES General Meeting. 2010. p. 1–7.

7. Mahapatra K, Wang H. Generator Dynamic Model Calibration using Multiple Disturbance Events. In: 2020 IEEE Power Energy Society Innovative Smart Grid Technologies Conference (ISGT). 2020. p. 1–5.

8. Sajjadi M, Seifi H, Delkhosh H. A new approach for system-wide power system frequency model validation via measurement data. Eng Reports [Internet]. 2021 Aug 17; Available from: https://onlinelibrary.wiley.com/doi/10.1002/eng2.12446

9. Kosterev D. Hydro Turbine-Governor Model Validation in Pacific Northwest. IEEE Trans Power Syst [Internet]. 2004 May;19(2):1144–9. Available from: http://ieeexplore.ieee.org/document/1295026/

10. den Boer TL. Validation of Dynamic Power System Models using Synchrophasor Measurements. TU Delft; 2019.

11. Gomez JE, Decker IC, Leon RA. Hybrid simulations, a smart way to perform parameter validation in power systems. In: 2011 IEEE PES Conference on Innovative Smart Grid Technologies Latin America (ISGT LA). 2011. p. 1–7.

12. Chen R, Wu W, Sun H, Zhang B. A two-level online parameter identification approach. In: 2013 IEEE Power Energy Society General Meeting. 2013. p. 1–6.

13. Hajnoroozi AA, Aminifar F, Ayoubzadeh H. Generating Unit Model Validation and Calibration Through Synchrophasor Measurements. IEEE Trans Smart Grid. 2015;6(1):441–9.

14.   Kittiwattanaphon S, Wangdee W, Katithummarugs S. Generator Excitation System Parameter Identification and Tuning by Using PSO. In: 2019 7th International Electrical Engineering Congress (iEECON). 2019. p. 1–4.

15.   Li C, Zhou J. Parameters identification of hydraulic turbine governing system using improved gravitational search algorithm. Energy Convers Manag. 2011;52(1):374–81.

16.   Yu P, Zhang J. Parameter Identification of Excitation System Based on Field Data and PSO. In: 2010 International Conference on E-Product E-Service and E-Entertainment [Internet]. IEEE; 2010. p. 1–4. Available from: http://ieeexplore.ieee.org/document/5660858/

17.   Bollinger KE, Gilchrist R. Voltage Regulator Models Using Automated Frequency Response Equipment. IEEE Trans Power Appar Syst [Internet]. 1982 Aug;PAS-101(8):2899–905. Available from: http://ieeexplore.ieee.org/document/4111680/

18.   Gibbard MJ, Kaan QH. Identification of excitation system parameters. IEEE Trans Power Appar Syst [Internet]. 1975 Jul;94(4):1201–7. Available from: http://ieeexplore.ieee.org/document/1601557/

19.   Huang R, Diao R, Li Y, Sanchez-Gasca J, Huang Z, Thomas B, et al. Calibrating Parameters of Power System Stability Models Using Advanced Ensemble Kalman Filter. IEEE Trans Power Syst. 2018;33(3):2895–905.

20.   Akhlaghi S, Zhou N, Chiang H. Starting point selection approach for power system model validation using event playback. IET Gener Transm Distrib [Internet]. 2020 Oct 7;14(19):3972–82. Available from: https://onlinelibrary.wiley.com/doi/10.1049/iet-gtd.2020.0094

21.   Delkhosh H, Seifi H. Quantitative model validation from the frequency perspective considering governor frequency ramp rate and activity range. Int J Electr Power Energy Syst [Internet]. 2019 May;107:668–79. Available from: https://linkinghub.elsevier.com/retrieve/pii/S0142061518325547

22.   Lin C, Wu C, Yang J, Liao C. Parameters identification of reduced governor system model for diesel-engine generator by using hybrid particle swarm optimisation. IET Electr Power Appl [Internet]. 2018 Nov 9;12(9):1265–71. Available from: https://onlinelibrary.wiley.com/doi/10.1049/iet-epa.2017.0851

23.   Stavrinos S, Petoussis AG, Theophanous AL, Pillutla S, Prabhakara FS. Development of a validated dynamic model of Cyprus transmission system. In: 7th Mediterranean Conference and Exhibition on Power Generation, Transmission, Distribution and Energy Conversion (MedPower 2010) [Internet]. IET; 2010. p. 238–238. Available from: https://digital-library.theiet.org/content/conferences/10.1049/cp.2010.0946

24.   Majka Ł, Paszek S. Mathematical model parameter estimation of a generating unit operating in the Polish National Power System. Bull Polish Acad Sci Tech Sci [Internet]. 2016 Jun 1;64(2):409–16. Available from: http://journals.pan.pl/dlibra/publication/98079/edition/84522/content

25.   Sun Y, Kuijpers WG, de Jong ECW, Pustjens H. Dynamic Study of Bonaire Island Power System: Model Validation and Project Experience. In: Proceedings of the 3rd Internation Hybrid Power Systems Workshop [Internet]. Energynautics; 2018. Available from: https://hybridpowersystems.org/wp-content/uploads/sites/9/2018/05/2A_1_TENE18_016_paper_Sun_Yin.pdf

26.   IEEE. IEEE Recommended Practice for Excitation System Models for Power System Stability Studies. IEEE Std 4215-2016 (Revision IEEE Std 4215-2005). 2016;1–207.

27.   The Power Company SEV. The Power Supply System [Internet]. The Power Company SEV. 2022 [cited 2022 Jan 13]. Available from: https://www.sev.fo/english/the-power-supply-system/

Title: Frequency and Voltage Stability Towards 100% Renewables in Suðuroy, Faroe Islands

Authors: *Helma Maria Tróndheim[1,2,3], Lutz Hofmann[4], Pascal Gartmann[5], Eckard Quitmann[5], Claus Leth Bak[2], Filipe Faria da Silva[2], Terji Nielsen[1] and Bárður A. Niclasen[3]

Affiliations: The Power Company SEV[1], Aalborg University[2] and the University of the Faroe Islands[3], Leibniz University Hannover[4] and Enercon GmbH[5]

Abstract: Frequency and voltage stability is a challenge as power systems move towards a more renewable future. This study focuses on the power system of Suðuroy, Faroe Islands, which is in the transition towards 100% renewables. The impact of three events on the frequency and voltage responses have been simulated in DIgSILENT's PowerFactory based on 2020, 2023, 2026 and 2030 and with different settings using a measurement validated model. These results show that additional ancillary services, provided by e.g. batteries and synchronous condensers, are required to keep the stability level at the same level as today. The isolated power system in Suðuroy (~10% of total annual demand) will be connected to the main grid (~90% of total annual demand) in the future (2026 according to the RoadMap), and thus the system has also been studied with this interconnection. According to the simulation results, the main grid contributes significantly to the power system stability in Suðuroy when the systems are interconnected. The impact of how the main grid has been represented is also analysed by conducting simulations using a detailed model of the main grid or approximated models. The results show that the suggested approximated models do not show a sufficiently accurate response compared to the detailed model; especially when batteries in the main grid are contributing with active power regulation. Therefore, new approximated models of power systems with high shares of inverter-based technologies, should be developed with this consideration. Finally the contribution from wind turbine inertia emulation is analysed, and shows that the system frequency nadir can be improved with the emulated inertia feature switched on.

Index Terms: Inertia emulation, isolated power system, network reduction, power system stability, renewable energy

Nomenclature: SEV: The Power Company in the Faroe Islands, SCP: Short circuit power, BESS: Battery energy storage system, SC: Synchronous condenser, AVR: Automatic voltage regulators, IE: Inertia emulation, PV: Photovoltaics, IBR: Inverter based resources, ROCOF: Rate of change of frequency, PDF: probability density function

1. Introduction

Suðuroy is the most southern island of the Faroe Islands in the North Atlantic Ocean, see Figure 1 [1]. The Faroese Power System has seven individual grids of different sizes and complexity, and the isolated power system on Suðuroy is one of these seven grids. The energy production in Suðuroy in 2020 was 35 GWh in total, which was 9% of the total generation in the Faroe Islands, and consisted of diesel and heavy fuel oil (85%), hydro (11.5%), wind (3%) and solar power generation (0.5%). The low wind power generation is due to the wind farm being inaguarated in February 2021, and thus only in operation in 2020 for test runs etc. The average demand in Suðuroy in 2020 was 4.0 MW, with minimum of 1.8 MW and maximum of 8.0 MW. The reason behind the great variation is a relatively large fish factory, which was in operation for around 2000 hours in 2020. A load curve for the demand in Suðuroy in 2020 can be found in Figure 2 plot (a). Plot (b) on Figure 2 shows the average hourly demand for months March-July in 2020, and thus shows how the daily and to some degree seasonally demand variations. January-February and August-December are not included in plot (b) as the previously mentioned factory was online during certain periods of these months, and an inclusion of these would not illustrate the daily and seasonally variations.
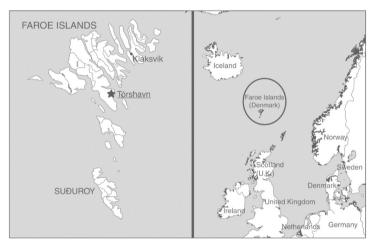
Figure 1 – Map of the Faroe Islands
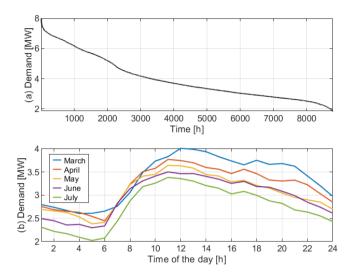
Figure 2 – (a) Load duration curve of demadn in Suðuroy 2020. (b) Average hourly demand for months March-July in 2020.

SEV, the local utility, is aiming for a 100% renewable electricity generation by 2030. This requires expansions in renewable generation capacity, storage systems, energy management systems and state of the art solutions to ensure a stable and reliable power system operation, as the share of traditional synchronous generators decreases.

Synchronous generators have the capability to provide the ancillary services needed to ensure a stable supply after a disturbance, i.e. active and reactive power provision for frequency and voltage control, respectively. However, these are becoming a smaller share of the total generation, as the synchronous generators are replaced with wind turbines and photovoltaics, which can results in a grid with decreased inertia, short circuit power (SCP) and active and reactive power provision. The integration of inverter-based generation, therefore will have a detrimental impact on stability, if traditional procedures continue to be used in all power systems, but especially smaller in isolated power systems like the Faroe Islands [2]–[4]. The specific challenges for power systems depend on the type of generation, and these have been addressed in previous review studies [5]–[7]. In order to ensure the stability of a power system with a high penetration of inverter-based renewables (IBR), it is therefore necessary to simulate and analyse the systems. This study addresses frequency and voltage stability challenges associated with reaching 100% renewables in an isolated grid, using a model, that has been dynamically validated based on measurements from trip tests. This is not an ordinary engineering task.

A relevant state-of-the-art characteristic of the power system is the probability density function (PDF) of voltage and frequency for the island. Any future change in the system should lead to a PDF which is close to, or at least not worse, than the present level. This would be the benchmark if a change has improved or detoriated the quality of power supply. Figure 3 shows the probability density function based on 10 Hz grid frequency measurements in Suðuroy before (2018-2020) and after (2021) the wind farm was installed. It is quite clear that the wind farm has led to a larger variance in the frequency, as 2021 differs from 2018-2020 and no other significant changes have been made in system.
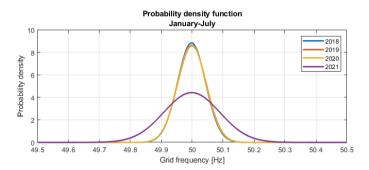
Figure 3 – Probability density function based on 10 Hz grid frequency measurements in Suðuroy in January to July in 2018 to 2021.

The power system stability in Suðuroy and in the main grid approaching 100% renewables has been studied previously, but all of these studies are considered as initial studies, as they have either had a narrow scope or have been done using power system models, which have not been validated [8]–[13]. The topics covered in previous publications include full system simulations [8]–[10] and providing ancillary services using batteries [11], heat pumps [12], synchronverters [13] and wind turbine controls [9]. Whilst studies on the power system stability in the Faroe Islands are limited, the potential investments in generation, storage and transmission system expansion towards 100% renewables in the Faroe Islands have been thoroughly investigated in multiple studies [14]–[20]. A detailed RoadMap for generation, storage and transmission can be found in [20]. The RoadMap contains project specific investments, which specify e.g. power plant sizes, locations and investment year, which are based on an economic optimisation and consider a demand increase from 369 GWh in 2020 to 633 GWh in 2030, due to an increase in the normal electricity usage and electrification of the heating and transport sectors. This RoadMap is used as a basis for expansions towards 2030, see section 1.2.

In many study cases only a part of a system is of interest, not the whole system. Including the whole system in computer simulations increases the calculation time and the complexity of the simulations, and therefore different network reduction methods have been developed to approximate the large system's static and dynamic behaviour over the past decades [21]. As the distributed generation has increased, newer approaches have been developed, which considers the distributed generation as well as synchronous generation [22]. While most reduction methods require the full system model to be computed, recent research also proposes methods using wide area measurements to compute dynamic equivalents [23]. Simulation softwares also have built-in models for network equivalents. For example in DIgSILENT's PowerFactory provides a model component called External Grid.ElmXnet [24].

This paper addresses an uncommon task, the transition of a small isolated system towards 100% renewables. The study focuses on the voltage and frequency stability of the the island Suðuroy, and how these are effected by 1) a sudden drop in wind power production, 2) an outage of a synchronous generator and 3) a load rejection. The events are analysed for the following expansion stages of the system: 2020, 2023, 2026 and 2030. Thus, the impact on the system stability of replacing thermal synchronous generators with renewables towards 2030 is addressed. The analysis of 2023 and 2026, shows that analysing the start (2020) and end (2030) date can result in missing problems in-between. The study is based on an existing system, which is under development to reach a cleaner energy production, and it uses validated dynamic models and an actual expansion plan. It is based on a scientific engineering approach to overcome the uncertainties and challenges in the actual expansion of the Faroese power system, in contrast to the mainly

theoretical approach of most such studies. Suðuroy will be connected to the main grid in 2026 via a single link [20], and a common method to analyse the stability on Suðuroy post connection, would be to simplify the main grid at the end of the cable connection, to reduce the computational time and the complexity of the system. This study shows that reducing the main grid, leads to some implications, e.g. capturing frequency triggered technologies which contribute to frequency stability accurately. This is done by comparing the simulation results using a detailed model of the main grid and two different approximations. The results therefore contribute to the discussion on whether or not present day equivalents are sufficient to represent a grid with high levels of inverter-based technologies, or if detailed models are needed. Based on the approximations used in this analysis, the dynamic response is inaccurate, so a detailed model is needed, or an approximated model, which considers frequency triggered technologies. The main contributions of this study are the results showing the implications with using approximated models in power system with a high share of inverter-based technologies, as well as the aspect of this being a study on the challenges in actual isolated system aiming for 100% renewables.

The power system of Suðuroy is presented in section section 2, while the investigation approach is described in section 3. The results of the study are presented and discussed in section section 4 and concluded in section 5.

2. The Existing and Future Power System

The power system in Suðuroy is a hybrid power system, which is under continuous development. Figure 4 shows a single line diagram of the power system in Suðuroy with respective capacities and introduces abbreviations for the different components. VG G1-VG G4 are synchronous thermal generators, which are rated at 13.4 MW in total, the hydro turbines with synchronous generators, BO G1 and BO G2, are rated at 3 MW in total, the wind farm PO has 7 wind turbines rated at 6.3 MW in total and finally there is a PV power plant of 260 kW. Installing a battery system of 7.5 MW/7.5 MWh (IH BS) and a synchronous condenser of 8 MVA (IH SC) is in progress as well. These are intended to provide ancillary services like active and reactive power reserves, inertia and SCP to the system. The voltage levels in Suðuroy are 20 kV, 10 kV and for distribution 0.4 kV. The TG and IH and the substation/diesel power plant VG have a rated voltage of 20 kV. The rated voltage at the hydro power plant BO is 10 kV. The demand in Suðuroy has been described in the introduction.
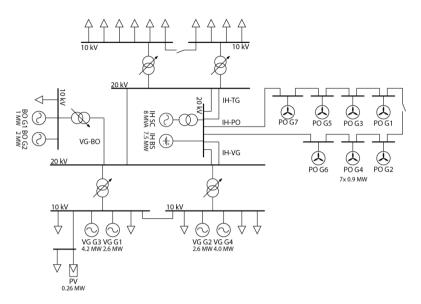
Figure 4 – Single line diagram of the power system in Suðuroy. BO is a hydro power plant, PO is a wind power plant, VG is a thermal power plant, while IH and TG are substations.

Each synchronous generator has a governor and an automatic voltage regulator (AVR). Under normal operation the frequency must be within 49.5 Hz and 50.5 Hz, and these limits are kept with droop primary control and manual secondary control. The installed wind turbines are the Enercon E44/900 kW model, which is a type 4 - full converter turbine. They have active and reactive power control capabilites, and the option of inertia emulation. However, ever since the wind turbines were inaugurated in February 2021, they have been controlled using only active and reactive power setpoints from the dispatch center. The PV plant is not controlled, due to its relatively small size. It therefore produces power according to the resource potential at any given moment with a power factor of 1.

2.1. Future Expansions According to RoadMap

The expansion steps in Suðuroy according to the RoadMap [20] are shown on Figure 5. There are expansions in wind power, PV power, a cable to the main grid and a second battery system (BESS) to balance the energy production on an hourly basis, i.e. this BESS is not intended for ancillary services as such, but more in terms of energy storage to lower the power exchange between Suðuroy and the main grid and the attributable losses. The focus in this study is the power system on Suðuroy, but according to the RoadMap Suðuroy will be connected to the main grid through a 60 kV subsea cable in 2026. The cable will be connected to 20 kV at substation TG trough a 60/20 kV transformer. Thus, the power composition in the main grid is relevant to this study from 2026 and forward. The main grid supplies 11 out of 18 islands. The generation capacity currently consists of 86 MW of heavy fuel oil and diesel power (synchronous), 2 MW of biogas (synchronous), 37 MW of hydro power (synchronous) and 18 MW of wind power (16 MW of type 4 and 2 MW of type 2 wind turbines). The future expansions in the main grid by 2026 and 2030 according to the RoadMap are tabulated in Table 1. These expansions consist of wind power, photovoltaics and a pumped storage system with synchronous turbines and pumps. Further details with regard to plant sizes and locations can be found in [20]. SEV also has preliminary plans with regards to investments of BESS and synchronous condensers (SC) in the main grid to provide active and reactive power reserves, inertia

and SCP to the system, just like the BESS and SC in Suðuroy. These plans include 3x16 MVA SC, 1x6 MVA SC and a BESS capacity of 30 MW in total, of which the first 12 MW BESS and 16 MVA SC are already procured. These components have been included in the simulations with the main grid.

Figure 5 – Expansions in Suðuroy according to RoadMap [20].

Table 1 – Additional expansion in wind power (WP), hydro power (HP), pumping power (PP) and photovoltaics (PV) in the main grid by 2026 and 2030 according to the RoadMap [20].

By 2026	By 2030
72 MW WP	66 MW WP
35 MW HP	39 MW HP
41 MW PP	38 MW PP
	40 MW PV

3. Investigation Approach

The future short term voltage and frequency stability of Suðuroy to large disturbances [25] and the impact of the main grid representation has been analysed using RMS simulations in DIgSILENT's PowerFactory. Three different events are investigated under one operation scenario, see section 3.2., in the study cases of 2020, 2023, 2026 and 2030. Different representations of the main grid and some wind turbine capabilities has also been investigated. Additionally the required BESS and SC sizes in the future to maintain the frequency and voltage stability in Suðuroy at the same levels as today, have been addressed.

3.1. Modelling

The grid model uses a load flow and dynamically validated model. The load flow model has been validated by defining load, generation, tap changers and circuit breakers according to historic operation scenarios, and then simulated currents and busbar voltages have been compared to measurements. The governors and automatic voltage regulators (AVRs) have been parameterized and validated by tripping generators, measuring the dynamic response and replicating the measurements in the simulation. Since models and parameters for multiple of these controllers were unavailable, standard models that fit with the actual regulators have been used. These were selected mainly based on [26], but also based on information in the available datasheets. These standard models have then been parameterized by minimizing the difference between simulated and measured primary response from the controllers. The wind power plants are modelled with models from Enercon with site specific parameters. The configuration of these models has been validated with the manufacturer. The future PV plants are modelled with IEC 614-27-1 WT 4B 2.0MW 50Hz models with adjusted rated power. This model is commonly used for PV modelling in the industry. The synchronous condensers are modelled based on a model of the synchronous condenser in Suðuroy, delivered by ABB. The main grid already has a BESS which contributes to frequency regulation during disturbances, and this model (Enercon) has been used for the BESS in Suðuroy and expansions in the main grid. The main grid has been modelled with a full size detailed model, and using two reduced models, both utilizing the "External Grid.ElmXnet" component in PowerFactory. The "External Grid.ElmXnet" used in RMS

simulations is basically a synchronous generator, neglecting saturation and leakage reactances. The SCP of the system to be reduced has to be defined, and the default acceleration time constant is infinite. The transient and subtransient time constants and the synchronous and transient reactances can be defined, but in this study default values have been used. In approximation 1 the external grid has been defined based on the SCP. This means that the inertia in approximation 1 is infinite. The difference between approximation 1 and 2, is that the inertia of the main grid is specified in approximation 2. The inertia in the main grid has been calculated based on the units online during the simulation. An overview of the models used can be found in Table 2.

Table 2 – Description of how different system components have been modelled.

Components	Model
Synchronous generation	Standard governor and AVR models, which have been parameterised and validated according to measurements.
Wind power	Wind turbine models and farm control unit models from the Enercon. Parameterised with actual parameters and validated in cooperation with Enercon.
Existing PV	Modelled as a negative load with set production.
Future PV	IEC 614-27-1 WT 4B 2.0MW Hz model, which is commonly used for PV in industry.
Synchronous condenser	Model and parameters from the manufracturer ABB
Battery system (ancillary)	Modelled using a Enercon model for the battery system in the main grid, which has similar capabilities. The model has been parameterised with the actual parameters in the main grid.
Battery system (2030)	Modelled as a load which charges with postive values and discharges with negative values.
Main grid detailed model	Full system model using models as decribed above.
Main grid approximation 1	"External grid" component in PowerFactory, considering only the short circuit power.
Main grid approximation 2	"External grid" component in PowerFactory, considering the short circuit power and inertia.

3.2. Operation Scenario

The previously discussed RoadMap [20] has been obtained based on an economic optimisation in the open source model Balmorel [27]. Balmorel optimises the hourly dispatch as well, thus the generation and load settings for the investigated events have been extracted from the optimisation for the years investigated (2020, 2023, 2026 and 2030). The operation scenario, i.e. the specific hour investigated, has been selected based on hourly input data (2017) and output (2020, 2023, 2026 and 2030) data in the RoadMap study. First the demand, wind speed and irradiation data (2017 input) were sorted based on the following criteria:

1. High load, i.e. ≥4.5 MW
2. Wind speeds at the wind farm in Suðuroy equal to or above average, i.e. 9.5 m/s
3. Irradiation in Suðuroy equal to or above average (night hours excluded), i.e. 201 W/m^2

41 hours of the input data from 2017 fit all requirements. In order to chose one of these 41 hours, the optimised dispatch (2020, 2023, 2026 and 2030) according to the output data in [20] was used to sort the hours, with the following criteria:

1. IBR shares should be equal to or less than 60% in 2020 and 80% in 2023. No criteria on IBR shares in 2026 and 2030, due to the system being connected to the main grid.
2. The diesel power plant should supply at least 20% in 2020, to ensure that the diesel engines are loaded above minimum.
3. The shares of PV should be equal to or lower than 25%. Higher shares than this will not be common due to the northern latitude, cloudy climate and installed capacity.
4. Import from the main grid should not supply over 40% of the demand in Suðuroy, so that the analysis includes significant amount of local production.

Only one of the 41 hours fits all criteria, and that is 12:00 on the 28th of March based on the input data. The production and import shares according to the optimised dispatch [20] are tabulated in Table 3. In order to be able to compare different years, it is important that the production composition is similar. The wind and PV dispatch according to Balmorel have been left unchanged, but the synchronous generation has been adjusted, so the hydro turbines in Suðuroy produce in total 1.8 MW every investigated year. In 2020 the 1.8 MW are extracted from the thermal generation, while in 2026 and 2030, the generation is moved from hydro turbines in the main grid to Suðuroy, thus, the import is decreased as well. The thermal generation in 2020 and 2023 is produced by VG G1 and VG G2.

The production in the main grid in 2026 and 2030 according to Balmorel consists of 3 hydro power plants, the biogas plant, wind power plants and PV (2030 only). Excess wind power is also being pumped during the investigated operation scenario, this pumping power has been divided between 3 and 4 pumps in 2026 and 2030, respectively.

Table 3 – Production and import in the selected operation scenario according to teh optimised dispatch [20] as percentages of demadn in Suðuroy (Rounded to integers).

	2020	2023	2026	2030
Diesel	42%	15%	0%	-
Hydro	0%	15%	0%	0%
Wind	58%	70%	66%	60%
Import	-	-	35%	18%
PV	-	-	-	23%

The loads, tap changers, circuit breakers etc. for the simulations in PowerFactory, have been set based on SCADA measurements from 12:00 on the 28th of March 2017 (the input data year) has been used. The loads have been scaled up to reflect the projected demand in 2020, 2023, 2026 and 2030. This is done to ensure a realistic load division between different substations. In cases where the voltage has been to high or low in future scenarios, the tap changers have been modified accordingly.

3.3. Events and Study Cases

Three events are investigated in this study, as listed following this paragraph. The first one is an outage of one of the hydro turbines, the second is a sudden loss of wind power production and finally a load rejection where a fish factory is disconnected. These three events have all been selected based on events which are considered as alarming. The events are analysed for the study cases of 2020, 2023, 2026 and 2030.

Additional simulations have been conducted to analyse the impact of the main grid representation and the contribution from the wind turbines' inertia emulation.

1. **BO G1 tripping:** In the future BO G1 and BO G2 will be the only synchronous generators in Suðuroy, therefore tripping one of these is interesting to investigate. In percentage of the total generation this trip corresponds to: 24% in 2020, 15% in 2023, 2% in 2026 (18% of production in Suðuroy) and 2% in 2030 (14% of production in Suðuroy).
   a. Additional simulations (2020 w/o BESS): With and without inertia emulation from the wind turbines in Suðuroy.
2. **Sudden loss of wind power:** Wind speeds often change suddenly, which can lead to a sudden loss of wind power. Therefore this scenario where the wind power changes from 0.7 to 0.0 p.u. in 17 seconds has been investigated. In percentage of the total generation this reduction corresponds to: 58% in 2020, 70% in 2023, 10% in 2026 (82% of production in Suðuroy) and 8% in 2030 (63% of production in Suðuroy).
   a. Additional simulations (2026): The main grid represented by approximation 1 and 2
3. **Load rejection:** This load rejection corresponds to a disconnection of a fish factory. As it is 18% of the total demand in Suðuroy, this load rejection can lead to power system instabilities.

3.4. Sizing Additional BESS and SC

The results of some of the scenarios showed a need for additional ancillary services, and there are many methods to provide ancillary services. A SC can provide inertia, SCP and reactive power regulation to the system, while BESS can provide active power regulation to support the frequency. In order to maintain the stability level in this study, it was decided to increase the SC and BESS capacities. The design criteria for sizing BESS and SC for future scenarios was that the responses should not be worse than in the base case, i.e. 2020. The validity of this design criteria set can be discussed, but this simple approach gives a good indication of the required size to maintain the dynamic stability at the same level as in the present system. The BESS has been increased by one BESS size at a time (2.3 MW) until the issues have been resolved. The SC was increased with 2 MVA intervals.

When a larger BESS or SC is needed in 2023 for one event, this additional capacity has been included in other 2023 events and in all events in 2026 and 2030.

4. Results and Discussion

The dynamic frequency and voltage responses to the study case, i.e. outage of one of the hydro turbines, are shown on Figure 6 for 2020, 2023, 2026 and 2030. The frequency in the base case, i.e. 2020, drops quite significantly, but stabilises at 49.8 Hz, which is when the batteries react to the sudden frequency deviation. The frequency reponse in 2023 is close to identical to the base case, because the only change between the two scenarios is an increase of the demand, which is covered by additional wind power production. The thermal generation is also lower, but the same units are online. Thus, the inertia of the system is the same and so is the production from the hydro turbine. The rate of change of frequency (ROCOF) decreases from 370 mHz/s to 35-40 mHz/s when Suðuroy is connected to the main grid, which was expected as the magnitude of the ROCOF is inversely proportional to system inertia, which increases when the two systems are interconnected. In 2026 the thermal generators in Suðuroy are not in operation, and the inertia provided by local apparatus in Suðuroy is therefore lower, this shows that the inertia of the hydro turbines, pumps and synchronous condensers in the main grid contribute quite significantly to stabilising the grid in Suðuroy in 2026, which is why a correct representation of the external grid is of significant importance to obtain accurate results. The frequency nadir in all years is around 49.8, due to the battery system, but the

time of the nadir varies from year to year due to the ROCOF. The difference between 2026 and 2030 is very limited. The ROCOF is sligthly higher in 2030, and the frequency reaches 49.8 Hz, which triggers the BESS to react. The threshold has been set according to the current configuration of the BESS in the main grid. The voltage (VG 20 kV in Figure 4) is not initialised at the same magnitude for the investigated years, but overall the disturbance in the voltage is relatively small and does not worsen from the base case to 2030. The behavoir is differnet depend on if the main grid is connected or not, i.e. different patterns are seen in the voltage for 2020/2023 and 2026/2030. No additional ancillary services need to be installed, to ensure grid stability in Suðuroy after an outage of BO G1 with this specific operation scenario and configuration, as the frequency and voltage responses are considered acceptable.
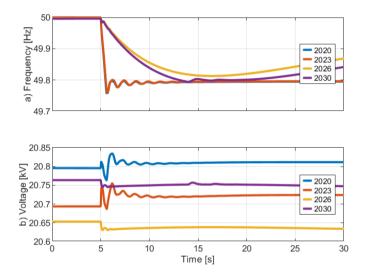
Figure 6 – Frequency and voltage response to the outage of BO G1 during different years.

A sudden drop in wind power production will also have a negative impact on the frequency and voltage stability, see Figure 7. In 2020 the grid is stabilised after the event at 49.7 Hz, but there are some issues with the frequency and voltage in 2023, when the frequency hits 49.6 Hz. An investigation of the data shows that the two frequency drops and voltage peaks after 15 seconds are caused by the wind turbine controllers, as these issues are not seen with the wind turbines' dynamic controllers deactivated Tuning the wind turbines controllers could resolve this, but in this study the controllers are parameterized according to the actual settings at the existing wind farm. If an additional BESS package (2.3 MW) is installed, the frequency is able to stay above 49.6 Hz, and a response very similar to the base is obtained, see "2023-1" on the figure. Similarly to the first study case, there are no issues with the frequency in 2026 and 2030 due to the ancillary services received from the main grid. The voltage drop is however larger in 2026 and 2030 than in previous years, due to the import from the main grid, but the drop is not large enough to lead to additional investments in ancillary services. These results therefore show that in order to ensure frequency stabilisation after the event of sudden wind power production loss in Suðuroy, additional active power regulation capabilities, e.g. a larger size of BESS, are required. Additionally the results show the importance of investigating the system step by step, and not only current state and final state, e.g. 2020 and 2030, as expansions in between might lead to some instabilities, even though the final system configuration does not.
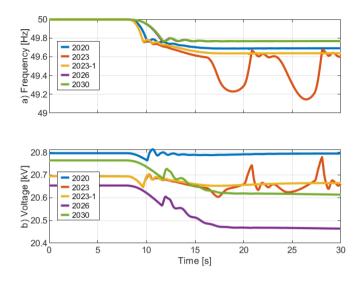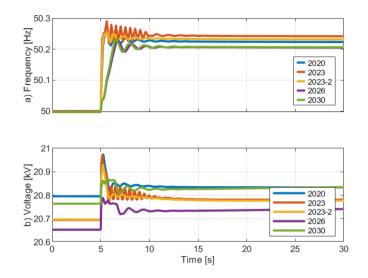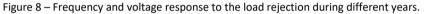
Figure 7 – Frequency and voltage response to wind power production in Suðuroy drop from 0.7 p.u. to 0.0 p.u. within 17 seconds during different years.

The final event investigated in this study is the load rejection, see Figure 8. In the simulations representing 2020 the system has a high ROCOF, but stabilises at 50.2, which is when the battery starts charging. In 2023 the demand has increased, and all loads have been increased proportionally, meaning that the power deficit is higher in 2023 than in 2020. The simulation results show that this higher load rejection leads to oscillations in both the frequency and the voltage. This issue can be avoided e.g. by increasing the SC from 8 MVA to 12 MVA. The "2023-2" lines in the figure show frequency and voltage responses similar to 2020, and have been obtained from simulations with the additional BESS package from event two and a 12 MVA SC. The main grid again contributes enough to the stability in Suðuroy in 2026 and 2030, to avoid any additional investments in ancillary services in Suðuroy based on the system configuration in this study.

Figure 8 – Frequency and voltage response to the load rejection during different years.

Overall it can be said that in order to ensure the stability in Suðuroy prior to the cable connection to the main grid, it will be necessary to make changes to the system, by e.g. investing in 4 MVA additional synchronous condenser and 2.3 MW additional battery power. The frequency and voltage stability on Suðuroy will benefit from the connection to the main grid.

4.1. Representation of the Main Grid

The main grid has in previously shown simulations been represented by a detailed model, since the simulated frequency and voltage with approximated models did not accurately replicate the detailed model. Figure 9 shows simulation results using different methods to represent the main grid during the second event, sudden drop of wind power production, in 2026. In approximation 1 - considering SCP but infinite inertia - the frequency is at 50 Hz during the whole simulation, while the detailed model shows a frequency drop. The voltage response using approximation 1, described in Table 2, is quite similar to the detailed model. Using approximation 2, the frequency response is closer to the detailed modelled, while the voltage response deviates more. The voltage drop is lower using approximation 2, because the power flow from the main grid is lower. The significant amount of power imported from the main grid, is the cause of the high voltage drop in the detailed model and approximation 1. In fact, up to 12 seconds, the frequency response is close to identical to the detailed model. The plot c) on Figure 9 explains the reason behind the differences from 12 seconds and forward. In the detailed model both the BESS in Suðuroy and the BESS in the main grid are injecting active power at 12s to stabilise the frequency in Suðuroy, but the active power regulation contribution from the BESS in the main grid cannot be captured by the approximation, thus this approximation is quite accurate regarding the frequency response as long as the frequency remains within 49.8 and 50.2 Hz, but can not be used as an accurate representation, for events which will trigger the BESS or other technologies which are frequency triggered. This indicates that when inverter based sources, e.g. BESS, are used to contribute to frequency and voltage regulation, using the approximated models shown here is not sufficient. The inverter-based sources like e.g. BESS have to be included in the approximation, e.g. using triggered behaviours, or a detailed model has to be used. This

finding is not only valid for the Faroese power system or isolated power systems, but for all systems that include frequency triggered technologies, and are being approximated in order to simplify simulations and reduce computational time.
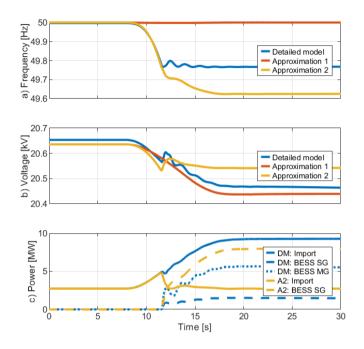

Figure 9 – Comparison of the dynamic response in Suðuroy using different modelling approaches of the main grid. Plot a) shows the frequency response and plot b) the voltage at VG 20 kV. The plot c) shows the import from the main grid (MG) to the Suðuroy grid (SG) and the power output from BESS using the detailed model (DM) and approximation 2 (A2) of the main grid. The specific scenario is sudden loss of wind power in 2026.

4.2. Inertia Emulation from Wind Turbines

The final simulation results included in this paper show the impact of activating inertia emulation (IE) from the wind turbines in Suðuroy. These simulations have been conducted without the BESS in Suðuroy, due to the fact that the BESS reacts as the frequency reaches 49.8 Hz, and the default IE settings are set to react at 49.5 Hz, which means that with the BESS online, the IE would not be activated, aside from events that can not be saved by the BESS, which are very unlikely on Suðuroy, as the BESS is similar in size to high load, and larger than the existing wind farm. However, the frequency and voltage response to the outage of BO G1 in the base case, without the BESS and with IE is shown on Figure 10. The initial frequency and voltage responses are are similar to 2020 simulations in Figure 6, and the ROCOF is the same, but since the batteries are deactivated, the frequency nadir reaches 49.4 Hz and 49.3 Hz with and without IE activated, compared to 49.8 with the battery activated. The grid frequency would clearly benefit from activating IE, as the frequency nadir is higher and the overshoot is decreased. The voltage is also impacted by this, as the overshoot increases, but the voltage deviations are relatively small.
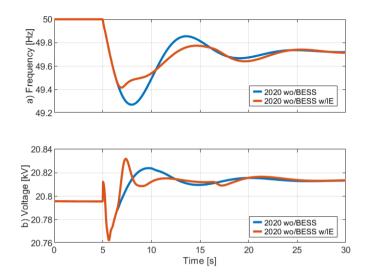
269

Figure 10 – Comparison of the frequency and voltage responses with and without inertia emulation from the wind turbines in Suðuroy. The specific scenario is an sudden outage of BO G1 in the base case without the BESS.

4.3 Discussion

Obtaining stability after the events investigated in this study will require additional investments in ancillary services already in 2023. In 2026 when the grid of Suðuroy is connected to the significantly larger main grid, stabilising the grid is not as challenging as in the isolated grid. The reason is that the severity of the events are proportionally decreased, as they are relatively small compared to the size and strength of the main grid. Aside from assessing the stability, the results also show some interesting findings with regards to expansions and network representation.

In study case 2 it was shown that maintaining a stable frequency becomes an issue in 2023, but this issue disappears when the Suðuroy is connected to the main grid. It is therefore important to simulate and analyse all expansion steps in the transition towards 100% renewables, and not only the initial and final stage of the system. Expansions in photovoltaic power are conducted in Suðuroy in 2028 and 2029, according to the RoadMap. These years should therefore also be investigated, and since the main grid has a significant impact on the stability in Suðuroy when interconnected, these steps should also be investigated.

Representing a network with an approximated model for dynamic simulations accurately, has been shown to be challenging, as neither of the two approximations showed an accurate representation of a detailed model. The main reason is that there is a BESS located in the main grid, which is frequency triggered, i.e. it reacts to frequency changes when the frequency reaches 49.8 Hz or 50.2 Hz. If an approximated model is used to represent the main grid, it has to be expanded with some kind of triggered frequency control, to represent the BESS or other frequency triggered technologies. Without this the approximated models simply will not show an accurate dynamic response, and this is not a site specific issue, i.e. it is not only an issue for the Faroese power system, but all power systems with frequency triggered technologies. The significant of this inaccuracy does however also depend on the power injected (proportional to the system) and the location.

5. Conclusion

This study has shown the impact different disturbances have on the isolated power system of Suðuroy. For the events, operation scenarios and cases studied, it can be concluded that additional ancillary services will be needed to maintain the voltage and frequency stability in 2023 at the same level as today, e.g. an additional investment of 4 MVA SC and 2.3 MW BESS. When the system is connected to the main grid, the analysed disturbances are relatively smaller, and no further expansions of BESS and SC in Suðuroy are required according to the simulation results in this study. However, the preliminary plans of installing 3x16 MVA and 1x6 MVA SC and 30 MW BESS on the main grid have been included in the investigation, and as shown the BESS in the main grid has a high impact on the frequency regulation in Suðuroy, and the inertia has also been shown to be significantly higher (lower ROCOF) in the whole system (2026/2030), than in Suðuroy in 2020/2023.

Analysing parts of systems, without including a detailed model of the whole system, will not lead to accurate results as the share of inverter based technologies increase. In this paper simulations have shown that as soon as the BESS contributes to frequency regulation, a typical approximation model deviates significantly from a detailed model. As synchronous generators are removed from the grid, the BESS capacity and other alternative methods to provide ancillary services will increase, which makes it challenging to use traditional approximation models.

There are many options with inverter-based generation, and this paper has shown that inertia emulation from the wind turbines can improve the frequency response, but the benefit is limited when BESS are present in systems. The contribution from the IE can however be increased if the thresholds of IE and BESS are well coordinated.

5.1. Future Works

In order to get a better understanding of the future frequency and voltage stability and needed future expansions in ancillary services, more operation scenarios should be investigated, as in this study only one operation scenario has been investigated. Other events, e.g. short circuits, should also be investigated.

This study focuses on Suðuroy, which is around 10 times smaller than the main grid. Thus, when connected to the main grid, the severity of large disturbances (relative to the Suðuroy grid), decreases significantly. When connected to the main grid, the grid on Suðuroy will notice much larger disturbances (on the main grid), and the impact of these on Suðuroy should be investigated.

6. References

[1]   M. G. Schug, A. Gottlieb, and J. DeLoache, '"Equal Children Play Best": Raising Independent Children in a Nordic Welfare State', in *A World of Babies*, Cambridge: Cambridge University Press, 2016, pp. 261–292.

[2]   D. Weisser and R. S. Garcia, 'Instantaneous wind energy penetration in isolated electricity grids: Concepts and review', *Renew. Energy*, vol. 30, no. 8, pp. 1299–1308, 2005, doi: 10.1016/j.renene.2004.10.002.

[3]   O. Erdinc, N. G. Paterakis, and J. P. S. Catalaõ, 'Overview of insular power systems under increasing penetration of renewable energy sources: Opportunities and challenges', *Renew. Sustain. Energy Rev.*, vol. 52, pp. 333–346, 2015, doi: 10.1016/j.rser.2015.07.104.

[4]   Y. Tan, L. Meegahapola, and K. M. Muttaqi, 'A review of technical challenges in planning and operation of remote area power supply systems', *Renew. Sustain. Energy Rev.*, vol. 38, pp. 876–889,

2014, doi: 10.1016/j.rser.2014.07.034.

[5]   T. R. Ayodele, A. A. Jimoh, J. L. Munda, and J. T. Agee, 'Challenges of Grid Integration of Wind Power on Power System Grid Integrity: A Review', *Int. J. Renew. ENERGY Res.*, vol. 2, no. 4, 2012.

[6]   R. Shah, N. Mithulananthan, R. C. Bansal, and V. K. Ramachandaramurthy, 'A review of key power system stability challenges for large-scale PV integration', *Renew. Sustain. Energy Rev.*, vol. 41, pp. 1423–1436, 2015, doi: 10.1016/j.rser.2014.09.027.

[7]   G. Pepermans, J. Driesen, D. Haeseldonckx, R. Belmans, and W. D'haeseleer, 'Distributed generation: Definition, benefits and issues', *Energy Policy*, vol. 33, no. 6, pp. 787–798, 2005, doi: 10.1016/j.enpol.2003.10.004.

[8]   Dansk Energi, 'Teknisk notat - Stabilitet og udbygning af elnettet'. Dansk Energi, Copenhagen, Denmark, 2017.

[9]   H. M. Tróndheim, J. R. Pillai, T. Nielsen, C. L. Bak, and B. A. Niclasen, 'Frequency Regulation in an Isolated Grid with a High Penetration of Renewables - the Faroe Islands', in *CIGRE e-Session 2020*, 2020.

[10]   H. M. Tróndheim *et al.*, 'Frequency and Voltage Analysis of the Hybrid Power System in Suðuroy, Faroe Islands', in *Proceedings of Virtual 5th International Hybrid Power Systems Workshop*, 2021.

[11]   H. M. Tróndheim, 'A Battery System Utilized for Ancillary Services - the Faroe Islands'. 2018.

[12]   H. M. Tróndheim, 'Aggregation and Control of Flexible Thermal Demand for Wind Power Based Power System Analysis', Aalborg, Denmark, 2018.

[13]   S. Østerfelt and J. Hansen, 'Transient stabilitet i elnet drevet af vedvaren- de energikilder', 2021.

[14]   H. M. Tróndheim, T. Nielsen, B. A. Niclasen, C. L. Bak, and F. F. Da Silva, 'The Least-Cost Path to a 100 % Renewable Electricity Sector in the Faroe Islands', in *Proceedings of 4th International Hybrid Power Systems Workshop*, 2019.

[15]   H. M. Tróndheim, B. A. Niclasen, T. Nielsen, C. L. Bak, and F. F. Da Silva, 'Introduction to the Energy Mixture in an Isolated Grid with 100% Renewable Electricity - the Faroe Islands', in *Proceedings of CIGRE Symposium Aalborg 2019*, 2019, pp. 1–12.

[16]   Norconsult AS, '100% fornybar kraft, Pumpekraft, vind og sol', Sandvika, Norway, 2018.

[17]   Ea Energy Analyse, 'Balancing a 100% renewable electricity system - Least cost path for the Faroe Islands', Copenhagen, Denmark, 2018.

[18]   D. Al Katsaprakakis, B. Thomsen, I. Dakanali, and K. Tzirakis, 'Faroe Islands: Towards 100% R.E.S. penetration', *Renew. Energy*, vol. 135, no. 2019, pp. 473–484, 2019, doi: 10.1016/j.renene.2018.12.042.

[19]   A. M. Skeibrok, M. Eriksen, and J. Stav, 'Optimized hybrid microgrid system integrated with renewable energy sources'. 2019.

[20]   H. M. Tróndheim, B. A. Niclasen, T. Nielsen, F. F. Da Silva, and C. L. Bak, '100% Sustainable Electricity in the Faroe Islands: Expansion Planning Through Economic Optimization', *IEEE Open Access J. Power Energy*, vol. 8, pp. 23–34, 2021, doi: 10.1109/OAJPE.2021.3051917.

[21]   L. Wang, M. Klein, S. Yirga, and P. Kundur, 'Dynamic reduction of large power sytems for stability studies', *IEEE Trans. Power Syst.*, vol. 12, no. 2, pp. 889–895, 1997.

[22]   A. Ishchenko, A. Jokic, J. M. A. Myrzik, and W. L. Kling, 'Dynamic reduction of distribution networks with dispersed generation', in *2005 International Conference on Future Power Systems*, 2005, pp. 7 pp. – 7, doi: 10.1109/FPS.2005.204320.

[23]   N. Tong *et al.*, 'Dynamic Equivalence of Large-Scale Power Systems Based on Boundary Measurements', in *2020 American Control Conference (ACC)*, 2020, pp. 3164–3169, doi: 10.23919/ACC45564.2020.9147425.

[24]   DIgSILENT, *PowerFactory 2020 User Manual*. 2020.

[25]   P. Kundur *et al.*, 'Definition and Classification of Power System Stability', *IEEE Trans. Power Syst.*, vol. 19, no. 3, pp. 1387–1401, 2004, doi: 10.1109/tpwrs.2004.825981.

[26]   IEEE, 'IEEE Recommended Practice for Excitation System Models for Power System Stability Studies', *IEEE Std 421.5-2016 (Revision IEEE Std 421.5-2005)*, pp. 1–207, 2016, doi: 10.1109/IEEESTD.2016.7553421.

[27]   H. Ravn, 'The Balmorel Model Structure', vol. 02, no. 2.12 Alpha, p. 96, 2005.